



More information available at:  
[www.iba.muni.cz/summer-school2010](http://www.iba.muni.cz/summer-school2010)



Institute of Biostatistics and Analyses  
Masaryk University

Proceedings of the 6<sup>th</sup> Summer  
School on Computational Biology

# Proceedings of the 6<sup>th</sup> Summer School on Computational Biology

## Deterministic and Stochastic Modelling in Biology and Medicine

23–25 September 2010  
Lednice, Czech Republic

Publication was supported by the ESF project no. CZ.1.07/2.2.00/07.0318  
"Multidisciplinary Innovation of Study in Computational Biology"  
and national budget of the Czech Republic



Editors:  
Jiří Hřebíček  
Jiří Holčík  
Jaroslav Urbánek



CRM<sup>®</sup>

ISBN 978-80-7204-690-4

LEDNICE 2010



**Institute of Biostatistics and Analyses  
Masaryk University**

# Proceedings of the 6<sup>th</sup> Summer School on Computational Biology

## **Deterministic and Stochastic Modelling in Biology and Medicine**

**23–25 September 2010  
Lednice, Czech Republic**

**Editors:  
Jiří Hřebíček  
Jiří Holčík**



european  
social fund in the  
czech republic



EUROPEAN UNION



MINISTRY OF EDUCATION,  
YOUTH AND SPORTS



OP Education  
for Competitiveness



INVESTMENTS IN EDUCATION DEVELOPMENT

**Proceedings of the 6<sup>th</sup> Summer School on Computational Biology  
Deterministic and Stochastic Modelling in Biology and Medicine**

Editors: Jiří Hřebíček, Jiří Holčík

Cover: Radim Šustr

Published by AKADEMICKÉ NAKLADATELSTVÍ CERM, s.r.o. Brno

Purkyňova 95a, 612 00 Brno

[www.cerm.cz](http://www.cerm.cz)

Printed by FINAL TISK s.r.o. Olomučany

1<sup>st</sup> edition, 2010

ISBN 978-80-7204-698-0

# Contents

<b>Foreword</b> Jiří Hřebíček, Jiří Holčík	5
<b>LECTURES</b>	7
<b>Solving least squares problems</b> Walter Gander	9
<b>Modeling infectious diseases in humans and animals</b> Luděk Berec	21
<b>Spatio-temporal modelling of air pollution</b> Daniela Cocchi, Francesca Bruno, Fedele Greco, Carlo Trivisano	76
<b>Exact vectorization of a bitmap in biological modelling</b> Stanislav Bartoň	86
<b>Stochastic modelling of signal transduction in olfactory neurons</b> Ondřej Pokora	97
<b>Stochastic modeling of biodiversity: f-diversity, self f-diversity and marginal f-diversity</b> Jana Zvárová and Karel Zvára	108
<b>Deterministic models of natural selection and their relation to ecology</b> Zdeněk Pospíšil	120
<b>COMPUTATIONAL BIOLOGY STUDENTS' ABSTRACTS</b>	149
<b>Gene prediction from non-annotated sequences</b> Michaela Bayerlová	151
<b>Mathematical modelling of biodegradable processes</b> Anna Gardavská	152
<b>Enabling pathway analysis - connecting genomic experiments and gene ontology databases</b> Hana Imrichová	153
<b>Creation of a single initiation application with GUI generated by MATLAB</b> Pavčina Krečmerová	154

<b>Changes in long time monitoring of macrozoobenthos in the Czech Republic</b> Simona Littnerová	155
<b>Population history of viruses causing rabies</b> Jiří Moravec	157
<b>Computational simulation of environmental pollution using Maple</b> Markéta Novotná	158
<b>Bioclimatic modelling</b> Roman Richard Štěrba	160
<b>Evaluation of stress test ECG signal parameters in horses</b> Jana Svačinová	161
<b>The application of clustering methods on data of clinical registries</b> Hana Švihálková	162
<b>Acquiring knowledge on anticancer chemotherapy from health insurance claims data</b> Alena Zolřáková	163

## Foreword

Computational Biology is a modern field of study at the Faculty of Science of Masaryk University (MU). The study programme is guaranteed by the Institute of Biostatistics and Analyses (IBA), which provides computationally oriented courses within the educational concept of the Faculty of Medicine and the Faculty of Science. The educational concept of IBA MU covers applied data analysis and informatics, specialized for biological and biomedical sciences. Progress in such an interdisciplinary field would not be possible without international cooperation, and indeed, collaboration with experts from other countries improves the quality of education in Computational Biology remarkably and helps us to incorporate new ideas and trends. This concept also covers mathematical modelling, both in theoretical lectures and in practical training.

IBA MU has initiated a yearly tradition of informal summer schools focused on various aspects of computational science in biology and biomedicine:

2005 - Computational Biology

2006 - Predictive Modelling and ICT in Environmental Epidemiology

2007 - Processing and Analysis of Biodiversity Data: from Genomic Diversity to Ecosystem Structure

2008 - Statistical Methods for Genetic and Molecular Data

2009 - Analysis of Clinical and Biomedical Data in an Interdisciplinary Approach (in Czech),

where the invited lecturers and other participants enhance the scope of the Computational Biology study programme. Modelling – both deterministic and stochastic – will be the main topic of the 6th Summer School on Computational Biology. These meetings were organized in close cooperation with the Research Centre for Toxic Compounds in the Environment (RECETOX) formerly the Research Centre for Environmental Chemistry and Ecotoxicology of Masaryk University and the Jaroslav Hájek Centre for Theoretical and Applied Statistics of Masaryk University.

This foreword introduces the proceedings of the 6th Summer School on Computational Biology which will take place in Lednice, Czech Republic, from 23 to 25 September 2010. The topic of the summer school is “Deterministic and Stochastic Modelling in Biology and Medicine”. This topic was chosen as a very important phenomenon which has generated exciting modelling research topics for centuries. The investigation of modelling in biology and medicine, particularly deterministic and stochastic modelling has always been closely linked to mathematical and statistical theory and to computational skills.

Even the simplest modelling of natural and human phenomena and visualization of monitored and processed data require a specific kind of frequency mathematical analyses and summary statistics. The deterministic and stochastic modelling and their reflection in contemporary computational techniques still present very progressive scientific goals, together with an ever-growing importance in this field in recent years. Our summer school has specifically addressed all fields that might be interesting for computational biology and medicine.

The programme of the summer school will include, among others, lectures by the following experts from abroad and the Czech Republic:

- Prof. Walter Gander, ETH Zurich, Switzerland: Solving least squares problems
- Dr. Luděk Berec, Institute of Mathematics and Biomathematics, Faculty of Science, South Bohemia University, Czech Republic: Modelling infectious diseases in humans and animals
- Prof. Daniela Cocchi, Facoltà di Scienze Statistiche Università di Bologna, Italy: Spatio-temporal modelling of air pollution

- Assoc. Prof. Stanislav Bartoň, Mendel University in Brno, Czech Republic: Exact vectorization of the bitmap in biological modelling
- Dr. Ondřej Pokora, Faculty of Science, Masaryk University, Czech Republic: Stochastic modelling of signal transduction in sensory neurons
- Prof. Jana Zvárová, Prof. Karel Zvára, Centre of biomedicine informatics, Prague, Czech Republic: Stochastic modelling of biodiversity
- Assoc. Prof. Zdeněk Pospíšil, Faculty of Science, Masaryk University, Czech Republic: Deterministic models of natural selection and their relation to ecology

Clearly there is a lot of work to do and matters to investigate within biology and medicine in relation with mathematical and statistical modelling and using information and communication technology. And what's more, the world of biology and medicine science is opened to new ideas and methods developed by mathematical and computational scientists. The educational mission of the summer school will cover modelling, processing and visualization of all types of biology and medicine-related data, using accessible software packages. Practical training in tutorials will be based on modern numerical and statistical methods. Participants should gain a comprehensive overview of all key modelling, numerical and computational methods in biology and medicine, as well as a critical summary of their advantages and limitations.

The summer schools on Computational Biology are expected to encourage collaboration among professors and junior scientists, as well as students of Computational Biology. Students can participate in informal discussions about novel methods in their field of study and can take advantage of this ideal opportunity to present their own results to the audience. An active contribution from advanced students forms a substantial part of the summer school's programme.

A student competition at the 6th Summer School of Computational Biology will be held under the auspices of assoc. prof. Ladislav Dušek, the IBA MU Director, who has announced a prize for the best contributions in two categories, students of bachelor programmes and students of master programmes.

Here we would like to thank to all participants, namely actively contributing teachers and students. We also greatly appreciate all the foreign experts that have participated in the meeting, especially teachers that helped students with their results published here.

We are also very grateful for the financial support of the Ministry of Education, Youth and Sports of the Czech Republic, project CZ.1.07/2.2.00/07.0318, Multidisciplinary Innovation of Study in Computational Biology, where this summer school is organized.

On behalf of the programme and organizing committee,

Brno, August 31, 2010

Jiří Hřebíček  
Jiří Holčík

# Deterministic and Stochastic Modelling in Biology and Medicine

## Lectures





# Solving Least Squares Problems

Walter Gander

ETH Zurich  
gander@inf.ethz.ch

## 1 Least Squares Principle

In science and engineering we often need to estimate values of parameters of a mathematical model from measured data.

*Example 1.* The amount  $f$  of a component in a chemical reaction decreases with time  $t$  exponentially according to:  $f(t) = a_0 + a_1 e^{-bt}$ . If the material is weighed for different times, we obtain a table of measured values:

$$\begin{array}{c|c} t & t_1, \dots, t_m \\ \hline f & f_1, \dots, f_m \end{array}$$

The problem is now to estimate the model parameters  $a_0$ ,  $a_1$  and  $b$  from the measured data. Each measurement point  $(t_i, f_i)$  yields an equation:

$$f(t_i) = f_i \approx a_0 + a_1 e^{-bt_i}, \quad i = 1, \dots, m \quad (1)$$

If there would be no *measurement error* then we could replace in Equations (1) the approximate symbol by an equality and use three equations from the set to determine the parameters. However, in practice, measurement errors are present and often also the model equations *approximate only* the physical behavior. The equations will therefore contradict each other and we need some mechanism to balance the measurement errors, e.g. by requiring that Equations (1) are satisfied as well as possible.

To find a solution to such problems, C. F. Gauss invented 1795 the *Least Squares Method*. Let us consider more generally some (non-linear) function  $f: \mathbb{R}^n \mapsto \mathbb{R}^m$  with  $n \leq m$ . We want to find a point  $x \in \mathbb{R}^n$  such that

$$\|f(x)\|_2^2 = \sum_{i=1}^m f_i(x)^2 = \min. \quad (2)$$

The principle of minimizing the sum of squares is abbreviated and known as *Least Squares*. Methods for solving (2) are called *Least Squares Methods*. For a given vector  $x$  we define  $r = f(x)$  to be the *residual vector* and the sum of squares in (2) is also called the *residual sum of squares*. The currently best and most thorough reference for least squares methods is the book by Åke Björck [1].

For our example we have  $x = (a_0, a_1, b)^\top \in \mathbb{R}^3$  and  $f \in \mathbb{R}^m$  where

$$f_i(x) = y_i - x_1 - x_2 e^{-x_3 t_i} \approx 0, \quad i = 1, \dots, m.$$

## 2 Linear Least Squares

If  $f$  is a linear function  $f(x) = b - Ax$ , then minimizing the length of the residual vector  $r = b - Ax$  is equivalent of minimizing the quadratic form

$$Q(x) = r^\top r = (b - Ax)^\top (b - Ax) = b^\top b - 2x^\top A^\top b + x^\top A^\top A x$$

Differentiating with respect to  $x$  and equating to zero we get the *Normal Equations of Gauss*:

$$A^\top A x = A^\top b. \quad (3)$$

*Example 2.* We want to fit a linear function through given points  $(t_i, f_i)$ ,  $i = 1, \dots, m$ . Using

$$f(t) = x_1 + x_2 t$$

and computing the coefficients  $x_1$  and  $x_2$  in the least squares sense is called *linear regression*. Inserting the points we get the equations

$$\begin{pmatrix} 1 & t_1 \\ \vdots & \vdots \\ 1 & t_m \end{pmatrix} \begin{pmatrix} x_1 \\ x_2 \end{pmatrix} \approx \begin{pmatrix} f_1 \\ \vdots \\ f_m \end{pmatrix}.$$

The normal equations which can be found in every statistics textbook become

$$\begin{pmatrix} m & \sum_i t_i \\ \sum_i t_i & \sum_i t_i^2 \end{pmatrix} \begin{pmatrix} x_1 \\ x_2 \end{pmatrix} = \begin{pmatrix} \sum_i f_i \\ \sum_i t_i f_i \end{pmatrix}.$$

### 2.1 Normal Equations and Condition

It is well known that when solving a linear system of equations  $Ax = b$  with  $A \in \mathbb{R}^{n \times n}$ , the relative error of numerically computed solution  $\tilde{x}$  is

$$\frac{\|\tilde{x} - x\|}{\|x\|} \simeq \underbrace{\|A^{-1}\| \|A\|}_{\kappa} \varepsilon \quad (4)$$

condition number

where  $\varepsilon$  denotes the machine precision. If we use as matrix norm the 2-norm then the condition number is computed by

$$\kappa = \frac{\sigma_{\max}(A)}{\sigma_{\min}(A)} = \text{cond}(A) \text{ in MATLAB.}$$

We have to expect that the numerical solution may deviate by about  $\kappa$  units in the last digit from the exact solution.

For the least squares problem Golub and Pereyra [4] showed that

$$\frac{\|\tilde{x} - x\|}{\|x\|} \simeq \left( 2\kappa + \kappa^2 \frac{\|r\|}{\|A\| \|x\|} \right) \varepsilon, \quad \text{where } \kappa := \|A\| \|A^+\| = \frac{\sigma_1(A)}{\sigma_r(A)}, \quad (5)$$

with  $A^+$  the *Pseudoinverse* and  $r$  the rank of the matrix (see Section 4).

Equation (5) tells us again what accuracy we can expect from the numerical solution. We have to distinguish between good and bad models. For good models, i.e. if the residual  $\|r\|$  is small, the error is proportional to  $\kappa$  as for linear equations (4). However, when the model is bad, i.e. when  $\|r\|$  is large then the error is proportional to  $\kappa^2$ . Using the normal equations, the error is always proportional to  $\kappa^2$  since  $\kappa(A^\top A) = \kappa(A)^2$ . Forming  $A^\top A$  also results in a loss of information as a famous example by P. Läuchli shows:

$$A = \begin{pmatrix} 1 & 1 \\ \delta & 0 \\ 0 & \delta \end{pmatrix}, \quad A^\top A = \begin{pmatrix} 1 + \delta^2 & 1 \\ 1 & 1 + \delta^2 \end{pmatrix}.$$

If  $\delta < \sqrt{\varepsilon}$  (with  $\varepsilon$  machine precision) then numerically  $1 + \delta^2 = 1$  and the matrix of the normal equations becomes singular though  $A$  has also numerically rank 2.

## 2.2 Avoiding Normal Equations

When solving linear systems  $Ax = b$  with  $A \in \mathbb{R}^{n \times n}$  by Gaussian elimination we use of the fact that *equivalent systems have the same solutions*:

$$Ax = b \iff BAx = Bb \quad \text{if } B \text{ is nonsingular.}$$

For a system of equations  $Ax \approx b$  to be solved in the least squares sense it is no longer true that multiplying by a nonsingular matrix  $B$  leads to an equivalent system. The transformation matrices have to be *orthogonal* (i.e.  $B^\top B = I$ ):

$$Ax \approx b \iff BAx \approx Bb \quad \text{if } B \text{ is orthogonal.}$$

This is clear from the fact that  $r = b - Ax$  and  $Br = Bb - BAx$  have the same length  $\|Br\|^2 = (Br)^\top (Br) = r^\top B^\top B r = r^\top r = \|r\|^2$ . Using the QR-decomposition of  $A$  we obtain an equivalent system by multiplying with  $B = Q^\top$ :

$$A = Q \begin{pmatrix} R \\ 0 \end{pmatrix} \Rightarrow Q^\top Ax = \begin{pmatrix} R \\ 0 \end{pmatrix} x \approx \begin{pmatrix} y_1 \\ y_2 \end{pmatrix}, \quad \text{with } \begin{pmatrix} y_1 \\ y_2 \end{pmatrix} := Q^\top b.$$

The square of the norm of the residual becomes

$$\|r\|^2 = \|y_1 - Rx\|^2 + \|y_2\|^2,$$

and is obviously minimal for  $x$  where

$$Rx = y_1, \quad x = R^{-1}y_1 \quad \text{and} \quad \min \|r\| = \|y_2\|.$$

This approach to solve a least squares problem is numerically preferable to the normal equations, since it leaves the condition number unchanged:  $\kappa(A) = \kappa(R)$ . This is true because the singular values are not changed by orthogonal transformations.

### 2.3 Elementary Orthogonal Matrices

There are two elementary orthogonal matrices useful for transforming  $Ax \approx b$  to  $Rx = y_1$ .

**Definition 1.**  $P = I - uu^\top$  with  $\|u\| = \sqrt{2}$  is an elementary orthogonal Householder matrix.

$P$  is used to introduce zeros in a matrix. The basic transformation is to map a given vector  $x$  to a multiple of the first unit vector:  $Px = \sigma e_1$ . Since  $P$  is orthogonal we have  $\|Px\|^2 = \|x\|^2 = \sigma^2$  thus  $\sigma = \pm\|x\|$ . Furthermore

$$P = (I - uu^\top)x = x - u(u^\top x) = \sigma e_1,$$

thus  $u(u^\top x) = x - \sigma e_1$  and we obtain by normalizing

$$u = \frac{x - \sigma e_1}{\|x - \sigma e_1\|} \sqrt{2}.$$

We choose the sign of  $\sigma$  to avoid cancellation in computing  $x - \sigma e_1$ :

$$\sigma = \begin{cases} \|x\|, & x_1 < 0 \\ -\|x\|, & x_1 \geq 0 \end{cases}.$$

Doing so the Householder-vector becomes

$$u = \frac{x - \sigma e_1}{\sqrt{\|x\|(|x_1| + \|x\|)}}.$$

**Definition 2.** An elementary Givens rotation is the matrix  $S(i, j, \alpha)$ , with  $1 \leq i < j \leq n$ , is an identity matrix with 4 elements changed:  $s_{ii} = s_{jj} = \cos \alpha$ ,  $s_{ij} = -s_{ji} = \sin \alpha$ .

$S(i, j, \alpha)$  is used to rotate elements to zero. Given  $x$ , we want the transformation  $x := Sx$  to change  $x_i$  and  $x_j \neq 0$  such that  $x_j^{new} = 0$ . Let  $s = \sin \alpha$  and  $c = \cos \alpha$ . Because  $x_j^{new} = sx_i - cx_j = 0$  we get

$$\cot = \frac{x_i}{x_j}, \quad s = \frac{1}{\sqrt{1 + \cot^2}}, \quad c = s \times \cot.$$

Note that we do not need to compute the angle  $\alpha$  explicitly to determine the matrix  $S(i, j, \alpha)$ . To compute the QR decomposition of a matrix  $A$  we now can apply Givens rotations to introduce zeros below the diagonal.

*Example 3.* The following problem can be stated as least squares problem, though there are no measurement errors. We consider two straight lines  $g$  and  $h$  in space. Assume they are given by a point and a direction vector:

$$\begin{aligned} g : X &= P + \lambda r \\ h : Y &= Q + \mu s \end{aligned}$$

If they intersect then there must exist a  $\lambda$  and a  $\mu$  such that  $P + \lambda r = Q + \mu s$ . Rearranging the equations we obtain

$$\begin{pmatrix} r_1 & -s_1 \\ r_2 & -s_2 \\ r_3 & -s_3 \end{pmatrix} \begin{pmatrix} \lambda \\ \mu \end{pmatrix} = \begin{pmatrix} Q_1 - P_1 \\ Q_2 - P_2 \\ Q_3 - P_3 \end{pmatrix} \quad (6)$$

a system of three linear equations with two unknowns. If the equations are consistent we can use two of them to determine the intersection point. If the straight lines are warped (and Equations (6) have no solutions) then we may be interested to find the the point  $X$  on  $g$  and  $Y$  on  $h$  which are closest, i.e. for which the distance vector  $r = X - Y$  has minimal length :  $\|r\|^2 = \min$ . Thus we are interested to solve Equations (6) as a least squares problem.

Applying three Givens rotations annihilating the (2, 1), (3, 1) and the (3, 2) element of the matrix we obtain an equivalent least squares problem:

$$\begin{pmatrix} r_{11} & r_{12} \\ 0 & r_{22} \\ 0 & 0 \end{pmatrix} \begin{pmatrix} \lambda \\ \mu \end{pmatrix} = \begin{pmatrix} y_1 \\ y_2 \\ y_3 \end{pmatrix}$$

which tells us all we want to know: if  $y_3 = 0$  the lines intersect and solving by back-substitution

$$\begin{pmatrix} r_{11} & r_{12} \\ 0 & r_{22} \end{pmatrix} \begin{pmatrix} \lambda \\ \mu \end{pmatrix} = \begin{pmatrix} y_1 \\ y_2 \end{pmatrix}$$

for  $\lambda$  and  $\mu$  we get the parameters which define the intersection point. If  $y_3 \neq 0$  then the parameters define the two nearest points and  $|y_3|$  is their distance.

### 3 Non-Linear Least Squares

We recall first Newton's method for a non-linear system of  $n$  equations for  $n$  unknowns. We want to find  $x$  such that  $f(x) = 0$ . Expanding  $f$  at some approximation  $x_k$  we obtain

$$f(x) \approx f(x_k) + J(x_k)h, \quad \text{with } h = x - x_k,$$

where  $J(x_k)$  denotes the Jacobian evaluated at  $x_k$ ,

$$J(x) = \begin{bmatrix} \frac{\partial f_1}{\partial x_1} & \frac{\partial f_1}{\partial x_2} & \cdots & \frac{\partial f_1}{\partial x_n} \\ \frac{\partial f_2}{\partial x_1} & \frac{\partial f_2}{\partial x_2} & \cdots & \frac{\partial f_2}{\partial x_n} \\ \vdots & \vdots & & \vdots \\ \frac{\partial f_n}{\partial x_1} & \frac{\partial f_n}{\partial x_2} & \cdots & \frac{\partial f_n}{\partial x_n} \end{bmatrix}.$$

Instead of solving  $f(x) = 0$  we solve the linearized system  $f(x_k) + J(x_k)h = 0$  for the *Newton correction*  $h$  and obtain a (hopefully better) approximation  $x_{k+1} = x_k + h$ .

Given now  $m$  non-linear equations with  $n$  unknowns ( $n \leq m$ ) we want to solve  $f(x) \approx 0$  in the least squares sense, that is, we want

$$\Phi(x) := \frac{1}{2} \|f(x)\|^2 = \min. \quad (7)$$

Necessary for minimizing  $\Phi(x)$  is  $\text{grad } \Phi = 0$ . We want to express this condition in  $f$ :

$$\frac{\partial \Phi(x)}{\partial x_i} = \sum_{l=1}^m f_l(x) \frac{\partial f_l}{\partial x_i},$$

or in matrix notation

$$\text{grad } \Phi(x) = J(x)^\top f(x).$$

Thus we obtain as a necessary condition for minimizing  $\Phi(x)$  a nonlinear system of  $n$  equations in  $n$  unknowns:

$$J(x)^\top f(x) = 0.$$

We want to compute a solution using Newton's method. We need the Jacobian of  $\text{grad } \Phi(x)$  which is the Hessian of  $\Phi(x)$ . If  $x_k$  is an approximation the we obtain the Newton correction by solving a linear system:

$$\text{hess } \Phi(x_k)h = -J(x_k)^\top f(x_k).$$

Let us express the Hessian also by the function  $f$ . We compute the second derivatives:

$$\frac{\partial \Phi(x)}{\partial x_i} = \sum_{l=1}^m f_l(x) \frac{\partial f_l}{\partial x_i} \quad (8)$$

$$\frac{\partial^2 \Phi(x)}{\partial x_i \partial x_j} = \sum_{l=1}^m \frac{\partial f_l}{\partial x_j} \frac{\partial f_l}{\partial x_i} + \sum_{l=1}^m f_l(x) \frac{\partial^2 f_l}{\partial x_i \partial x_j}. \quad (9)$$

Now  $\partial^2 f_l / \partial x_i \partial x_j$  is the  $ij$ -element of the Hessian of  $f_l(x)$ . Furthermore  $(\mathbf{cJ}_i$  denotes the  $i$ -th column of the matrix  $J$ )

$$\sum_{l=1}^m \frac{\partial f_l}{\partial x_j} \frac{\partial f_l}{\partial x_i} = \mathbf{cJ}_j^\top \mathbf{cJ}_i.$$

Therefore we obtain in matrix notation

$$\text{hess } \Phi(x) = J^\top J + \sum_{l=1}^m f_l(x) \text{hess } f_l(x).$$

A Newton step for the non-linear least squares problem  $f(x) \approx 0$  becomes

1. solve for the correction  $h$  the linear system

$$\left( J(x_k)^\top J(x_k) + \sum_{l=1}^m f_l(x_k) \text{hess } f_l(x_k) \right) h = -J(x_k)^\top f(x_k) \quad (10)$$

2. iterate:  $x_{k+1} = x_k + h$ .

**Simplifications:** The matrix for the computation of the correction  $h$  in Equation (10) is complicated. Therefore an approximation of the sum of the Hessians, called *Tikhonov regularization* or *method of Levenberg-Marquart*, is considered:

$$\left( J(x_k)^\top J(x_k) + \tau^2 D^2 \right) h = -J(x_k)^\top f(x_k) \iff \begin{pmatrix} J(x_k) \\ \tau D \end{pmatrix} h \approx \begin{pmatrix} f(x_k) \\ 0 \end{pmatrix}.$$

The matrix  $D$  is often chosen as diagonal matrix. It is straightforward to see that this way one minimizes the expression

$$\|J(x_k)h - f(x_k)\|^2 + \tau^2 \|Dh\|^2,$$

which is again equivalent to the problem

$$\min \|J(x_k)h - f(x_k)\|^2 \quad \text{subject to} \quad \|Dh\|^2 \leq \alpha^2$$

for some  $\alpha$ . Since by that the stepsize  $h$  is restricted to  $\|Dh\|^2 \leq \alpha^2$  the resulting method is called *Trust Region Method*.

## 4 The Singular Value Decomposition (SVD)

**Theorem 1.** (*Singular Value Decomposition*) Let  $A \in \mathbb{R}^{m \times n}$  with  $m \geq n$ . Then there exist orthogonal matrices  $U \in \mathbb{R}^{m \times m}$ ,  $V \in \mathbb{R}^{n \times n}$  and a diagonal matrix  $\Sigma = \text{diag}(\sigma_1, \dots, \sigma_n) \in \mathbb{R}^{m \times n}$  with  $\sigma_1 \geq \sigma_2 \geq \dots \geq \sigma_n \geq 0$ , such that  $A = U\Sigma V^\top$  holds. If  $\sigma_r > 0$  is the smallest singular value greater than zero then the matrix  $A$  has rank  $r$ .

**Definition 3.** Let  $A = U\Sigma V^\top$  be the singular value decomposition with

$$\Sigma = \begin{pmatrix} \Sigma_r \\ 0 \end{pmatrix} \in \mathbb{R}^{m \times n}, \quad \Sigma_r := \text{diag}(\sigma_1, \dots, \sigma_r, 0, \dots, 0) \in \mathbb{R}^{n \times n}$$

The matrix  $A^+ = V\Sigma^+ U^\top$  with

$$\Sigma^+ = (\Sigma_r^+ \ 0) \in \mathbb{R}^{n \times m}, \quad \Sigma_r^+ := \text{diag}\left(\frac{1}{\sigma_1}, \dots, \frac{1}{\sigma_r}, 0, \dots, 0\right) \in \mathbb{R}^{n \times n} \quad (11)$$

is called the *pseudo-inverse* of  $A$ .

The SVD allows us to compute the general solution of the linear least squares problem with (possibly) rank deficient coefficient matrix  $Ax \approx b$ :

1. Compute the SVD:  $[U \ S \ V] = \text{svd}(A)$ .
2. Make a rank decision, i.e. choose  $r$  such that  $\sigma_r > 0$  and  $\sigma_{r+1} = \dots = \sigma_n = 0$ . This decision is necessary because rounding errors will prevent the zero singular values to be exactly zero.
3. Set  $V1=V[:, 1:r]$ ,  $V2= V[:, r+1:n]$ ,  $Sr=S[1:r, 1:r]$ ,  $U1=U[:, 1:r]$ .
4. The solution with minimal norm is  $xm=V1*(Sr \setminus U1' * b)$ .

5. The general solution is  $x = x_m + V_2 * c$  with an arbitrary  $c \in \mathbb{R}^{n-r}$ .

If  $A$  has full rank ( $\text{rank}(A) = n$ ) then the solution of the linear least squares problem is unique:  $x = V \Sigma^{-1} U^T b$ . It is computed in Matlab by the statement  $x = A \backslash b$ .

If  $A$  has  $\text{rank}(A) = r < n$  then the solution is not unique and given in theory by

$$x = A^+ b + (I - A^+ A) w, \quad w \text{ arbitrary.}$$

The SVD gives us explicit expressions for the various projectors on the four fundamental subspaces:

$$\begin{aligned} 1. P_{\mathcal{R}(A)} &= AA^+ = U_1 U_1^T & 2. P_{\mathcal{R}(A^T)} &= A^+ A = V_1 V_1^T \\ 3. P_{\mathcal{N}(A^T)} &= I - AA^+ = U_2 U_2^T & 4. P_{\mathcal{N}(A)} &= I - A^+ A = V_2 V_2^T \end{aligned}$$

**Theorem 2.** Let  $A = U \Sigma V^T$  and  $V = [v_1, \dots, v_n]$ . Then the problem

$$\|Ax\|_2 = \min, \quad \text{subject to } \|x\|_2 = 1 \quad (12)$$

has the solution  $x = v_n$  and the value of the minimum is  $\min_{\|x\|_2=1} \|Ax\|_2 = \sigma_n$ .

*Example 4.* We consider the problem of fitting lines by minimizing the sum of squares of the distances to given points (see [2], Chapter 6). In the plane we can represent a straight line uniquely by the equations

$$c + n_1 x + n_2 y = 0, \quad n_1^2 + n_2^2 = 1. \quad (13)$$

The unit vector  $(n_1, n_2)$  is orthogonal to the line. A point is on the line if its coordinates  $(x, y)$  satisfy the first equation. On the other hand if  $P = (x_P, y_P)$  is some point not on the line and we compute

$$r = c + n_1 x_P + n_2 y_P$$

then  $|r|$  is its distance from the line. Therefore if we want to determine the line for which the sum of squares of the distances to given points is minimal, we have to solve the constrained least squares problem

$$\begin{pmatrix} 1 & x_{P_1} & y_{P_1} \\ 1 & x_{P_2} & y_{P_2} \\ \vdots & \vdots & \vdots \\ 1 & x_{P_m} & y_{P_m} \end{pmatrix} \begin{pmatrix} c \\ n_1 \\ n_2 \end{pmatrix} \approx \begin{pmatrix} 0 \\ 0 \\ \vdots \\ 0 \end{pmatrix} \quad \text{subject to } n_1^2 + n_2^2 = 1. \quad (14)$$

Let  $A$  be the matrix of the linear system (14). Using the QR decomposition  $A = QR$  we can reduce the the linear system to  $Rx \approx 0$ , i.e., the problem becomes

$$\begin{pmatrix} r_{11} & r_{12} & r_{13} \\ 0 & r_{22} & r_{23} \\ 0 & 0 & r_{33} \end{pmatrix} \begin{pmatrix} c \\ n_1 \\ n_2 \end{pmatrix} \approx \begin{pmatrix} 0 \\ 0 \\ 0 \end{pmatrix} \quad \text{subject to } n_1^2 + n_2^2 = 1. \quad (15)$$

Since the nonlinear constraint only involves two unknowns; we now have to solve

$$\begin{pmatrix} r_{22} & r_{23} \\ 0 & r_{33} \end{pmatrix} \begin{pmatrix} n_1 \\ n_2 \end{pmatrix} \approx \begin{pmatrix} 0 \\ 0 \end{pmatrix}, \quad \text{subject to } n_1^2 + n_2^2 = 1. \quad (16)$$

The solution is obtained using Theorem 2. Inserting the values into the first equation of (15), we then can compute  $c$ .

## 5 Constrained Least Squares

Given the matrices  $A^{m \times n}$ ,  $C^{p \times n}$  and the vectors  $b$  and  $d$  we are interested to find a vector  $x$  such that

$$\|Ax - b\|_2^2 = \min \quad \text{subject to} \quad Cx = d. \quad (17)$$

We are interested in the case  $p \leq n \leq m$ . A solution exists only if the constraints are consistent i.e. if  $d \in \mathcal{R}(C)$ . The classical solution is obtained by minimizing the Lagrangian

$$L(x, \lambda) = \frac{1}{2} \|Ax - b\|_2^2 + \lambda^\top (Cx - d).$$

Setting the partial derivatives to zero we obtain:

$$\frac{\partial L}{\partial x} = A^\top (Ax - b) + C^\top \lambda = 0 \quad \text{and} \quad \frac{\partial L}{\partial \lambda} = Cx - d = 0.$$

Thus

$$\begin{pmatrix} A^\top A & C^\top \\ C & 0 \end{pmatrix} \begin{pmatrix} x \\ \lambda \end{pmatrix} = \begin{pmatrix} A^\top b \\ d \end{pmatrix} \quad \text{Normal Equations.} \quad (18)$$

The matrix of the Normal Equations (18) is symmetric, however, not positive definite. So we cannot use the Cholesky decomposition, we need Gaussian elimination with pivoting to solve the system.

If both  $A$  and  $C$  have full rank then we may make use of the structure. Consider the ansatz for an LU-decomposition:

$$\begin{pmatrix} A^\top A & C^\top \\ C & 0 \end{pmatrix} = \begin{pmatrix} R^\top & 0 \\ G & -U^\top \end{pmatrix} \begin{pmatrix} R & G^\top \\ 0 & U \end{pmatrix}.$$

Multiplying the right hand side and equating terms we obtain

$$R^\top R = A^\top A \quad \text{thus} \quad R = \text{chol}(A^*A)$$

$$R^\top G^\top = C^\top \quad \text{or} \quad GR = C \quad \text{thus} \quad G = CR^{-1}$$

and

$$GG^\top - U^\top U = 0 \quad \text{thus} \quad U = \text{chol}(G*G').$$

The whole algorithm becomes:

1. Compute the Cholesky decomposition  $R^\top R = A^\top A$ .
2. Solve for  $G^\top$  by forward substituting  $R^\top G^\top = C^\top$ .
3. Compute the Cholesky decomposition  $U^\top U = GG^\top$
4. Solve for  $y_1$  and  $y_2$  by forward substituting

$$\begin{pmatrix} R^\top & 0 \\ G & -U^\top \end{pmatrix} \begin{pmatrix} y_1 \\ y_2 \end{pmatrix} = \begin{pmatrix} A^\top b \\ d \end{pmatrix}$$

5. Solve for  $x$  and  $\lambda$  by back substituting

$$\begin{pmatrix} R & G^\top \\ 0 & U \end{pmatrix} \begin{pmatrix} x \\ \lambda \end{pmatrix} = \begin{pmatrix} y_1 \\ y_2 \end{pmatrix}$$

There are several possibilities to avoid the numerically not favored Normal Equations (18) by directly eliminating the constraints. In the following we present the *Null Space Method*. Since we assume that  $C$  has full rank  $p$ , we can express the general solution of  $Cx = d$  using the QR decomposition. We compute the QR decomposition of  $C^\top$ :

$$C^\top = [Q_1, Q_2] \begin{pmatrix} R \\ 0 \end{pmatrix}.$$

With  $Q = [Q_1, Q_2]$  and the new unknowns  $\begin{pmatrix} y_1 \\ y_2 \end{pmatrix} := Q^\top x$  the constraints become

$$Cx = [R^\top, 0] Q^\top x = R^\top y_1 = d.$$

The general solution of the constraints is  $y_1 = R^{-T}d$  and  $y_2$  arbitrary. Introducing this in  $\|Ax - b\|$  we get:

$$Ax = AQQ^\top x = AQ \begin{pmatrix} y_1 \\ y_2 \end{pmatrix} = A(Q_1 y_1 + Q_2 y_2)$$

and the problem becomes an unconstrained least squares problem

$$\|Ax - b\| = \|AQ_2 y_2 - (b - AQ_1 y_1)\| = \min. \quad (19)$$

Thus we obtain the algorithm:

1. compute the QR decomposition of  $C^\top$ :  $[Q, R] = \text{qr}(C^\top)$
2. compute  $y_1$  by forward substitution  $R^\top y_1 = d$  and  $x_1 = Q_1 y_1$ .
3. Form  $\tilde{A} = AQ_2$  and  $\tilde{b} = b - Ax_1$ .
4. Solve  $\tilde{A}y_2 \approx \tilde{b}$ .
5.  $x = Q \begin{pmatrix} y_1 \\ y_2 \end{pmatrix} = x_1 + Q_2 y_2$ .

```
function [x] = lsqcn(A,C,b,d);
%
% x = LSQCN(A,C,b,d) solves the constrained least squares problem
% ||Ax-b|| = min subject to Cx=d by the Nullspace Method.
% For the change of variables and for solving the reduced least
% squares problem the Matlab built-in Householder QR decomposition
% is used.
[p n] = size(C);
[Q R ] = qr(C');
y1 = R(1:p,1:p)'\d;
x1 = Q(:,1:p) *y1;
y2 = (A*Q(:,p+1:n))\ (b -A*x1);
x = x1 + Q(:,p+1:n)*y2;
```

*Example 5.* If we interpolate the 7 points

```
>> x = [ 1; 2.5; 3; 5; 13; 18; 20];
>> y = [ 2; 3; 4; 5; 7; 6; 3];
>> m = length(x);
>> plot(x,y,'o'); hold;
```

by the interpolating polynomial of degree 6

```
>> xx = 1:0.1:20;
>> P = polyfit(x,y,6); plot(xx, polyval(P,xx),':')
```

we obtain the dashed curve shown in Figure 1. The interpolation is really not what one would like. We can obtain a smoother approximation e.g. by giving up the interpolation

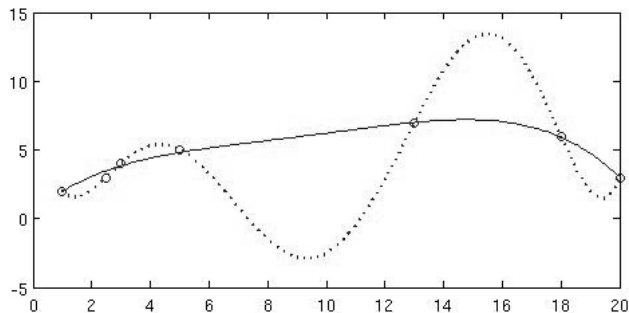


**Fig. 1.** Polynomial Interpolation

condition or maybe relaxing it by demanding interpolation only for a few points and a least squares fit for the remaining others.

In MATLAB polynomials of degree  $d$  are represented with coefficients  $p$  as

$$P_d(x) = p_1x^d + p_2x^{d-1} + \dots + p_dx + p_{d+1}.$$

The interpolation- and approximation-conditions  $P_d(x_i) = y_i$  resp.  $P_d(x_i) \approx y_i$  lead to a constraint least squares problem

$$Vp \simeq y,$$

with the  $m \times (d+1)$  Vandermonde matrix  $V = (v_{ij})$  with  $v_{ij} = x_i^{d-j+1}$ . We now choose the degree  $d = 4$  and want to interpolate  $p = 3$  points: the first, the last and the fifths.

```
>> degree = 4;
>> n = degree+1;
>> V(:,n) = ones(m,1);
>> for j = degree:-1:1
>>     V(:,j) = x.*V(:,j+1);
>> end
>> p = 3; % number of interpolating points
>> in = [1 5 7 2 3 4 6]; % permute equations: the first p interpolate
```

We reorder the equations so that the first 3 are the one with the interpolation conditions:

```
>> Vp = V(in,:); yp = y(in);
>> C = Vp(1:p,:); A = Vp(p+1:m,:);
```

```

>> d = yp(1:p); b = yp(p+1:m);
>> % Solve constrained least squares problem
>> P1 = lsq1cn(A,C,b,d);

P1' =   -0.0005    0.0176   -0.2367    1.6531    0.5665

>> plot(xx, polyval(P1,xx))
>> [V*P1 y]
ans =
    2.0000    2.0000
    3.4758    3.0000
    3.8313    4.0000
    4.8122    5.0000
    7.0000    7.0000
    5.9036    6.0000
    3.0000    3.0000

```

As we can see from Figure 1 we obtain a much better interpolation this time. Comparing  $V \times P1$  with  $y$  we see the three interpolation points and that the others are only approximated by least squares.

## References

1. Åke Björck, "Numerical Methods for Least Squares Problems", SIAM, 1996.
2. W. Gander and J. Hřebíček, "Solving Problems in Scientific Computing using Maple and Matlab", Springer Verlag, third edition 1997.
3. W. Gander, G. H. Golub and R. Strebler, "Least-Squares Fitting of Circles and Ellipses", BIT 34, 1994, pp. 558-578.
4. GENE H. GOLUB AND VICTOR PEREYRA, *The Differentiation of Pseudoinverses and Nonlinear Least Squares Problems Whose Variables Separate*, SIAM J. Numer. Anal. 10, 413-432, 1973.

# Modeling Infectious Diseases in Humans and Animals

Luděk Berec

Department of Theoretical Ecology, Institute of Entomology, Biology Centre ASCR, and  
Institute of Mathematics and Biomathematics, Faculty of Science, University of South Bohemia,  
Branišovská 31, 37005 České Budějovice, Czech Republic berec@entu.cas.cz,  
[www.entu.cas.cz/berec](http://www.entu.cas.cz/berec)

**Abstract.** Mathematical models play a vital role in present-day epidemiology. The aim of this material is to provide an introduction to mathematical epidemiology, that is, to the art of mathematical modeling of infectious diseases. We introduce the fundamental concepts and principles of modeling infectious diseases in humans and animals, starting with the basic epidemiological models that assume constant host population size. We show how these simple models can help us interpret data on infectious diseases and facilitate designing of strategies for controlling them. Although the assumptions behind these basic models are necessarily unrealistic, their main value is in telling us what is possible in a system as simple and abstract as possible where everything except the actual host-parasite interaction is removed. In addition, these simple models can capture many of the qualitative properties of more complex, detail-rich models, and the latter models actually use the simple ones as the basic building blocks. Next, we consider dynamic models of wildlife infections, as these infections tend to increasingly affect humans. In these models, the host population size is no longer assumed to be constant, but rather is subject to its own dynamics, whether exponential growth, logistic growth, or constant rate immigration. The wildlife models are often used to explore the extent to which parasites can depress the (natural) growth rate or steady state of their host populations and what characteristics of infectious agents are most decisive in this. In addition, the wildlife models can be adequate descriptions of infectious disease dynamics in human populations in developing countries. Finally, we present models of a few specific infectious diseases, and discuss their epidemiological as well as ecological consequences.

**Note:** This material is intended to be lecture notes, not an original scientific treatise. As such, it is mostly composed of the work of others (books and scientific papers), to which the material refers where appropriate. Although I have strived to not repeat the original wording, it might be that some portions of the text have remained virtually unchanged compared with the original work. This by no means implies that I credit the work of others to myself. Rather, it means that the original wording was so dense and accurate that I could hardly write it any better.

## 1 Introduction

### 1.1 The Why and How of Mathematical Modeling

The word “model” is not unambiguous, but in science, a model is generally considered to be a representation of (a part of) reality that we aim to study. One familiar type of

models is *physical models* – a material, pictorial, or analogical representation of (a part of) an actual system, such as scale material models used in wind tunnel experiments or flight simulators. In many fields of science, however, *mathematical models* play a far more important role, especially in studies of dynamics of all sorts of systems. Mathematical models represent the systems examined in the form of mathematical objects and their relationships, often in the form of various types of (dynamic) equations or in the form of governing rules assembled as computer algorithms.

Unfortunately, only the simplest mathematical models are analytically tractable, that is, can be completely solved using standard tools of mathematical analysis. As model complexity increases, all that one can usually obtain is numerical solutions corresponding to specific initial conditions. For models of intermediate complexity, analytical tools and numerical simulations are standardly combined and complement one another.

Whether formally analyzed or run as numerical simulations, mathematical models are useful experimental tools for building and testing theories, generating hypotheses, assessing quantitative conjectures, answering specific questions, determining system sensitivity to changes in parameter values, and estimating key parameters from data. Models often identify behaviors that are unclear in experimental data, often because data are hardly reproducible and the number of data points is often limited and subject to measurement errors. From the applied perspective, models can be used to supplant experiments that we, for some reason, cannot conduct practically, and/or to assess and compare various management actions before they are actually employed.

Practically, mathematical modeling proceeds in several steps [31]:

1. *Formulate the question*: formulate the question of interest in terms of the original scientific discipline;
2. *Determine the basic ingredients*: choose the ingredients perceived as essential for addressing the question, such as variables, their interactions, time scales and parameters;
3. *Qualitatively describe the examined system* through diagrams or tables;
4. *Quantitatively describe the examined system* by writing down equations or governing rules;
5. *Solve the model*: analyze the equations, run numerical simulations, carry out analysis relevant to the question of interest;
6. *Perform checks and balances*: check whether the results are in agreement with what is known, if not, refine the model and repeat steps 2–5;
7. *Relate the results back to the question*: interpret the results in terms of the original scientific discipline, discuss generality of the results, embed them in current theories, suggest potential experiments.

Interestingly, the contribution of the original scientific discipline can mostly be detached from the contribution of mathematics; we can often put aside the real world when solving mathematical models (steps 4–5).

Any model is necessarily a *simplified* representation of reality – one is always forced to prioritize, that is, to consider only those aspects of the examined system that are essential for its understanding and/or prediction of its behavior, and neglect those aspects that seem marginal for the question of interest. Because of this, no model can be considered the best one; there is always a place for improvement, no matter how large. It

is also important to realize that from no model can one require more than conditional predictions of the type “what effects would a given situation imply if it occurs”.

## 1.2 What Is a Parasite?

Epidemiology deals with parasites. In completing their life cycle, parasites need one or more host species. A Parasite may spend most of its life in such a host-parasite association, or alternatively only a short periods of time, adopting a free-living mode for the major part of its life cycle. During the parasitic phase of their life cycle, parasites depend on their hosts for synthesis of one or more nutrients essential for their own metabolism. Also, it is within their hosts that many parasites reproduce. The host-parasite association is traditionally regarded as obligatory for the parasite and harmful for the host. A species should therefore satisfy three conditions to be considered parasitic. It should (i) utilize its host as a habitat; (ii) nutritionally depend on it; and (iii) cause harm to its host. The parasite, although potentially inducing the death of the host, does not kill its host as a prerequisite for successful development (this distinguishes parasites from parasitoids).

Parasites exhibit a high between-species variability in the degree of harm they cause to their hosts. At one extreme, deaths will result from a parasite infection, but (in contrast to parasitoids) such host deaths will also kill the parasites contained within. At the other extreme lie symbionts that live on or in the host and cause negligible, if any, harm to the host even if present in very large numbers.

The effect of parasites on the hosts varies. The most common effect of parasites is presumably an increase in the mortality rate of the affected hosts. Parasitism can also lead to a reduced birth rate, which can even reach the state of parasitic castration [23, 29]. Interestingly, by decreasing the energy outlay on reproduction due to a fecundity-reducing parasite, infected individuals with lowered reproduction might live longer [15, 5, 33]. Parasites can also induce morphological changes in the hosts or changes in host behavior [34], or bias the host’s sex ratio at birth [21], so as to increase their transmission efficiency.

## 1.3 Role of Mathematical Modeling in Epidemiology

Identification of new infectious diseases, including Lyme disease, the human immunodeficiency virus (HIV) as the etiological agent of the acquired immunodeficiency syndrome (AIDS), hepatitis C, or the severe acute respiratory syndrome (SARS), frequent reappearance of such infections as plague, cholera, and viral hemorrhagic fevers (Ebola, Marburg, etc.), emergence of antibiotic-resistant strains of tuberculosis or gonorrhea, or the apparently never-ending fight against malaria, all maintain a general interest in infectious diseases and their control. This interest is also fed by many recent popular books, movies and television series that have given us exciting accounts of the emergence and detection of new diseases. It is quite obvious that human or animal invasions of new ecosystems, increased international travel, and changes in social and economic patterns will continue to provide opportunities for new and existing infectious diseases.

Scientific experiments are usually the means to obtain information and to test hypotheses. Experiments in epidemiology are often difficult or impossible to design. Even

if we were able to arrange an experiment there are serious ethical questions involved in withholding treatment from a control group. Sometimes data may be collected from reports of epidemics or of endemic disease levels, but they are often incomplete or inaccurate. Hence, parameter estimation and model fitting are very difficult.

In spite of, or perhaps because of this, the ecological and public health challenges that infectious diseases present have been addressed with mathematical models. Mathematical models have become important tools in understanding the fundamental mechanisms that drive the spread of infectious diseases and in suggesting strategies for their control. In particular, understanding the transmission characteristics of infectious diseases can lead to better approaches to reducing the transmission of these diseases. More specifically, mathematical models (Pauline van den Driessche, unpublished material):

1. Help clarify assumptions, variables, and parameters, e.g. pathways involved in parasite spreading or the degree of heterogeneity needed;
2. Provide conceptual results such as thresholds for disease invasion or the plausibility of parasite eradication;
3. Can contribute to the design and analysis of epidemiological surveys, especially by suggesting crucial data that should be collected;
4. Can be used as experimental tools for testing control measures and determining sensitivities to changes in parameter values;
5. Can be used to compare and optimize the costs and efficiency of various detection, prevention and control programs;
6. Can provide, when parasites are used as control agents, qualitative insights into the circumstances under which parasites are capable of regulating their host population, and of doing so in an adequate and stable manner.

Mathematical modeling of infectious diseases has a long history in mathematical biology, starting with the works of Sir Ronald Ross at the beginning of the 20th century and of William Ogilvy Kermack and Anderson Gray McKendrick in the 1920s and 1930s. In recent years, it has even become part of epidemiology policy decision-making in several countries, including the United Kingdom, Canada, and the United States. Modeling studies of diseases such as HIV/AIDS, BSE, foot and mouth disease, measles and SARS have had an impact on public health policy in these countries. Apart from these hot spots, a tremendous variety of mathematical models have been developed, analyzed, and applied to a large number of infectious diseases, such as malaria, rabies and Lyme disease. The majority of epidemiological models focus on human diseases, accounting for aspects such as passive immunity, vaccination, gradual loss of vaccine- and disease-acquired immunity, stages of infection, vertical transmission, disease vectors, age structure, social and sexual mixing groups, and spatial spread. Analogous models have also been developed for animal diseases, an issue of increasing importance as global climate changes and other anthropogenic stressors render natural populations of animals increasingly susceptible to diseases contracted by spillover from domestic animals, as well as render humans increasingly susceptible to diseases originally restricted to wildlife. The breadth of the subject can be appreciated by flipping through the books on epidemiology modeling, such as [9] or [20].

There is always a trade-off between simple (or strategic or generic) models which omit most details and are designed to highlight general qualitative behavior of a host-

parasite interaction, and detailed (or tactic or specific) models usually designed for specific diseases and situations including short-term quantitative predictions. Detailed models are often impossible to solve analytically and hence their usefulness for theoretical purposes is limited, although their practical value may be high. In this material we deal with simple models in order to establish broad principles of mathematical epidemiology. Furthermore, these simple models have an additional value as they are the building blocks of models that include more detailed structure. As a matter of fact, we will never be able to predict the precise course of a disease, or which individuals will be infected. The best that we can hope for are models that provide confidence intervals on disease behavior and determine the risk of infection for various groups of hosts.

#### 1.4 Basic Concepts in Epidemiology

It is useful to distinguish two broad groups of parasites, *microparasites* and *macroparasites*, as differences in their life cycles and their impact on hosts call for development of different epidemiological models. Microparasites, the term used to describe viruses, bacteria, fungi and some (parasitic) protozoa, are characterized by small size (they generally cannot be seen with the naked eye), short generation times, extremely high rates of direct reproduction within the host (usually inside the host cells), and a tendency to induce immunity to reinfection. The duration of infection is typically short relative to the expected lifespan of the host. Microparasites can complete their full life cycle inside a single host.

Macroparasites can be either external (ectoparasitic) or internal (endoparasitic), and include some (parasitic) protozoa, (parasitic) helminths, such as nematodes and tapeworms, and some arthropods, such as ticks and mites. Unlike microparasites, they are large enough to be seen with the naked eye, they tend to have much longer generation times, direct multiplication within the host is either absent or occurs at a low rate, and they elicit immune responses that tend to be of a relatively short duration. Macroparasitic infections therefore tend to be of a persistent nature, with hosts being continually reinfected. Macroparasites typically need more than one host species to complete their life cycle. Last but not least, many host responses to macroparasites generally depend on the number of parasite individuals present in a given host. We will not treat models of macroparasitic infections in this material.

Parasites may complete their life cycle by passing from one host to the next either directly or indirectly via one or more intermediate host species. The *intermediate host* is an organism in which the parasites reproduce asexually or in which the parasitic larvae simply grow. The intermediate hosts are mostly invertebrates, but can also include vertebrates, including humans. The *definitive host*, on the other hand, is an organism in which the parasites mature and sexually reproduce (if they have the ability to do so), and in which the life cycle of the parasite begins as well as ends. The definitive host can be the only host of a parasite. *Direct transmission* is achieved by direct physical contact between hosts (as in, for example, sexually transmitted diseases) or by transmission stages of the parasite which leave a host and are then picked up by another host by inhalation (e.g. influenza), ingestion (such as pinworms) or penetration of the skin (e.g. hookworms). A special case of direct transmission arises when an infection passes from a parent to its unborn offspring (egg, embryo or host chromosomes), as

can happen in AIDS/HIV, syphilis and many viral infections of arthropods; this process has been termed *vertical transmission*, as opposed to the variety of *horizontal transmission* processes just described. *Indirect transmission* occurs when the life cycle of the parasite involves one or more intermediate hosts. It can involve biting by vectors (mosquitoes, flies, ticks, and others) that serve as intermediate hosts, or penetration by free-living transmission stages that are produced by other (e.g. molluscan) intermediate hosts. The parasite can also be ingested when an infected intermediate host is eaten by the predatory or scavenging definitive host.

Infectious diseases can display two different temporal patterns, epidemic and endemic. An *epidemic*, which acts on a short time scale, may be described as a sudden outbreak of a disease that infects a substantial portion of the population in a region before it disappears. Epidemics usually leave many individuals untouched. Epidemics such as the 2002 outbreak of SARS, the Ebola virus and avian flu are just some recent examples. An *endemic* situation is one in which a disease is always present. We observe relatively small fluctuations in monthly cases counts, and only slow increase or decrease over the course of years. Diseases such as malaria, typhus, and cholera are endemic in many parts of the world. One can also think of an intermediate scenario where diseases are constantly present but outbreak frequently. Stochastic effects can sometimes play a role in classifying a disease as epidemic or endemic. Ultimately endemic diseases, the prevalence of which settles to be so small as to give a high probability of their stochastic fade-out, can actually be viewed as recurrent epidemics. Other useful concepts that we occasionally use are summarized in Table 1.

## 1.5 Basic Reproduction Number $R_0$

A quantity of central importance in epidemiology is the *basic reproduction number*, traditionally denoted as  $R_0$ . From time to time, people also call it the basic reproductive rate or ratio, or the basic reproduction ratio. For microparasitic infections (our focus in this material),  $R_0$  is defined as *the mean number of secondary infections produced when one infected individual is introduced into a host population where everyone is susceptible*. Values of  $R_0$  for a number of infectious diseases are given in Table 2.

For most epidemiological models (and in fact all models in this material), an infection invades a fully susceptible host population if  $R_0 > 1$  and dies out if  $R_0 < 1$ . If  $R_0 > 1$  ( $R_0 < 1$ ), then on average each infectious individual produces more (less) than one new infection. Thus, the basic reproduction number  $R_0$  is a threshold quantity that determines when an infection invades a host population and when it does not. Examples of models where infections can invade hosts even for some  $R_0 < 1$  include models involving stochasticity [20] and models in which disease dynamics are seasonally forced [3, and references therein].

For epidemiological models with a single infected compartment,  $R_0$  is simply the product of the contact rate, the mean duration of the infection, and the fraction of infected hosts surviving the latent period of the infection (provided the model works with the latent period). For more complex models that involve several infected compartments (e.g. models with age structure), the simple heuristic definition of  $R_0$  is insufficient. Van den Driessche and Watmough [36] presented a precise definition of  $R_0$  for a

**Table 1.** Definition of some common terms in epidemiology.

Term	Definition
Contact rate	The average number of “adequate” or potentially infectious contacts per host individual per unit time. An adequate or potentially infectious contact is one that is sufficient for transmission of infection from an infective to a susceptible.
Disease prevalence	Fraction of infected individuals in the population. This fraction can vary with different age classes, for example.
Force of infection	The per capita rate at which susceptibles catch the disease or equivalently the probability per unit time that a susceptible individual becomes infected. Note that its inverse is the mean time an individual spends in the susceptible class, which is the mean age at infection provided all individuals are born susceptible. Force of infection can likewise vary with different age classes, for example.
Disease incidence	The rate of occurrence of new cases or equivalently the number of new cases per unit time (= force of infection $\times$ number of susceptibles). Also called the <i>transmission rate</i> . Do not confuse with prevalence – incidence conveys information about the risk of contracting the disease, prevalence indicates how widespread the disease is.
Virulence	A measure of how much a parasite harms its host. From an evolutionary perspective, virulence can be defined as the host’s loss of fitness due to infection (reduced fecundity and/or increased mortality).
Mortality rate	The ratio of deaths due to an infection during a given time interval and in an area, to the population of that area; often expressed per 1000 hosts per year.

**Table 2.** Some estimates of  $R_0$ . After Keeling and Rohani (2008).

Infectious disease	Host	$R_0$
Measles	Humans (UK)	16-18
Pertussis (whooping cough)	Humans (UK)	16-18
Chickenpox (varicella)	Humans (UK)	10-12
Rubella	Humans (UK)	6-7
Smallpox	Humans	3.5-6
FIV	Domestic cats	1.1-1.5
Rabies	Dogs (Kenya)	2.44
Phocine distemper	Seals	2-3
Tuberculosis	Cattle	2.6
Influenza	Humans	3-4
Foot-and-mouth disease	Livestock farms (UK)	3.5-4.5
Mumps	Humans	12
Poliomyelitis (polio)	Humans	5
HIV	Male homosexuals in England and Wales	4
HIV	Female prostitutes in Kenya	11
Malaria	Humans	$\approx 100$

general compartmental disease transmission model based on a system of ordinary differential equations, and a method of its calculation.  $R_0$  is defined as *the mean number of secondary infections produced by a typical infective individual in a population at a disease-free equilibrium (DFE)*. If  $R_0 < 1$  then the DFE is locally asymptotically stable and the disease cannot invade the population. On the other hand, if  $R_0 > 1$  then the DFE is unstable and the disease can invade the host population in the sense that any trajectory starting with a small positive size of infectives moves into the positive quadrant where the disease persists. The method of calculation assumes a heterogeneous population whose individuals can be classified by age, behavior, spatial location and/or stage of the disease and which can be grouped into a finite number of homogeneous compartments; this is sketched in Sect. 5.

The basic reproduction number  $R_0$  can be used to assess the efficiency of any disease control policy and the likelihood that a disease may be eliminated. In general, assuming that an infection invades a fully susceptible host population if  $R_0 > 1$  and dies out if  $R_0 < 1$ , any management action (such as vaccination) that decreases the magnitude of  $R_0$  below 1 effectively prevents the infection from successfully invading and spreading. We discuss some models involving vaccination in Sect. 2.3.

Closely related to  $R_0$  is the concept of *replacement number*  $R$ , defined as *the mean number of secondary infections produced when one infected individual is introduced into a host population*, not necessarily one where all individuals are susceptible. Some authors use the term (*effective*) *reproduction number* instead. Although  $R_0$  is defined only at the moment of disease invasion,  $R$  is defined at all times, and  $R = R_0$  at the moment of invasion. Because after the disease invasion everyone is no longer susceptible,  $R < R_0$  as time goes on.

## 2 Basic Epidemiological Models

### 2.1 Models of Microparasitic Infections

Many epidemiological models of microparasitic infections use the conventional assumption that the host population is held constant, independent of the presence or absence of the infection, by an unspecified mechanism. This assumption stems from a history of medical interest in human diseases, predominantly in developed countries, where population densities usually do remain roughly constant on time scales appropriate to the operation of most diseases. On the other hand, the densities of human populations in developing countries and most animal populations need to be treated as a dynamic variable. As expected, models with a variable host population size are often more difficult to analyze because this additional variable requires an extra equation. We consider models with a constant host population size in this section and models in which the host population size varies with time in Sect. 3.

For *microparasitic infections*, modelers distinguish several classes of hosts according to their status with respect to the disease:

**Passively immune,  $M$**  If a mother has been infected, then some IgG antibodies<sup>1</sup> are transferred across the placenta, so that her newborn infant has temporary passive

---

<sup>1</sup> IgG = immunoglobulin G. Antibodies (also called immunoglobulins) are proteins that are found in blood or other bodily fluids of vertebrates, and are used by the immune system to

immunity to an infection. This class contains only infants with passive immunity. After the maternal antibodies disappear, the infant moves to the susceptible class  $S$ . Infants who do not have any passive immunity, because their mothers were never infected, enter the susceptible class directly.

**Susceptible,  $S$**  Individuals susceptible to infection; they can contract the disease if they are exposed to it.

**Exposed,  $E$**  Latent period of the disease; individuals are infected but not yet infectious and hence not yet able to pass the disease to the others. During this period the parasite reproduces rapidly within the host but its abundance is still too low for active transmission to other susceptible hosts.

**Infectious (or infective),  $I$**  Individuals that are infectious and hence capable of transmitting the infection to any susceptible individual that they come into contact with. Do not commute for *infected* individuals which are those who are either exposed or infectious,  $E + I$ .

**Recovered (or removed),  $R$**  Individuals that were previously infected but now are neither infected nor susceptible; they now have infection-acquired immunity (permanent or temporary).

Not all epidemiological models will include all of these classes, but some will include more (such as a class of chronic carriers of the disease, [20]). In addition, many host populations are structured to various extents, so the models must divide the heterogeneous population into classes within which the individuals have similar characteristics. This division into groups can be based not only on the mode of transmission, contact pattern, latent period, infectious period, genetic susceptibility or resistance, type and amount of control, but also on social, cultural, economic, demographic (age or sex), or geographic (spatial location) factors. We also stress here that the exposed and infectious periods cannot be mistaken with the incubation (or asymptomatic) and symptomatic periods, respectively. This is because one can transmit parasites long before becoming symptomatic, and one can still be symptomatic while no longer infectious. Table 3 lists incubation, latent and infectious periods for a variety of infections.

The choice of which classes to include in a model depends on the characteristics of the modeled disease and the purpose of the model. The passively immune class  $M$  and the exposed class  $E$  are often omitted as not crucial for the host-parasite interaction. Acronyms are often used to name epidemiological models, and these are based on the classes they contain and the flow patterns between these classes. So, for example, in the MSEIR model, passively immune infants first become susceptible, then exposed, then infectious, and finally recover with permanent immunity. An SEIRS model is similar, but there is no passively immune class, and the immunity is only temporary so that recovered individuals regain their susceptibility after the temporary immunity fades away. An SIS model contains no passively immune class, no disease latency, and no immunity whatsoever.

---

identify and neutralize foreign objects, such as bacteria and viruses. Antibodies are produced by a kind of white blood cells called B cells. IgG is the only immunoglobulin that can pass through the human placenta, thereby providing protection to the fetus in its first weeks of life before its own immune system has developed.

**Table 3.** Incubation, latent and infectious periods for a variety of viral and bacterial infections. Table 3.1 of Anderson and May (1991).

Infectious disease	Incubation period (day)	Latent period (day)	Infectious period (day)
Measles	8-13	6-9	6-7
Mumps	12-26	12-18	4-8
Pertussis	6-10	21-23	7-10
Rubella	14-21	7-14	11-12
Diphtheria	2-5	14-21	2-5
Chickenpox	13-17	8-12	10-11
Hepatitis B	30-80	13-17	19-22
Poliomyelitis	7-12	1-3	14-20
Influenza	1-3	1-3	1-3
Smallpox	10-15	8-11	2-3
Scarlet fever	2-3	1-2	14-21

Given a decision on the type and number of classes involved, equations are standardly derived which describe dynamics of densities of hosts within these classes. An ordinary differential equation classically corresponds to each class which describes the rate of change in the size of individuals in the respective class as a result of all processes affecting this rate. For a generic state variable  $X$ , we may formally write:

$$\frac{dX}{dt} = \text{rates of all processes affecting } X$$

## 2.2 SIR Models

SIR models are a traditional point of departure in the exploration of infection dynamics in any textbook on mathematical biology or epidemiology. A SIR model is composed of susceptible ( $S$ ), infectious ( $I$ ), and recovered ( $R$ ) classes of individuals. Assuming hosts are born as susceptible individuals, the specific dynamic equations are as follows:

$$\begin{aligned} \frac{dS}{dt} &= \text{rates of ... births} - \text{natural deaths} - \text{new infections} \\ \frac{dI}{dt} &= \text{rates of ... new infections} - \text{natural deaths} - \text{disease-induced deaths} - \text{recovery} \\ \frac{dR}{dt} &= \text{rates of ... recovery} - \text{natural deaths} \end{aligned} \tag{1}$$

Note that mortality in model (1) is divided into two components, natural deaths experienced by individuals in all classes, and an extra mortality due to the disease. All infectious hosts are commonly assumed to be equally susceptible to disease-induced mortality, no matter how long they are infected (models do exist in which disease-induced mortality of an infected individual is a function of the time since becoming

infected, [7]). The number of susceptible hosts declines due to infection, while that of infectious hosts increases at the same rate.

We shall now set down formal mathematical equations. We start with an *epidemic* SIR model and go on with an *endemic* SIR model. Whereas epidemic models are used to describe rapid disease outbreaks that occur in less than one year, endemic models are used to study the impact of diseases over longer periods during which there is a renewal of susceptible individuals by births or recovery from no or temporary immunity. The two classic SIR models formulated and analyzed below provide a basis for an intuitive understanding of the results of more complex epidemiological models.

**Epidemic SIR Model** Epidemics have often had a large impact on population sizes and historical events. For example, the Black Death, widely thought to have been an outbreak of bubonic plague caused by the bacterium *Yersinia pestis*, caused population decreases of between 25% and 50% and led to social, economic, and religious changes in Europe in the 14th century. A neat account of the major epidemics occurring in the past and how they affected human populations is provided by [8].

One of the questions that first attracted the attention of researchers interested in the spread of infectious diseases was why diseases suddenly appear in a community and then disappear just as suddenly without infecting everyone in the community. It was actually one of the early triumphs of mathematical epidemiology that a simple model was able to predict just this type of behavior. The model proposed in 1927 by Kermack and McKendrick and especially its special case that has become known as the Kermack-McKendrick epidemic model – which we shall now study – forms the core of virtually any epidemiological model developed so far.

Public health officers confronted with a possible epidemic are always interested in how severe the epidemic will be. This question can actually be made more precise in a number of ways. For example, when will the epidemic start? How many individuals will be affected and thus require treatment? What is the maximum number of people needing care at any particular time? How long will the epidemic last? How much good do vaccination or quarantine programs do in reducing severity of the epidemic? These are some of the questions we would like to study with the aid of mathematical models and we indeed can do so.

The Kermack-McKendrick epidemic model is based on relatively simple assumptions on the rates of flow between different classes of hosts (e.g. [7]). First, epidemics are assumed to be sufficiently short for births and natural deaths to not affect their course, so that births = natural deaths = 0 in our conceptual model (1). Second, diseases to be modeled are assumed to be virtually non-lethal, so that disease-induced deaths = 0 in (1)<sup>2</sup>. We are thus left to specify the rate at which new infections occur and the rate at which infectious individuals recover. As a matter of fact, description of disease transmission, determining the rate at which new infections occur, is the core part of any epidemiological model and is of crucial importance in determining disease dynamics.

In the following, we assume the disease transmission rate to equal  $\Phi(N)pSI/N$ , for which we provide an explanation in Box 1;  $\Phi(N)$  is the per-individual contact rate and

---

<sup>2</sup> In Sect. 2.4, we will allow the possibility that some infectives recover while the others die of the disease.

$p$  is the probability that the disease will be transmitted when an infective individual and a susceptible individual meet. Now, assuming that  $\Phi(N)$  is constant,  $\Phi(N) = \phi$ , the disease transmission rate becomes  $\beta SI/N$ , with  $\beta = \phi p$ . This form is commonly referred to as *standard incidence* or *frequency-dependent transmission*. Alternatively, assuming  $\Phi(N)$  to be proportional to host population size,  $\Phi(N) = \phi N$ , the disease transmission rate becomes  $\beta SI$ , with  $\beta = \phi p$ . This form usually termed *mass action incidence* or *density-dependent transmission*, has been the most widely used model of disease transmission, and is also the one used in the Kermack-McKendrick epidemic model. Note that  $\phi$  in both expressions has a different meaning and a different unit. In what follows, we define  $\beta(N) \equiv \Phi(N)p$ .

Assuming further that the recovery rate scales linearly with the population size of infectives,  $\gamma I$  (Box 2), our epidemic SIR model is as follows:

$$\begin{aligned}\frac{dS}{dt} &= -\beta(N)\frac{SI}{N} \\ \frac{dI}{dt} &= \beta(N)\frac{SI}{N} - \gamma I \\ \frac{dR}{dt} &= \gamma I\end{aligned}\tag{2}$$

Here,  $N = S + I + R$  is the total host population size. Since  $dN/dt = 0$ ,  $N$  does not vary with time. The parameter  $\gamma$  is the (per capita) recovery rate; its reciprocal  $1/\gamma$  determines the *mean duration of the infectious period* (Box 2). Upon recovery from the disease, individuals are here assumed to gain permanent immunity against reinfection. As we effectively start with a fully susceptible host population to which an infective is introduced, the initial conditions for model (2) are  $S(0) = N - \varepsilon$ ,  $I(0) = \varepsilon$ , and  $R(0) = 0$  for a small positive  $\varepsilon$ . With model (2) we shall now address some fundamental questions concerning epidemics: ‘When does an epidemic start?’, ‘Once an epidemic has started, how will it proceed?’, and ‘How many susceptibles escape an epidemic?’.

### Box 1 How do we model disease transmission?

The behavior of epidemiological models is considerably affected by the way we model transmission between infectious and susceptible hosts. The key issue here is how to model the number of contacts with other individuals per unit time per individual. Infections spread via different kinds of contact (social, in school, within families, on public transportation, etc.) each of which occurs at a different rate and with a different chance per contact of disease being transmitted. The first (and only) term on the right-hand side of the first equation of model (2) describes only the disease transmission rate resulting from contacts between infectives and susceptibles. How is this term derived? The disease transmission rate as a result of *random* contacts between infectives ( $I$ ) and susceptibles ( $S$ ) can be viewed as a product of four elements:

1. contact rate  $\Phi(N)$
2. proportion of contacts that occur with susceptibles  $S/N$
3. proportion of such contacts that actually result in infection  $p$

#### 4. number of infectives $I$

Together, the disease transmission rate is thus  $\Phi(N)pSI/N$ .

There has been much controversy over which of the two most common models of disease transmission, mass action incidence with  $\Phi(N) = \phi N$  or standard incidence with  $\Phi(N) = \phi$ , is more appropriate (if either) and under what circumstances. Mass action incidence has been suggested as the more appropriate term for e.g. air-borne diseases. The idea is that by doubling the number of people in a bus, a child with a runny nose is likely to infect twice as many people. This does not seem to be the case of sexually transmitted diseases, however. An average woman or man typically has only a few sexual partners (per year), irrespectively of the total population size, and standard incidence here seems much more adequate. Also, for malaria and many other vector-borne infections, vectors tend to make a fixed number of bites per day, independent of how many hosts are available for their feeding; simple vector-host models are presented in Sect. 4.3.

Mena-Lorca and Hethcote [27] tested the idea that for human diseases the contact rate is only very weakly dependent on the absolute population size. Modeling the disease transmission rate as  $\beta N^\nu SI/N$  and using data for five human diseases in communities with population sizes ranging from 1,000 to 400,000, they estimated  $\nu$  to lie between 0.03 and 0.07. This strongly suggests that standard incidence corresponding to  $\nu = 0$  is more appropriate to use for human diseases than mass action incidence corresponding to  $\nu = 1$ . This result is consistent with the idea that people are infected through their daily encounters and the patterns of daily encounters are largely independent of community size. Standard incidence is also a better formulation than mass action incidence for animal populations in a herd, because disease transmission primarily occurs locally from nearby animals.

A number of authors have proposed a saturation relationship between the contact rate and host size – at low densities, contacts are directly proportional to host size, but a maximum rate of contacts and actual density-independence is reached at high host densities; see [13] and [14]. Figure 1 is just an example of such a situation, with the contact rate  $\Phi(N) = bN/(1 + cN)$ .

In fact, the random-mixing assumption underlying the disease transmission models specified above – that a proportion  $S/N$  of all contacts made by an infectious host are with susceptibles – is merely a simplification. The proportion of all contacts taking place between susceptible and infectious hosts may differ from this assumption for a number of reasons, including a spatial patchiness of the infection or a physiological heterogeneity in the susceptibility of hosts to contracting the disease. Actually, there is a desperate need for more relevant experimental and observational data on transmission dynamics because models of disease transmission generally outnumber sets of actual data. A variety of other functions used to model disease transmission were summarized

by McCallum et al. [26]. Thorough discussions surrounding the issue of choice of an adequate model of transmission rate can also be found in [22], [4], and [16].

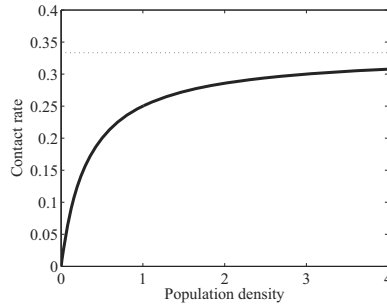


**Fig. 1.** A saturation relationship between the contact rate and host size;  $\Phi(N) = bN/(1 + cN)$ , with  $b = 1$  and  $c = 3$ .

### Box 2 What does a linear rate of recovery mean?

Box 2 follows [8]. Many mathematical models involve rates at which subjects leave a model class. Often, these rates are modeled as linear functions of the abundance of the class which remains behind. For example, model (2) assumes that infectives leave the  $I$  class at rate  $\gamma I$ . What does this mean precisely from the perspective of an infectious individual? To address this question, consider a “cohort” of hosts who were all infected at the same time and let  $I(\tau)$  denote the number of these who are still infective  $\tau$  time units after having been infected. If these leave the infectious class at rate  $\gamma$ , then

$$dI/d\tau = -\gamma I$$

the solution of which is

$$I(\tau) = I(0)e^{-\gamma\tau} \quad (3)$$

Thus, the fraction of infectives remaining infective  $\tau$  time units after having been infected is  $e^{-\gamma\tau}$ . Changing now the perspective from cohort to individual infectives, (3) means that the probability that an individual recovers before time  $\tau$  after contracting the disease is  $P(\text{recovery time} < \tau) = 1 - e^{-\gamma\tau}$ . This implies that the length of the individuals’ infectious period is exponentially distributed, with the mean

$$\int_0^{\infty} \gamma\tau e^{-\gamma\tau} d\tau = 1/\gamma$$

So, the linear recovery rate  $\gamma I$  means that the mean time an individual is infectious is  $1/\gamma$ , and that the actual times of infection are exponentially distributed around this mean. Although unrealistically simple, mathematically it is quite “elegant”. Alternative models can be formulated, with more realistic distributions of the recovery time (e.g. with a recovery time more or less the same for each infectious individual), but these require a consideration of time delays or a subdivision of the time of infection into smaller periods and thus make the model mathematically much more complex [20]. Actually, it turns out that many more realistic models exhibit qualitative behavior very similar to the model with linear recovery rate [20].

When does an epidemic start? Let us begin with calculating the basic reproduction number. We can calculate  $R_0$  as the rate at which new cases are produced by an infectious individual when the entire population is susceptible,  $\beta(N)S(0)/N = \beta(N) \times 1 = \beta(N)$ , multiplied by the mean infectious period,  $1/\gamma$ ; hence

$$R_0 = \beta(N)/\gamma \quad (4)$$

Now, the infection will spread if initially  $dI/dt > 0$  and die out if initially  $dI/dt < 0$ . The second equation of model (5) implies that the infection will spread provided that

$$\left. \frac{dI}{dt} \right|_{t=0} = I(0) \left( \beta(N) \frac{S(0)}{N} - \gamma \right) > 0$$

which happens in a fully susceptible population if  $\beta(N)/\gamma > 1$ , and in a partially susceptible population if  $(\beta(N)/\gamma)(S(0)/N) > 1$ . Analogously, it will die out if  $\beta(N)/\gamma < 1$  or  $(\beta(N)/\gamma)(S(0)/N) < 1$ , respectively. This result is referred to as the threshold phenomenon since initially the proportion of susceptibles in the population  $S(0)/N$  must exceed the threshold  $\gamma/\beta(N)$  for an infection to invade. Putting  $R_0$  and the threshold behavior together, an epidemic will start in a fully susceptible population as soon as  $R_0 > 1$  and dies out if  $R_0 < 1$ , as discussed in Sect. 1.5. This also implies that a disease can invade a partially susceptible host population if and only if the fraction of susceptibles is greater than  $1/R_0$ ; hence, to eliminate the disease we need to reduce the fraction of susceptibles below  $1/R_0$ .

Quite an important distinction exists in frequency-dependent transmission, with  $\beta(N) = \beta$ , and density-dependent transmission, with  $\beta(N) = \beta N$ . For the former, we have  $R_0 = \beta/\gamma$  so that whether an epidemic starts or not depends just on the parasite and host properties. On the other hand, for density-dependent transmission we have  $R_0 = \beta N/\gamma$ . Thus, it is also the host population size which drives the infection fate. For any fixed values of  $\beta$  and  $\gamma$ , small enough populations cannot be invaded; the host population size must exceed the threshold values  $N > N_T \equiv \gamma/\beta$  for an epidemic to start.

Once an epidemic has started, how will it proceed? To address this question, we divide all three equations of model (2) by the (constant) total host population size  $N$ ,

yielding the rescaled model

$$\begin{aligned}\frac{ds}{dt} &= -\beta(N)si \\ \frac{di}{dt} &= \beta(N)si - \gamma i \\ \frac{dr}{dt} &= \gamma i\end{aligned}\tag{5}$$

where  $s = S/N$ ,  $i = I/N$ , and  $r = R/N$  are now *proportions* of hosts in the respective classes. Since  $r = 1 - s - i$ , knowing  $s$  and  $i$  allows us to calculate  $r$  and we can thus “ignore” the last equation of model (5). The initial conditions now become  $s(0) = 1 - \varepsilon \approx 1$ ,  $i(0) = \varepsilon \approx 0$ , and  $r(0) = 0$  for a small  $\varepsilon > 0$ . Since the triangle  $X$  in the  $si$  phase plane given by

$$X = \{(s, i) \mid s \geq 0, i \geq 0, s + i \leq 1\}$$

is positively invariant and thus unique solutions exist in  $X$  for all times  $t \geq 0$ , model (5) is mathematically and epidemiologically well-posed.

Obviously, as  $ds/dt < 0$  the proportion of susceptibles will decrease over time, and as  $dr/dt > 0$  the proportion of recovered individuals will increase over time. In addition, as the equation for  $r$  implies that  $i(t) \rightarrow 0$  as  $t \rightarrow \infty$  ( $dr/dt = 0$  has the only solution  $i = 0$ ), then if  $R_0 > 1$  the proportion of infectives will initially increase and eventually decrease to zero. So the disease spreads, reaches a maximum prevalence and then recedes and vanishes, the behavior observed in countless real epidemics.

The epidemic loses its strength and eventually dies out because the replacement number  $R = \beta(N)s(t)/\gamma$  decreases as  $s(t)$  decreases and eventually falls below 1 or equivalently  $s(t) < 1/R_0$  (otherwise  $i(t)$  would never go to zero). At the moment  $R = 1$  or equivalently  $s = 1/R_0 = \gamma/\beta(N)$ , the disease prevalence reaches its maximum. By the chain rule,  $di/dt = (di/ds)(ds/dt)$ , so that

$$\frac{di}{ds} = \frac{di}{dt} \bigg/ \frac{ds}{dt} = -1 + \frac{\gamma}{\beta(N)s}$$

and hence

$$i = -s + \frac{\gamma}{\beta(N)} \ln s + c\tag{6}$$

where the constant of integration  $c$  is determined by the initial values  $s(0)$  and  $i(0)$ :

$$c = i(0) + s(0) - \frac{\gamma}{\beta(N)} \ln s(0)$$

Inserting  $s = \gamma/\beta(N)$  into (6), the peak value  $i_{\max}$  of infectives is

$$i_{\max} = -\frac{\gamma}{\beta(N)} + \frac{\gamma}{\beta(N)} \ln \frac{\gamma}{\beta(N)} + i(0) + s(0) - \frac{\gamma}{\beta(N)} \ln s(0)$$

For a fully susceptible host population, this further simplifies to

$$i_{\max} = 1 - \frac{\gamma}{\beta(N)} + \frac{\gamma}{\beta(N)} \ln \frac{\gamma}{\beta(N)}$$

Figure 2A shows a typical solution of model (2), demonstrating the features just derived.

The speed at which an epidemic progresses depends on the characteristics of the disease. In particular, higher values of  $R_0$  lead to a shorter and more severe epidemic (Fig. 2C). Note that Fig. 2C plots disease incidence, not disease prevalence; for model (2), disease incidence equals  $\beta(N)SI/N$ . An example of a plague epidemic in Bombay lasting from December 17, 1905 to July 21, 1906 is given in Fig. 2D (after [20]).

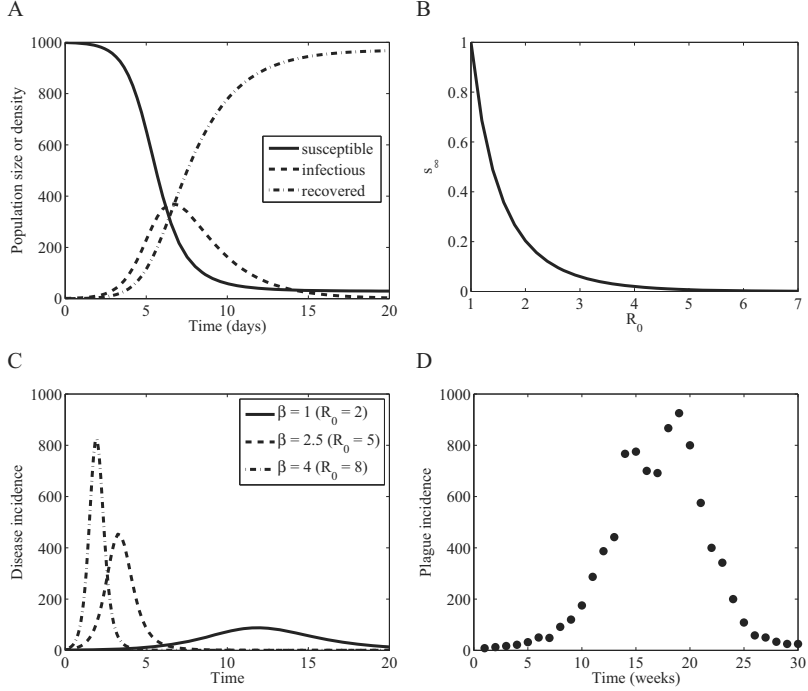


**Fig. 2.** Epidemic SIR model (2) with frequency-dependent disease transmission,  $\beta(N) = \beta$ . A. Temporal disease dynamics. Parameter values correspond to the best fit of the model to the influenza epidemic data in an English school in 1978 (Keeling and Rohani 2008):  $\beta = 1.66$  per day and  $1/\gamma = 2.2$  days, and hence  $R_0 = 3.65$ ;  $N = 1000$ . B. The fraction of susceptibles that escape the epidemic  $s_\infty$  as a function of the basic reproduction number  $R_0$ . C. Temporal progress of disease incidence for different values of  $R_0$ . D. Example of a plague epidemic in Bombay from December 17, 1905 to July 21, 1906 (Keeling and Rohani 2008).

Finally, how many susceptibles escape an epidemic? In other words, what will be the final fraction of susceptibles as  $t \rightarrow \infty$ ? By the chain rule,  $ds/dt = (ds/dr)(dr/dt)$ , so that

$$\frac{ds}{dr} = \frac{ds}{dt} \bigg/ \frac{dr}{dt} = -\frac{\beta(N)}{\gamma} s = -R_0 s$$

Upon integrating with respect to  $r$  and assuming  $r(0) = 0$ ,

$$s(t) = s(0) \exp(-r(t)R_0)$$

This implies that  $s$  always remains positive as  $\exp(-r(t)R_0)$  is always positive. The constraint  $r(t) \leq 1$  implies  $s(t) \geq s(0) \exp(-R_0)$  so that there will always be some susceptibles in the population that escape an epidemic. As a result, the progress of the epidemic will eventually break down because new infections cannot keep pace with recoveries, not because of a complete lack of susceptibles. Given that  $s + i + r = 1$  and that the epidemic ends with  $i = 0$ , we can write

$$s_\infty = s(0) \exp(-(1 - s_\infty)R_0) \quad (7)$$

where  $s_\infty$  is the proportion of host population that remains susceptible after the epidemic ends;  $s(t) \rightarrow s_\infty$  as  $t \rightarrow \infty$ . For any  $R_0$ , equation (7) has a unique solution which cannot, however, be calculated analytically. By solving it numerically, we find that  $s_\infty$  rapidly approaches 0 as  $R_0$  increases (Fig. 2B). Therefore, for sufficiently large  $R_0$  essentially everyone is likely to contract the disease. An application of equation (7) is given in Box 3.

### Box 3 Using equation (7) to estimate $R_0$ for an epidemic.

Consider an isolated village experiencing an outbreak of influenza in which 812 of its 1100 residents contract the infection. The question is to estimate  $R_0$  assuming that the outbreak started with a single case contracted from outside the village, with all others susceptible at the start of the outbreak. Solving equation (7) for  $R_0$ , we have

$$R_0 = -\frac{\ln(s_\infty/s(0))}{1 - s_\infty}$$

From what we know,  $r_\infty = 812/1100$  and hence  $s_\infty = 1 - r_\infty = 288/1100$ , and  $s(0) = 1$ . As a result,  $R_0 \approx 1.8$ .

In summary, the hallmark of a typical epidemic is that the number of infectious individuals first increases from an initial  $I(0)$  near zero (as long as  $R_0 > 1$ ), reaches a peak, and finally decreases to zero. The number of susceptibles  $S$  monotonously decreases with time, yet the final value  $S_\infty$  remains positive; there are always host individuals that escape the epidemic. Finally, the number of recovered individuals  $R$  monotonically increases with time.

**Endemic SIR Model** Due to permanent immunity to reinfection, epidemics race through the host population as waves of infection. However, new susceptible individuals are born behind these waves. There are diseases which are endemic in many parts of the world. To model an endemic disease we must envision a longer time scale and thus include births and deaths. The simplest way to incorporate births and deaths into a model of infectious disease dynamics is to assume the same number of births and deaths per

unit time so that the total population size still remains constant. This is, of course, possible only if there are no deaths due to the disease. The second SIR model we shall formulate and analyze is just such an *endemic* model:

$$\begin{aligned}\frac{dS}{dt} &= \mu N - \beta(N) \frac{SI}{N} - \mu S \\ \frac{dI}{dt} &= \beta(N) \frac{SI}{N} - \gamma I - \mu I \\ \frac{dR}{dt} &= \gamma I - \mu R\end{aligned}\tag{8}$$

This model assumes that all hosts produce offspring at the same rate (equal to the natural death rate)  $\mu$ ;  $1/\mu$  can thus be viewed as the natural host life expectancy. Both birth and (natural) death rates are assumed to be density-independent; there is no density dependence in either due to, for example, competition for resources. The model is thus most appropriate for the study of human infections in developed countries. The approach would be different if the host population exhibited its own dynamics as is often the case with human populations in developing countries or wildlife populations; Sect. 3 will deal with such situations.

Threshold behavior for this model can be deduced in the same way as for the epidemic one – the infection dies out in a partially susceptible population if  $S(0)/N < (\gamma + \mu)/\beta(N)$  and in a fully susceptible population if the basic reproduction number  $R_0 = \beta(N)/(\gamma + \mu) < 1$ ; the infection invades if the opposite inequalities hold. Note that this  $R_0$  is lower than that for the epidemic SIR model (2). This is because the death rate reduces the mean length of the period in which an individual is infectious. Rescaling model (8) by dividing it by the (constant) total host population size  $N$  yields

$$\begin{aligned}\frac{ds}{dt} &= \mu - \beta(N)si - \mu s \\ \frac{di}{dt} &= \beta(N)si - \gamma i - \mu i \\ \frac{dr}{dt} &= \gamma i - \mu r\end{aligned}\tag{9}$$

Since the inclusion of host demography may permit a disease to persist in the host population in the long run, we seek system equilibria. Obviously, one such equilibrium is  $(s^*, i^*, r^*) = (1, 0, 0)$ . This is the *disease-free equilibrium* (DFE) as in this case the parasite is not present and all hosts are susceptible. There is one more equilibrium, the *endemic equilibrium* at which there is a positive proportion of infectives,  $i^* > 0$ . The second equation of model (8) implies

$$s^* = \frac{\gamma + \mu}{\beta(N)} = \frac{1}{R_0}$$

Inserting this formula to the first equation then gives

$$i^* = \frac{\mu}{\gamma} \left( 1 - \frac{1}{R_0} \right) = \frac{\mu}{\beta(N)} (R_0 - 1)$$

This implies that the endemic equilibrium is feasible (i.e.  $i^* > 0$ ) if and only if  $R_0 > 1$ , which makes perfect sense as we already know that the disease can invade and potentially persist in the host population if and only if  $R_0 > 1$ . The equilibrium proportion of recovered individuals can eventually be calculated as  $r^* = 1 - s^* - i^*$ . At the endemic equilibrium, the replacement number equals 1, since if it were greater than or less than 1, the proportion of infectives  $i$  would be increasing or decreasing, respectively. Local stability analysis shows that if  $R_0 > 1$  (disease invades) the DFE is unstable and the endemic equilibrium is locally asymptotically stable; conversely, if  $R_0 < 1$  (the disease dies out), the DFE is locally asymptotically stable. So, if  $R_0 > 1$ , supplementing the pool of susceptibles by newborns ensures disease persistence in the long run.

Local stability analysis also shows that system trajectories might approach the endemic equilibrium in an oscillatory manner, that is, they fluctuate around the equilibrium and the amplitude of these fluctuations declines over time (Fig. 3). Intuitively, this could be seen as follows. If  $R_0 > 1$ ,  $i(0)$  is small, and  $s(0)$  is large with  $s(0) > 1/R_0$ , then  $s$  decreases and  $i$  increases up to a peak and then decreases, just as it would for an epidemic. However, after the proportion of infectives has decreased to a low level, the slow processes of the deaths of recovered individuals and the births of new susceptibles gradually increase the proportion of susceptibles until  $s$  is large enough that another smaller epidemic occurs. This process of alternating rapid epidemics and slow regeneration of susceptibles continues as the trajectories approach the endemic equilibrium. Mathematically, the damped fluctuations occur if eigenvalues of the system composed of the first two equations of model (9) are complex numbers with negative real parts. The eigenvalues are

$$\lambda_{1,2} = -\frac{\mu R_0}{2} \pm \sqrt{\frac{\mu^2 R_0^2}{4} - \mu(\gamma + \mu)(R_0 - 1)}$$

and these become complex if and only if

$$\mu R_0^2 < 4(\gamma + \mu)(R_0 - 1)$$

This inequality is satisfied for parameter values used to plot Fig. 3A. For  $R_0 = 1.05$ , for example, the eigenvalues are complex provided that  $\gamma/\mu > 4.5125$ . This certainly holds if  $\mu$  is very small, such as for human populations in developed countries where  $1/\mu$  can be about 70 years, but at least in theory we might have cases where this is not true and the eigenvalues are real, such as for  $\mu = \gamma = 1$ .

**Summary** Upon successful invasion, an epidemic followed by disease extinction occurred in the epidemic model (2) and an approach to endemic equilibrium was observed in the endemic model (8). In both models, the total host population size was assumed to be constant. We also emphasized an important distinction between frequency-dependent transmission (or standard incidence,  $\beta(N) = \beta$ ) and density-dependent transmission (or mass action incidence,  $\beta(N) = \beta N$ ). Whereas for the former  $R_0$  depends only on model parameters, for the latter it is also the host population size that matters: small host populations cannot be invaded.

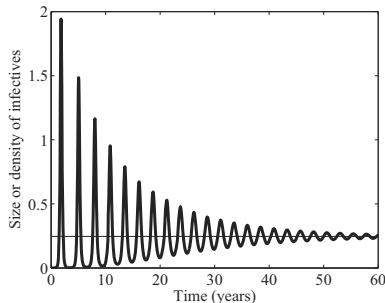


**Fig. 3.** Temporal dynamics of endemic SIR model (8) with frequency-dependent disease transmission,  $\beta(N) = \beta$ , when the infection approaches the endemic equilibrium. Model parameters:  $1/\mu = 70$  years,  $\beta = 520$  per year,  $1/\gamma = 7$  days,  $N = 1000$ ,  $S(0) = 0.1N - 2.5 \times 10^{-4}$ ,  $I(0) = 2.5 \times 10^{-4}$ ,  $R(0) = N - S(0) - I(0)$ .

We also saw that for a disease to be endemic (i.e. to persist indefinitely) there must be a supply of fresh susceptibles, through births in our case. Endemicity also occurs once the susceptible class is steadily supplied by “new” individuals recovering only to be immediately susceptible again (no immunity), or returning back to the susceptible class thanks to merely temporary immunity (e.g. [20]). Generally, diseases transmitted by viral agents, such as influenza, measles, rubella, and chicken pox, confer immunity against reinfection, while diseases transmitted by bacteria, such as tuberculosis, meningitis, and gonorrhea, confer no immunity against reinfection [8]. An SIRS model as an extension of the endemic SIR model (8) can be as follows:

$$\begin{aligned}
 \frac{dS}{dt} &= \mu N - \beta(N) \frac{SI}{N} - \mu S + \sigma R \\
 \frac{dI}{dt} &= \beta(N) \frac{SI}{N} - \gamma I - \mu I \\
 \frac{dR}{dt} &= \gamma I - \mu R - \sigma R
 \end{aligned}
 \tag{10}$$

where  $\sigma$  is the rate at which immunity is lost and recovered individuals move back to the susceptible class;  $1/\sigma$  can thus be viewed as the mean duration of immunity against reinfection.

The simple SIR models presented here have obvious limitations. They assume that the host population is uniform and homogeneously mixing (in reality, children usually have more adequate contacts per day than adults, different geographic and socio-economic groups have different contact rates, etc.), that there is no latent period of the disease, that there are no dynamics of the host population when the disease is absent, etc. Still, despite these limitations, these models have contributed much to our understanding of the course of real epidemics and the way endemic equilibria can be attained; they can also be useful in obtaining some parameter estimates and between-infections comparisons [19].

### 2.3 Vaccination

The ultimate goal of any vaccination program is to vaccinate enough people to achieve a replacement number less than 1, so that an infection fades away and herd immunity is achieved [19]. *Herd immunity* occurs for a disease if enough people have disease-acquired or vaccination-acquired immunity, so that the introduction of one infective into the population does not cause an invasion of the disease.

Successful vaccination moves individuals from the susceptible class straight into the recovered class so that they can no longer catch or spread the infection. If it is newborns who are vaccinated and  $p$  denotes the proportion of newborns vaccinated, we might compose the following model as an extension of the endemic SIR model (8):

$$\begin{aligned}\frac{dS}{dt} &= \mu N(1-p) - \beta \frac{SI}{N} - \mu S \\ \frac{dI}{dt} &= \beta \frac{SI}{N} - \gamma I - \mu I \\ \frac{dR}{dt} &= bNp + \gamma I - \mu R\end{aligned}\tag{11}$$

Analysis of this model shows that the disease cannot invade the host population if

$$p > p_c = 1 - (\gamma + \mu) / \beta = 1 - 1/R_0\tag{12}$$

This follows from two facts: first, in the absence of infection, the equilibrium value of susceptibles is (setting the right-hand side of the first equation of (11) to zero, inserting  $I = 0$ , and solving it for  $S$ )  $S = (1-p)N$ ; second,  $R_0 = \beta(S/N)/(\gamma + \mu)$  when evaluated at this equilibrium, so  $R_0 = \beta(1-p)/(\gamma + \mu)$ . Finally, solving the inequality  $R_0 < 1$  for  $p$  gives the resulting expression (12).

Table 4 lists some specific examples of  $p_c$ . Smallpox is actually the only infectious disease for which successful vaccination has been achieved worldwide and smallpox has been eliminated (the last known case was in Somalia in 1977). For measles, on the other hand, the herd immunity against measles has not been achieved and probably will never be, as the minimum required proportion of newborns vaccinated is extremely high (and the vaccine for measles is not always effective).

**Table 4.** Minimum proportion of newborns vaccinated for smallpox and measles, based on  $R_0$ . After Keeling and Rohani (2008).

Disease	$R_0$	$p_c$ [%]
Smallpox	3-5	66-80
Measles	16-18	93-95
Chickenpox	8-10	87.5-90

Even if  $p < p_c$ , for which the disease persists, the equilibrium size of infectives

$$I^* = \frac{\mu N(1-p)}{\gamma + \mu} - \frac{\mu N}{\beta}$$

shows that vaccination reduces the disease prevalence.

Alternatively, if it is susceptibles who are vaccinated, and  $\theta$  is the rate at which they are vaccinated (vaccination of  $I$  and  $R$  individuals is assumed to have no effect):

$$\begin{aligned}\frac{dS}{dt} &= \mu N - \beta \frac{SI}{N} - \mu S - \theta S \\ \frac{dI}{dt} &= \beta \frac{SI}{N} - \gamma I - \mu I \\ \frac{dR}{dt} &= \theta S + \gamma I - \mu R\end{aligned}\tag{13}$$

In this case, the same method as above for the vaccination of newborns can be applied to see that the disease cannot invade the host population if

$$\theta > \theta_c = \mu(\beta/(\gamma + \mu) - 1) = \mu(R_0 - 1)\tag{14}$$

Again, there is a minimum rate at which susceptibles need be vaccinated for the disease to be eliminated.

In reality, vaccination is only partly effective, decreasing the rate of infection and also decreasing infectivity of a vaccinated person which has become infected. More complex models are needed to come up with sound quantitative recommendations on applicable vaccination strategies.

## 2.4 Epidemic SIR Model with Disease-Induced Mortality

This section follows [8]. We differentiate between members of the population who die due to the disease and those that recover and become permanently immune. Disease-induced deaths require adding an equation for the total host population size, as this quantity is no longer a constant. Let us assume that infectious individuals leave the  $I$  class at rate  $\alpha I$  of which a proportion  $f$  recovers and the remaining proportion  $1 - f$  dies due to the disease. We obtain the following model

$$\begin{aligned}\frac{dS}{dt} &= -\Phi(N)p\frac{SI}{N} \\ \frac{dI}{dt} &= \Phi(N)p\frac{SI}{N} - \alpha I \\ \frac{dR}{dt} &= f\alpha I \\ \frac{dN}{dt} &= -(1-f)\alpha I\end{aligned}\tag{15}$$

Note that  $R$  is determined once  $S$ ,  $I$ , and  $N$  are known, so we may “ignore” it. Once  $f = 1$  there are no disease-induced deaths and the model (15) reduces to the epidemic SIR model (2).

Before we start with the analysis, we make some assumptions regarding the contact rate  $\Phi(N)$ . We require that it be a positive ( $\Phi(N) > 0$ ), increasing ( $\Phi'(N) > 0$ ), and saturating function of  $N$  ( $(\Phi(N)/N)' \leq 0$  or equivalently  $\Phi'(N) \leq \Phi(N)/N$ ); the

function plotted in Fig. 1 is an example. Given this, we would like to demonstrate that the model (15) has the same qualitative behavior as the model (2), namely that it demonstrates a threshold behavior and that some hosts escape the disease after the epidemic passes. According to [8], *these two properties are the central features of all epidemic models.*

Assume that initially all hosts are susceptible and that the total host population size is  $K$ . The basic reproduction number is then given by

$$R_0 = \frac{\Phi(K)p}{\alpha}$$

This is because a single infective introduced to a fully susceptible population makes  $\Phi(K)$  contacts in unit time of which all are with susceptibles, each contact results in a new infection with probability  $p$ , and the mean length of the infectious period is  $1/\alpha$ . Since  $I'(0) = \alpha(R_0 - 1)I(0)$ , then if  $R_0 > 1$ , an epidemic starts, and if  $R_0 < 1$ , the disease dies out.

From (15) we obtain

$$S' + I' = -\alpha I$$

$$N' = -(1-f)\alpha I$$

Integration of these equations from 0 to  $t$  gives

$$S(t) + I(t) - S(0) - I(0) = -\alpha \int_0^t I(s) ds$$

$$N(t) - N(0) = -(1-f)\alpha \int_0^t I(s) ds$$

When we combine these two equations, and note that  $N(0) = S(0) + I(0) = K$ , we obtain

$$K - N(t) = (1-f)[K - S(t) - I(t)]$$

If we let  $t \rightarrow \infty$ ,  $S(t)$  and  $N(t)$  decrease monotonically to limits  $S_\infty$  and  $N_\infty$ , respectively, and  $I(t) \rightarrow 0$ . This implies

$$K - N_\infty = (1-f)(K - S_\infty)$$

In this equation,  $K - N_\infty$  is the change in population size due to disease deaths over the course of the epidemic, while  $K - S_\infty$  is the change in the size of susceptibles due to infections over the course of the epidemic.

To show that  $S_\infty > 0$ , let us assume that  $B = \lim_{N \rightarrow 0} \Phi(N)/N$  is finite, thus ruling out standard incidence. If we let  $t \rightarrow \infty$  in the first of the above integral equations, we obtain

$$\alpha \int_0^\infty I(s) ds = K - S_\infty$$

The first equation of (15) may be written as

$$-\frac{S'}{S} = \frac{\Phi(N)}{N} p I$$

Since  $\Phi(N)/N \leq B$ , integration from 0 to  $\infty$  gives

$$\ln \frac{S(0)}{S_\infty} = \int_0^\infty \frac{\Phi(N(t))}{N(t)} p I(t) dt \leq B p \int_0^\infty I(t) dt = \frac{B p (K - S_\infty)}{\alpha}$$

Since the right-hand side of this inequality is finite, the left-hand side is also finite and this implies that  $S_\infty > 0$ . In addition, if we use the same integration together with the inequality  $\Phi(N)/N \geq \Phi(K)/K$ , we obtain

$$\ln \frac{S(0)}{S_\infty} = \int_0^\infty \frac{\Phi(N(t))}{N(t)} p I(t) dt \geq \frac{\Phi(K)}{K} p \int_0^\infty I(t) dt = R_0 \left( 1 - \frac{S_\infty}{K} \right)$$

If  $\Phi(N)/N \rightarrow \infty$  as  $N \rightarrow 0$ , such as for standard incidence, a different approach must be used to analyze the limiting behavior. According to [8], it is possible to show that  $S_\infty = 0$  only if  $f = 0$ , that is, only if all infectives die due to the disease. As we have already emphasized above, the assumption that  $\Phi(N)/N$  is unbounded as  $N \rightarrow 0$  is, however, biologically unreasonable. In particular, standard incidence is not realistic for small populations. A more realistic assumption would be that the number of contacts per individual in unit time is linear for small population densities and saturates for large population densities – a saturation transmission term discussed in Box 1.

## 2.5 Latent Period of the Disease

Many diseases have a latent period during which hosts are infected but not yet infectious, which is comparable in length with the infectious period; see Table 3. This calls for accounting for the latent period in epidemiological models, by introducing the exposed class  $E$  of individuals. Extending the endemic SIR model (8), we may have the following (endemic) SEIR model:

$$\begin{aligned} \frac{dS}{dt} &= \mu N - \beta(N) \frac{SI}{N} - \mu S \\ \frac{dE}{dt} &= \beta(N) \frac{SI}{N} - \sigma E - \mu E \\ \frac{dI}{dt} &= \sigma E - \gamma I - \mu I \\ \frac{dR}{dt} &= \gamma I - \mu R \end{aligned} \tag{16}$$

In this model,  $\sigma$  is the rate at which individuals leave the exposed class and enter the infectious one;  $1/\sigma$  can thus be viewed as the mean latent period. In the limiting case when  $\sigma \rightarrow \infty$ , the latent period is negligible and the SEIR model (16) reduces to the endemic SIR model (8).

The basic reproduction number  $R_0$  is here the product of the contact rate, the probability of surviving the latent period  $\sigma/(\mu + \sigma)$ , and the mean length of the infectious period:

$$R_0 = \frac{\beta(N)}{\gamma + \mu} \times \frac{\sigma}{\mu + \sigma}$$

Note that  $R_0$  is now slightly different than what we saw above for SIR models, due to the death of some individuals when in the exposed class – an individual has to survive the latent period in order to produce new infectives. However, we have already noted above that for human populations in developed countries a typical value of  $\mu$  can be about  $1/70 \text{ year}^{-1}$ , that is, the mean life expectancy  $1/\mu$  is about 70 years. With this value,  $\sigma/(\mu + \sigma) \sim 1$  (the latent period is negligible relative to the mean life expectancy) and we get close to the basic reproduction number corresponding to the endemic SIR model,  $R_0 = \beta(N)/(\gamma + \mu)$ .

As with the previous models, the model (16) (more precisely its rescaled version with class densities divided by  $N$ ) also possesses both the DFE  $(1, 0, 0, 0)$  and the endemic equilibrium  $(s^*, e^*, i^*, r^*)$  with

$$\begin{aligned} s^* &= \frac{(\gamma + \mu)(\mu + \sigma)}{\beta(N)\sigma} = \frac{1}{R_0} \\ e^* &= \frac{\mu(\gamma + \mu)}{\beta(N)\sigma}(R_0 - 1) \\ i^* &= \frac{\mu}{\beta(N)}(R_0 - 1) \end{aligned}$$

and  $r^* = 1 - s^* - e^* - i^*$ , which is feasible provided that  $R_0 > 1$ . Local stability analysis shows that the endemic equilibrium is asymptotically stable (and the DFE unstable) for  $R_0 > 1$ , and the DFE is locally asymptotically stable if  $R_0 < 1$ . Much like in the endemic SIR model (8), here also perturbations die out in an oscillatory manner (Fig. 4A).

Panels B and C of Fig. 4 clearly show that the latent period is of importance only if the mean life expectancy is comparable in size to the mean length of the latent period. For human infections, we thus usually need not regard the exposed class  $E$  as an important aspect of epidemiological models. This is not the case, however, of infections in which the latent period plays a considerable role (Fig. 4C and D). The addition of a latent period is essentially akin to introducing a time delay – individuals need to pass the exposed class before becoming infectious and transmitting the disease to susceptibles. In epidemic SEIR models, we thus expect and indeed observe that longer latent periods cause the epidemic to begin at a slower rate, reach a lower peak prevalence, but last much longer (Fig. 4D). Still, the behavior of SEIR models is qualitatively similar to those of the analogous SIR models.

For some diseases, rather than a latent period, there is an asymptomatic period  $E$  during which individuals have some infectivity. If the infectivity during this period is reduced by a factor  $\varepsilon$  relative to the infectious period, then the corresponding model can be formulated as follows [8]:

$$\begin{aligned} \frac{dS}{dt} &= \mu N - \beta(N) \frac{S(I + \varepsilon E)}{N} - \mu S \\ \frac{dE}{dt} &= \beta(N) \frac{S(I + \varepsilon E)}{N} - \sigma E - \mu E \\ \frac{dI}{dt} &= \sigma E - \gamma I - \mu I \\ \frac{dR}{dt} &= \gamma I - \mu R \end{aligned} \tag{17}$$

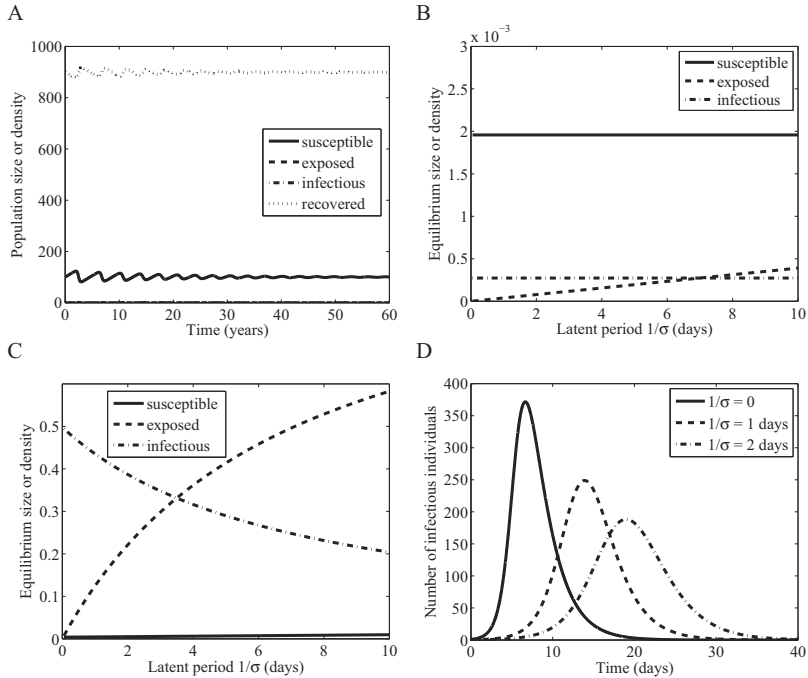


**Fig. 4.** SEIR model (16) with frequency-dependent disease transmission. A. Temporal disease dynamics when the disease approaches the endemic equilibrium. Parameter values:  $1/\mu = 70$  years,  $\beta = 520$  per year,  $1/\gamma = 7$  days,  $1/\sigma = 5$  days,  $N = 1000$ ,  $S(0) = 0.1N - 2.5 \times 10^{-4}$ ,  $E(0) = 2.5 \times 10^{-4}$ ,  $I(0) = 0$ ,  $R(0) = N - S(0) - I(0)$ . B. Equilibrium values for  $\mu = 70$  years,  $\beta = 73$  per day, and  $1/\gamma = 7$  days. C. Equilibrium values for  $\mu = 7$  days,  $\beta = 73$  per day, and  $1/\gamma = 7$  days. D. Results of an epidemic SEIR model (just removing the  $\mu$ -terms from model (16)) for  $\beta = 1.66$  per day,  $1/\gamma = 2.2$  days,  $N = 1000$ , and various values of  $\sigma$ .

## 2.6 Epidemiological Models on the Web

There are some publicly available tools through which one can play with the epidemiological models discussed in this section (and many others):

1. Epidemic SIR model:  
<http://math.colgate.edu/~wweckesser/solver/DiseaseSIR.shtml>
2. Endemic SIR model:  
<http://math.colgate.edu/~wweckesser/solver/DiseaseSIRwBD.shtml>
3. SIR models: <http://user.mendelu.cz/marik/dmb/sir.html>
4. Populus – software tool for simulations in population biology:  
<http://cbs.umn.edu/populus/> then to Model → Multi-species dynamics → Host-parasite models → Infectious microparasitic diseases
5. Source code accompanying the book “Modeling infectious diseases in humans and animals” by Keeling and Rohani (2008):

<http://www.modelinginfectiousdiseases.org/> (available in C++, Fortran and Matlab; some are also coded in web-based Java)

### 3 Modeling Wildlife Diseases

#### 3.1 Why Study Wildlife Diseases?

There are (at least) three major reasons for studying wildlife diseases:

1. For wildlife species of conservation interest there are concerns about the impact of diseases on population survival. Wildlife diseases thus pose a threat to biodiversity. Two situations can be distinguished:
  - (a) Diseases can be contracted by spillover from domestic animals, as is e.g. the case of canine distemper virus transmitted from domesticated dogs to African wild dogs
  - (b) Diseases can be innate to wildlife, such as chytridiomycosis (an infection due to the fungal pathogen *Batrachochytrium dendrobatidis*) in amphibians
2. There are increasing concerns about the possibility of either transmission from wildlife to humans or to domestic animal species. In this case we often think of wildlife as the reservoir species. According to the World Health Organization, zoonoses (zoonosis, sing.) or zoonotic diseases are those diseases and infections which are naturally transmitted between vertebrate animals and man.
3. Many natural phenomena are driven by parasites. These include sexual selection, population dynamics, population genetics, diet selection (through manipulation of hosts by parasites), and biogeography. Thus, we need to understand natural host-parasite interactions in order to understand more general concepts of biology.

Zoonoses often occur because of anthropogenic changes to the environment. These changes result in increased contact with wildlife species which allows a disease to jump between species. Examples of wildlife diseases that are transmitted to humans include hantavirus pulmonary syndrome (transmitted by wild rodents such as rats and mice), bird or swine flu, and plague from prairie dogs and rats. Rabies cases in humans are often due to bites by infected bats. Vector-transmitted diseases affecting wildlife as well as humans include West Nile virus and Lyme disease. A fine exposition of emerging infectious diseases of wildlife, including their implications for biodiversity and human health, is provided by Daszak et al. [12].

The major differences between modeling human and wildlife diseases are that

1. Wildlife populations do not remain constant over time. Populations can be highly variable due to environmental factors, landscape, or because of their internal dynamics.
2. Multiple species interactions are often involved. For example, a reservoir for infection does not have to consist of one species, but can be made up of a number of species which interact via the parasite and also otherwise through direct inter-specific competition.

3. In many cases, wildlife populations are believed to be controlled by parasites. Parasites can thus be added to the weaponry aimed at controlling pest populations. On the other hand, parasites need to be limited in their ability to invade endangered populations of hosts, to prevent biodiversity degradation.
4. Data can be more easily obtained from animal disease systems; it is often possible to experiment on wildlife populations or individual animals without the ethical issues involved with human disease systems.

Human populations in developing countries or populations of rapidly multiplying animals such as insects do not conform to the assumption of a constant population size made in Sect. 2. In what follows, we will in turn assume that the host population is subject to exponential growth, logistic growth, or constant rate immigration. The epidemiological model we will study in all three cases is the SI model

$$\begin{aligned}\frac{dS}{dt} &= b(N)N - \beta(N)\frac{SI}{N} - d(N)S \\ \frac{dI}{dt} &= \beta(N)\frac{SI}{N} - d(N)I - \alpha I\end{aligned}\tag{18}$$

where  $\beta(N)SI/N$  represents either the mass action incidence term  $\beta SI$  or the standard incidence term  $\beta SI/N$ ,  $b(N)$  and  $d(N)$  represent possibly density-dependent per capita birth rate and death rate, respectively, and  $\alpha$  is an extra mortality rate induced by the disease. The total host population size  $N = S + I$  thus evolves as

$$dN/dt = b(N)N - d(N)N - \alpha I$$

### 3.2 Exponential Host Population Growth

We start by assuming that in the absence of disease, the host population grows exponentially:

$$\frac{dN}{dt} = bN - dN\tag{19}$$

Hence,  $b(N) = b$  and  $d(N) = d$  are density-independent per capita birth and death rates, respectively; the intrinsic growth rate of the host population is thus  $r = b - d$ . The general solution of model (19) is  $N(t) = N(0)e^{rt}$ ; populations grow if  $r > 0$  and decline to extinction if  $r < 0$  (Fig. 5).

The major question here is whether and how a disease may modify dynamics of an exponentially growing host population. It seems plausible that infections can slow down its exponential growth. Whether a disease can regulate the host population to a steady state or even make it extinct is not at all clear. Mathematical models will help us address this question.

**Mass Action Incidence** With mass action incidence, the model we will study is as follows:

$$\begin{aligned}\frac{dS}{dt} &= bN - \beta SI - dS \\ \frac{dI}{dt} &= \beta SI - dI - \alpha I\end{aligned}\tag{20}$$

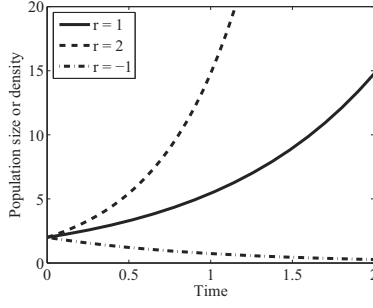


**Fig. 5.** A couple of solutions of model (19) of exponential host population growth.

The total host population evolves as  $dN/dt = rN - \alpha I$ , where  $r = b - d$ ; we assume  $b > d$  for the host population to grow exponentially in the absence of infection.

If a parasite will invade a host population of size  $N$ , the basic reproduction number is

$$R_0 = \frac{\beta S}{\alpha + d} \Big|_{S=N} = \frac{\beta N}{\alpha + d} \quad (21)$$

The condition  $R_0 > 1$  for the disease to successfully invade a fully susceptible host population thus translates to the need to surpass a threshold host population size  $N_T$ :

$$N > N_T \equiv \frac{\alpha + d}{\beta} \quad (22)$$

Provided that  $N > N_T$ , the density of infectious individuals  $I$  will increase. If  $N < N_T$ , however,  $I$  will decrease and  $S$  will thus grow at a rate close to  $r$ . After some time, however,  $N$  will exceed  $N_T$  and the condition (22) for successful disease invasion will be satisfied:  $I$  will eventually increase. So, in an exponentially growing host population, the disease driven by mass action incidence will always spread, the spread being lagged if  $N < N_T$  initially.

Now, let us seek for positive equilibria of model (20). As the equation for  $I$  can be written as  $dI/dt = \beta I(N - I - N_T)$ , the positive equilibria, if they exist, are solutions of the equations

$$rN - \alpha I = 0 \quad \text{and} \quad N - I - N_T = 0$$

This gives

$$N^* = N_T \frac{\alpha}{\alpha - r} \quad \text{and} \quad I^* = N_T \frac{r}{\alpha - r} \Rightarrow S^* = N^* - I^* = N_T \quad (23)$$

Obviously,  $I^* > 0$  provided that the disease-induced mortality rate  $\alpha$  exceeds a threshold value:

$$\alpha > \alpha_T \equiv r \quad (24)$$

In addition, the unique positive equilibrium (23) of model (20) is locally asymptotically stable if it exists (check by analyzing its Jacobian). If  $\alpha < \alpha_T$  then no positive equilibrium exists and  $N$  undergoes an unbounded exponential increase, since

$$\frac{dN}{dt} = rN - \alpha I = (r - \alpha)N + \alpha S > (r - \alpha)N \Rightarrow N(t) > N(0)e^{(r-\alpha)t}$$

To see even more, let us explore the dynamic equation for the proportion of infected individuals  $i = I/N$  (recall that  $N$  now depends on time):

$$\frac{di}{dt} = \frac{d}{dt} \left( \frac{I}{N} \right) = \frac{1}{N} (I' - iN') = i[\beta N(1 - i) - (\alpha + d + r) + \alpha i]$$

Since  $N$  grows exponentially and  $0 \leq i \leq 1$ , it must be  $i \rightarrow 1$  for the first term in the square brackets to disappear in the long run. Given that  $dN/dt = N(r - \alpha i)$ ,  $N$  grows asymptotically exponentially at a reduced (with respect to no disease case) rate  $\rho = r - \alpha$ . Finally, knowing that  $N(t) \rightarrow c \exp(\rho t)$ ,  $i \rightarrow 1$  and  $I = iN$ , then  $I(t) \rightarrow c \exp(\rho t)$ . Inserting this last term to the equation  $I' = \beta I(S - N_T)$  gives  $\rho = \beta(\hat{S} - N_T)$ , so that asymptotically there will be a constant density of susceptibles,

$$\hat{S} = \frac{\rho + (\alpha + d)}{\beta} = \frac{b}{\beta} \quad (25)$$

In summary, the disease will regulate the host population to stable equilibrium provided that  $\alpha > \alpha_T$  and only slow its exponential growth relative to no disease case if  $\alpha < \alpha_T$  (Fig. 6A).

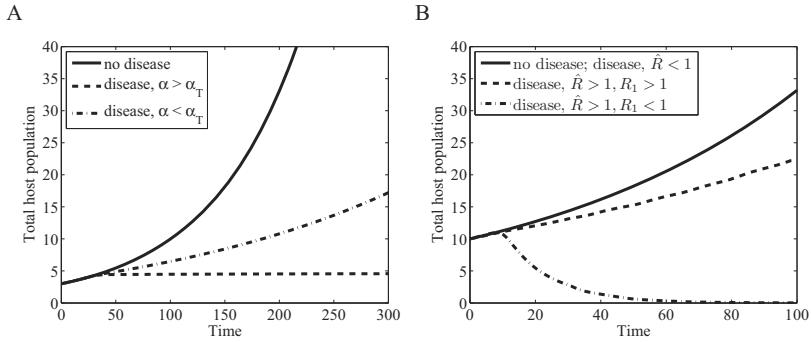


**Fig. 6.** Exponential growth of the host population, embedded in an SI model. A. Mass action incidence. B. Standard incidence.

**Standard Incidence** With standard incidence, the SI model with exponential host population growth is:

$$\begin{aligned}\frac{dS}{dt} &= bN - \beta \frac{SI}{N} - dS \\ \frac{dI}{dt} &= \beta \frac{SI}{N} - dI - \alpha I\end{aligned}\quad (26)$$

The total host population evolves as  $dN/dt = rN - \alpha I$ , where  $r = b - d$ ; also here, we assume  $b > d$  for the host population to grow exponentially in the absence of infection.

Whatever the initial population density  $N$ , the basic reproduction number is now

$$R_0 = \left. \frac{\beta S/N}{\alpha + d} \right|_{S=N} = \frac{\beta}{\alpha + d}\quad (27)$$

The condition  $R_0 > 1$  for the disease to successfully invade a fully susceptible host population thus translates to the condition  $\beta > \alpha + d$ . If  $\beta < \alpha + d$ , the disease will die out, irrespectively of the initial host population density, and the host population goes on to grow at rate  $r$ .

We go on by changing variables from densities of infectives to proportions of infectives:

$$\frac{di}{dt} = \frac{d}{dt} \left( \frac{I}{N} \right) = \frac{1}{N} (I' - iN') = i[\beta(1-i) - (d + \alpha + r) + \alpha i]\quad (28)$$

This equation has as its *proportional* equilibria

$$i_0^* = 0 \quad \text{and} \quad i_e^* = (\beta - (b + \alpha)) / (\beta - \alpha) = 1 - b / (\beta - \alpha)$$

While the proportional disease-free equilibrium  $i_0^*$  always exists, the proportional endemic equilibrium  $i_e^*$  is feasible ( $0 < i_e^* < 1$ ) only if  $\hat{R} \equiv \beta / (\alpha + b) > 1$ . Note that  $b > d$  implies  $R_0 > \hat{R} > 1$  so that existence of  $i_e^*$  means successful disease invasion. When it exists,  $i_e^*$  is locally asymptotically stable and  $i_0^*$  is unstable; otherwise,  $i_0^*$  is locally asymptotically stable.

Once  $i_0^*$  is stable,  $dN/dt = N(r - \alpha i) \rightarrow rN$  and the host population thus grows exponentially at rate  $r$ . In addition, because  $dI/dt$  can be written as

$$dI/dt = I[\beta S/N - (d + \alpha)] = I(d + \alpha)(R_0 S/N - 1) \rightarrow I(d + \alpha)(R_0 - 1)$$

as  $t \rightarrow \infty$  ( $S/N = s = 1 - i$ ), it follows that if  $R_0 > 1$  the disease invades and thus  $I \rightarrow \infty$ , and if  $R_0 < 1$  the disease dies out and thus  $I \rightarrow 0$ . The asymptotic rate of increase (if  $R_0 > 1$ ) or decrease (if  $R_0 < 1$ ) is  $(d + \alpha)(R_0 - 1)$ . If  $i_e^*$  exists (and is stable), the host population  $N$  will decline to extinction as soon as  $r - \alpha i_e^* < 0$  or equivalently  $R_1 \equiv b / (d + \alpha i_e^*) < 1$ , and grow exponentially, albeit at a reduced rate  $r - \alpha i_e^*$ , if  $R_1 > 1$ .

In summary, we observe the following four types of behavior of model (26) (see also Fig. 6B):

1. If  $\hat{R} < 1$ , the proportional disease-free equilibrium  $i_0^* = 0$  (that always exists) is locally asymptotically stable and the host population grows exponentially at rate  $r$ ; in addition,
  - (a) when  $R_0 > 1$  disease invades and  $I \rightarrow \infty$

- (b) when  $R_0 < 1$  disease dies out and  $I \rightarrow 0$
2. If  $\hat{R} > 1$  (which implies  $R_0 > 1$  so that disease always invades in this case), the proportional disease-free equilibrium  $i_0^* = 0$  is unstable and the proportional endemic equilibrium  $i_e^* > 0$  exists and is locally asymptotically stable; in addition,
- (a) when  $R_1 > 1$  the host population grows exponentially, at a reduced rate  $r - \alpha i_e^*$ , and  $I \rightarrow \infty$
- (b) when  $R_1 < 1$  the host population dies out and  $I \rightarrow 0$

Note that the proportion of infectives  $i$  may tend to an endemic value  $i_e^*$ , while the density of infectives declines to zero ( $\hat{R} > 1, R_1 < 1$ ). Conversely, the proportion of infectives  $i$  may tend to zero, while the density of infectives increases ( $\hat{R} < 1, R_0 > 1$ ). There are therefore two distinct ways of considering a disease as being brought under control in a host population – the stricter way requires that the density of infectives  $I$  tends to 0 with time, while a weaker requirement is that the proportion of infectives  $i$  tends to 0 with time.

### 3.3 Logistic Host Population Growth

Many populations are limited in growth by a finite amount of resources (such as food or territories) so that their per capita growth rate declines as population density increases, and logistic growth is the simplest formalization of this concept of negative density dependence.

Logistic growth of a disease-free population due to negative density dependence is often formalized via the Verhulst or logistic equation

$$\frac{dN}{dt} = rN \left( 1 - \frac{N}{K} \right) \quad (29)$$

where  $r > 0$  is the intrinsic population growth rate (i.e. the actual population growth rate when  $N$  is small) and  $K > 0$  is the carrying capacity of the environment (i.e. the density which the population eventually attains). This equation, though neat and simple, has a substantial drawback: it does not distinguish between birth and death rates and considers only the net growth rate of the population. However, such a distinction is precisely what we would like to have for models of disease transmission, as the death rate commonly enters equations for all epidemiological classes, while the birth rate standardly enters only the equation for the susceptible class. Various attempts have been made to reformulate equation (29) as a sum of a birth and a death part, such as

$$\frac{dN}{dt} = \left( b - ar \frac{N}{K} \right) N - \left( d + (1-a)r \frac{N}{K} \right) N, \quad 0 \leq a \leq 1 \quad (30)$$

but these commonly suffer from the problem that the birth rate becomes negative once  $N$  becomes sufficiently large (e.g. [17, 30]). Although the problem can be overcome by setting the parameters so that the birth rate becomes negative only for relatively large  $N > K$  which actually cannot be attained, we rather prefer to start from first principles on reproduction and survival and revert the flow of thinking such that birth and death rates are specified first and only then an equation for the population's net growth rate such as (29) is derived.

In the simplest modeling framework, negative density dependence can affect the birth rate, the death rate, or both – the birth rate decreases and the death rate increases with increasing population density, but both must stay non-negative. Writing the equation for population growth as

$$\frac{dN}{dt} = b(N)N - d(N)N \quad (31)$$

we can formalize the per capita birth rate  $b(N)$  as, for example,  $b(N) = b - b_1N$  if  $N \leq b/b_1$  and  $b(N) = 0$  otherwise,  $b(N) = b \exp(-b_1N)$  (Ricker formulation), or  $b(N) = b/(1 + b_1N)$  (Beverton-Holt formulation), and the per capita death rate  $d(N)$  as, for example,  $d(N) = d + d_1N$  or  $d(N) = dN/(d_1 + N)$ . It is just  $d(N)$  as a linear function of  $N$ ,  $d(N) = d + d_1N$ , that is mathematically quite neat to analyze in many cases and is therefore used by many authors to account for negative density dependence in epidemiological models (e.g. [25, 28]). In what follows, we too use this form of negative density dependence in which  $d$  represents the intrinsic death rate (i.e. the actual death rate when  $N$  is small) and  $d_1$  the strength of negative density-dependent effects. We avoid using the word “negative” in the following, as we do not consider any other type of density dependence here, but the reader should be aware that there are also positive density-dependent effects (Allee effects, [11]). So, in the absence of disease the host population is assumed to grow as

$$\frac{dN}{dt} = bN - (d + d_1N)N, \quad b > d \quad (32)$$

This model can also be written in the form (29), with  $r = b - d > 0$  and  $K = (b - d)/d_1 > 0$ . A couple of solutions of model (32) are plotted in Fig. 7.

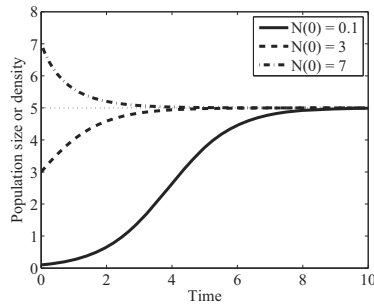


**Fig. 7.** A couple of solutions of model (32) of logistic host population growth;  $r = 1$ ,  $K = 5$ .

**Mass Action Incidence** Consider an SI model with logistic host population growth and mass action incidence:

$$\begin{aligned}\frac{dS}{dt} &= bN - \beta SI - (d + d_1 N)S \\ \frac{dI}{dt} &= \beta SI - (d + d_1 N)I - \alpha I\end{aligned}\tag{33}$$

Again, the total host population density  $N = S + I$  evolves as  $dN/dt = bN - (d + d_1 N)N - \alpha I = rN(1 - N/K) - \alpha I$ , where  $r = b - d$  and  $K = (b - d)/d_1$ . The basic reproduction number now equals

$$R_0 = \left. \frac{\beta S}{d + d_1 N + \alpha} \right|_{S=N=K} = \frac{\beta K}{d + d_1((b - d)/d_1) + \alpha} = \frac{\beta K}{b + \alpha}$$

If we rescale the state variables as  $s = S/N$  and  $i = I/N$ ,  $N$  will not disappear from the resulting equations. Therefore, we analyze equations corresponding to rescaled  $I$  ( $i = I/N$ ) and to  $N$ . This leads to

$$\begin{aligned}\frac{di}{dt} &= i[\beta(1 - i)N - \alpha - b + \alpha i] \\ \frac{dN}{dt} &= N[b - (d + d_1 N) - \alpha i]\end{aligned}\tag{34}$$

Four candidate equilibria of model (34) are  $(0, 0)$ ,  $(0, K = (b - d)/d_1)$ ,  $(1 + b/\alpha, 0)$ , and an endemic equilibrium  $(i_e^*, N_e^*)$ . Obviously, the third equilibrium is not feasible as  $1 + b/\alpha > 1$ , that is, the equilibrium proportion of infectives would be greater than one. While  $(0, 0)$  and  $(0, K)$  always exist, the endemic equilibrium  $(i_e^*, N_e^*)$  is feasible provided that  $R_0 > 1$  (Box 4).

#### Box 4 Existence of the endemic equilibrium of model (34)

We use graphical analysis to prove that the endemic equilibrium  $(i_e^*, N_e^*)$  of model (34) is feasible provided that  $R_0 > 1$ . The equilibrium is a solution of the system of two algebraic equations:

$$\begin{aligned}\beta(1 - i)N - \alpha - b + \alpha i &= 0 \\ b - (d + d_1 N) - \alpha i &= 0\end{aligned}\tag{35}$$

Expressing  $N$  from the second equation as a function of  $i$ ,  $N = K - \alpha i/d_1$ , we get a decreasing linear function that equals  $K$  for  $i = 0$  and crosses the  $i$ -axis at  $N = (b - d)/\alpha$ ; recall that  $K = (b - d)/d_1$  (Fig. 8). Now, expressing  $i$  from the first equation as a function of  $N$ ,

$$i = 1 - \frac{b}{\beta N - \alpha}$$

we have a hyperbolic function that has  $N = \alpha/\beta$  as its vertical asymptote and  $i = 1$  as its horizontal asymptote; moreover, it crosses the  $N$ -axis at  $N = (b + \alpha)/\beta$  (Fig. 8). Hence,

for these two functions to cross in the feasibility region for the endemic equilibrium ( $0 < i < 1, 0 < N < K$ ), we require that the hyperbolic function crosses the  $N$ -axis below  $K$ , that is, we require that  $(b + \alpha)/\beta < K$ . This inequality translates to  $\beta K/(b + \alpha) > 1$  and because the left-hand side of this last inequality equals  $R_0$ , we conclude that the endemic equilibrium  $(i_e^*, N_e^*)$  is feasible provided that  $R_0 > 1$ . The shape of the two functions also implies that if an endemic equilibrium exists it is unique. Graphical analysis in two-dimensional systems is often a quite powerful tool in proving the existence (and also number) of system equilibria.

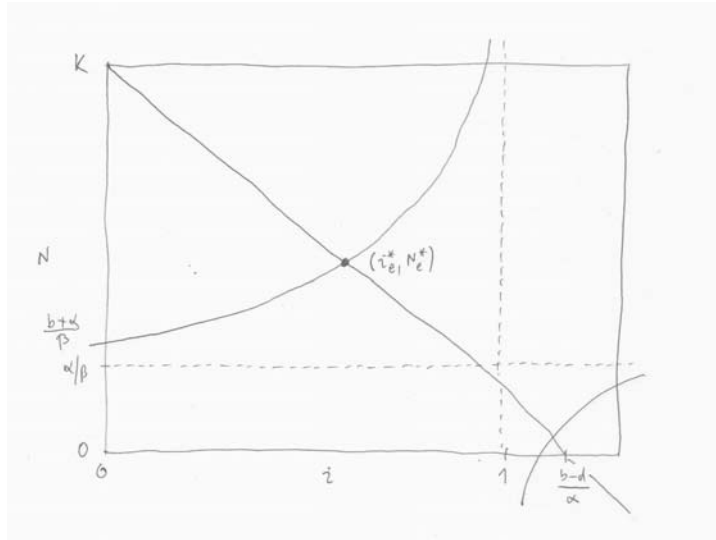


**Fig. 8.** Graphical analysis of model (34).

Regarding local stability of the equilibria of model (34), its Jacobian is:

$$J = \begin{bmatrix} -2\beta Ni + 2\alpha i + \beta N - \alpha - b & \beta(1-i)i \\ -\alpha N & -2d_1 N + b - d - \alpha i \end{bmatrix} \quad (36)$$

This can be used to show that for  $b > d$ :

1. The extinction equilibrium  $(0, 0)$  is always unstable.
2. The DFE  $(0, K)$  is locally asymptotically stable if  $R_0 < 1$  and unstable if  $R_0 > 1$ .
3. The endemic equilibrium  $(i_e^*, N_e^*)$  is locally asymptotically stable if it exists (i.e. if  $R_0 > 1$ ); see Box 5.

**Box 5 Local stability of the endemic equilibrium of model (34)**

Using equations (35) that the endemic equilibrium satisfies allows us to simplify the Jacobian (asterisks and subscripts  $e$  dropped) (36) to

$$J = \begin{bmatrix} -\beta Ni + \alpha i \beta(1-i)i \\ -\alpha N & -d_1 N \end{bmatrix} \quad (37)$$

Local asymptotic stability requires the trace of  $J$  to be negative and the determinant of  $J$  to be positive. Since

$$\begin{aligned} \text{Tr}J &= -i(\beta N - \alpha) - d_1 N \\ \det J &= d_1 Ni(\beta N - \alpha) + \alpha N \beta(1-i)i \end{aligned} \quad (38)$$

a sufficient condition for local asymptotic stability of the endemic equilibrium is  $\beta N > \alpha$ . To prove that this inequality indeed holds, note that at the endemic equilibrium the replacement number  $R$  of the infection must equal 1 (i.e. the current infectives produce the same amount of future infectives). Since

$$R = \frac{\beta S}{d + \alpha} = \frac{\beta N s}{d + \alpha} = \frac{\beta N(1-i)}{d + \alpha} = 1$$

this implies

$$\beta N - \alpha = d + i\beta N > 0$$

and hence

$$\beta N > \alpha$$

This completes the proof.

Biologically, the model outcomes can be summarized as follows (Fig. 9A): the disease either does not invade and the host population attains its environmental carrying capacity, or it invades and attains an endemic equilibrium. With mass action incidence, the infection cannot cause the host population to go extinct.

**Standard Incidence** With standard incidence, an equivalent SI model is:

$$\begin{aligned} \frac{dS}{dt} &= bN - \beta \frac{SI}{N} - (d + d_1 N)S \\ \frac{dI}{dt} &= \beta \frac{SI}{N} - (d + d_1 N)I - \alpha I \end{aligned} \quad (39)$$

Note that we assume equal density dependence for susceptibles and infectives. The total host population density  $N = S + I$  evolves as

$$dN/dt = bN - (d + d_1 N)N - \alpha I = rN(1 - N/K) - \alpha I$$

where  $r = b - d$  and  $K = (b - d)/d_1$ . As we require  $b > d$ , in the absence of disease the population attains the environmental carrying capacity  $K$ . The disease-free equilibrium (DFE) of model (39) is thus  $(K, 0)$ .

As always, we start with calculating the basic reproduction number  $R_0$ :

$$R_0 = \frac{\beta S/N}{d + d_1 N + \alpha} \Big|_{S=N=K} = \frac{\beta}{b + \alpha} \quad (40)$$

The condition  $R_0 > 1$  for the disease to invade a fully susceptible population at the DFE thus translates to the condition  $\beta > \alpha + b$ . If  $R_0 < 1$  or equivalently  $\beta < \alpha + b$ , the disease will die out.

We go on by rescaling state variables of model (39) as  $s = S/N$  and  $i = I/N$  (note that  $N$  is a function of time). This leads to (note that  $N$  disappeared from the resulting equations, contrary to mass action incidence):

$$\begin{aligned} \frac{ds}{dt} &= b(1 - s) + (\alpha - \beta)si \\ \frac{di}{dt} &= \beta si - i(\alpha + b) + \alpha i^2 \end{aligned} \quad (41)$$

Since  $s = 1 - i$ , we can write the equation for  $i$  as

$$\frac{di}{dt} = i[\beta(1 - i) - (\alpha + b) + \alpha i]$$

Obviously,  $i_0^* = 0$  solves the equation  $di/dt = 0$  which implies  $s_0^* = 1$ ;  $(1, 0)$  is thus the proportional disease-free equilibrium. Setting the term in square brackets to zero and solving it for  $i$ , we get

$$i_e^* = \frac{\beta - (\alpha + b)}{\beta - \alpha} = 1 - \frac{b}{\beta - \alpha}$$

as a proportional endemic equilibrium ( $0 < i_e^* < 1$ ) if  $\beta > \alpha + b$  or equivalently  $R_0 > 1$ ;  $s_e^* = b/(\beta - \alpha)$ . Local stability analysis shows that if  $R_0 < 1$  then  $(s_0^*, i_0^*)$  is locally asymptotically stable; if  $R_0 > 1$ , on the other hand,  $(s_0^*, i_0^*)$  is unstable and  $(s_e^*, i_e^*)$  is locally asymptotically stable.

In addition, since

$$dN/dt = N[(b - d - d_1 N) - \alpha i]$$

we have that  $N \rightarrow N^*$  as  $t \rightarrow \infty$  where

1.  $N^* = K$  if  $R_0 < 1$
2.  $N^* = (b - d - \alpha i_e^*)/d_1 < K$  if  $R_0 > 1$  and  $b - d > \alpha i_e^*$
3.  $N^* = 0$  if  $R_0 > 1$  and  $b - d < \alpha i_e^*$

Model equilibria in the original state variables can be calculated as  $S^* = s^* N^*$  and  $I^* = i^* N^*$ .

Biologically, the model outcomes can be summarized as follows (Fig. 9B): the disease either does not invade and the host population attains its environmental carrying capacity, or it invades and then proportions of susceptibles and infectives attain an endemic equilibrium. In the latter case, the total host population may either attain an endemic equilibrium if the effect of the disease is not too strong, or go extinct if it is.

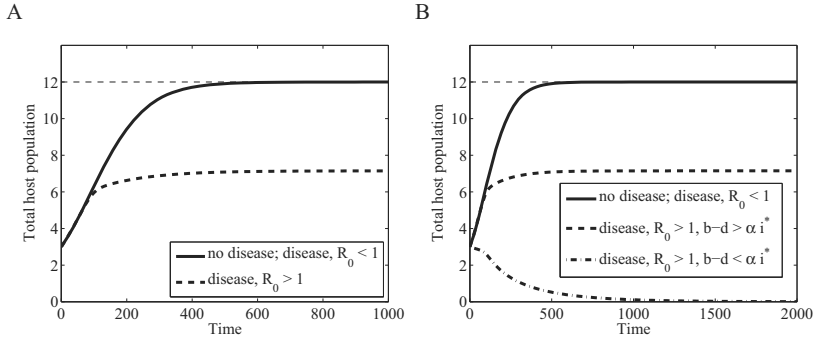


**Fig. 9.** Logistic growth of the host population, embedded in an SI model. A. Mass action incidence. B. Standard incidence.

### 3.4 Host Population Growth with Constant Rate Immigration

A number of published epidemiological models consider immigration at a constant rate instead of a density-dependent birth term [2, 27]e.g. . With immigration rate  $\Lambda > 0$ , the host population in the absence of disease is thus assumed to evolve as

$$\frac{dN}{dt} = \Lambda - dN \quad (42)$$

This implies that the host population never goes extinct in the absence of disease (population extinction is not even a model equilibrium) and attains the environmental carrying capacity  $K = \Lambda/d$ . A couple of solutions of model (42) are plotted in Fig. 10.

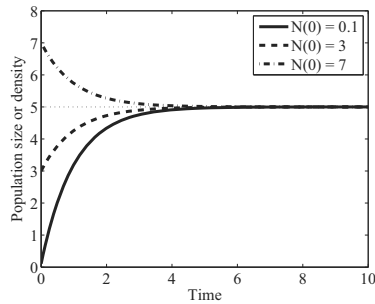


**Fig. 10.** A couple of solutions of model (42) of host population growth with constant immigration;  $d = 1, \Lambda = 5$ .

**Generic Incidence** Let us now work with a generic incidence term  $\beta(N)SI/N$ ; the SI model is then

$$\begin{aligned}\frac{dS}{dt} &= \Lambda - \beta(N)\frac{SI}{N} - dS \\ \frac{dI}{dt} &= \beta(N)\frac{SI}{N} - dI - \alpha I\end{aligned}\quad (43)$$

The total host population size or density  $N = S + I$  evolves as

$$dN/dt = \Lambda - dN - \alpha I$$

First,  $I = 0$  solves the equation  $dI/dt = 0$  which implies  $S = \Lambda/d$  from the equation  $dS/dt = 0$ :  $(\Lambda/d, 0)$  is thus the DFE. For the disease to invade the host population, we must have

$$\frac{1}{I} \frac{dI}{dt} = \beta(N)S/N - d - \alpha > 0$$

when evaluated at the DFE which implies  $\beta(\Lambda/d) > d + \alpha$ . As the basic reproduction number is

$$R_0 = \frac{\beta(N)S/N}{d + \alpha} \Big|_{S=N=K=\Lambda/d} = \frac{\beta(\Lambda/d)}{d + \alpha}$$

the disease invades the host population if and only if  $R_0 > 1$ .

Evaluating the Jacobian of model (43) at the DFE, we have

$$J = \begin{bmatrix} -d - \beta(\Lambda/d) & \\ 0 & \beta(\Lambda/d) - (d + \alpha) \end{bmatrix}\quad (44)$$

The DFE  $(\Lambda/d, 0)$  is thus locally asymptotically stable provided that  $\beta(\Lambda/d) < d + \alpha$ , that is, if  $R_0 < 1$ , and unstable if the opposite inequality holds.

Solving model (43) for an endemic equilibrium, we eventually get that (asterisks dropped)

$$\beta(N)S = (d + \alpha)N \quad (\text{from the equation for } I)$$

$$\Lambda + \alpha S = (d + \alpha)N \quad (\text{from the equation for } N)$$

This can be solved for  $S$  and  $N$  if a specific form of  $\beta(N)$  is given. Once solved, the equilibrium density of infectives can be calculated as

$$I = \frac{\Lambda - dS}{(d + \alpha)} \quad (\text{from the equation for } S)$$

In particular, standard incidence  $\beta(N) = \beta$  implies a unique solution

$$S^* = \frac{\Lambda}{\beta - \alpha} \quad \text{and} \quad I^* = \Lambda \frac{\beta - (d + \alpha)}{(d + \alpha)(\beta - \alpha)}\quad (45)$$

whereas mass action incidence  $\beta(N) = \beta N$  implies a unique solution

$$S^* = \frac{d + \alpha}{\beta} \quad \text{and} \quad I^* = \frac{\Lambda\beta - d(d + \alpha)}{\beta(d + \alpha)}\quad (46)$$

In both cases,  $S^* > 0$  and  $I^* > 0$  if and only if  $R_0 > 1$ . Also, in both cases, this unique endemic equilibrium of model (43) is locally asymptotically stable if it exists.

Biologically, regardless of the type of incidence (mass action or standard) the disease either does not invade and the host population attains its environmental carrying capacity, or it invades and attains an endemic equilibrium (Fig. 11). The disease can never bring the host population to extinction (population extinction is not even a model equilibrium).

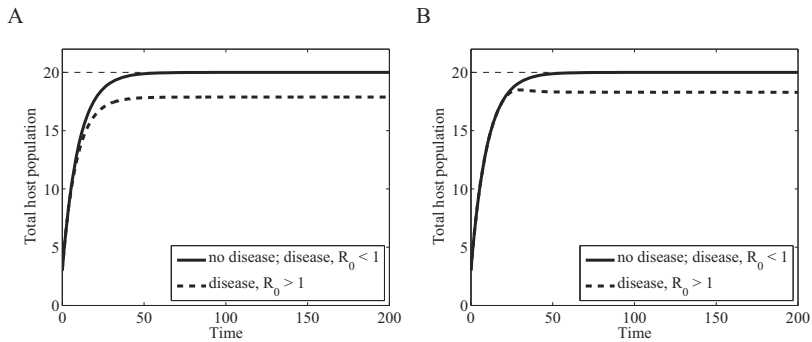


**Fig. 11.** Host population growth with constant rate immigration, embedded in an SI model. A. Mass action incidence. B. Standard incidence.

### 3.5 Summary

The above three sections have demonstrated several important points. First, we now know that parasites can regulate the (dynamic) host populations. This regulation does not mean a merely quantitative change, such as a decrease in the exponential growth rate or a decrease in the steady state. It may also result in a qualitative change: exponentially growing populations can be stabilized or even made extinct, just like populations that grow logistically in the absence of infection.

Second, disease-induced extinction of host populations requires that the disease transmission not decline to zero as population density declines. If that is so, such as in the case of mass action transmission, low-density populations are virtually free of parasites and can thus recover. On the other hand, populations subject to standard incidence do not suffer from this limitation and can be made extinct if the infection is strong enough as regards disease-induced mortality – transmission efficiency simply does not fade out with declining population density.

Third, the exception from this are models with a constant immigration rate. Since this type of immigration causes the susceptibles to arrive at a steady rate, such populations cannot be made extinct by any disease regardless of whether mass action or standard incidence drives the parasite transmission.

We have presented and analyzed here only the simplest epidemiological models (the SI models), in part because this is an adequate description for many wildlife diseases and in part because they can be treated analytically to greater detail relative to more complex models and thus the basic principles that drive disease dynamics can be more easily revealed. Nevertheless, researchers have extended this analysis to epidemiological models with a more complex structure, and we absolutely encourage interested readers to consult those for more insight. Nevertheless, it turns out that the basic types of dynamics revealed for the simplest SI model are conserved in those more complex models, too (see Table 5 and references therein).

**Table 5.** Examples of studies that analyzed more complex epidemiological models with internal host growth. The results of these studies were qualitatively similar to those of the SI models analyzed in this material.

Host growth	Model type	Incidence	Reference
Exponential	SIRS	mass action	Anderson and May [2]
	SIRS	standard	Busenberg and van den Driessche [10]
	SIRS	saturation	Mena-Lorca and Hethcote [27]
	many	mass action	Anderson and May [2]
	SEIR	standard	Li et al. [24]
Logistic	SI(S)	standard	Lockhart et al. [25]
	SEI <sup>a</sup>	mass action	Gao et al. [18]
	SEI <sup>a</sup>	standard	Gao et al. [18]
	SIS and SIRS <sup>b</sup>	standard	Gao and Hethcote [17]
Constant rate immigration	SIRS	mass action	Mena-Lorca and Hethcote [27]
	SIRS	standard	Mena-Lorca and Hethcote [27]
	SIRS	mass action	Anderson and May [2]

Note: <sup>a</sup>This model also optionally includes reduced reproduction due to disease.

<sup>b</sup>These models also optionally include vertical disease transmission.

An interesting study was provided by Ryder et al. [32]. They considered the situation in which transmission occurred through two different types of contact (e.g. sexual vs. non-sexual/social contacts), one of which was density-dependent, the other frequency-dependent, and asked how do deviations from solely density-dependent or frequency-dependent transmission affected dynamics. The model is as follows:

$$\begin{aligned} \frac{dS}{dt} &= (b - b_1 N)N - \beta(\beta_1 + \beta_2 N) \frac{SI}{N} - dS \\ \frac{dI}{dt} &= \beta(\beta_1 + \beta_2 N) \frac{SI}{N} - dI - \alpha I \end{aligned} \tag{47}$$

Ryder et al. [32] showed that when the major type of transmission was density-dependent transmission ( $\beta_1 \approx 0$ ), allowing for even small amounts of transmission to occur through frequency-dependent contacts lowered the threshold for disease invasion and led to

the possibility of disease-induced extinction. On the contrary, assuming frequency-dependent transmission to be dominant ( $\beta_2 \approx 0$ ) and adding a small amount of density-dependent one did not affect the propensity to disease-induced extinction, but still increased the chance of disease invasion.

This section, together with the previous one, make clear the point that we need to make a number of decisions when considering a host-parasite interaction, even in the framework of the simplest host-parasite models. We must consider the type of host population demography (constant population density [epidemic or endemic disease], exponential growth, logistic growth, or constant rate immigration), whether to use no, transient or permanent immunity to infection, and which form to choose for the (horizontal) transmission term (frequency-dependent, density-dependent or other). Also, we need to decide if there is no or some disease-induced mortality, no or some vertical transmission, and no or some sort of depression of reproduction due to infection. The essential message here is that qualitative properties at the level of individual hosts and parasites create qualitative differences at the whole-population level, and the connection between these is mediated through adequate epidemiological models.

We have not discussed at all models of infectious diseases that reduce host fecundity and/or are transmitted vertically. Just to get a feeling of how such models could look like, we give an example here:

$$\begin{aligned}\frac{dS}{dt} &= b(S + (1-p)(1-\sigma)I) - \beta(N)\frac{SI}{N} - dS \\ \frac{dI}{dt} &= bp(1-\sigma)I + \beta(N)\frac{SI}{N} - dI - \alpha I\end{aligned}\tag{48}$$

where  $\sigma$  denotes the proportional decrease in fecundity of infectives, and  $p$  is the proportion of newborns produced by infectives to which the disease is transmitted vertically.

## 4 Some Applications

In this section, we present four applications of models analyzed in this material. Each of these applications has an added value not discussed above, so it extends the scope of this material. Whereas the dynamic model of HIV/AIDS considers treatment of HIV+ individuals as another disease control strategy, modeling the hantavirus infection requires an explicit account of both host sexes. We go on with modeling vector-borne infections for which both the host and the vector populations need to be subdivided according to the disease status. Finally, an infection is shown to explain the successful invasion of the alien gray squirrels over the native red ones across Europe.

### 4.1 Dynamics of HIV/AIDS

This example comes from [31] and originally from [6]. AIDS (acquired immunodeficiency syndrome), results from the deterioration of the immune system and is the final stage of infection by HIV (human immunodeficiency virus). HIV is transmitted through the exchange of bodily fluids, predominantly through unprotected sexual intercourse,

but also through sharing of unsterilized needles or transfusion with infected blood supplies. AIDS can now be classified as a pandemic. According to the Joint United Nations Programme on HIV/AIDS (UNAIDS) and World Health Organization (WHO), 33.2 million people worldwide were estimated to be infected by HIV in 2007. In addition, 2.1 million people, including 330,000 children, were estimated to have been killed by AIDS.

Blower et al. [6] developed and analyzed a model to predict an advance of HIV infection among gay males in San Francisco. There is a general concern that effective antiretroviral therapies (ART) might cause people to be less cautious when engaging in behavior posing a risk for HIV transmission. Blower et al. [6] asked what this might mean for the further progression of the disease relative to when no ART was available. We present here a simplified version of their model due to [31] which ignored the evolution of HIV resistance. The major assumption of the model was that the mean number of sexual partners with whom an HIV- individual has unprotected sex per year increased from  $c$  before ART was available to  $c(1+i)$ , for a constant  $i > 0$ .

The model assumes three classes of gay males, uninfected individuals  $X(t)$ , HIV+ individuals taking ART  $Y_T(t)$ , and untreated HIV+ individuals  $Y_U(t)$ . The rate of change of the number of individuals in each class is as follows:

$$\begin{aligned}\frac{dX}{dt} &= \pi - c(1+i)\lambda X - \mu X \\ \frac{dY_U}{dt} &= c(1+i)\lambda X + gY_T - \sigma Y_U - \mu Y_U - \nu_U Y_U \\ \frac{dY_T}{dt} &= -gY_T + \sigma Y_U - \mu Y_T - \nu_T Y_T\end{aligned}\tag{49}$$

where  $\pi$  is the rate at which HIV- men enter the gay community in San Francisco,  $\mu$  is the rate at which gay man leave the community (by moving away, becoming sexually inactive, or dying for reasons other than HIV/AIDS),  $\sigma$  is the rate at which untreated HIV+ men enter treatment,  $g$  is the rate at which treated HIV+ men abandon treatment,  $\nu_U$  is the death rate of untreated HIV+ men from AIDS, and  $\nu_T$  is the death rate of treated HIV+ men from AIDS. The force of infection  $\lambda$ , i.e. the per capita rate at which susceptibles catch the disease, is the probability that a sexual partner is HIV+ times the probability of acquiring HIV from this partner during sex, summed over the treated and untreated classes:

$$\lambda = \beta_U \frac{Y_U}{N} + \beta_T \frac{Y_T}{N}\tag{50}$$

where  $N = X + Y_U + Y_T$  is the total number of gay males in the community; the untreated partners are assumed to have a higher probability of HIV transmission than the treated ones,  $\beta_U > \beta_T$ .

Following [6], Otto and Day [31] showed that “43% of the AIDS deaths that would have occurred within the gay population of San Francisco within the next ten years will be avoided by the use of ART if risky behavior does not increase [ $i = 0$ ], but only 24% of deaths will be averted if risky behavior doubles [ $i = 1$ ].” From another perspective, there will be a much higher probability of contracting HIV through upon sexual intercourse when risky behavior doubles compared to when it does not increase (Fig. 12).

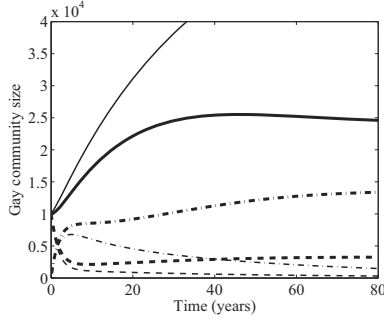


**Fig. 12.** Dynamics of uninfected (solid), treated HIV+ (dash-dot), and untreated HIV+ (dashed) individuals when the risky behavior does not change (thin) and when it doubles (thick). Parameters from Otto and Day (2007).

## 4.2 Hantavirus Infection in Rodents

This example comes from [1]. Hantaviruses are primarily a source of infection in rodents that might nonetheless be occasionally transmitted to humans. Human infection occurs primarily through the inhalation of aerosolized saliva and/or excreta of infected rodents, or after individuals have been bitten by infected rodents. Humans infected by hantaviruses suffer from a hemorrhagic fever with renal syndrome – HFRS (in Europe and Asia) or a hantavirus pulmonary syndrome – HPS (in North and South America). The mortality rate for HPS in the United States is 37%.

None of the models studied above discerned between male and female hosts, assuming that an infection affects both sexes equally. With hantavirus infection this is different, as two aspects of the disease call for an explicit consideration of host sex structure: (i) as males are more aggressive than females, contacts between two males generally result in greater transmission of the disease than contacts between two females or a male and a female, so that males have a higher disease prevalence than females, and (ii) the infectious period is longer for males than for females. In addition, because the life expectancy of rodents is relatively short, the latent period of the disease needs to be accounted for. The population is thus subdivided according to disease status: susceptible ( $S$ ), exposed ( $E$ ), infective ( $I$ ), and recovered ( $R$ ), and then into males (subscript  $m$ ) and females (subscript  $f$ ). For male rodents, the SEIR model is as follows:

$$\begin{aligned}
 \frac{dS_m}{dt} &= \frac{B(N_m, N_f)}{2} - \beta_f S_m I_f + \beta_m S_m I_m - d(N) S_m \\
 \frac{dE_m}{dt} &= \beta_f S_m I_f + \beta_m S_m I_m - \sigma E_m - d(N) E_m \\
 \frac{dI_m}{dt} &= \sigma E_m - \gamma_m I_m - d(N) I_m \\
 \frac{dR_m}{dt} &= \gamma_m I_m - d(N) R_m
 \end{aligned} \tag{51}$$

and for female rodents,

$$\begin{aligned}
\frac{dS_f}{dt} &= \frac{B(N_m, N_f)}{2} - \beta_f S_f I_f + \beta_{mf} S_f I_m - d(N) S_f \\
\frac{dE_f}{dt} &= \beta_f S_f I_f + \beta_{mf} S_f I_m - \sigma E_f - d(N) E_f \\
\frac{dI_f}{dt} &= \sigma E_f - \gamma_f I_f - d(N) I_f \\
\frac{dR_f}{dt} &= \gamma_f I_f - d(N) R_f
\end{aligned} \tag{52}$$

where total density of males is  $N_m = S_m + E_m + I_m + R_m$ , total density of females is  $N_f = S_f + E_f + I_f + R_f$ , and total population density is  $N = N_m + N_f$ . The function  $B(N_m, N_f)$  is the birth function, and one assumes a 1:1 sex ratio of newborns. One of the most commonly used birth functions in sex-structured models is

$$B(N_m, N_f) = b \frac{N_m N_f}{(N_m + N_f)/2}$$

where  $b$  is the average litter size and the fraction  $N_m N_f / [(N_m + N_f)/2]$  is the pair formation rate. In the model,  $\beta_f$  scales the disease transmission between an infective female and a susceptible female or a susceptible male,  $\beta_{mf}$  scales the disease transmission between an infective male and a susceptible female, and  $\beta_m$  scales the disease transmission between an infective male and a susceptible male. The above stated differences between male and female epidemiology translate to the following conditions:

$$\beta_m \geq \beta_{mf} \geq \beta_f \text{ and } \gamma_f > \gamma_m$$

The density-dependent death rate  $d(N) = d + d_1 N$ , with  $0 < d < b/2$  and  $d_1 > 0$  is the same for males and females; we thus assume a logistic growth of the rodent population in the absence of infection (see Sect. 3.3).

There is a globally stable positive equilibrium for the total population density in the absence of infection,  $N = K \equiv (b/2 - d)/d_1$ . At this equilibrium, densities of males and females equal,  $N_m = N_f = K/2$ . Therefore, because there is no disease-induced mortality in the model, every equilibrium of the model (51) and (52) must satisfy

$$S_m + E_m + I_m + R_m = S_f + E_f + I_f + R_f = K/2$$

One particular equilibrium with this property is the disease-free equilibrium (DFE), where  $S_m = K/2 = S_f$  and  $E_m = I_m = R_m = E_f = I_f = R_f = 0$ . The stability of the DFE depends on the magnitude of the basic reproduction number. Using the method of [36], sketched in Sect. 5, one can show that

$$\begin{aligned}
R_0 &= \frac{\sigma K/4}{b/2 + \sigma} \left[ \frac{\beta_m}{b/2 + \gamma_m} + \frac{\beta_f}{b/2 + \gamma_f} + \right. \\
&\quad \left. \frac{\sqrt{[\beta_m(b/2 + \gamma_f) + \beta_f(b/2 + \gamma_m)]^2 - 4\beta_f(\beta_m - \beta_{mf})(b/2 + \gamma_f)(b/2 + \gamma_m)}}{(b/2 + \gamma_m)(b/2 + \gamma_f)} \right] \tag{53}
\end{aligned}$$

Importantly,  $R_0$  is proportional to the environmental carrying capacity of the rodents  $K$ . As  $K$  increases,  $R_0$  also increases and so does the chance of a disease invasion. This relationship between  $R_0$  and  $K$  is a consequence of the assumption of mass action incidence, a reasonable assumption for rodent populations. This result agrees well with what happened in New Mexico in 1993. There, the outbreak of Sin Nombre virus (a hantavirus strain) was associated with increased densities of deer mice *Peromyscus maniculatus*, its primary host.

### 4.3 Vector-Host Models

Vector-host modeling is a fruitful area of research, mainly because many important diseases of humans are transmitted by vectors and especially mosquitoes, but also flies and ticks. Examples include malaria (where the parasite is transmitted from human to human via mosquitoes), bubonic plague (where the parasite is transmitted from rodent to rodent via fleas and occasionally to humans), and Lyme disease (where the parasite is transmitted from deer to deer via ticks and occasionally to humans). Actually, malaria is currently the most frequently modeled vector-borne disease.

Vector-host modeling introduces a new problem, the need to include the population dynamics of the vector. As an illustration, assume an SIS model for the host and an SI model for the vector (vectors rarely recover from the disease but are also rarely affected by it). The four model compartments then consist of susceptible hosts ( $S_H$ ), infectious hosts ( $I_H$ ), susceptible vectors ( $S_V$ ) and infectious vectors ( $I_V$ ). Hosts are infected by contacts with infectious vectors and vectors are in turn infected by contacts with infectious hosts. Let the disease transmission correspond to standard incidence (vectors are assumed to bite a fixed number of hosts per unit time). The vector-host epidemiological model is then as follows:

$$\begin{aligned}
 \frac{dS_H}{dt} &= \mu N_H - \beta_V I_V \frac{S_H}{N_H} - \mu S_H + \gamma I_H \\
 \frac{dI_H}{dt} &= \beta_V I_V \frac{S_H}{N_H} - \mu I_H - \gamma I_H \\
 \frac{dS_V}{dt} &= c N_V - \beta_H S_V \frac{I_H}{N_H} - c S_V \\
 \frac{dI_V}{dt} &= \beta_H S_V \frac{I_H}{N_H} - c I_V
 \end{aligned} \tag{54}$$

where  $N_H = S_H + I_H$  and  $N_V = S_V + I_V$  are total population densities of hosts and vectors, respectively; note that both populations are assumed constant here since births and natural deaths are balanced and there is no disease-induced mortality. Once  $a$  is the per capita bite rate of vectors (the number of bites a vector makes per unit time) and  $p_{HV}$  ( $p_{VH}$ ) is the probability that an infectious vector biting a susceptible host transmits the infection (the probability that an infection is transmitted upon a susceptible vector biting an infectious host), we can write  $\beta_V = ap_{HV}$  and  $\beta_H = (1 - (1 - p_{VH})^a) \approx ap_{VH}$ .

Following the procedure developed by [36], shortly presented as Sect. 5, the basic reproduction number  $R_0$  for model (54) is

$$R_0 = \sqrt{\frac{\beta_H \beta_V N_V}{\mu + \gamma} \frac{N_V}{c N_H}} \quad (55)$$

The biological meaning of  $R_0$  can be readily given. Near the DFE equal to  $(N_H, 0, N_V, 0)$ , each infectious vector produces  $\beta_V(S_H/N_H)/c|_{S_H=N_H}$  new infectious hosts over its mean infectious period  $1/c$ , and each infectious host produces  $\beta_H(S_V/N_H)/(\mu + \gamma)|_{S_V=N_V}$  new infectious vectors over its mean infectious period  $1/(\mu + \gamma)$ . The product gives the total basic reproduction number from vector to vector or from host to host. The square root then represents the geometric mean, i.e. the basic reproduction number for an average individual of both species combined. We get  $R_0 < 1$  if and only if

$$\frac{N_H}{N_V} > \frac{\beta_H \beta_V}{\mu + \gamma c} \quad (56)$$

Therefore, if the ratio of the total host population to the total vector population becomes large, the infection dies out. Intuitively, this is because when there are many hosts (such as humans) relative to vectors (such as mosquitoes), the chance of someone being bitten twice in a quick succession – once to catch the infection and once to pass it on before recovery – is very small. Therefore, for a vector-borne infection to successfully invade the host population, the ratio of vectors to hosts has to be sufficiently large that double bites are common.

Rescaling  $S_H$  as  $s_H = S_H/N_H$ ,  $I_H$  as  $i_H = I_H/N_H$ ,  $S_V$  as  $s_V = S_V/N_V$ ,  $I_V$  as  $i_V = I_V/N_V$ , and setting  $\hat{\beta}_V = \beta_V(N_V/N_H)$  allows us to simplify the model as

$$\begin{aligned} \frac{ds_H}{dt} &= \mu - \hat{\beta}_V i_V s_H - \mu s_H + \gamma i_H \\ \frac{di_H}{dt} &= \hat{\beta}_V i_V s_H - \mu i_H - \gamma i_H \\ \frac{ds_V}{dt} &= c - \beta_H s_V i_H - c s_V \\ \frac{di_V}{dt} &= \beta_H s_V i_H - c i_V \end{aligned} \quad (57)$$

Realizing further that  $s_H = 1 - i_H$  and  $s_V = 1 - i_V$  and inserting these expressions to the second and fourth equations of the model (57), respectively, we end up with just two equations

$$\begin{aligned} \frac{di_H}{dt} &= \hat{\beta}_V i_V (1 - i_H) - \mu i_H - \gamma i_H \\ \frac{di_V}{dt} &= \beta_H (1 - i_V) i_H - c i_V \end{aligned} \quad (58)$$

The last model (58) has two equilibrium points. One is  $(0, 0)$  which corresponds to the DFE ( $s_H = s_V = 1$ ); that is, only the susceptible individuals of both species are present;

$(N_H, 0, N_V, 0)$  is then the DFE of the original unscaled system. The other is the unique endemic equilibrium

$$(i_H^*, i_V^*) = \left( \frac{\beta_H \hat{\beta}_V - c(b + \gamma)}{\beta_H(\hat{\beta}_V + b + \gamma)}, \frac{\beta_H \hat{\beta}_V - c(b + \gamma)}{\hat{\beta}_V(\beta_H + c)} \right) \quad (59)$$

The endemic equilibrium of the original unscaled system is then  $S_H^* = (1 - i_H^*)N_H$ ,  $I_H^* = i_H^*N_H$ ,  $S_V^* = (1 - i_V^*)N_V$ ,  $I_V^* = i_V^*N_V$ , and replacing  $\hat{\beta}_V$  back by  $\beta_V(N_V/N_H)$ . Trivial calculations show that  $i_H^*$  and  $i_V^*$  are always less than 1, and that  $I_H^* = i_H^*N_H$  and  $I_V^* = i_V^*N_V$  are positive as soon as  $R_0 > 1$ . Local stability analysis of the equilibria would then show that

1. if  $R_0 < 1$  then there is only the DFE  $(N_H, 0, N_V, 0)$  which is locally asymptotically stable,
2. if  $R_0 > 1$  then the DFE is unstable and there is a unique endemic equilibrium  $(S_H^*, I_H^*, S_V^*, I_V^*)$  which is locally asymptotically stable.

A number of variations of model (54) exist in the literature. Here we shall briefly present a model of the West Nile virus (WNV) infection developed by [37]. The primary hosts of WNV are birds, especially crows, and the virus is transmitted via mosquitoes of the genus *Culex*. Mammals (e.g. horses and humans) are secondary hosts, generally considered unimportant to disease persistence in the wild. WNV is widespread in Africa, the Middle East and western Asia, with occasional European outbreaks introduced by migrating birds. In North America, the first recorded epidemic was initially detected in the New York state in 1999 and spread rapidly across the continent, with many bird, horse and human deaths left behind. The simplest possible biologically relevant model for WNV transmission contains four compartments for mosquitoes (larvae, susceptible, exposed and infectious adults) and three compartments for birds (susceptible, infectious and recovered birds) and is as follows (see also Fig. 13):

$$\begin{aligned} dS_B/dt &= -abI_M S_B/N_B \\ dI_B/dt &= abI_M S_B/N_B - \mu_V I_B - gI_B \\ dR_B/dt &= gI_B \\ dL_M/dt &= \beta_M(S_M + E_M + I_M) - mL_M - \mu_L L_M \\ dS_M/dt &= -acS_M I_B/N_B + mL_M - \mu_A S_M \\ dE_M/dt &= acS_M I_B/N_B - kE_M - \mu_A E_M \\ dI_M/dt &= kE_M - \mu_A I_M \end{aligned} \quad (60)$$

Parameter values for this model have been extracted primarily for the American crow, *Corvus brachyrhynchos* Brehm, the bird that suffered one of the highest mortalities in the North American WNV epidemic, and for the mosquito *Culex pipiens* ssp., a major North American WNV vector, can be found in [37]. The basic reproduction number equals

$$R_0 = \sqrt{\frac{ab S_M(0)}{\mu_A N_B(0)} \frac{ac}{\mu_V + g} \frac{k}{k + \mu_A}} \approx 0.465 \sqrt{\frac{S_M(0)}{N_B(0)}}$$

using those mean parameter values. As usual, when  $R_0 < 1$  the DFE is locally stable; when  $R_0 > 1$  it is locally unstable, and the disease is able to invade the vector-host system. The virus will therefore invade if  $S_M(0)/N_B(0) > 4.625$ . For New York in 2000, a 40 – 70% reduction of the initial mosquito population, i.e. reducing  $S_M(0)/N_B(0)$  from 7.5 – 15 to less than about 4.6, would have prevented the WNV outbreak. Bird control, however, would have had the opposite effect.

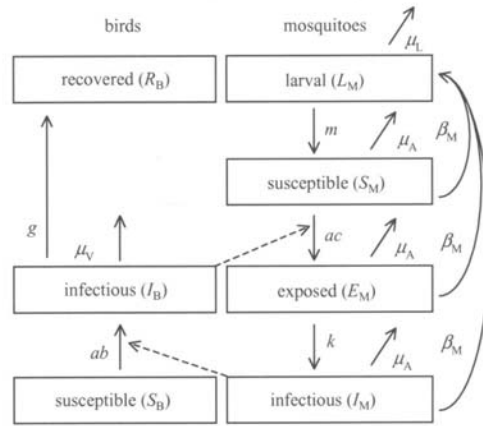


**Fig. 13.** Progression diagram for the West Nile virus model (60). Adapted from Wonham et al. (2004).

#### 4.4 Multi-Host Models: System with Parapoxvirus and the Red versus Gray Squirrel

The gray squirrel was introduced to Europe from America at the beginning of the 20th century. Since then, it has successfully spread across the continent and displaced the red squirrel from much of its home range. Although an innate competitive advantage of the gray squirrel over the red one was found, this advantage was not sufficient to explain the rate of the gray's expansion and the intensity of the red's decline. Parapoxvirus has been postulated to speed up competitive replacement. To test this hypothesis, a two-host disease model is needed. Tompkins et al. [35] considered the following SIR (gray) – SI

(red) model with interspecific competition:

$$\begin{aligned}
 \frac{dS_G}{dt} &= \left( a_G - \frac{N_G + c_R N_R}{K_G} \right) N_G - \beta_{GG} S_G I_G - \beta_{GR} S_G I_R - b_G S_G \\
 \frac{dI_G}{dt} &= \beta_{GG} S_G I_G + \beta_{GR} S_G I_R - \gamma_G I_G - b_G I_G \\
 \frac{dR_G}{dt} &= \gamma_G I_G - b_G R_G \\
 \frac{dS_R}{dt} &= \left( a_R - \frac{N_R + c_G N_G}{K_R} \right) N_R - \beta_{RG} S_R I_G - \beta_{RR} S_R I_R - b_R S_R \\
 \frac{dI_R}{dt} &= \beta_{RG} S_R I_G + \beta_{RR} S_R I_R - b_R I_R - \alpha_R I_R
 \end{aligned} \tag{61}$$

Note that this model is non-spatial so that it is suitable for model squirrel competition only at the level of an individual forest. Application of the parameter values of [35] indeed shows that the red squirrels are replaced by the gray ones faster when parapoxvirus is present in the system relative to when it is absent (Fig. 14).

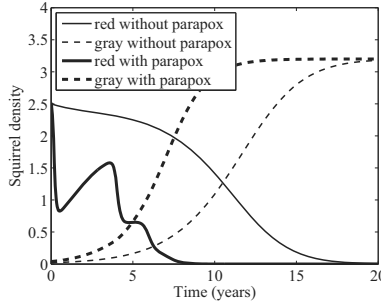


**Fig. 14.** Competition between gray and red squirrels in the presence or absence of the parapoxvirus in the system. Adapted from Keeling and Rohani (2008).

Of course, a more realistic model needs to account for space (to allow exploration of the invasion across Europe) and must be stochastic (as invasions and extinctions involve a low number of individuals). Tompkins et al. [35] developed and simulated such a model as well, clearly showing that parapoxvirus is indeed a potential agent of the observed displacement of the red squirrels by gray ones in Europe. But as we can see, even the simple, non-spatial and deterministic model highlights the importance of parasites in affecting competition.

## 5 Appendix: A Method for Calculating $R_0$

Here we briefly sketch and apply to a more complex epidemiological model the method by van den Driessche and Watmough [36] on calculating the basic reproduction number  $R_0$ . Consider a heterogeneous population whose individuals are distinguishable by age, behavior, spatial position and/or stage of the disease, but nevertheless can be grouped into  $n$  homogeneous compartments. That is, the parameters may vary from compartment to compartment, but are identical for all individuals within a given compartment. Let  $x = (x_1, \dots, x_n)'$ ,  $x_i \geq 0$  for all  $i = 1, \dots, n$ , be the vector of densities of individuals in each compartment. Let us sort the compartments so that the first  $m$  compartments correspond to infected individuals.

In order to compute  $R_0$ , it is important to distinguish new infections from all other changes in the host population. Let  $\mathcal{F}_i(x)$  be the rate of appearance of new infections in compartment  $i$ ,  $\mathcal{V}_i^+(x)$  be the rate of transfer of individuals into compartment  $i$  by all other means, and  $\mathcal{V}_i^-(x)$  be the rate of transfer of individuals out of compartment  $i$ . It is assumed that each function is continuously differentiable at least twice in each variable. Any model of infectious disease dynamics can be formulated as

$$\frac{dx_i}{dt} = f_i(x) = \mathcal{F}_i(x) - \mathcal{V}_i(x), \quad i = 1, \dots, n \quad (62)$$

where  $\mathcal{V}_i(x) = \mathcal{V}_i^-(x) - \mathcal{V}_i^+(x)$  and the functions satisfy some technical yet epidemiologically plausible assumptions described in detail in [36]. These authors showed that if  $x_0$  is the DFE of (62) and  $f_i(x)$  satisfy those technical assumptions, then the derivatives  $D\mathcal{F}(x_0)$  and  $D\mathcal{V}(x_0)$  can be partitioned as

$$\begin{bmatrix} F & 0 \\ 0 & 0 \end{bmatrix} \text{ and } \begin{bmatrix} V & 0 \\ J_3 & J_4 \end{bmatrix}$$

where  $F$  and  $V$  are the  $m \times m$  matrices defined by

$$F = \left[ \frac{\partial \mathcal{F}_i}{\partial x_j}(x_0) \right] \text{ and } V = \left[ \frac{\partial \mathcal{V}_i}{\partial x_j}(x_0) \right] \text{ with } 1 \leq i, j \leq m$$

Moreover,  $F$  is non-negative,  $V$  is invertible with eigenvalues whose real parts are positive, and all eigenvalues of  $J_4$  have positive real part.

Now, consider the fate of an infected individual introduced into compartment  $k$  of a disease-free population. The  $(j, k)$  entry of  $V^{-1}$  is the mean length of time this individual spends in compartment  $j$  during its lifetime, assuming that the population remains near the DFE and barring reinfection. The  $(i, j)$  entry of  $F$  is the rate at which infected individuals in compartment  $j$  produce new infections in compartment  $i$ . Hence, the  $(i, k)$  entry of the product  $FV^{-1}$  is the expected number of new infections in compartment  $i$  produced by the infected individual originally introduced into compartment  $k$ . The matrix  $FV^{-1}$  is usually referred to as the *next generation matrix* for model (62). Setting

$$R_0 = \rho(FV^{-1}) \quad (63)$$

where  $\rho(A)$  denotes the spectral radius of a matrix  $A$  (that is, the eigenvalue of  $A$  with the maximum absolute value), the following theorem of [36] states that  $R_0$  is a threshold

parameter for local stability of the DFE: Consider the disease transmission model given by (62) with  $f_i(x)$  satisfying the above-mentioned technical assumptions. If  $x_0$  is the DFE of this model, then  $x_0$  is locally asymptotically stable if  $R_0 < 1$  and unstable if  $R_0 > 1$ , where  $R_0$  is defined by (63).

As an example, we apply the procedure described above to the following epidemiological model:

$$\begin{aligned}\frac{dS}{dt} &= b(S+I) - (d+d_1N)S - \beta \frac{S(I+Z)}{N} \\ \frac{dI}{dt} &= (1-\sigma)\beta \frac{S(I+Z)}{N} - (d+d_1N)I - \alpha I \\ \frac{dZ}{dt} &= \sigma\beta \frac{S(I+Z)}{N} - (\delta d+d_1N)Z - \alpha Z\end{aligned}\quad (64)$$

This is an SI model of an infection that causes both disease-induced mortality  $\alpha$  as well as reduction in the birth rate – a fraction  $\sigma$  ( $0 \leq \sigma \leq 1$ ) of infectious individuals are assumed to be sterilized due to the disease ( $Z$ ) and the remaining fraction is able to both spread the virus and reproduce ( $I$ ). As the sterilized individuals do not “waste” resources in reproduction, they are assumed to live longer; that is why their intrinsic death rate  $d$  is reduced by a factor  $\delta$  ( $0 < \delta \leq 1$ ). In the absence of infection the total host population density evolves as

$$\frac{dN}{dt} = bN - (d+d_1N)N = rN \left(1 - \frac{N}{K}\right)$$

where  $r = b - d$  and  $K = (b - d)/d_1$ ; this implies the DFE  $(K, 0, 0)$ .

Let us first sort the state variables so that the first two of them represent infected classes:  $(I, Z, S)$ . We have

$$\mathcal{F} = \begin{bmatrix} (1-\sigma)\beta S(I+Z)/N \\ \sigma\beta S(I+Z)/N \\ 0 \end{bmatrix}, \mathcal{V} = \begin{bmatrix} (d+d_1N)I + \alpha I \\ (\delta d+d_1N)Z + \alpha Z \\ -b(S+I) + (d+d_1N)S + \beta S(I+Z)/N \end{bmatrix}$$

as only the transmission terms generate new infections in the model (64). This implies

$$F = \beta \begin{bmatrix} 1-\sigma & \sigma \\ 1-\sigma & \sigma \end{bmatrix}, V = \begin{bmatrix} b+\alpha & 0 \\ 0 & b-(1-\delta)d+\alpha \end{bmatrix}$$

and hence

$$FV^{-1} = \beta \begin{bmatrix} (1-\sigma)/(b+\alpha) & (1-\sigma)/(b-(1-\delta)d+\alpha) \\ \sigma/(b+\alpha) & \sigma/(b-(1-\delta)d+\alpha) \end{bmatrix}$$

of which the maximum (in the absolute value) eigenvalue, equal to  $R_0$ , is

$$R_0 = \frac{\beta}{2} \left( \frac{1-\sigma}{b+\alpha} + \frac{\sigma}{b-(1-\delta)d+\alpha} \right)$$

Note that  $R_0$  is independent of  $d_1$ , the strength of negative density dependence in the natural mortality rate of hosts. We can deduce that the first term of  $R_0$  is the contribution of those infectives that stay fertile, while the latter is due to those infectives that become sterilized, and  $R_0$  is the average of the two.

## References

1. Allen, L. J. S., R. K. McCormack and C. B. Jonsson. 2006. Mathematical models for hantavirus infection in rodents. *Bulletin of Mathematical Biology* 68:511–524.
2. Anderson, R. M. and R. M. May. 1979. Population biology of infectious diseases: part I. *Nature* 280:361–367.
3. Bacaër, N. and M. G. M. Gomes. 2009. On the final size of epidemics with seasonality. *Bulletin of Mathematical Biology* 71:1954–1966.
4. Begon, M., M. Bennett, R. G. Bowers, N. P. French, S. M. Hazel and J. Turner. 2002. A clarification of transmission terms in host-microparasite models: numbers, densities and areas. *Epidemiology and Infection* 129:147–153.
5. Bennett, P. M. and I. P. F. Owens. 2002. *Evolutionary ecology of birds*. Oxford University Press, Oxford.
6. Blower, S. M., H. B. Gershengorn and R. M. Grant. 2000. A tale of two futures: HIV and antiretroviral therapy In San Francisco. *Science* 287:650–654.
7. Brauer, F. 2005. The Kermack-McKendrick epidemic model revisited. *Mathematical Biosciences* 198:119–131.
8. Brauer, F. 2008. Compartmental models in epidemiology. *in* F. Brauer, P. van den Driessche and J. Wu, eds. *Mathematical epidemiology*. Springer.
9. Brauer, F., P. van den Driessche and J. Wu. 2008. *Mathematical epidemiology*. Springer.
10. Busenberg, S. and P. van den Driessche. 1990. Analysis of a disease transmission model in a population with varying size. *Journal of Mathematical Biology* 28:257–270.
11. Courchamp, F., L. Berec and J. Gascoigne. 2008. *Allee effects in ecology and conservation*. Oxford University Press, Oxford.
12. Daszak, P., A. A. Cunningham and A. D. Hyatt. 2000. Emerging infectious diseases of wildlife – threats to biodiversity and human health. *Science* 287:443–449.
13. Deredec, A. and F. Courchamp. 2003. Extinction thresholds in host-parasite dynamics. *Annales Zoologici Fennici* 40:115–130.
14. Deredec, A. and F. Courchamp. 2006. Combined impacts of Allee effects and parasitism. *Oikos* 112:667–679.
15. Eilers, J. 1995. Fat and eggs: an alternative method to measure the trade-off between survival and reproduction in insect parasitoids. *Netherlands Journal of Zoology* 46:227–235.
16. Fenton, A., J. P. Fairbairn, R. Norman and P. J. Hudson. 2002. Parasite transmission: reconciling theory and reality. *Journal of Animal Ecology* 71:893–905.
17. Gao, L. Q. and H. W. Hethcote. 1992. Disease transmission models with density-dependent demographics. *Journal of Mathematical Biology* 30:717–731.
18. Gao, L. Q., J. Mena-Lorca and H. W. Hethcote. 1995. Four SEI endemic models with periodicity and separatrices. *Mathematical Biosciences* 128:157–184.
19. Hethcote, H. W. 2000. The mathematics of infectious diseases. *SIAM Review* 42:599–653.
20. Keeling, M. J. and P. Rohani. 2008. *Modeling infectious diseases in humans and animals*. Princeton University Press.
21. Kelly, A., A. M. Dunn and M. J. Hatcher. 2001. Population dynamics of a vertically transmitted, parasitic sex ratio distorter and its amphipod host. *Oikos* 94:392–402.
22. Knell, R. J., M. Begon and D. J. Thompson. 1998. Transmission of *Plodia interpunctella* granulosis virus does not conform to the mass action model. *Journal of Animal Ecology* 67:592–599.
23. Lafferty, K. D. 1993. Effects of parasitic castration on growth, reproduction and population dynamics of the marine snail *Cerithidea californica*. *Marine Ecology Progress Series* 96:229–237.

24. Li, M. Y., J. R. Graef, L. Wang and J. Karsai. 1999. Global dynamics of a SEIR model with varying total population size. *Mathematical Biosciences* 160:191–213.
25. Lockhart, A. B., P. H. Thrall and J. Antonovics. 1996. Sexually transmitted diseases in animals: ecological and evolutionary implications. *Biological Reviews* 71:415–471.
26. McCallum, H., N. Barlow and J. Hone. 2001. How should pathogen transmission be modelled? *Trends in Ecology & Evolution* 16:295–300.
27. Mena-Lorca, J. and H. W. Hethcote. 1992. Dynamic models of infectious diseases as regulators of population sizes. *Journal of Mathematical Biology* 30:693–716.
28. Mena-Lorca, J., J. X. Velasco-Hernandez and C. Castillo-Chavez. 1999. Density-dependent dynamics and superinfection in an epidemic model. *IMA Journal of Mathematics Applied in Medicine and Biology* 16:307–317.
29. Newey, S. and S. Thirgood. 2004. Parasite-mediated reduction in fecundity of mountain hares. *Proceedings of the Royal Society of London B* 271:S413–S415.
30. O’Keefe, K. J. and J. Antonovics. 2002. Playing by different rules: the evolution of virulence in sterilizing pathogens. *American Naturalist* 159:597–605.
31. Otto, S. P. and T. Day. 2007. *A biologist’s guide to mathematical modeling in ecology and evolution*. Princeton University Press, Princeton and Oxford.
32. Ryder, J. J., M. R. Miller, A. White, R. J. Knell and M. Boots. 2007. Host-parasite population dynamics under combined frequency- and density-dependent transmission. *Oikos* 116:2017–2026.
33. Thomas, F., A. T. Teriokhin, F. Renaud, T. D. Meeus and J. F. Guegan. 2000. Human longevity at the cost of reproductive success: evidence from global data. *Journal of Evolutionary Biology* 13:409–414.
34. Thomas, F., J. Moore, R. Poulin and S. Adamo. 2007. Parasites that manipulate their hosts. *in* M. Tibayrenc, ed. *Encyclopedia of Infectious Diseases: Modern Methodologies*. John Wiley & Sons, Inc.
35. Tompkins, D. M., A. R. White and M. Boots. 2003. Ecological replacement of native red squirrels by invasive greys driven by disease. *Ecology Letters* 6:189–196.
36. van den Driessche, P. and J. Watmough. 2002. Reproduction numbers and sub-threshold endemic equilibria for compartmental models of disease transmission. *Mathematical Biosciences* 180:29–48.
37. Wonham, M. J., T. de Camino-Beck and M. A. Lewis. 2004. An epidemiological model for West Nile virus: invasion analysis and control applications. *Proceedings of the Royal Society of London B* 271:501–507.

# Spatio-temporal modelling of air pollution

Daniela Cocchi<sup>1</sup>, Francesca Bruno<sup>1</sup>, Fedele Greco<sup>1</sup>, Carlo Trivisano<sup>1</sup>

<sup>1</sup> Department of Statistics, Faculty of Statistics, University of Bologna,  
via delle Belle Arti 41, 40126 Bologna, Italy

**Abstract.** In this paper two examples of spatio-temporal modeling of air pollution data are illustrated. In the first one, the attention focuses on the issue of separability while in the second, under the separability hypothesis, the emphasis is on the advantages of the hierarchical specification of a space-time model. The motivating examples of the two ways of modeling came from the same region and concern, respectively, daily ozone and PM10 concentration.

**Keywords:** air pollution data, Hierarchical Bayesian models, ozone, particulate matter, separability, spatio-temporal models

## 1. Introduction

Quantitative analysis of air pollution data has a long tradition. This kind of data very often comes from dedicated monitoring sites equipped by devices that measure, by means of techniques that may be not completely standardized across a territory, the level of pollutants, each one separately. The location of the monitoring sites is decided by local authorities and follows national and international directives. Summaries of these data, and subsequent models for interpolating and forecasting not necessarily rely on statistics. Deterministic models based on ideas coming from chemistry or physics can constitute a very effective tool for helping in decisions, without keeping the randomness due to variability and uncertainty into account, where variability represents a natural characteristics of phenomena and uncertainty can be reduced by means of suitable statistical models relying on probability.

Data on air pollution have the peculiarity of being collected at different locations and along times, so spatial and spatio-temporal models are a natural way for analysis. Non-homogeneity of spatial and time data sets and missing data are typical problems in this context. Data are collected with methods that are born in laboratories but suffer of the measurement errors and the confounding issues typical of observational data. They are collected for reasons that are almost administrative, and the values they

---

<sup>1</sup> The research leading to this paper has been partially funded by a 2008 grant (Project no. 2008CEFF37-001, sector 13: Economics and Statistics) for research of national interest by the Italian Ministry of the University and Scientific and Technological Research.

assume may be influenced by human activities and natural environmental chemical reactions.

Trends detection is fundamental for monitoring the state of the environment. The analysis of the spatio-temporal trend, or expected value, is typical of the investigation of large-scale variation; for small-scale variability the focus is rather on the spatio-temporal covariance, or correlation function. A common purpose of this data collection is, however, monitoring the effects on human and animal health, the possible effects on biodiversity and forecasting

The most commonly analyzed pollutants are CO, SO<sub>2</sub>, particulate matter, O<sub>3</sub>, NO<sub>x</sub>, but, because of their danger on human health, also data on benzene and other carcinogenic pollutants are being extensively collected.

The behavior of ozone is frequently explored in these studies, see for instance [1], [2] and [3]. This secondary pollutant, even if not catastrophic for human health, is important as a benchmark for monitoring more complex pollution situations.

The way of collecting data on air pollution is continuously evolving. The example of particulate matter is worth to be mentioned: in current air pollution studies, it is measured by weighting. Since it was discovered, along years, that the finest particulate is the most harmful for health, the measurements of interest changed from total suspended particulate TSP, to PM<sub>10</sub> [4], then to PM<sub>2.5</sub> [5] and ever finer particles. Other types of studies, rather, investigate the compositions of different sizes of particulate along vertical profiles [6].

Studies on single pollutants will be presented. However, the most promising studies concern the effect of interactions between pollutants on human health [7]. Information on meteorology may also be included in studies on air pollution: this ought to reduce the uncertainty of the model, mainly for prediction and be successful in taking confounding effects into account [8].

In what follows two examples of spatio-temporal modeling of air pollution data will be given. In the first one [9], the attention focuses on the issue of separability while in the second [10], under the separability hypothesis, the emphasis is on the advantages of the hierarchical specification of a space-time model. The motivating examples of the two ways of modeling came from the same region and concern, respectively, daily ozone and PM<sub>10</sub> concentration.

## **2. Spatio-temporal non-separable models**

For studying a spatio-temporal process, the hypothesis of normality is frequently assumed. Data transformations (like square root, logarithm or Box-Cox transformations) are proposed in order to be allowed to use the Gaussian model, that is very convenient since it is fully defined by its first two moments.

The construction of a suitable model for the covariance is the tool for embodying both the temporal and spatial components [11]. The estimation of space-time covariance models is facilitated by simplifying assumptions that ought to be proposed and tested. The simplest models assume therefore spatio-temporal stationarity, and the separability of spatial and temporal components. A further simplifying assumption is isotropy.

A spatio-temporal random field  $Z(t, \mathbf{x})$  is considered to be strictly stationary within its space-time domain  $T \times S$  if its spatio-temporal law is invariant under translations. A more restrictive property based on moments of the spatio-temporal process is second-order stationarity, involving only the first two moments of the spatio-temporal random field  $Z(t, \mathbf{x})$ : the mean function is modelled as a constant, and the space-time covariance function is assumed to depend exclusively on the spatial and temporal lags. Strict stationarity alone implies second order stationarity if the first two moments exist, whereas second-order stationarity only implies strict stationarity if the  $Z(t, \mathbf{x})$  random field has a Gaussian distribution.

Isotropy is an additional assumption of stationarity about the spatial component of the spatio-temporal correlation function, when it does not depend on direction but only on distance. Appropriate adjustments are often made to the coordinate system, such that the correlation structure may be considered isotropic [12], [13].

A spatio-temporal model is separable if its space-time covariance function can be expressed as a product of two functions: a function of space and a function of time. The first contribution about non-separability is due to [14], who used an approach based on Fourier transforms. Then [15] proposed a general class of non-separable, stationary covariance functions for spatio-temporal random fields directly in the space-time domain (via a construction not based on the inversion of a Fourier transformation). These two contributions share one important feature: the assumption of stationarity in both time and space. A number of statistical tests for separability have been proposed, based on parametric models [16], likelihood ratio tests and subsampling [17], or spectral methods [18] and [19].

## 2.1 A general spatio-temporal model

A general model for spatio-temporal data  $\{Y(t, \mathbf{x})\}$  measured in discrete time ( $t = 1, \dots, T$ ) and continuous space ( $x \in \mathfrak{R}^2$ ) may be formulated as follows:

$$Y(t, \mathbf{x}) - \mu(t, \mathbf{x}) = Z(t, \mathbf{x}) = W(t, \mathbf{x}) + \varepsilon(t, \mathbf{x}) \quad (1)$$

where  $\mu(t, \mathbf{x})$  is the spatio-temporal mean field or trend, and the stochastic component is a single term  $Z(t, \mathbf{x}) = W(t, \mathbf{x}) + \varepsilon(t, \mathbf{x})$ , with zero-mean, while the spatio-temporal correlation function is still to be specified. The component  $W(t, \mathbf{x})$  is a zero-mean smooth Gaussian spatio-temporal underlying process, and  $\varepsilon(t, \mathbf{x})$  is an independent zero-mean random-error term. Model (1) has three independent additive components  $\mu$ ,  $W$  and  $\varepsilon$ .

Due to this independence, model estimation is usually performed component-wise. A) In some cases the focus is on trend estimation: generally speaking, the mean component can be viewed as deterministic or stochastic. When covariates are available, a regression-type estimator may effectively represent the trend component [8]. When there is no specific focus on trend detection, and no covariate is available, a trend component may be expressed as a simple function of spatial coordinates. B)

When interest is on the spatio-temporal structure, the process  $Z(t, \mathbf{x})$  is analyzed. Separable spatio-temporal models are relatively easy to estimate, but situations requiring non-separable models are very common. Non-separability may arise from process non-stationarity.

The original process  $Z$  can be expressed, via an appropriate transformation, as a function of a separable process  $Z^*(t, \mathbf{x})$ :  $Z(t, \mathbf{x}) = f(Z^*(t, \mathbf{x}))$ . For a separable process  $V$ , the spatio-temporal correlation function is the product:

$$\text{Corr}(V(t, \mathbf{x}), V(t', \mathbf{x}')) = \rho_1(|t - t'|) \rho_2(\|\mathbf{x} - \mathbf{x}'\|) \quad t, t' = 1, \dots, T, \quad \mathbf{x}, \mathbf{x}' \in \mathfrak{R}^2 \quad (2)$$

and  $\rho_1$  and  $\rho_2$  are, respectively, functions of time and space only.

A way for modelling spatio-temporal processes starts from the specification of their spatio-temporal correlation function. This is particularly suitable when the removal of temporal non-stationarity leads to a separable spatio-temporal correlation function.

## 2.1 Ozone in Emilia Romagna, Po Valley

Following a conjecture about the spatio-temporal distribution of ozone in a region of the Po valley, we explored [9] the idea of non-separability due to temporal non-stationarity through the transformation:

$$Y(t, \mathbf{x}) - \mu(t, \mathbf{x}) = \sigma_{\langle t \rangle, \mathbf{x}} Z^*(t, \mathbf{x}); \quad t = 1, \dots, T, \quad \mathbf{x} \in \mathfrak{R}^2 \quad (3)$$

leading to  $Z(t, \mathbf{x})$  in the spatio-temporal model (1). In (3), the multiplicative parameter  $\sigma_{\langle t \rangle, \mathbf{x}}$  represents the component of non-stationary temporal variability which, when removed, leads to separable space and time correlation components. The subscript  $\langle t \rangle$  denotes an empirically derived temporal reference set for this scale parameter, and the subscript  $\mathbf{x}$  denotes the spatial coordinates at each site.

Let us assume that a large-scale temporal process underlies the separable spatio-temporal process  $Z^*(t, \mathbf{x})$  in (3), which can be further modelled as a combination of simpler processes:

$$Z^*(t, \mathbf{x}) = \beta_{\mathbf{x}} Z_1(t) + Z_2(t, \mathbf{x}) \quad t = 1, \dots, T, \quad \mathbf{x} \in \mathfrak{R}^2 \quad (4)$$

a time-dependent process, that applies over the entire spatial domain, denoted by  $Z_1(t)$ , and a temporally uncorrelated space-time process,  $Z_2(t, \mathbf{x})$ , which is suitable when the spatio-temporal process does not radically change with time, *i.e.* when it displays similar temporal structures across space;  $\beta_{\mathbf{x}}$  is a site-specific coefficient for the process  $Z_1(t)$  that may vary from site to site.

Anisotropy, can be removed by deformation analysis, see [12] and [13]. Deformation may be applied to  $Z^*(t, \mathbf{x})$ , when the spatio-temporal model considered is (3), or to  $Z_2(t, \mathbf{x})$ , when model (4) is assumed.

In our work on tropospheric ozone in a sub-region of the Italian Po Valley [9], we detected a high spatial correlation structure, similar temporal structures along space and strong persistence as temporal lags increase. This agrees with other studies on fine particulate in the same region [10], confirming that the area may be perceived, for geographical, meteorological and anthropic reasons, as a part of a unique metropolitan area covering the entire Po Valley.

The data set at disposal consists of tropospheric ozone measurements from 31 monitoring stations situated throughout the Emilia-Romagna Region of Italy. Ozone concentrations are measured on a daily time scale, expressed in terms of daily maximum 8-h moving averages computed from hourly ozone concentration data recorded in micrograms per cubic meter,  $\mu\text{g}/\text{m}^3$ , over a five-year period (between 1998 and 2002).

The trend component  $\mu(t, \mathbf{x})$  in (1) is estimated using a Median Polish algorithm, and includes a seasonal effect, meaning that the annual ozone cycle is very important, a yearly effect and a spatial effect. The seasonal cycle shows higher values during the summer days, and lower values during colder winter days. The year effect seems to be slightly decreasing over the five-year period considered. The spatial effect underlies higher values in the central area of the region, corresponding to Bologna, the largest city in the entire area.

The decreasing behavior of the spatio-temporal correlation function is modelled exponentially, as a function of spatial lag  $\mathbf{d}$  that can be defined as in (2) for each temporal lag  $l$  (currently  $l=1, \dots, 3$ , since temporal correlations fall near to zero beyond 3 days), as follows:

$$\text{Corr}(l, \mathbf{d}) = \alpha_l \cdot \exp(-\mathbf{d}/\theta_l) \quad (5)$$

The two coefficients  $\alpha_l$  and  $\theta_l$  are estimated for each lag and for each spatio-temporal process.

After the estimation of  $\sigma_{(l), \mathbf{x}}$ , an empirical check is performed to assess whether a separable spatio-temporal process  $Z^*(t, \mathbf{x})$  has been obtained. This is performed checking whether the ARMA model that better fits every spatial point have the same parameters. Indeed, an ARMA(1,1) with very similar parameters was obtained, that indicates the spatial invariance of the structure in time.

The empirical check of the invariance of the temporal correlation structure in space suggests a spatio-temporal process  $Z^*(t, \mathbf{x})$  as in (3), with separable spatio-temporal correlation function (2); the temporal correlation  $\rho_1$  is expressed as an ARMA(1,1) autocorrelation function found to be suitable, whereas for the spatial correlation function  $\rho_2$  we retain the exponential model (5).

The  $Z^*(t, \mathbf{x})$  process is then decomposed in the process  $Z_1(t)$  using a principal component analysis and the  $Z_2(t, \mathbf{x})$  is finally estimated. Removal of the large scale process  $Z_1(t)$  overcomes the correlation for large distances, leading to correlations that tend towards zero within the spatial range of the data.

### 3. Separable spatio-temporal hierarchical modeling

Hierarchical modeling is a different way for managing spatio-temporal data. The aspects that can be underlined are again the detection of long-term space and time trends, the consideration of confounding effects and measurement errors, adjustment for missing data, prediction for locations where data are not available. Meteorological variables can be also considered. Different forms of variability, due respectively to space, time, presence of specific meteorological conditions can be modeled and assessed: each component can be attributed to relatively simple sub-models that together constitute a complex general model [20].

#### 3.1 A general separable hierarchical space-time model

Consider a pollutant ( $Y$ ) observed at  $S$  spatial locations and  $T$  time points, and a set of  $p$  meteorological variables ( $M$ ) and  $q$  spatially varying constant in time explanatory variables ( $X$ ). In a three stage hierarchical model [10], the first stage specifies a measurement error model for the observed pollutant level, the second stage deals with temporal and spatial modelling, while the final stage completes the Bayesian formulation by specifying hyperpriors on the hyperparameters.

Let  $\mathbf{Y}_{t,\bullet}$  denote the  $S$ -dimensional vector of observed pollutant concentrations at day  $t$  ( $t=1, \dots, T$ ). At the first level of the hierarchy, observations are modelled as independently distributed under the assumption of normality:

$$\mathbf{Y}_{t,\bullet} | \boldsymbol{\mu}_{t,\bullet}, \boldsymbol{\sigma}_{t,\bullet}^2 \sim MVN\left(\boldsymbol{\mu}_{t,\bullet}, \text{diag}(\boldsymbol{\sigma}_{t,\bullet}^2)\right) \quad (6)$$

Let  $\mathbf{M}_{t,\bullet}$  denote the  $p \times S$  matrix covariates varying in time  $t$  ( $t=1, \dots, T$ ) for the  $S$  spatial locations and let  $\mathbf{X}$  be the  $q \times S$  matrix of the constant-in-time spatial covariates:

$$\boldsymbol{\mu}_{t,\bullet} = \mathbf{X}'\boldsymbol{\gamma} + \mathbf{M}_{t,\bullet}'\boldsymbol{\beta}_{t,\bullet} + \theta_t \mathbf{1}_s + \boldsymbol{\varepsilon}_{t,\bullet} \quad (7)$$

where  $\boldsymbol{\gamma}$  and  $\boldsymbol{\beta}_{t,\bullet}$  are respectively  $q \times 1$  and  $p \times 1$  vectors of coefficients,  $\mathbf{1}_s$  is a  $s$ -dimensional unit vector,  $\boldsymbol{\mu}_{t,\bullet}$  denotes the  $S$ -dimensional vector of pollutant mean levels at day  $t$ ,  $\theta_t$  and  $\boldsymbol{\varepsilon}_{t,\bullet}$  are respectively temporal and spatial random effects. In this model  $\boldsymbol{\sigma}_{t,\bullet}^2 = (\sigma_1^2, \sigma_2^2, \dots, \sigma_s^2)$  represents the vector of residual variances in the  $S$  monitoring sites. The error variance does not depend on time, while different

monitoring sites are allowed to have different unexplained variances, *i.e.* different measurement errors. In (6) and (7) data are viewed as a time series of spatial processes.

With regard to  $\beta$ , the most general model is characterised by coefficients varying in space and time, see [21] and [22] for a detailed discussion. The vector of parameters  $\gamma$  models the overall site-specific mean, according to site-specific constant-in-time features and capture the overall mean level at each monitoring site, without effect on the temporal dynamics.

Spatial and temporal dependence which remains unexplained by the relationship with explanatory variables is modelled at the second level of the hierarchy by means of the temporal random effect  $\theta_t$  and the spatial random effects  $\epsilon_{t,s}$ . At each time  $t$ , data are generated from the same spatial process while, at each location  $s$ , each time series is generated from the same temporal process. Modelling space and time independently allows a straightforward evaluation of the sources of variability of the pollutant generating process.

Parameters  $\theta$  model the residual temporal dynamics characterising the pollutant generating process, once the effect of meteorological conditions has been accounted for, by a random walk model, as a first-order smoothing non-stationary temporal model:

$$\theta_t = \theta_{t-1} + \omega_t, \quad \omega_t \sim N(0, \sigma_\omega^2) \quad (8)$$

Equations (6)-(8) have a representation in terms of dynamic linear models [23]. With regard to spatial modelling, the terms  $\epsilon_{t,s}$  in equation (7) represent spatially correlated random effects: at each time  $t$ , the random effects  $\epsilon_{t,\bullet} = (\epsilon_{t,1}, \epsilon_{t,2}, \dots, \epsilon_{t,S})$  follow a multivariate normal distribution with mean vector  $\mathbf{0}_S$  and  $S \times S$  correlation matrix  $\Sigma$ :

$$\epsilon_{t,\bullet} | \sigma_\epsilon^2, \Sigma \sim MVN(\mathbf{0}_S, \sigma_\epsilon^2 \Sigma) \quad (9)$$

Parameter  $\sigma_\epsilon^2$  plays the role of between-site variance. The  $ss'$  entry of the correlation matrix denotes the correlation between sites  $s$  and  $s'$ , and can be specified in several ways, as a function of the decay of correlation with distance. A popular correlation function is the exponential:

$$\Sigma_{ss'} = \exp(-\phi d_{ss'})$$

This covariance model is isotropic, since the correlation between two generic sites depends only on the distance between them. The logarithm of the correlation is a linearly decreasing function of distance  $d_{ss'}$ . The parameter  $\phi > 0$  describes the decay rate of correlation as a function of distance. This spatial structure is assumed constant over time, the underlying assumption being that spatial and temporal processes are separable.

A constraint is needed for model identifiability, because of the simultaneous presence of the random effects  $\theta$  and  $\epsilon$ , in this case a zero mean constraint on the spatial random effects at each time  $t$ . With this parameterisation, parameters  $\theta_t$ 's can

be viewed as time dependent intercepts capturing the regional mean pollutant level,  $\varepsilon_{ts}$  is the deviation from the regional mean at day  $t$  for the site  $s$ , due to the spatial process unexplained by the dependence on the explanatory variables.

In the Bayesian framework, model hierarchy is completed by the specification of prior probability distributions for parameters and hyperparameters. If, at the second stage, a model is proposed for the regression coefficients, then hyperpriors are needed for model hyperparameters. As regards spatial and temporal model hyperparameters, a prior distribution is needed for parameters  $\sigma_\theta^2$ ,  $\sigma_\varepsilon^2$  and  $\phi$ .

Inference about the parameters of interest is based on their posterior distribution given the data. These posterior distributions are seldom available in analytical form because of the complexity of the probability distributions involved and have to be approximated via MCMC algorithms.

This modelisation allows for assessing the contribution of the spatial and temporal components together with that of meteorological variables to total variability. We used an approach that follows [24] for decomposing the variability of the complete hierarchical model by means of the relationship:

$$E[V(\boldsymbol{\mu}_s | \mathbf{Y})] = E\left[V(\boldsymbol{\theta} | \mathbf{Y}) + V(\mathbf{M}'_{s'}\boldsymbol{\beta} | \mathbf{Y}) + V(\boldsymbol{\varepsilon}_s | \mathbf{Y}) + \right. \\ \left. + Cov(\boldsymbol{\theta}, \boldsymbol{\varepsilon}_s | \mathbf{Y}) + Cov(\boldsymbol{\theta}, \mathbf{M}'_{s'}\boldsymbol{\beta} | \mathbf{Y}) + Cov(\mathbf{M}'_{s'}\boldsymbol{\beta}, \boldsymbol{\varepsilon}_s | \mathbf{Y})\right]$$

The proposed model permits also the spatial prediction at unmonitored sites, possible after a suitable interpolation of meteorological covariates for that site. Sampling is performed from the posterior predictive distribution

$$\mu_{ts'} | \mathbf{Y} = \mathbf{X}'_{s'}(\boldsymbol{\gamma} | \mathbf{Y}) + \mathbf{M}'_{ts'}(\boldsymbol{\beta} | \mathbf{Y}) + (\theta_t | \mathbf{Y}) + (\varepsilon_{ts'} | \mathbf{Y})$$

where  $\mathbf{X}'_{s'}$  and  $\mathbf{M}'_{ts'}$  are respectively space varying constant-in-time and space-time-varying covariates observed at site  $s'$ .

### 3.2 Particulate in Emilia Romagna, Po Valley

The model has been applied [10] to daily mean PM<sub>10</sub> concentrations measured at 11 monitoring sites located in the main cities of the Italian Emilia-Romagna Region from January 1<sup>st</sup> 2000 to December 31<sup>st</sup> 2002. Data have been logarithmically transformed to obtain a symmetric distribution for each monitoring site and to stabilize the mean-variance relationship. A strong correlation among site measurements occurred, ranging from 0.86 for the nearest sites to 0.6 for those further away. A strong correlation between distant monitoring sites time series remains: a considerable amount of the between-sites correlation is due to the common temporal dynamics of the data.

Meteorological variables for each site are obtained from a meteorological forecasting model. In this way, homogeneous covariates for the spatial detail of the PM<sub>10</sub> monitoring sites are available, thus avoiding the problem of spatial misalignment as well as missing values in covariates. In the model we used daily

mean mixing height ( $MH$ ) and daily mean wind speed ( $WS$ ). The dependence of  $PM_{10}$  levels on  $MH$  has a physical explanation since, when  $MH$  is low, the particulate matter does not spread throughout the atmosphere, and thus a negative relationship is expected between  $MH$  and  $PM_{10}$ .

If  $Y_{ts}$ ,  $MH_{ts}$  and  $WS_{ts}$  denote, respectively, the log of  $PM_{10}$  concentration, the mixing height and the wind speed at spatial location  $s$  ( $s=1, \dots, 11$ ) on day  $t$  ( $t=1, \dots, 1096$ ), and  $(C_{1s}, C_{2s})$  are the spatial coordinates of site  $s$ , equation (7) is specified as:

$$\mu_{ts} = \gamma_1 Z_s + \gamma_2 C_{1s} + \gamma_3 C_{2s} + \beta_1 MH_{ts} + \beta_2 WS_{ts} + \theta_t + \varepsilon_{ts}.$$

where the variable  $Z$  is defined as follows:  $Z_s = 1$  if the site  $s$  is a background urban area like a park, otherwise  $Z_s = -1$ . Parameters  $\gamma_2$  and  $\gamma_3$  capture the large-scale spatial trend, while coefficients  $\beta_1$  and  $\beta_2$  capture the dependence of log- $PM_{10}$  concentrations on the considered meteorological variables. The isotropy assumption does not seem to be overly restrictive, since the meteorology of the Po Valley Region is spatially stable. Model hierarchy is completed by the prior specification of the hyperparameters distributions.

The posterior distributions of model parameters  $\gamma_2$  and  $\gamma_3$  indicate a decreasing spatial trend in North-South and West-East directions. A negative relationship has been estimated between the meteorological variables and the level of  $PM_{10}$  concentrations. Using the original scale of meteorological variables, when  $MH$  increases by 100  $m$ , there is an estimated decrease of 0.02 in  $PM_{10}$  concentrations (in the log scale); whereas when  $WS$  increases by 1  $m/s$ , a decrease of 0.04 in  $PM_{10}$  concentrations (on the log scale) is estimated.

As regards the decomposition of the overall model variance  $E[V(\boldsymbol{\mu}_s | \mathbf{Y})]$  it is mainly attributable to the time process  $\boldsymbol{\theta}$ , which accounts for about 68% of the total explained variance. Spatial random effects account for a smaller portion of variability (about 18%), while the contribution of meteorological variables is about 5%. Covariances between spatial, temporal and meteorological components are negligible.

Analogously to ozone concentration studied in Section 2, the observed time series can be broadly thought of as replications of the same temporal process, with a weak large-scale spatial trend and a spatial correlation that, for  $PM_{10}$ , vanishes altogether at a distance of 90  $km$ . This feature is the premise for a good predictability in non sampled sites: the generating process is quite homogeneous within the study region.

## References

1. Cox, W.M., Chu, S.: Meteorologically adjusted ozone trends in urban areas: a probabilistic approach. *Atmos Environ* 27, 425–434 (1993)

2. Guttorp, P., Meiring, W., Sampson, P.D.: A space-time analysis of ground-level ozone data. *Environmetrics*, 5, 241–254 (1994)
3. Huerta, G., Sanso, B., Stroud, J.R.: A spatiotemporal model for Mexico City ozone levels. *Applied Statistics*, 53, 231–248 (2004)
4. Harrison, R., Stedman, J., Derwent, D.: New directions: Why are PM10 concentrations in Europe not falling? *Atmos. Environ.* 42, 603–606 (2008)
5. Smith, R.L., Kolenikov, S., Cox, L.H.: Spatio-temporal modelling of PM2.5 data with missing values. *Journal of Geophysical Research* 108, D24 (2003).
6. Ferrero, L., Perrone, M. G., Petraccone, S., Sangiorgi, G., Ferrini, B. S., Lo Porto, C., Lazzati, Z., Cocchi, D., Bruno, F., Greco, F., Riccio, A., and Bolzacchini, E.: Vertically-resolved particle size distribution within and above the mixing layer over the Milan metropolitan area, *Atmos. Chem. Phys.*, 10, 3915-3932, doi:10.5194/acp-10-3915-2010 (2010)
7. Samet, M. (Ed.): *The National Morbidity, Mortality, and Air Pollution Study*. Health Effect Institute, Cambridge, MA (2000).
8. Carroll, R.J., Chen, R., George, E.I., Li, T.H., Newton, H.J., Schmiediche, H., Wang, N., Ozone exposure and population density in Harris County, Texas, *J Am Stat Assoc* 92, 392–404 (1997)
9. Bruno, F., Guttorp, P., Sampson, P. D., Cocchi, D.: A simple non-separable, non-stationary spatiotemporal model for ozone, *Environ Ecol Stat*, 16, 515–529 (2009)
10. Cocchi, D., Greco, F., Trivisano C.: Hierarchical space-time modelling of PM10 pollution, *Atmospheric Environment*, 41, 532–541 (2007)
11. Cressie, N.: *Statistics for Spatial Data*, (2nd ed.) New York: Wiley (1993)
12. Sampson, P.D., Guttorp, P., Nonparametric estimation of nonstationary spatial covariance structure. *J Am Stat Assoc* 87, 108–119 (1992)
13. Damian, D., Sampson, P.D., Guttorp, P.: Bayesian estimation of semi-parametric non-stationary spatial covariance structure. *Environmetrics*, 12, 161–176 (2000)
14. Cressie, N., Huang, H.C.: Classes of nonseparable, spatio-temporal stationary covariance functions. *J Am Stat Assoc*, 94, 1330–1340 (1999)
15. Gneiting, T.: Nonseparable, stationary covariance functions for space-time data. *J Am Stat Assoc*, 97, 590–600 (2002)
16. Roberts, G.O., Kareson, K., Brown, P., Tonellato, S.: Blur-generated non-separable space-time models, *J R Stat Soc, Ser B*, 62, 847–860 (2000)
17. Mitchell, M.W., Genton, M.G., Gumpertz, M.L.: A likelihood ratio test for separability of covariances. *J Multivar Anal*, 97, 1025–1043 (2006)
18. Scaccia, L., Martin, R.J.: Testing axial symmetry and separability of lattice processes. *J Stat Plan Inference*, 131, 19–39 (2005)
19. Fuentes, M.: Testing for separability of spatial-temporal covariance functions. *J Stat Plan Inference*, 136, 447–466 (2005)
20. Wikle, C.K.: Hierarchical models in environmental science. *Int. Stat. Rev.* 71, 181–199 (2003)
21. Wikle, C.K., Berliner, L.M., Cressie, N.: Hierarchical Bayesian space-time models. *Environmental and Ecological Statistics*, 5, 117-154 (1998)
22. Banerjee, S., Carlin, B., Gelfand, A.: *Hierarchical Modeling and Analysis for Spatial Data*. Monographs on Statistics and Applied Probability. Chapman and Hall, New York (2004)
23. West, M., Harrison, J.: *Bayesian forecasting and dynamic linear models*. Springer-Verlag, New York (1997)
24. Gelman, A., Pardoe, I.: Bayesian measures of explained variance and pooling in multilevel (hierarchical) models, *Technometrics*, 40(2), 241-251 (2005)

# Exact vectorization of a bitmap in biological modelling

Stanislav Bartoň,

Mendel University in Brno, Faculty of Agronomy, Dept. of Automobile Transport,  
Zemědělská 1, 613 00 Brno, Czech Republic

**Abstract.** The paper presents a software procedure (using MAPLE13) intended for considerable reduction of a digital image data set to a more easily treatable extent. An example with image of a carrot is presented. The carrot, displayed on the digital photo, was represented as a polygon described by the coordinates of the pixels creating its perimeter. The photos taken in high resolution (and corresponding data sets) contain coordinates of thousands of pixels – the vertexes of the polygon. The approach presented substitutes this polygon by a new one, where a smaller number of vertexes is used. The task is solved by using an adapted least squares method. The presented algorithm enables reduction of number of vertexes to 10% of its original extent with acceptable accuracy  $\pm$  one pixel (distance between initial and final polygon). The procedure can be used for processing of similar types of 2D images and acceleration of following computations.

**Keywords:** Image processing, data reduction, least square method.

## 1. Introduction

The acquisition and analysis of visual information represents a powerful tool for interpretation of a large range of input data. The origin of computer vision is intimately intertwined with computer history, having been motivated by a wide spectrum of important applications such as robotics, biology, medicine, industry and physics, but also agricultural and food sciences over the last decades. Among the different aspects underlying visual information, the shape of the objects certainly plays a special role. The multidiscipline nature of image analysis, with respect to both techniques and applications, has motivated a rich and impressive set of information resources represented e.g. by [4].

Precise and correct image processing enables solving problems of a multidisciplinary nature, completing images and objects in terms of features (implying several distinct objects to be mapped into the same representation), pattern recognition used for segmenting an image into its constituent parts, proper validation of algorithms, and/or improving the relation between continuous and discrete approaches.

In fact “computer vision” (or generally image processing) often requires, sometimes in real time, processing of very large and heterogeneous data sets (including shape, spatial orientation, color, texture, motion, etc.). Extensive image

files or series of images are processed e.g. in biological studies [10], [8], but also in agricultural sciences [13] or food sciences [5], [9]. In spite of increasing hardware performance, large or sometimes huge data sets often cause problems and certain data reduction, regularization and/or modification is needed. There are several generally accepted approaches to achieve this task. One of the most commonly used methods is Principal Component Analysis (PCA). Principal Component Analysis is a technique that simplifies data sets by reducing their dimensionality. It is often used to decompose shape variability into a reduced set of interpretable components. It is an orthogonal linear transformation that spans a subspace, which approximates the data optimally in a least-squares sense, see [7]. This is accomplished by maximizing the variance of the transformed coordinates. If the dimensionality of the data is to be reduced to  $N$ , an equivalent formulation of PCA is to find the  $N$ -set of orthonormal vectors, grouped in the  $P$  matrix, which minimizes the error made when reconstructing the original data points in the data set. This method has been successfully used in number of works – see e.g. [11], [6], [5]. There are alternative approaches such as LDA (Linear Discriminant Analysis) – see e.g. [12] or PFA (Principal Factor Analysis) – see e.g. [1].

This paper presents a completely different approach, where input image data are significantly reduced (up to 10% of the original extent) by means of the MAPLE13 algorithm without loss of precision. An example with carrot is presented. Reduced data sets can be consequently used for faster processing and/or further utilization. The MAPLE software environment has been successfully used for determination of the shape of agricultural products [2], [3], [4].

## 2. Material and methods

### 2.1 Digital photo

A sample digital photo of a carrot (bought in May 2010 in Kaufland, Jičín) has been used. But any similar object of natural or artificial origin could have been used. The photo was taken with a Panasonic DMC-T27 digital camera with a resolution of 10.5 megapixels, see Fig. 1.

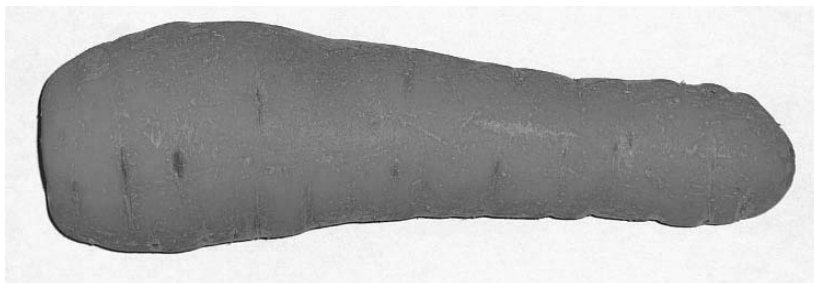


**Fig. 1.** A sample digital photo of the carrot

## 2.2 Processing software

The software MAPLE13, classic has been used to perform all presented calculations.

## 2.3 Mathematical background

### The best line

Let us assume a polygon given by the list of  $N$  points with coordinates  $[[X_1, Y_1], \dots, [X_b, Y_b], \dots, [X_N, Y_N]]$ . Let us select sublist of vertexes  $N_1, \dots, N_2, 1 \leq N_1 < N_2 \leq N, N_2 - N_1 \geq 2$ . The task is to find parameters of common line  $p1$  which will minimize  $\sum_{i=1}^N d_i^2$ , where  $d_i$  = length of the line segment between  $i_{th}$  and  $p_{i,th}$  point. The point  $p_{i,th}$  is the intersection of the line perpendicular to the line  $p1$  going through  $i_{th}$  point with the line  $p1$ .

### Lists of lines and corresponding points

After defining the best line, the procedure can continue in computing the best line for remaining points from the list of the vertexes and smoothing the polygon.

### Estimation of accuracy

After polygon approximation it is possible to compute distances  $d_i$  for input polygon vertexes using corresponding line segments. It is possible to compute their average values and variance. These values may be used to determine accuracy of approximation.

### Maple procedure

The complete Maple procedure for the presented approach can be seen at the end of this article.

## 3. Results and discussion

### 3.1 The best line

The best form of the line  $p1$ , corresponding to the above-mentioned problem is,  $p1 = (x - Q_x) \sin(\phi) + (Q_y - y) \cos(\phi)$ , where  $[Q_x, Q_y]$  are coordinates of the point lying on this line and  $\phi$  is its direction angle, see Fig. 2.

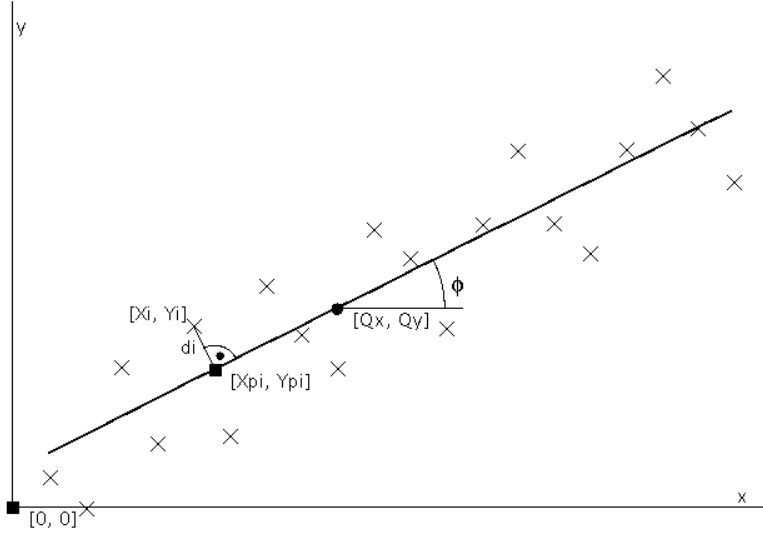


**Fig. 2.** The best line

In this case the coordinates of the  $p_i$ th point are as follows:

$$\begin{aligned} X_{p_i} &= (-Q_x \cos(\phi) - \sin(\phi) Q_y + \sin(\phi) Y_i + X_i \cos(\phi)) \cos(\phi) + Q_x \\ Y_{p_i} &= (-Q_x \cos(\phi) - \sin(\phi) Q_y + \sin(\phi) Y_i + X_i \cos(\phi)) \sin(\phi) + Q_y. \end{aligned} \quad (1)$$

The square of the distance from the line  $p_i$  is  $d_i^2 = (X_i - X_{p_i})^2 + (Y_i - Y_{p_i})^2$ , where  $X_{p_i}$  and  $Y_{p_i}$  are defined by the equation (1). The sum of the squares of the distances  $d_i$  for all  $N$  points is  $\sum_{i=1}^N d_i^2 = SoS$ ,

$$\begin{aligned} SoS &= -2 \cos(\phi) \sin(\phi) (Q_x Q_y (N2 - N1 + 1) + \Sigma_2 - Q_y \Sigma_3 - Q_x \Sigma_4) \\ &\quad + ((N2 - N1 + 1) Q_x^2 - 2 Q_x \Sigma_3 + \Sigma_3) \sin(\phi)^2 \\ &\quad + ((N2 - N1 + 1) Q_y^2 - 2 Q_y \Sigma_4 + \Sigma_4) \cos(\phi)^2, \end{aligned} \quad (2)$$

where

$$\begin{aligned} \Sigma_1 &= \sum_{i=N1}^{N2} X_i^2, \quad \Sigma_2 = \sum_{i=N1}^{N2} X_i Y_i, \quad \Sigma_3 = \sum_{i=N1}^{N2} X_i, \\ \Sigma_4 &= \sum_{i=N1}^{N2} Y_i, \quad \Sigma_5 = \sum_{i=N1}^{N2} X_i^2. \end{aligned} \quad (3)$$

These substitutions accelerate computation of  $\sum_{i=1}^N d_i^2$ , because it is faster to calculate all sums only once and to substitute obtained results instead of computing

each sum as indicated in (2) or in the following expressions. The condition for the global minimum of  $SoS(Q_x, Q_y, \phi)$  is  $\delta SoS/\delta Q_x = 0$ ,  $\delta SoS/\delta Q_y = 0$ , and  $\delta SoS/\delta \phi = 0$ . The first and second equation consequently yields in  $Q_x = \Sigma_3/(N2 - N1 + 1)$ , and  $Q_y = \Sigma_4/(N2 - N1 + 1)$ . If these values are substituted into the third equation, the result has the following form:

$$\begin{aligned} S_2 \sin(\phi)^2 + S_1 \cos(\phi) \sin(\phi) + S_3 \cos(\phi)^2 &= 0, \text{ where} \\ S_1 &= 2 (\Sigma_4^2 + (1 + N2 - N1) (\Sigma_1 - \Sigma_3) - \Sigma_3^2), \\ S_2 &= 2 (\Sigma_2 (1 - N1 + N2) - \Sigma_4 \Sigma_3), \\ S_3 &= 2 (\Sigma_2 (-1 + N1 - N2) + \Sigma_4 \Sigma_3) \end{aligned} \quad (4)$$

simplify equation (4) and its solution for  $\phi$ . Equation (4) has two roots:

$$\phi_1 = \arctan\left(-\frac{S_1}{2} + \frac{\sqrt{S_1^2 - 4 S_2 S_3}}{2 S_2}\right) \text{ and } \phi_2 = -\arctan\left(\frac{S_1}{2} + \frac{\sqrt{S_1^2 - 4 S_2 S_3}}{2 S_2}\right). \quad (5)$$

The first root leads to the global minimum of the  $SoS$ , the second one to the global maximum. Therefore it is possible to continue with  $\phi = \phi_1$ . Following substitution

$$\cos(\phi) = \frac{S_2}{\sqrt{2 S_2^2 + S_1^2 + S_1 \sqrt{S_1^2 - 4 S_2 S_3} - 2 S_2 S_3}}$$

(6)

and

$$\sin(\phi) = \frac{(S_1 + \sqrt{S_1^2 - 4 S_2 S_3}) \sqrt{2}}{\sqrt{2 S_2^2 + S_1^2 + S_1 \sqrt{S_1^2 - 4 S_2 S_3} - 2 S_2 S_3}}$$

will simplify computations of  $\cos(\phi)$  and  $\sin(\phi)$ . In special cases, when line  $p1$  is parallel with  $x$  or  $y$  axis  $S_2 = 0$  this substitution converts into  $\cos(\phi) = 0$ ,  $\sin(\phi) = 1$ , or  $\cos(\phi) = 1$ ,  $\sin(\phi) = 0$ . In these cases, proper values of  $\cos(\phi)$  and  $\sin(\phi)$  must be found, to obtain a smaller value of  $SoS$ .

### 3.2 Lists of lines and corresponding points

The best line for the first three points from the list of vertexes can be computed as follows. Let us assume  $N1=1$  and  $N2=3$  for this particular case. The best line  $p1$  can be found for each point with consequent computing of corresponding square of the distance  $d_i$  and finding the maximum of distances  $Dist = \max([d_{N1}, \dots, d_i, \dots, d_{N2}])$  the value is smaller than predefined accuracy  $L$ , it is possible to increase  $N2=N2+1$  and repeat the whole process until accuracy is satisfying. Values of  $N2$ , corresponding values of  $Q_x$ ,  $Q_y$ ,  $\cos(\phi)$ ,  $\sin(\phi)$  describing the best line for the vertexes  $N1 \dots N2$ , and  $Dist$  can be stored into the lists.

The highest  $N2$  satisfying condition  $Dist < k L$  can be determined from these lists, where  $k$  is the correction value depending on smoothness of the polygon. If the polygon is smooth  $k \rightarrow 0.5$ , while for non-smooth polygons  $k \rightarrow 0.2$ . It is possible to use a value of  $k \sim 0.5$ , but it must be considered that value  $Dist$  is a function of  $N2$  and if it once exceeds  $k L$ , it may be again lower for higher value of  $N2$ . This approach leads to a higher number of final polygon vertexes. In this case the data reduction will not be so effective. The reason that the value  $k=1$  cannot be used will be discussed later.

As the next step, the points  $[X_{P_{N1}}, Y_{P_{N1}}], [X_{P_{N2}}, Y_{P_{N2}}]$ , must be recorded into the list  $LXY$ , ordinary numbers of the border points  $N2$  are recorded into list  $LN2$ , and value  $N1$  put equal to  $N2$ , ( $N1=N2$ ). The whole process can be repeated with the subsequent vertexes from the list of polygon vertexes. The procedure is repeated until  $N2 < N$ . Finally, both lists will contain  $n$  elements. The list  $LXY$  can be displayed as a list of separate line segments approximating the initial polygon. The ordinary numbers of vertexes of the input polygon corresponding to the  $i$ -th line can be picked from the list  $LN2$  as a series of integer numbers from  $LN2_{i-1}$  to  $LN2_i$ . These lists contain information about line segments – best line and input polygon vertexes corresponding to the line segment. But the line segments are not connected with one another – see Fig. 3.

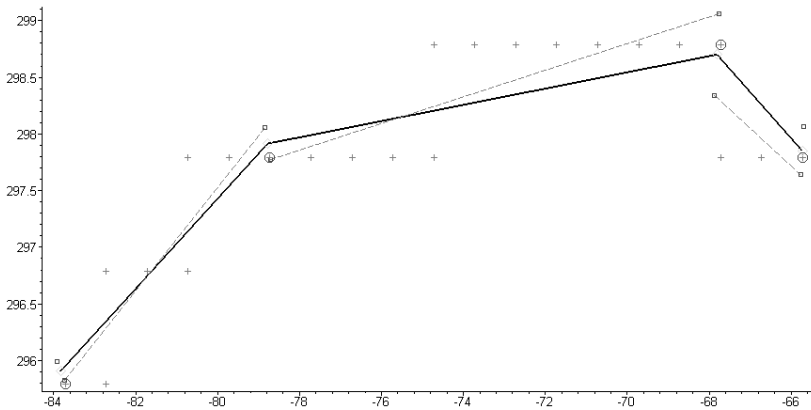


**Fig. 3.** The best line segments and part of corresponding polygon

The best line segments are displayed as a red-dashed line, input polygon vertexes are displayed as red crosses and polygon vertexes with ordinary numbers  $N2$  are blue-circled. These points correspond to endpoints of the best line segments.

The endpoint of one line segment  $[X_{P_{N2}}, Y_{P_{N2}}]$ , and the initial point of the subsequent line segment  $[X_{P_{N1}}, Y_{P_{N1}}]$ , correspond to the same vertex of the input polygon. These points are very close, but not identical, because they correspond to the different line segments. The points are displayed in Fig. 3 as blue boxes – end points of the best line segments. These couples of points can be substituted by their midpoints  $[X_C, Y_C] = 0.5([X_{P_{N2}}, Y_{P_{N2}}] + [X_{P_{N1}}, Y_{P_{N1}}])$ , and they are displayed as green diamonds in Fig. 3. As a result, a continuous curve is obtained, displayed as black line segments, creating a polygon with a reduced number of vertexes

approximating the input polygon. Center points will be recorded in a new list  $LC$ . Because the new polygon vertex  $[X_C, Y_C]$  is a midpoint corresponding to the projection of the same vertex of the initial polygon to different best lines, this point does not lay on these best lines, but it is close to both of them and the new line segments do not correspond to the preceding line segments – best lines. Therefore, it is necessary to put  $k < 1$ . As  $k \rightarrow 0$ , these line segments are shorter and the number of vertexes of the final polygon increases, but accuracy of the approximation is better. A different scale for  $x$  and  $y$  axis is used for a better overview of Fig. 3. Thus, expected right angles are displayed as distorted.

The result can be displayed graphically, see Fig. 4. The figure displays the carrot perimeter described by 1848 colored points. The corresponding polygon is substituted by a polygon with 53 vertexes with a predefined accuracy of 1 pixel. Line segments and corresponding points all have the same color. The approximating polygon is displayed with a blue line and its vertexes are indicated by blue circles. Since the difference between line segments – polygon sides and corresponding points is smaller than line thickness itself, the points are not visible. It can be seen that with data reduction 1:35, the accuracy is satisfying.

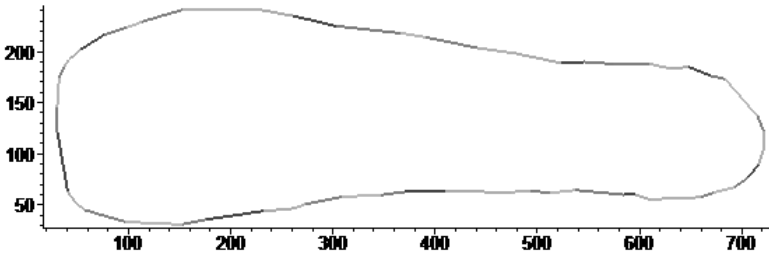


Fig. 4. Carrot shape and its approximation

### 3.3. Estimation of accuracy

The most effective method is to compute absolute value  $d_i$  and argument  $\phi_i$  the vector  $v_i = [X_i - X_{p_i}, Y_i - Y_{p_i}]$ , see Fig. 2, which can be used for the demonstration of accuracy precision. If the best line segment is defined by its endpoints,  $[X_{C_1}, Y_{C_1}]$  and  $[X_{C_2}, Y_{C_2}]$ , see previous section, the distance  $d_i$  and orientation  $\phi_i$  can be computed using very simple expressions:

$$d_i = \frac{(X_{c2} - X_{c1}) Y_i - (Y_{c2} - Y_{c1}) X_i + X_{c1} Y_{c2} - X_{c2} Y_{c1}}{\sqrt{(X_{c2} - X_{c1})^2 + (Y_{c2} - Y_{c1})^2}}, \quad (7)$$

$$\phi_i = \arctan\left(\frac{Y_{cl} - Y_{c2}}{X_{c2} - X_{cl}}\right),$$

where

$$X_{c2} = LC_{2j-1,1}, \quad Y_{c2} = LC_{2j-1,2}, \quad X_{cl} = LC_{2j,1}, \quad Y_{cl} = LC_{2j,2},$$

$$LN2_j \leq i \leq LN2_{j+1} \quad \text{and} \quad 1 \leq j \leq n.$$

This approach enables displaying accuracy in polar coordinates. For the carrot presented in Fig. 4, the corresponding accuracy is visualized in Fig. 5. As can be seen, the real accuracy is  $\pm 0.5$  pixels only. This means that the worst accuracy achieved is about 0.2 % of the object size and the average accuracy indicated by the thick blue line is  $\pm 0.5$  pixels, approximately 0.07% of the object size. Variances of the accuracy are displayed as the thin blue lines.

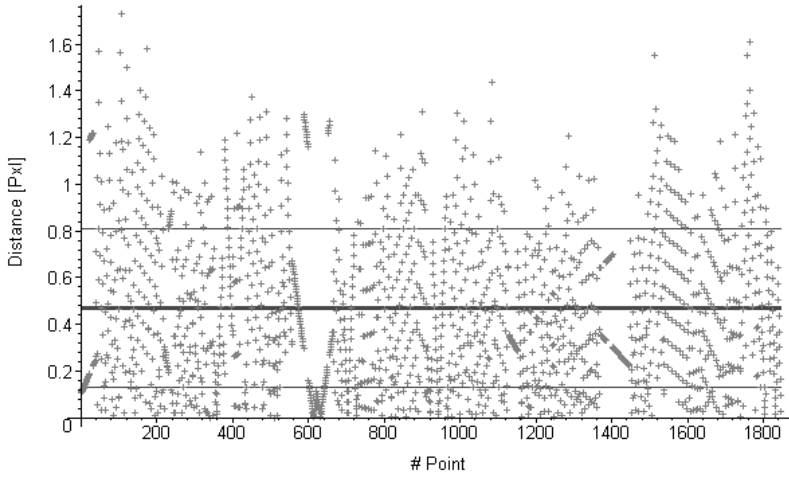


**Fig. 5.** Accuracy of the approximation

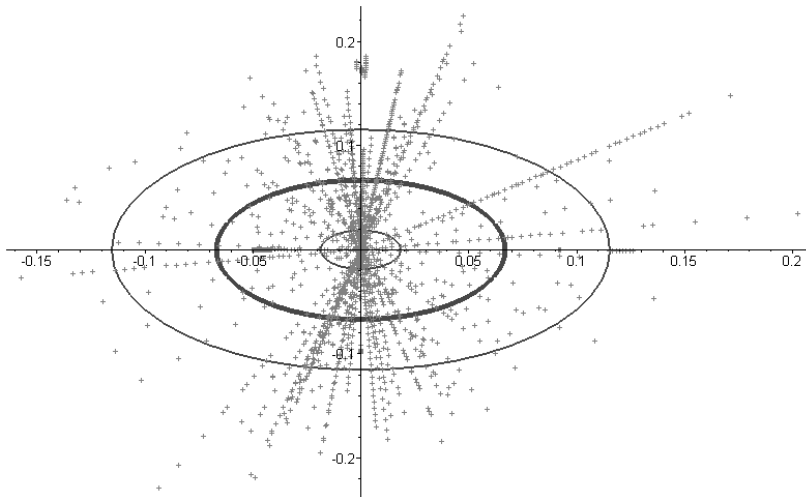


**Fig. 6.** Accuracy of the approximation, relative scale, polar coordinates

It is possible to plot vertexes of the input polygon and the resulting polygon. The example with distances  $d_i$  magnified 100 times is shown in Fig. 7.

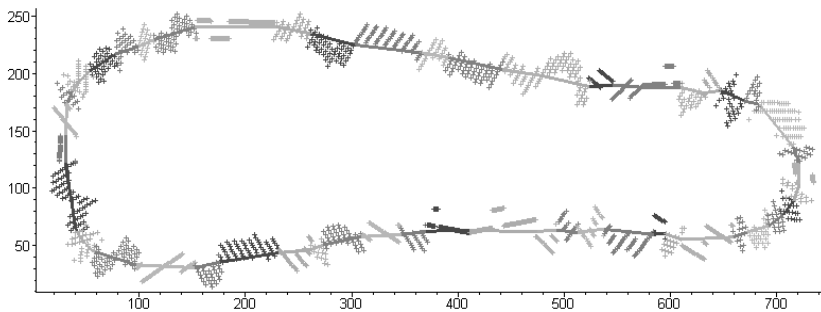


**Fig. 7.** The distance between input and resulting polygons ( $d_i$  magnified 100x)

#### 4. Program Code

The complete Maple procedure for the presented approach can be seen on the author's personal website: [user.mendelu.cz/barton](http://user.mendelu.cz/barton).

## 5. Conclusion

The proposed procedure is of a general nature and can be used for data reduction in the case of other biological as well as artificial shapes. It can serve as an effective and precise tool for acceleration of processing computing and for enabling the calculation itself on less powerful hardware, such as a common PC with a computer algebra program and/or in case of data processing using non-linear regression methods.

**Acknowledgments** The research has been supported by the Grant Agency of the Czech Academy of Sciences under Contract No. IAA201990701.

## References

1. 2005: On the adequacy of principal factor analysis for the study of shape variability. Proceedings of Medical Imaging 2005: Image Processing, San Diego, CA, USA, 17 Ballester, M. A. G., Lingrau, M. G., Aquirre, M. R. and Ayache, N., February 2005, pp. 1392
2. Bartoň, S., 2000: Quick algorithms for calculation of coefficients of non-linear and partially continuous functions using the Least Square Method, solution in Maple 6. Proceedings of 8th International Research Conference CO-MAT-TECH 2000, Trnava, October 2000. STU Bratislava, pp. 79–85. ISBN 80–227–1413–5.
3. Bartoň, S., 2007: Stanovení tvaru zemědělské plodiny. Proceedings of 6. Matematický workshop. Brno: FAST VUT Brno, November 2007, pp. 1–12. ISBN 80–214–2741–8.
4. Bartoň, S., 2008. Three dimensional modelling of the peach in Maple. In CHLEBOUN, J. Programs and Algorithms of numerical Mathematics. 1st ed. Praha. Matematický ústav AV ČR, 2008, pp. 7–14. ISBN 978–80–85823–55–4.
5. Havlíček, M., Nedomová, Š., Simeonová, J., Severa, L. and Křivánek, I., 2008: On the evaluation of chicken egg shape variability. Acta Universitatis agriculture et silviculture Mendelianae Brunensis 56(5), 69–74.
6. Iglesias, J. E., Bruijne, M., Loog, M., Lauze, F. and Nielsen, M., 2007: A Family of Principal Component Analyses for Dealing with Outliers. Proceedings of 10th MICCAI International Conference, October 29 - November 2, Brisbane, Australia, pp. 178–185. ISBN 978-3-540-75758-0
7. Jolliffe, I., 1986: Principal component analysis. Springer, New York, 1986
8. Klotz, B., Pyle, D. L. and Mackey, M., 2007: New Mathematical Modeling Approach for Predicting Microbial Inactivation by High Hydrostatic Pressure. Applied and Environmental Microbiology 73(8), 2468–2478.
9. Severa, L., 2008: Development of the peach firmness during harvest period. Acta Universitatis agriculture et silviculture Mendelianae Brunensis 56(4), 169–176.
10. Tománková, K., Jeřábková, P., Zmeškal, O., Veselá, M. and Haderka, J., 2006: Use of Image Analysis to Study Growth and Division of Yeast Cells. Journal of Imaging Science and Technology 50(6), 583–587.
11. Vidal, R., Ma, Y. and Sastry, S., 2005: Generalized Principal Component Analysis (GPCA). IEEE Transactions on Pattern Analysis and Machine Intelligence 27(12), 1–15.
12. Wang, M., Perera, A. and Guitterrez-Osuna, R., 2004: Principal Discriminants Analysis for small-sample-size problems: Application to chemical sensing. Proceedings of IEEE Sensors 2, 591-594.

13. Zadavec, M. and Žalik, B., 2009: A geometric and topological system for supporting agricultural subsidies in Slovenia. *Computers and Electronics in Agriculture* 69, 92-92.

# Stochastic modelling of signal transduction in olfactory neurons

Ondřej Pokora

Department of Mathematics and Statistics, Faculty of Science, Masaryk University,  
Kotlářská 2, 611 37 Brno, Czech Republic  
pokora@math.muni.cz

**Abstract.** Several models of olfactory sensory neurons (concentration detectors, flux detectors) are investigated. Their behavior is described by stochastic processes of binding and activation. The models assume that the response, concentration of activated receptors, is determined by the signal, fixed log-concentration of odorant in perireceptor space. An approach used is based on stochastic variant of the law of mass action as a neuronal model. The statistical steady-state characteristics of the models are derived.

## 1 Introduction

Characterization of the input-output properties of sensory neurons and their models is commonly done by using the so called input-output response functions,  $R(s)$ , in which the response is plotted against the input  $s$ . The output is usually the spiking frequency, or rate of firing, but it can be also concentration of activated receptors as presented e.g. in [13, 15] and also in this contribution. The response curves are usually monotonously increasing functions (most often of sigmoid shape) assigning a unique response to an input signal (see Fig. 1 for illustration).

The intuitive concept of “just noticeable difference”, which has been deeply studied in psychophysics, is also implicitly involved in understanding of signal optimality in neurons. Having the transfer function  $R(s)$  and minimum detectable increment  $\varepsilon$  of the response, we can calculate  $\Delta_s$  which is the just noticeable difference in the signal. If the response curve is nonlinear (e.g. sigmoidal as in Fig. 1) we can see that  $\Delta_s$  varies along  $D$  and the smallest values of the just noticeable difference in the signal are achieved where the response curve is steepest. The stimulus intensity for which the signal is optimal, that is the best detectable, is where the slope of the transfer function is highest. However, in practice, an identical signal does not always yield the same response. The presence of noise complicates the concept of signal optimality based on the just noticeable difference. Not only a fixed response is assigned to every level of the stimulus (as in the classical frequency coding schema), but also a probability distribution of the responses. A concept of using more statistical characteristics of the response (not only the mean value) for classification of the stimuli is depicted in Fig. 1b, where, for simplicity, the mean value and the standard deviation of the response are shown.

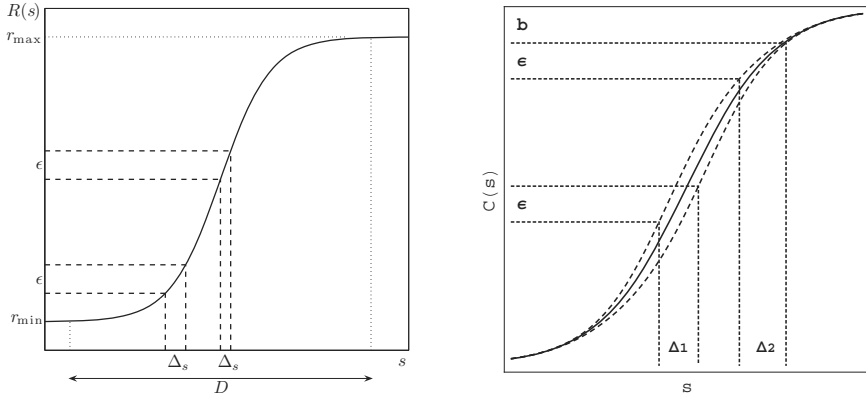


**Fig. 1.** (left) A schematic example of deterministic transfer function  $R(s)$  (solid curve). The dynamic range  $D$ , threshold response  $r_{\min}$ , maximal discharge  $r_{\max}$  and just noticeable difference  $\Delta_s$  in the signal corresponding to the just noticeable difference  $\epsilon$  in the response are given. (b) Stochastic point of view: mean transfer function  $C(s)$  (solid) equipped with standard deviations (dashed curves) of  $R(s)$ . Note, that both quantities play important role in understanding the relation between changes  $\epsilon$  in the response and corresponding  $\Delta$  in the signal.

## 2 Modelling the Number of Activated Receptors

Signal processing in olfactory systems is initialized by binding of odorant molecules to receptor molecules embedded in the membranes of sensory neurons. Binding of odorants and receptor activation trigger a sequence of biochemical events that result in the opening of ionic channels, the generation of receptor potential which triggers a train of action potentials. Models of the binding and activation of receptors investigated in the following sections are based on models proposed in [2, 3, 7, 6, 10, 12, 13, 16].

The models can be, in general, classified into two categories, concentration detectors and flux detectors. In the concentration detector models (see Fig. 2) it is assumed that the neuronal membrane is directly exposed to the odorant molecules present in the external space. In other words, it is assumed that the transfer of odorant molecules between the external space and the perireceptor space is very fast and reversible. Thus the odorant concentrations in both compartments are the same.

We investigate three types of the concentration detectors which differ in the binding and activation mechanisms. In the flux detector model (see Fig. 3) it is assumed that the transfer of odorants from the external to the perireceptor space is relatively slow and irreversible. Here, the degradation must be included to compensate for the fact that no possible outflow of the odorant occurs (see [7] for details).

Under the statistical approach the behaviour of the number of activated receptors is represented as a stochastic process with the odorant concentration as a parameter. Such a description was used in [1, 5, 8, 9, 14, 17]. We assume that there is only one odorant substance, that each receptor molecule possesses only one binding site and that

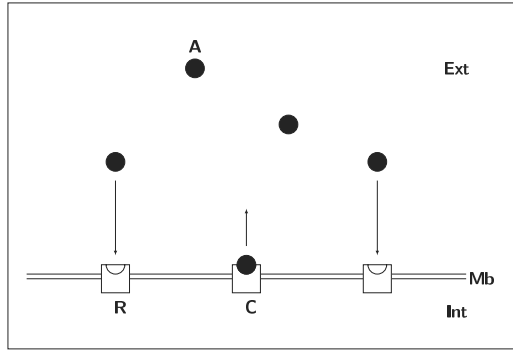


**Fig. 2.** Schema of the concentration detector. **Ext** external air space, **Int** sensory cell interior, **Mb** cell membrane, **A** odorant, **R** free receptor, **C** activated odorant-receptor complex.

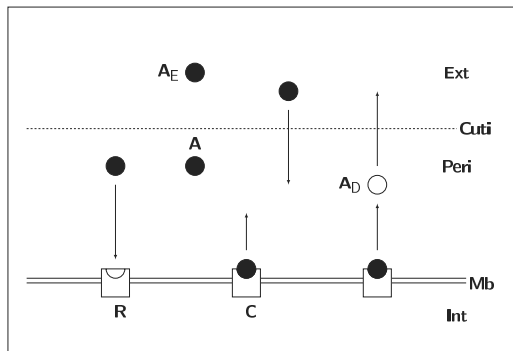


**Fig. 3.** Schema of the flux detector. **Ext** external air space, **Cuti** cuticle, **Peri** perireceptor space, **Int** sensory cell interior, **Mb** cell membrane,  $A_E$  odorant in external space, **A** odorant in perireceptor space, **R** free receptor, **C** activated odorant-receptor complex,  $A_D$  degraded form of the odorant.

the total number of the receptors on the surface of the membrane is fixed and equal to  $N$ . Let  $A$  denote the odorant molecule in perireceptor space and  $A_E$  in external space, with concentration  $A = e^s$  (in concentration detector) or  $A_E = e^s$  (in flux detector), which is assumed to be fixed until the olfactory system achieves the steady state.

We distinguish three states in which the receptors can appear: unbound (free) state,  $R$ , bound inactive state,  $C^*$ , and bound activated state  $C$ . Only activated receptors trigger the response. The models assume that the response, the count of activated receptors,  $C(s)$ , in steady state is completely determined by the signal, which is fixed log-concentration,  $s$ , of odorant. Thus, in the models investigated here the count is a dependent variable with the odorant log-concentration,  $s$ , as a parameter.

### 3 Basic Model

At first we consider the simplest model in which each occupied receptor becomes activated instantaneously with its occupation. Thus, the number of bound but not activated receptors is always zero. It is assumed that each receptor is occupied and released independently of others in accordance with stochastic reaction schema (as usually used for the description of chemical reactions)



where  $A$  represents an unbound molecule of odorant,  $R$  unoccupied receptor and  $C$  stands for bound activated receptor (complex of the odorant molecule and the receptor),  $k_1$  and  $k_{-1}$  are fixed reaction rates coefficients of association and dissociation of the odorant molecules. The ratio  $K_1 = k_{-1}/k_1$  is commonly called the dissociation constant. A receptor unbound at time  $t$  becomes bound (and activated) in time interval  $(t, t + \Delta t]$  with probability  $\lambda \Delta t + o(\Delta t)$ , a receptor activated at time  $t$  becomes unbound in time interval  $(t, t + \Delta t]$  with probability  $\mu \Delta t + o(\Delta t)$ . The parameter  $\lambda$  is an increasing function of the concentration,  $A$ , of the odorant. We consider this dependency to be linear,  $\lambda = k_1 A = k_1 e^s$ , with the constant of proportionality  $k_1$  equal to the rate of association. The parameter  $\mu$  is considered to be equal to the rate of dissociation,  $\mu = k_{-1}$ . As the total number of receptor sites on the surface of the membrane is equal to  $N$ , relation  $R_t + C_t = N$  is satisfied for all  $t \geq 0$ .

In line with these assumptions the continuous-time stochastic process  $\{C_t; t \geq 0\}$  giving the count of bound activated receptors at time  $t$  can be described as a birth and death process (see [8, 9, 11]) with birth rates  $\lambda_i$  and death rates  $\mu_i$ ,

$$\lambda_i = \lambda (N - i) = k_1 (N - i) e^s \quad , \quad \mu_i = \mu i = k_{-1} i \quad (2)$$

for  $i \in \{0, 1, \dots, N\}$ . It means that the transition probabilities are

$$\begin{aligned} P\left\{ (i) \xrightarrow{\Delta t} (i+1) \right\} &= k_1 (N - i) e^s \Delta t + o(\Delta t) \quad , \\ P\left\{ (i) \xrightarrow{\Delta t} (i-1) \right\} &= k_{-1} i \Delta t + o(\Delta t) \quad . \end{aligned} \quad (3)$$

This process, independently of the initial condition, achieves a stationary state with probability distribution with mass function,

$$\pi_i = P\{C(s) = i\} = \left(1 + \frac{e^s}{K_1}\right)^{-N} \binom{N}{i} \left(\frac{e^s}{K_1}\right)^i, \quad i \in \{0, 1, \dots, N\}. \quad (4)$$

Using this stationary distribution to derive the mean and variance of the count of activated receptors in steady state,  $C(s)$ , we obtain

$$E(C(s)) = \frac{N}{1 + K_1 e^{-s}}, \quad (5)$$

$$\text{Var}(C(s)) = \frac{NK_1 e^{-s}}{(1 + K_1 e^{-s})^2}. \quad (6)$$

As a function of  $s$ , the steady-state mean given by equation (5) monotonically increases from 0 to  $N$  and it has typical sigmoidal shape with inflexion point located at  $s = \ln K_1$ . Variance (6) has unimodal shape and its maximum value is achieved for the same odorant log-concentration  $s = \ln K_1$ . For extremely low and high odorant concentrations the variance tends to zero,  $\text{Var}(C(\pm\infty)) = 0$ . The mean and standard deviation as functions of the log-concentration of odorant are plotted in Fig. 4.

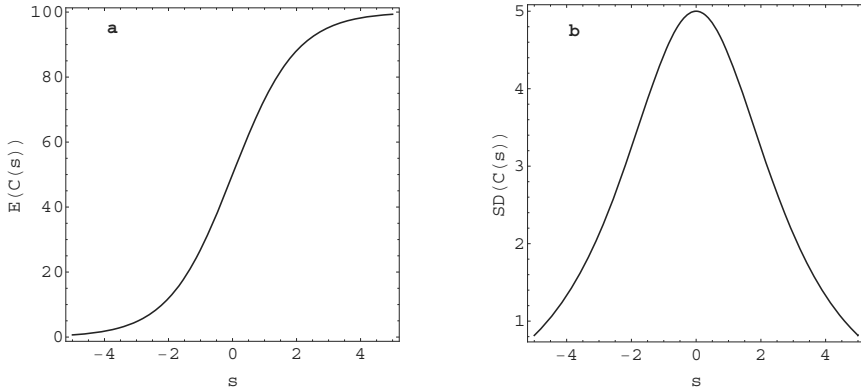


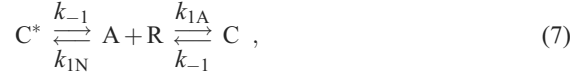
**Fig. 4.** (a) Mean  $E(C(s))$  and (b) standard deviation  $SD(C(s))$  of the number of activated receptors in the basic model, as functions of the odorant log-concentration,  $s$ , in perireceptor space. Parameters are  $K_1 = 1$  and  $N = 100$ . Both the inflexion point of the mean and the point of maximal standard deviation are located at  $s = \ln K_1 = 0$ .

If the number of receptor sites,  $N$ , is sufficiently high, it is natural to consider continuous variant of the steady-state count of activated receptors  $C(s)$  and we need to know the distribution of such continuous approximation. One possibility how to do it is to use the central limit theorem. Other legitimate approach is to use the diffusion approximation of the birth and death process (2), as described e.g. in [17]. Then,  $C(s)$

is assumed to be continuous Gaussian random variable with the prescribed mean and variance,  $C(s) \sim N(E(C(s)), \text{Var}(C(s)))$ .

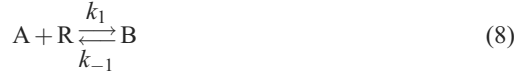
#### 4 Model of Simple Activation

Consider now the model where not every bound receptor (complex) is activated immediately. The receptors really appear in three states: unbound, R, occupied but not activated,  $C^*$ , and occupied activated, C. Model described in [11] supposes that each occupied receptor can either become activated, C, with probability  $p \in (0, 1)$ , or stay inactive,  $C^*$ , with probability  $1 - p$ , independently of its past behavior and of the behavior of other receptors. Such an interaction corresponds to the following reaction schema,



where  $k_{1A} = pk_1$  and  $k_{1N} = (1 - p)k_1$  are association rate coefficients for the activated and inactive state and  $k_1, k_{-1}$  have the same meaning as in basic model (1).

Denoting by  $B_t$  the number of bound receptors, B, at time  $t$ , regardless of their activation, the relation  $B_t = C_t + C_t^*$  is satisfied. Then, because of the independence of behaviour of the receptor sites the binding process follows reaction schema



(compare this with schema (1)), the conditional steady-state distribution is binomial,  $(C_\infty | B_\infty = b) \sim \text{Bi}(b, p)$ . From the knowledge of the mass function (4) of the random variable  $B_\infty$ , the unconditional probability distribution of  $C(s)$  can be derived,

$$\pi_i = P\{C(s) = i\} = \binom{N}{i} q(s)^i (1 - q(s))^{N-i}; \quad i \in \{0, 1, \dots, N\}, \quad (9)$$

where  $q(s) = p/(1 + K_1 e^{-s})$ . Hence, the steady-state number of activated receptors has binomial distribution  $C(s) \sim \text{Bi}(N, q(s))$  and its mean and variance can be directly derived,

$$E(C(s)) = \frac{Np}{1 + K_1 e^{-s}}, \quad (10)$$

$$\text{Var}(C(s)) = \frac{NpK_1 e^{-s}}{(1 + K_1 e^{-s})^2} + \frac{Np(1 - p)}{(1 + K_1 e^{-s})^2}. \quad (11)$$

Steady-state mean (10) monotonically increases from 0 to  $Np$  and has sigmoidal shape. Its inflexion point is located at  $s = \ln K_1$ , independently of the value of activation probability  $p$ . For  $p \in (0, 0.5]$ , variance (11) is monotonically increasing from zero to the limit value  $\text{Var}(C(\infty)) = Np(1 - p)$ . For  $p \in (0.5, 1)$ , it increases from zero to maximal value  $N/4$  achieved at  $s = \ln K_1 - \ln(2p - 1)$  and then decreases to the limit value  $\text{Var}(C(\infty)) = Np(1 - p)$ . Both the mean and the standard deviation as functions of the log-concentration of odorant are plotted in Fig. 5. Model (1) is a limit case of model (7) for  $p$  converging to 1.

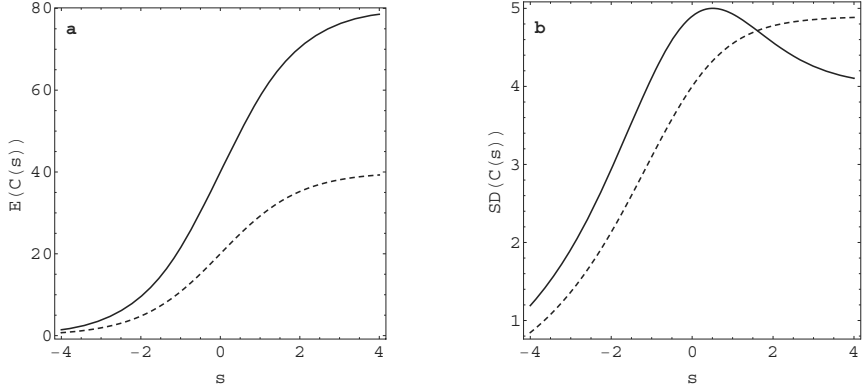


**Fig. 5.** (a) Mean  $E(C(s))$  and (b) standard deviation  $SD(C(s))$  of the number of activated receptors in model of simple activation, as functions of the odorant log-concentration,  $s$ , in perireceptor space. Parameters are  $K_1 = 1$  and  $N = 100$ . Activation probability  $p$  is set to 0.8 (solid curves) and 0.4 (dashed curves). Inflexion points of the mean curves are located at  $s = \ln K_1 = 0$  (independently on the activation probability  $p$ ). The variance is either monotonically increasing (for  $p = 0.4$ ) or has a maximum located at  $s = \ln K_1 - \ln(2p - 1) \approx 0.511$  (for  $p = 0.8$ ).

## 5 Double-step Model

This model has often been used for describing odorant-receptor interaction, see [6, 5, 16]. As in the previous model, the receptors may appear in three different states. The interaction between unbound,  $R$ , bound not activated,  $C^*$ , and bound activated receptors,  $C$ , is formed by the transitions via the stochastic reaction schema



where rate coefficients  $k_2$  and  $k_{-2}$  characterize the activation-deactivation process. In contrast with the model of interaction with simple activation (7), in the double-step interaction it is assumed that occupied receptor can become activated only with a delay after the binding. Analogously as in the basic model, the stochastic process  $\{C_t; t \geq 0\}$  giving the count of activated receptors at time  $t$  can be described as a homogenous Markov chain with  $(N+1)(N+2)/2$  states  $\{(i, j); 0 \leq i+j \leq N\}$  and transition probabilities (for time interval  $\Delta t$ )

$$\begin{aligned} P\left\{(i, j) \xrightarrow{\Delta t} (i+1, j)\right\} &= k_1(N-i-j)e^s \Delta t + o(\Delta t), \\ P\left\{(i, j) \xrightarrow{\Delta t} (i-1, j)\right\} &= k_{-1}i \Delta t + o(\Delta t), \\ P\left\{(i, j) \xrightarrow{\Delta t} (i-1, j+1)\right\} &= k_2i \Delta t + o(\Delta t), \\ P\left\{(i, j) \xrightarrow{\Delta t} (i+1, j-1)\right\} &= k_{-2}j \Delta t + o(\Delta t), \end{aligned} \quad (13)$$

where the first coordinate denotes the count of bound not activated receptors and the second one denotes the count of activated receptors.

The stationary distribution of  $C(s)$  is multinomial; see [4] for general formulae. The steady-state mean number of activated receptors,  $C(s)$ , is

$$E(C(s)) = \frac{N}{1 + K_2(1 + K_1 e^{-s})}, \quad (14)$$

where  $K_2 = k_{-2}/k_2$ . The analytical expression of the steady-state variance is very complicated. Nevertheless, it can be computed numerically and as its good approximation we found the function

$$\text{Var}(C(s)) \approx \frac{a + b e^{-s}}{1 + c e^{-s} + d e^{-2s}} \quad (15)$$

with general parameters  $a, b, c, d$ . The steady-state mean given by equation (14) monotonically increases from zero to  $N/(1 + K_2)$  and has (in general) asymmetric sigmoidal shape with inflexion point located at  $s = \ln K_1 + \ln K_2 - \ln(1 + K_2)$ . The steady-state variance fulfills relations  $\text{Var}(C(-\infty)) = 0$  and  $\text{Var}(C(\infty)) = a > 0$ . Both the mean and the standard deviation as functions of the log-concentration of odorant are depicted in Fig. 6.

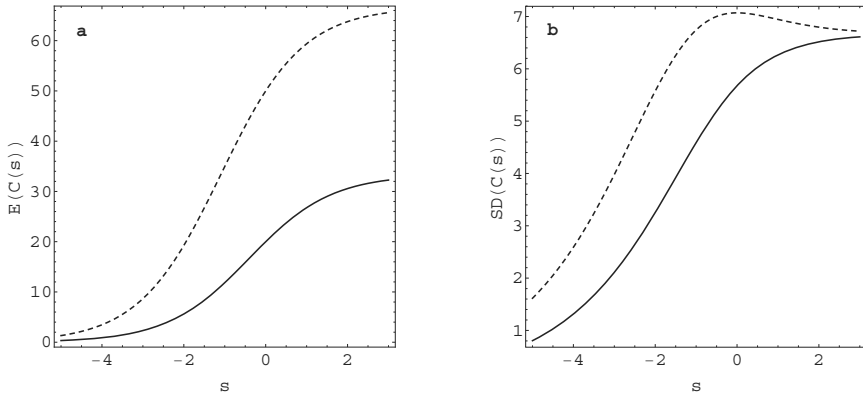
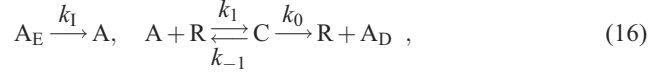


**Fig. 6.** (a) Mean  $E(C(s))$  and (b) standard deviation  $SD(C(s))$  of the number of activated receptors in the double-step model, as functions of the odorant log-concentration,  $s$ , in perireceptor space. Parameters are  $N = 100$ ;  $K_1 = 1$  and  $K_2 = 2$  (solid curves),  $K_1 = 1$  and  $K_2 = 0.5$  (dashed curves). Inflexion points of the mean curves are located at  $s \approx -0.405$  (solid) and  $s \approx -1.099$  (dashed). The standard deviation is either monotonically increasing (solid) or has a local maximum (dashed).

## 6 Flux Detector

In contrast with the concentration detector, in the flux detector model, the rate of influx of odorant from the external to the perireceptor space is quantitatively taken into ac-

count. This scenario has been introduced in [7] and further analyzed in [10, 16]. The transfer of odorant molecules between the external and perireceptor spaces is relatively slow and irreversible (no outflux is permitted). The concentration of the odorant in perireceptor space can be substantially higher than outside. Stochastic schema of the single-step reaction is



where  $A_E$  denotes the odorant of fixed concentration  $A_E = e^s$  in the external space,  $A$  odorant in the perireceptor space and  $A_D$  denotes degraded form of the odorant (cannot interact with receptors anymore). The parameter  $k_1$  is the rate of influx of the odorant molecules from the external to the perireceptor space and  $k_0$  is the rate of degradation of molecules of the odorant. Because of irreversible reaction, the Michaelis-Menten constant  $K_M = (k_{-1} + k_0)/k_1$  should be used for description of reaction rate instead of the dissociation constant  $K_1$ . Further, let us denote the ratio of the influx and the degradation rates by  $K = k_1/k_0$ .

Continuous-time stochastic process  $\{C_t; t \geq 0\}$  giving the count of activated receptors at time  $t$  can be described by inhomogeneous birth and death process with transition rates

$$\lambda_{i,t} = k_1(N-i)A_t, \quad \mu_i = \mu i = (k_{-1} + k_0)i; \quad i \in \{0, 1, \dots, N\}, \quad (17)$$

where  $A_t$  is the odorant concentration in the perireceptor space at time  $t$ . The birth rates  $\lambda_{i,t}$  are time-dependent (inhomogeneous) because of the stable influx of the odorant from the external to the perireceptor space.

The process has a stationary state  $C(s)$  if the relation  $s \leq \ln N - \ln K$  is fulfilled. In this case the concentration of the odorant in the perireceptor space reaches an equilibrium  $A(s) < \infty$ . For  $s > \ln N - \ln K$  the process  $C_t$  converges to the value  $C(s)$  whereas the odorant concentration  $A_t$  in the perireceptor space grows without bounds. Using the law of mass action, the deterministic behaviour of the flux detector model can be described by two independent differential equations for  $C_t$  and  $A_t$ . Their asymptotical solution gives the steady-state odorant concentration in the perireceptor space,

$$A(s) = \frac{K_M K e^s}{(N - K e^s)}. \quad (18)$$

Now we can replace the inhomogeneous birth and death process of the reaction (16) with the homogenous one according to reaction (1),

$$\lambda_i = k_1(N-i)A(s), \quad \mu_i = k_{-1}i; \quad i \in \{0, 1, \dots, N\}. \quad (19)$$

This is justified by the Markovian property of the birth and death stochastic process. Analogously as in Section 3 we derive the stationary probability distribution  $\{\pi_i\}$  of the birth and death process  $\{C_t; t \geq 0\}$  with rates (19). Assuming  $s \leq \ln N - \ln K$ , the moments of the count of activated receptors have shapes plotted in Fig. 7,

$$E(C(s)) = K e^s, \quad (20)$$

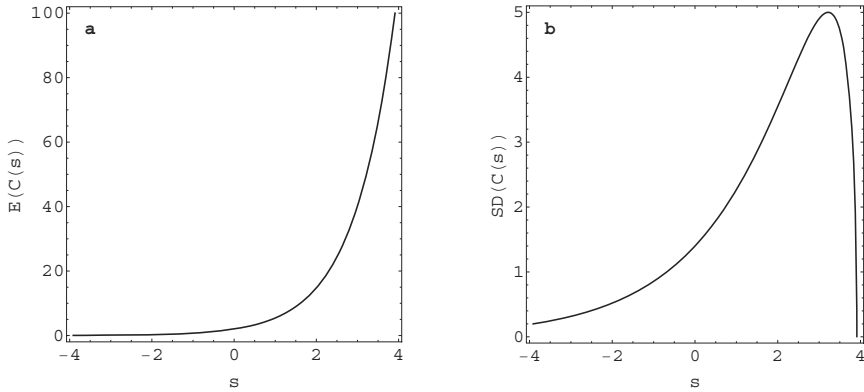


**Fig. 7.** (a) Mean  $E(C(s))$  and (b) standard deviation  $SD(C(s))$  of the number of activated receptors in the flux detector model, as functions of the odorant log-concentration,  $s$ , in perireceptor space. Parameters are  $K = 1$  and  $N = 100$ .

$$\text{Var}(C(s)) = Ke^s \left( 1 - \frac{Ke^s}{N} \right). \quad (21)$$

The steady-state mean given by equation (20) is increasing function of the odorant concentration. The variance (as a function of the odorant concentration) given by equation (21) has unimodal asymmetric shape with maximum value  $N/4$  achieved for  $s = \ln N - \ln K - \ln 2$ . For low as well as possible high odorant log-concentrations it becomes practically zero. Note the fact that the Michaelis-Menten constant  $K_M$  does not play any role in the behaviour of  $C(s)$ .

## 7 Conclusion

The stochastic modelling of signal transduction has wide applications in the theory of classification of the stimuli. An important question "How precisely can be the stimulus (odorant concentration) estimated from the knowledge of the response (concentration of activated receptors)?" is given. For answering this question in a stochastic concept, the statistical characteristics of the response presented in this contribution are required.

## Acknowledgement

This work was supported by Jaroslav Hájek Center for Theoretical and Applied Statistics LC06024.

## References

1. Arányi, P., Tóth, J.: A Full Stochastic description of the Michaelis-Menten reaction for small systems. *Acta Biochimica et Biophysica Academiae Scientificarum Hungariae* 12, 375–388 (1977)

2. Brown, D., Rothery, P.: *Models in Biology: Mathematics, Statistics and Computing*. Wiley, Chichester (1993)
3. Cleland, T. A., Linster, C.: Concentration tuning by spare receptor capacity in olfactory sensory neurons: a theoretical study. *Neural Computation* 11, 1673–1690 (1999)
4. Érdi, P., Tóth, J.: *Mathematical Models of Chemical Reactions*. Princeton University Press, Princeton (1989)
5. Gurewich, K. G., Agutter, P. S., Wheatley, D. N.: Stochastic description of the ligand-receptor interaction of biologically active substances at extremely low doses. *Cellular Signalling* 15, 447–453 (2003)
6. Kaissling, K. E.: Kinetics of olfactory receptor potentials. In: *Olfaction and Taste III*. Rockefeller University Press, New York (1969)
7. Kaissling, K. E.: Flux detectors vs. concentration detectors: two types of chemoreceptors. *Chemical Senses* 23, 99–111 (1998)
8. Kurtz, T. G.: The relationship between stochastic and deterministic models for chemical reactions. *Journal of Chemical Physics* 57, 2976–2978 (1972)
9. Lam, H. S., Lampard, D. G.: Modelling of drug receptor interaction with birth and death processes. *Journal of Mathematical Biology* 12, 153–172 (1981)
10. Lánský, P., Rospars J.-P.: Odorant concentration and receptor potential in olfactory sensory neurons. *BioSystems* 48, 131–138 (1998)
11. Lánský, P., Rospars J.-P.: Coding of odor intensity. *BioSystems* 31, 15–38 (1993)
12. Lauffenburger, D. A., Linderman, J.: *Receptors: Models for Binding, Trafficking and Signaling*. Oxford University, Oxford (1993)
13. Mankin, R. W., Mayer, M. S.: A phenomenological model of the perceived intensity of single odorants. *Journal of Theoretical Biology* 100, 123–138 (1983)
14. McNeil, D. R., Schach, S.: Central limit analogues for Markov population processes. *Journal of the Royal Statistical Society, Series B* 35, 1–23 (1973)
15. Pokora, O., Lánský, P.: Statistical approach in search for optimal signal in simple olfactory neuronal models. *Mathematical Biosciences* 214, 100–108 (2008)
16. Rospars, J.-P., Křivan, V., Lánský, P.: Perireceptor and receptor events in olfaction. Comparison of concentration and flux detectors: a modeling study. *Chemical Senses* 25, 293–311 (2000)
17. Tuckwell, H. C.: Diffusion approximations to channel noise. *Journal of Theoretical Biology* 127, 427–438 (1987)

# Stochastic Modeling of Biodiversity

## f-diversity, self f-diversity and marginal f-diversity

Jana Zvárová and Karel Zvára \*

Center of Biomedical Informatics, Department of Medical Informatics,  
Institute of Computer Science AS CR,  
Pod Vodárenskou věží 2, 182 07 Prague, The Czech Republic  
zvarova@euromise.cz

**Abstract.** The paper is devoted to stochastic modeling of biodiversities, that are presented as selected f-diversities frequently used in biology and medicine. The most often used in biology and medicine are f-diversities called Number of Alleles, Gini-Simpson diversity and Shannon diversity. We have introduced two new general concepts, named marginal f-diversity and self f-diversity. The statistical properties of sample estimates of the selected f-diversities are mentioned. Results of simulations of f-diversities, self f-diversities and marginal f-diversities for Number of Alleles, Gini-Simpson and Shannon type diversities on the example of three alleles with fixed probabilities of occurrence and several sample sizes used are presented.

**Keywords.** Biodiversity, modeling, f-entropy, f-diversity, self f-diversity, marginal f-diversity

## 1 Introduction

For the complete genetic characteristics of the individual in a given population it should be necessary to determine the forms of nucleotides in all its loci. In the event that we are able for a given gene  $X$  to determine alleles  $A_1, \dots, A_{k-1}$ , then the rest (till unknown alleles) we summarize in the category "others" and we understand this category as the allele  $A_k$ . In the event that all individuals of a given population have the same allele in a considered gene we call the corresponding loci monomorphic. The concept of a polymorphism is a more complicated because for a given gene there can be one prevailing allele, but there are other alleles with very small probabilities of occurrence. The corresponding loci are thus called q-polymorphic if the probability of occurrence of the prevailing allele is greater or equal to a given number  $q < 1$ . Mostly  $q$  is chosen as 0.99 or 0.995. We then call a given population q-polymorphic for a given gene. Some known measures of diversity of genes were based on q-polymorphism.

Let us consider  $r$  genes with  $r$  corresponding pairs of loci, where  $s$  pairs are q-polymorphic. The ratio  $P = r/s$  is then called the **proportion of q-polymorphic loci**.

---

\* The work was supported by the project 1M06014 of the Ministry of Education of the Czech Republic and by the research institutional plan AV0Z10300504 of the Institute of Computer Science AS CR

This measure is a very rough measure of diversity. On a considered loci a variety can essentially change (change of a probability of an allele), but the  $P$  value will not change. Another known measure of diversity is the number  $k - 1$  of known alleles called the **Number of Alleles**. This measure is able to show a disappearing of an allele, but gives no information on probabilities of alleles. In the literature the three following measures of diversity are often introduced: **heterozygosity**, the **Gini-Simpson index** and the **Shannon index** of diversity.

Let us denote as  $p_{ij}$  a probability that on two corresponding loci an allele  $A_i$  is on the first loci and an allele  $A_j$  on the second loci. These measures are then calculated as follows:

**heterozygosity**  $H$  is the probability that on two corresponding loci there are different alleles, i.e.

$$H = \sum_{\substack{i=1,\dots,k,j=1,\dots,k \\ i \neq j}} p_{ij} = 1 - \sum_{i=1}^k p_{ii}. \quad (1)$$

It is obvious that  $H$  reaches its maximum if and only if  $\sum_{i=1}^k p_{ii} = 0$ , therefore  $p_{ii} = 0$  for  $i = 1, 2, \dots, k$ . The minimum is reached in the event that  $\sum_{i=1}^k p_{ii} = 1$ .

The **Gini-Simpson index**  $H_{GS}(p)$  is calculated from the probability distribution  $p = (p_1, \dots, p_k)$  of  $k$  alleles on a given loci as

$$H_{GS}(p) = 1 - \sum_{i=1}^k p_i^2. \quad (2)$$

The Gini-Simpson index has its values in the interval  $[0, (k - 1)/k]$ , where the lower boundary 0 is reached if and only if the loci is monomorphic and the upper boundary  $(k - 1)/k$  for  $p = u_k = (1/k, 1/k, \dots, 1/k)$ , uniform probability distribution. In the event of a panmictic population the Gini-Simpson index and heterozygosity are the same. However, in the event that the population is not panmictic, these measures can be different. In genetic literature gene variation known as gene diversity was popularized in the early 1970s by Nei [8]. In ecological literature it has a much older history. Originally it was suggested as a measure of ecological diversity by Gini [3] and later discussed by Simpson [11]. Apart from the Gini-Simpson index modifications of it are used as well, e.g. **gene identity**  $J = \sum_{i=1}^k p_i^2$  and **effective number of alleles**  $A = 1/J$ .

The **Shannon information index**  $H_S(p)$  is calculated from the probabilities  $p_1, \dots, p_k$  of  $k$  alleles on a given loci as

$$H_S(p) = - \sum_{i=1}^k p_i \log p_i. \quad (3)$$

The Shannon information index has its values in the interval  $[0, \log k]$ , where the lower boundary 0 is reached if and only if the loci is monomorphic and the upper boundary  $\log k$  for uniform probability distribution  $p = u_k = (1/k, \dots, 1/k)$ .

It is hard to give a universal preference to either of these two measures. Some researchers are more familiar with Shannon entropy and it is easier for them to interpret concrete numerical values of  $H_S(p)$  than those of  $H_{GS}(p)$ . On the other hand, the Gini-Simpson index is a traditional measure of diversity that has an easy interpretation in

biology as the probability that two alleles on paired loci are different or as heterozygosity in a panmictic population.

Apart from the above mentioned measures of diversity, the paper of Chakraborty and Rao [2] introduces the following measures of diversity:  $\alpha$ -order entropy of Havrda and Charvát, paired Shannon entropy, Rényi entropy of order  $\alpha$  and  $\gamma$ -entropy function. We show further that some of them are special cases of the more general concept of f-diversity.

## 2 f-diversities

The Shannon information  $I_S(X;Y)$  is defined in information theory as a measure of association between two random variables  $X$  and  $Y$ .

$$I_S(X;Y) = \sum_{x,y} p(x,y) \log \frac{p(x,y)}{p(x) \cdot p(y)}, \quad (4)$$

where  $p(x,y)$  are the joint probabilities and  $p(x), p(y)$  marginal probabilities of values of random variables  $X$  and  $Y$ .

The Shannon information  $I_S(X;Y)$  is non-negative and equal to zero if and only if the random variables are independent. Maximal information is Shannon entropy obtained when  $Y = X$ . In the event that the random variable  $X$  is a gene on a given loci with the alleles  $A_1, A_2, \dots, A_k$  and probability distribution  $p = (p_1, p_2, \dots, p_k)$ , then **Shannon entropy** of the gene  $X$  is the same as Shannon information index  $H_S(p) = -\sum_{i=1}^k p_i \log p_i$ . We will further call this measure of diversity **Shannon diversity**.

The Shannon information can be generalized to the f-information

$$I_f(X;Y) = \sum_{x,y} f\left(\frac{p(x,y)}{p(x) \cdot p(y)}\right) p(x) \cdot p(y), \quad (5)$$

where  $f(t)$  is a convex function on the interval  $[0, \infty)$ , strictly convex at  $t = 1$  with  $f(1) = 0$ . For more details about f-information derived from the concept of f-divergence see Vajda [12]. In case of  $f(t) = t \log t$ , f-information  $I_f(X;Y)$  reduces to Shannon information  $I_S(X;Y)$ . The f-information was first systematically studied by Zvárová [13] who proved the representation of the maximal f-information and called it f-entropy. In the case that the random variable  $X$  is a gene on a given loci with the alleles  $A_1, A_2, \dots, A_k$  and probability distribution  $p = (p_1, p_2, \dots, p_k)$ , then **f-entropy** of the gene  $X$  is

$$H_f(p) = \sum_{i=1}^k p_i^2 f(1/p_i) + f(0) \sum_{i=1}^k p_i(1 - p_i). \quad (6)$$

The f-entropy  $H_f(p)$  can be interpreted as an average unpredictability of the individual alleles  $A_i$  of the gene  $X$  (Zvárová and Vajda, [16]). In this sense f-entropy  $H_f(p)$  is a measure of genetic diversity depending on the distribution  $p$ .  $H_f(p)$  will be called **f-diversity** if it moreover satisfies the following conditions:

- $H_f(p)$  is non-negative,

- $H_f(p)$  reaches its minimal value in case of the monomorphism,
- $H_f(p)$  reaches its maximal value in the case that  $p = u_k$  is the uniform distribution,
- $H_f(p)$  is symmetric function of  $p$ ,
- $H_f(p)$  is a concave function on the system of all probability distributions  $p$ .

f-diversity  $H_f(p)$  was first introduced into genetics by Zvárová [14] and discussed in further detail in (Zvárová and Mazura [15]). We can see that  $H_f(p)$  is a sum of two expressions where the second one is none other than the well-known Gini-Simpson index  $H_{GS}(p)$  multiplied by the constant  $f(0)$ . We will further call the Gini-Simpson index **Gini-Simpson diversity**. In the paper (Zvárová [13]) it was proved that f-diversities can be found among f-entropies satisfying the condition  $g(t) = (f(t) - f(0))/t$  is a concave function. Then the f-entropy  $H_f(p)$  of the gene  $X$  will reach its maximal value for uniform distribution of alleles  $p = u_k$ . We can see that Gini-Simpson diversity  $H_{GS}(p)$  is the f-diversity with  $f(t) = t - 1$  for  $t > 1$ , otherwise  $f(t) = 0$ . Similarly, Shannon diversity is the f-diversity with  $f(t) = t \log t$ . Apart from the above mentioned measures of genetic diversity there are other measures of f-diversities e.g.  $\alpha$ -order entropy of Havrda-Charvát (Havrda, Charvát [4]) further called  **$\alpha$ -order diversity of Havrda-Charvát**

$$H_{H-Ch}(p) = \frac{1}{2^{\alpha-1} - 1} \left( 1 - \sum_{i=1}^k p_i^\alpha \right), \quad (7)$$

with  $f(t) = 1/(2^{\alpha-1} - 1)t(1 - t^{1-\alpha})$ , where  $0 < \alpha < 2, \alpha \neq 1$ . As proved by Kocmanová and Zvárová [7] **paired Shannon entropy**

$$H_{PS}(p) = - \sum_{i=1}^k p_i \log p_i - \sum_{i=1}^k (1 - p_i) \log(1 - p_i), \quad (8)$$

is the measure of f-diversity with  $f(t) = t^2 \log t + t(1 - t) \log(t - 1)$  for  $1 < t < \infty$  and  $f(t) = 0$  for  $0 \leq t \leq 1$ .

The third f-diversity Number of Alleles (often used in biology under the name Species Count) is

$$H_{NA}(p) = k - 1. \quad (9)$$

It is also f-diversity with  $f(t) = t(t - 1)$  (Horáček and Zvárová [5]) and simultaneously it belongs to the class of power  $\alpha$ -diversities

$$H_\alpha(p) = \begin{cases} \frac{1}{\alpha-1} (1 - \sum_{i=1}^k p_i^\alpha) & \text{for } 0 < \alpha < 2, \alpha \neq 1, \\ \sum_{i=1}^k \chi_{(0,1)}(p_i) - 1 & \text{for } \alpha = 0, \\ - \sum_{i=1}^k p_i \log p_i & \text{for } \alpha = 1. \end{cases} \quad (10)$$

Diversity  $H_\alpha(p)$  is, up to a multiplying constant, equal to Havrda-Charvát diversity  $H_{H-Ch}(p)$ .

In this framework of information theory we have introduced the concept of f-diversity and showed several measures of f-diversity used in biology and medicine which we call **biodiversities**.

### 3 Measures of rarity, self and marginal f-diversity

In the case that a random variable  $X$  is a gene on a given loci with alleles  $A_1, \dots, A_k$  and a probability distribution  $p = (p_1, \dots, p_k)$  then according to Patil and Tailie [10] the rarity of allele  $A_i$  depends only on the numerical value of  $p_i$ . Denoting the rarity of an allele  $A_i$  by  $R(p_i)$  the **diversity index** associated with the measure of rarity  $R$  is its average rarity calculated as

$$\sum_{i=1}^k p_i R(p_i). \quad (11)$$

Three widely used indexes of ecological diversity are:  
Number of Alleles (Number of Alleles diversity)

$$H_{NA} = k - 1 \quad \text{with } R(p_i) = (1 - p_i)/p_i, \quad (12)$$

Gini-Simpson index (Gini-Simpson diversity)

$$H_{GS}(p) = \sum_{i=1}^k p_i(1 - p_i) \quad \text{with } R(p_i) = 1 - p_i \quad (13)$$

and Shannon index (Shannon diversity)

$$H_S(p) = - \sum_{i=1}^k p_i \log p_i \quad \text{with } R(p_i) = - \log p_i. \quad (14)$$

These three indexes of diversity belong to the family of diversity indexes of order  $\beta$  (Patil and Tailie [10]) defined as

$$R_i(p_i) = \begin{cases} (1 - p_i^\beta)/\beta & \text{if } \beta \geq -1, \beta \neq 0, \\ - \log p_i & \text{if } \beta = 0, \end{cases} \quad (15)$$

where for  $\beta = 0$  we receive Shannon diversity, for  $\beta = 1$  Gini-Simpson diversity and for  $\beta = -1$  Number of Alleles diversity. As it was shown above, all three indexes of diversity belong to the family of f-diversity.

Let us present the new concept of self f-diversity that is a generalization of the rarity introduced by Patil and Tailie [10]. **Self f-diversity** of the  $j$ -th component ( $j$ -th allele) is

$$R_{f,j}(p) = p_j f(1/p_j) + f(0)(1 - p_j). \quad (16)$$

Then it can be proved that f-diversity

$$H_f(p) = \sum_{i=1}^k p_i (p_i f(1/p_i) + f(0)(1 - p_i)) \quad (17)$$

$$= \sum_{i=1}^k R_{f,i}(p). \quad (18)$$

Self f-diversity  $R_{f,i}(p)$  shows the additive influence of the probability  $p_i$  on the value of f-diversity.

For the often used Shannon diversity the **Shannon self diversity** is equal to

$$R_{S,j}(p) = -\log(p_j) \quad (19)$$

also known in information theory as **self information**. Similarly, for Gini-Simpson diversity the **Gini-Simpson self diversity** is equal to

$$R_{GS,j}(p) = 1 - p_j. \quad (20)$$

Another perspective on the impact of the  $j$ -th allele comes if do not distinguish among other alleles. In this case we formally work with two alleles (dichotomy) with probabilities  $p_j$  and  $1 - p_j$ . Then **marginal f-diversity** of the  $j$ -th component is defined as

$$H_{f,j}(p) = p_j^2 f(1/p_j) + (1 - p_j) f(1/(1 - p_j)) + 2f(0)p_j(1 - p_j). \quad (21)$$

We shall further introduce several propositions about f-diversities and marginal f-diversities.

**Proposition 1.** *Let us have two one-dimensional probability distributions  $p$  and  $q$  such that  $q_r = 1 - p_j$  for some  $j, r$ . Then*

$$H_{S,j}(p) = H_{S,r}(q). \quad (22)$$

For  $f(t) = t \log t$  we obtain **Shannon marginal f-diversity** as

$$H_{S,j}(p) = -p_j \log p_j - (1 - p_j) \log(1 - p_j). \quad (23)$$

**Proposition 2.** *For  $p_i > 0$  Shannon marginal diversity is positive, i.e.*

$$H_{S,j}(p) > 0 \quad (24)$$

**Proposition 3.** *Paired Shannon diversity  $H_{PS}(p)$  is the sum of Shannon marginal diversities  $H_{S,j}(p)$  for all components of  $p$ :*

$$H_{PS}(p) = \sum_{j=1}^k H_{S,j}(p). \quad (25)$$

**Proposition 4.** *Paired Shannon marginal diversity of the  $j$ -th component is equal to Shannon marginal diversity multiplied by 2:*

$$H_{SP,j}(p) = 2H_{S,j}(p) \quad (26)$$

**Proposition 5.** *(Monotony) If  $0 < p_j < p_r < 1/2$  then the Shannon marginal diversity of the  $j$ -th component  $H_{S,j}(p)$  is smaller than Shannon marginal diversity of the  $r$ -th component  $H_{S,r}(p)$ , i.e.*

$$H_{S,j}(p) < H_{S,r}(p). \quad (27)$$

**Proposition 6.** Let  $p_{ij} > 0$ ,  $j = 1, \dots, n_i$ ,  $i = 1, \dots, k$  and  $\sum_{i=1}^k \sum_{j=1}^{n_i} p_{ij} = 1$ . Let us denote

$$\begin{aligned} p_i &= (p_{i1}, \dots, p_{in_i}), \\ p &= (p_1, \dots, p_k), \\ p_{i+} &= \sum_{j=1}^{n_i} p_{ij}, \\ p_+ &= (p_{1+}, \dots, p_{k+}). \end{aligned}$$

Then

$$H_S(p) = H_S(p_+) + \sum_{i=1}^k p_i H_S(p_i) \quad (28)$$

Next proposition is a special case of the Proposition 6.

**Proposition 7.**

$$H_S(p) = H_{S,j}(p) + (1 - p_j) H_S((p_1, \dots, p_{j-1}, p_{j+1}, \dots, p_k) / (1 - p_j)) \quad (29)$$

## 4 Sample estimates of Gini-Simpson and Shannon diversities

Let us have a random sample of the size  $n$  of diploid individuals. Let us denote for paired loci of a gene  $X$  the number of observed alleles  $A_i$  as  $N_i$  for  $i = 1, \dots, k$  from a total number of observed alleles  $N = 2n$ . Then the relative frequency  $\hat{p}_i = N_i/N$  is an unbiased estimate of the probability  $p_i$  of the occurrence of the allele  $A_i$ ,  $i = 1, 2, \dots, k$ . We denote  $\hat{p} = (\hat{p}_1, \dots, \hat{p}_k)$  the vector of relative frequencies  $\hat{p}_i$  and  $p = (p_1, \dots, p_k)$  corresponding probability distribution.

The sample estimate of Gini-Simpson diversity is then

$$H_{GS}(\hat{p}) = 1 - \sum_{i=1}^k \hat{p}_i^2. \quad (30)$$

As shown in a paper (Nei and Roychoudhury [9]) this naive estimate is not the unbiased estimate of the Gini-Simpson diversity, because its mean value  $E(H_{GS}(\hat{p}))$  is equal to  $((2n-1)/2n)H_{GS}(p)$ . They therefore proposed an unbiased estimate  $H_{GS}^*(\hat{p})$  as

$$H_{GS}^*(\hat{p}) = \frac{2n}{2n-1} \left( 1 - \sum_{i=1}^k \hat{p}_i^2 \right), \quad (31)$$

where  $E(H_{GS}^*(\hat{p})) = H_{GS}(p)$ .

In the estimated variance published in a paper (Chakraborty and Rao [2]) a small misprint was found that was corrected in Kocmanová and Zvárová [7]. The variance of

the unbiased estimate  $H_{GS}^*(\hat{p})$  is then

$$\begin{aligned} \text{Var} (H_{GS}^*(\hat{p})) &= \frac{4(n-1)}{n(2n-1)} \left( \sum_{i=1}^k p_i^3 - \left( \sum_{i=1}^k p_i^2 \right)^2 \right) \\ &+ \frac{1}{n(2n-1)} \sum_{i=1}^k p_i^2 \left( 1 - \sum_{i=1}^k p_i^2 \right). \end{aligned} \quad (32)$$

The naive sample estimate of the Shannon diversity  $H_S(p)$  is

$$H_S(\hat{p}) = - \sum_{i=1}^k \hat{p}_i \log \hat{p}_i. \quad (33)$$

However, the naive Shannon diversity estimators such as  $H_S(\hat{p})$ , in which  $p$  is simply replaced by  $\hat{p}$  are always biased and they deviate from the true value of the Shannon diversity not only randomly but also systematically. It should be emphasized that an ideal estimator does not exist. The paper (Bonachela, Hinrichsen and Muños [1]) discusses different Shannon diversity estimators. For the purpose of this paper we stay with the naive sample estimate of Shannon diversity given by (33). The estimate  $H_S(\hat{p})$  is not unbiased and its mean value can be approximated by

$$E (H_S(\hat{p})) \doteq H_S(p) - \frac{k-1}{4n} \quad (34)$$

and its variance can be approximated by

$$\text{Var} (H_S(\hat{p})) \doteq \frac{1}{2n} \left( \sum_{i=1}^k p_i (\log p_i)^2 - \left( \sum_{i=1}^k p_i \log p_i \right)^2 \right) + \frac{k-1}{2n^2}, \quad (35)$$

see Hutcheson [6].

Gini-Simpson and Shannon diversities have been used in a number of studies for measuring genetic diversity. However, their numerical values are not influenced by alleles with small probabilities of occurrence. Therefore, even in the event that there are many alleles in the population, but only a small number of alleles are prevailing and others are very rare, Gini-Simpson and Shannon diversities are small. Therefore the Number of Alleles diversity remains the simple important measure of genetic diversity.

We will show sample behaviour of Shannon, Gini-Simpson and Number of Alleles diversities, as well as corresponding self and marginal diversities, in the following section.

## 5 Stochastic Modeling of Number of Alleles, Gini-Simpson and Shannon diversities and corresponding self and marginal diversities

Let us consider the following example. In the sample of  $n=97$  patients suffering with Alzheimer's disease we examined the distribution of alleles  $e_1$ ,  $e_2$  and  $e_3$  of the gene

ApoE. In the total number  $N = 194$  of examined alleles, the allele  $e_1$  occurred in 27 cases, the allele  $e_2$  in 67 cases and the allele  $e_3$  in 100 cases. Therefore the sample estimates of the probabilities of the alleles  $e_1$ ,  $e_2$  and  $e_3$  are given by corresponding relative frequencies  $p_1 = 27/194$ ,  $p_2 = 67/194$  and  $p_3 = 100/194$ . In the case that we will consider the relative frequencies as the real probabilities of the alleles in the population, we can simulate the behaviour of sample estimates of different forms of diversities for Number of Alleles, Gini-Simpson and Shannon types of diversities.

Table 1 displays simulations of means and standard deviations of the following estimates of diversities Number of Alleles, Gini-Simpson, Gini-Simpson unbiased, Shannon and Shannon unbiased for  $N=2n=10, 50, 100$  and  $500$ . We generated 1000 random samples for mean and standard deviation estimates of each diversity.

**Table 1.** Behaviour of several sample estimates of Number of Alleles, Gini-Simpson and Shannon diversities

Diversity	Simulations			Theoretical values		
	$N$	mean	SD	mean	SD of est.	Asympt. SD of est.
NumberOfAlleles	10	1.757	0.432	2.000		
GiniSimpson	10	0.535	0.097	0.596		0.083
GiniSimpson Unbiased	10	0.595	0.108	0.596	0.107	0.083
Shannon	10	0.868	0.176	0.983	0.092	
Shannon Unbiased	10	0.968	0.176	0.983		
NumberOfAlleles	50	2.000	0.020	2.000		
GiniSimpson	50	0.583	0.039	0.596		0.037
GiniSimpson Unbiased	50	0.595	0.040	0.596	0.040	0.037
Shannon	50	0.962	0.066	0.983	0.059	0.055
Shannon Unbiased	50	0.982	0.066	0.983		0.055
NumberOfAlleles	100	2.000	0.000	2.000		
GiniSimpson	100	0.590	0.027	0.596		0.026
GiniSimpson Unbiased	100	0.596	0.027	0.596	0.027	0.026
Shannon	100	0.973	0.045	0.983	0.043	0.041
Shannon Unbiased	100	0.983	0.045	0.983		0.041
NumberOfAlleles	500	2.000	0.000	2.000		
GiniSimpson	500	0.594	0.012	0.596		0.012
GiniSimpson Unbiased	500	0.596	0.012	0.596	0.012	0.012
Shannon	500	0.981	0.020	0.983	0.020	0.019
Shannon Unbiased	500	0.983	0.020	0.983		0.019

We can see in Table 1 that Gini-Simpson and Shannon diversity unbiased estimates are better than corresponding naive estimates for small sample sizes  $n$ .

We furthermore display mean values of naive estimates of self and marginal diversities for Number of Alleles type diversities (Table 2), Gini-Simpson type diversities (Table 3) and Shannon type diversities (Table 4).

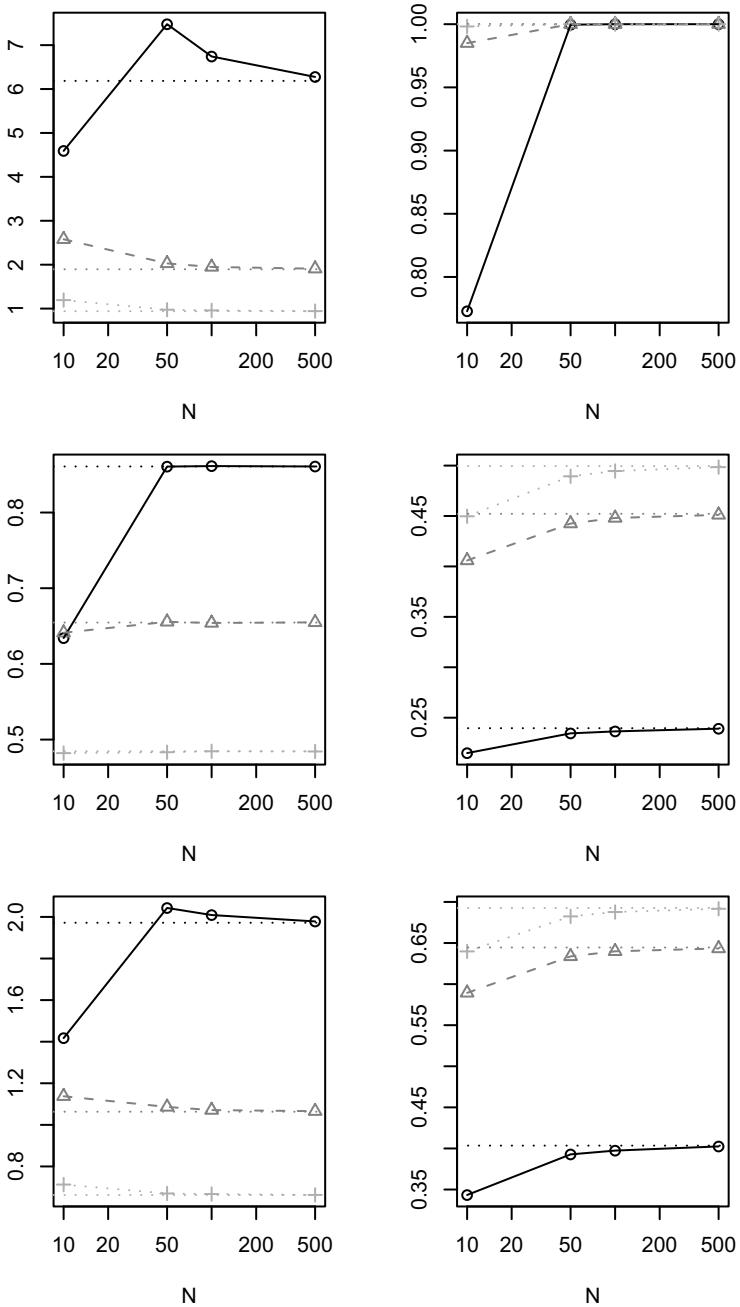


**Fig. 1.** Pairs of graphs in each row of the figure display simulated means of self and marginal diversities. In the upper row are Number of Alleles type diversities, in the row are Gini-Simpson type diversities and in the lower row are Shannon type diversities. In each graph the symbols  $\circ, \Delta, +$  denote the corresponding diversity derived from probabilities  $p_1, p_2, p_3$ .

**Table 2.** Number of Alleles self and marginal diversities

Probability	Self diversity					Marginal diversity				
	Theor.	$N=10$	$N=50$	$N=100$	$N=500$	Theor.	$N=10$	$N=50$	$N=100$	$N=500$
$p_1 = 27/194$	6.19	4.59	7.48	6.74	6.28	1.00	0.77	1.00	1.00	1.00
$p_2 = 67/194$	1.90	2.58	2.03	1.95	1.91	1.00	0.99	1.00	1.00	1.00
$p_3 = 100/194$	0.94	1.19	0.97	0.96	0.94	1.00	1.00	1.00	1.00	1.00

**Table 3.** Gini-Simpson self and marginal diversities

Probability	Self diversity					Marginal diversity				
	Theor.	$N=10$	$N=50$	$N=100$	$N=500$	Theor.	$N=10$	$N=50$	$N=100$	$N=500$
$p_1 = 27/194$	0.86	0.63	0.86	0.86	0.86	0.24	0.21	0.23	0.24	0.24
$p_2 = 67/194$	0.65	0.64	0.66	0.65	0.65	0.45	0.41	0.44	0.45	0.45
$p_3 = 100/194$	0.48	0.48	0.48	0.48	0.48	0.50	0.45	0.49	0.49	0.50

**Table 4.** Shannon self and marginal diversities

Probability	Self diversity					Marginal diversity				
	Theor.	$N=10$	$N=50$	$N=100$	$N=500$	Theor.	$N=10$	$N=50$	$N=100$	$N=500$
$p_1 = 27/194$	1.97	1.42	2.04	2.01	1.98	0.40	0.34	0.39	0.40	0.40
$p_2 = 67/194$	1.06	1.14	1.09	1.07	1.07	0.64	0.59	0.63	0.64	0.64
$p_3 = 100/194$	0.66	0.71	0.67	0.67	0.66	0.69	0.64	0.68	0.69	0.69

We can see (Fig. 1) that for small sample sizes the estimates of self diversity and marginal diversity of the Number of Alleles are worse than estimates for Gini-Simpson and Shannon type diversities.

## References

1. Bonachela, J.A., Hinrichsen, H., Munoz, M.A.: Entropy estimates of small data sets. *Journal of Physics A: Mathematical and Theoretical* **41** (2009) 1–11
2. Chakraborty, R., Rao, C.R.: Measurement of genetic variation for evolutionary studies. *Statistical and Medical Sciences*. Elsevier Science Publ (1991) 271–316
3. Gini, C.: Variabilità e Mutabilità. *Studi Economico-Giuridici della R. Univ. di Cagliari*. **3** (1912) Part 2 80
4. Havrda, S., Charvát, F.: Quantification methods of classification processes: Concept of structural  $\alpha$ -entropy. *Kybernetika* **3** (1967) 95–100
5. Horáček, M., Zvárová, J. (supervisor): Biodiversity measures and their applications (in Czech), MSc. diploma thesis, Charles University of Prague, Faculty of Mathematics and Physics (2009)

6. Hutcheson K.: A test for comparing diversities based on the Shannon formula. *Journal of the Theoretical Biology* **29** (1970) 151–154
7. Kocmanová, D., Zvárová, J. (supervisor): Study of influence of genetic factors on the start and development some diseases (in Czech), MSc. diploma thesis, Charles University of Prague, Faculty of Mathematics and Physics (1999)
8. Nei, M.: Genetic distance between populations. *Amer. Nat.* **106** (1982) 283–292
9. Nei M., Roychoudhury A.K.: Sampling variance of heterozygosity and genetic distance. *Genetics* **76** (1974) 379–390
10. Patil, G.P., Tailie, C.: Diversity as a concept and its measurement. *Journal of Americal Statistical Association*, **77** (1982) 548–561
11. Simpson, E. H.: Measurement of diversity. *Nature* **163** (1949) 688
12. Vajda, I.: *Theory of Statistical Inference and Information*. Boston, Kluwer (1989)
13. Zvárová, J. On measures of statistical dependence. *Casopis pro pestovani matematiky* (1974) **99** 15–29
14. Zvárová, J.: *Information Measures of Stochastic Dependence and Diversity: Theory and Medical Informatics Applications*. Disertaition for Doctor of Sciences Degree, Academy of Sciences of the Czech Republic (1998)
15. Zvárová, J., Mazura, I.: *Stochastic Genetics* (in Czech) Charles University, Karolinum, Prague (2001)
16. Zvárová, J., Vajda, I.: On genetic information, diversity and distance. *Methods of Information in Medicine* **2** (2006) 173–179

# Deterministic models of natural selection and their relation to ecology

Zdeněk Pospíšil

Masaryk University, Faculty of Science, Department of Mathematics and Statistics, Kotlářská 2,  
Brno, Czech Republic,  
pospisi1@math.muni.cz,  
WWW home page: <http://www.math.muni.cz/~pospisi1/>

**Abstract.** The theory of evolution and ecology are very important components of theoretical biology. The contribution presents some links between them that emerges on the level of mathematical models. It introduces replicator equations (ordinary differential equations modeling natural selection) and shows their equivalence with the Lotka-Volterra equations of population dynamics and their connection to the game theory. It mentions two alternative models of selection as well.

The contribution can serve as an introductory text on the subject and a basic source of references.

## 1 Introduction

John Maynard Smith and George Price published a pioneering paper on logic of animal conflicts in *Nature*, 1973 [13]. They aimed to model mathematically some aspects of biological evolution, in particular, the natural selection perceived as a mutual contest of non-intelligent participants that are not able to evaluate information on contenders. Maynard Smith and Price adopted concepts of game theory for the purpose.

Similar ideas were formulated in terms of ordinary differential equations by Peter Taylor and Leo Jonker in 1978 [15]. The paper met no reception until 1981 when Peter Schuster and Karl Sigmund independently rediscovered the same equation [11] and applied them to point out a mistake appearing in a famous book by Richard Dawkins [2].

The combination of differential equations and game theory proved to be very fruitful. Recently, it has been explored in monographs in various ways, e.g. [12], [8], [16], [3], [14] and it reaches applications not only in evolutionary biology but also in economics, psychology, and decision theory. Indeed, the theory admits applications for describing any conflict with incomplete or even none information, hence, it allows one to understand behavior of complex and complicated systems (or to get some insight, at least); community ecology represents an important example.

The present article is not intended to be a comprehensive text on evolutionary dynamics. It is meant to be a mere introduction to the subject and to allow a reader to get an impression of it. The book [8] was utilized as the main source for the article. The subsequent section introduces a dynamical model of the deterministic part of biological

evolution, that is, of the natural selection. Then, the main result (Theorem 3) shows that, under some assumptions, the model presented is equivalent to the fundamental model of population ecology. Section 3 goes back to game theory and demonstrates how the “static” results obtained by it correspond to “dynamical” ones yielded by the qualitative theory of differential equations. Moreover, Theorem 6 suggest that the differential equations under consideration may play a fundamental role in theoretical biology. This “strong assertion” is weakened in the next section that presents some alternative models of the selection.

Sufficient preliminaries to understand the text are calculus and linear algebra as taught in university courses. Some knowledge on qualitative theory of ordinary differential equations might be useful as well.

The symbols used are standard. To refresh,  $\mathbb{R}$ ,  $\mathbb{R}_+$  and  $\bar{\mathbb{R}}_+$  denote set of reals, of positive reals and of non-negative reals, respectively. Vectors are denoted by bold symbols, their entries by symbols in italic and indexed by subscripts, i.e the vector  $x$  contains the entries  $x_i$ . Sometimes, it is useful to denote vector entries by a vector symbol in parentheses supplemented by a subscript, i.e.  $x_i = (x)_i$ . Vector  $e_k$  is the  $k$ -th vector of standard basis (all of its entries equal to zero with the exception of the  $k$ -th which equals one,  $(e_k)_j = \delta_{jk}$ , where  $\delta_{jk}$  denotes the Kronecker symbol), symbol  $I$  denotes the vector with all of entries equal to one. A support of  $n$ -dimensional vector  $x$  is the set of subscripts such that corresponding entries differ from zero,

$$\text{supp}x = \{i \in \{1, 2, \dots, n\} : x_i \neq 0\}.$$

Matrices are denoted by sans serif font, their entries by italic and indexed by double subscripts; the matrix  $A$  possesses the entry  $a_{ij}$  in the  $i$ -th row and in the  $j$ -th column. The symbols  $E$  and  $O$  denote the unity and the zero matrices, respectively. The matrix multiplication is implicit, ( $AB$  stands for the product of matrices  $A$  and  $B$ ). Vectors appearing in formulas including matrices are considered to be column ones. The transpose of a matrix is denoted by  $^T$ , symbol  $\circ$  denotes the Hadamard product of matrices with equal shape;  $A \circ B$  is a matrix with the entries  $a_{ij}b_{ij}$  in the  $i$ -th row and in the  $j$ -th column.

The symbols  $S_n$ ,  $S_n^\circ$  and  $S_n^\partial$  denote the  $n$ -dimensional probability simplex, its interior and its boundary, respectively; that is

$$S_n = \{(x_1, x_2, \dots, x_n) \in \bar{\mathbb{R}}_+^n : x_1 + x_2 + \dots + x_n = 1\} = \{x \in \bar{\mathbb{R}}_+^n : I^T x = 1\},$$

$$S_n^\circ = \{x \in \mathbb{R}_+^n : I^T x = 1\}, \quad S_n^\partial = S_n \setminus S_n^\circ.$$

## 2 Replicator equation

The notion of evolutionary stability relies upon implicit dynamical considerations. In certain situations, the underlying dynamic can be modeled by a differential equation on the simplex  $S_n$ . In this section, we introduce considerations and assumptions leading to equations describing the evolution of the frequencies of traits in a population. A particular case of this equation can be transformed to the Lotka-Volterra equations, i.e. to the standard model of population dynamics. Hence, from a mathematical point of view, the natural selection is the same process as ecology.

## 2.1 Derivation/construction of the equation

Let us consider a population (biological community in a broad sense) of some individuals which is split up into several “types”. The individuals “produce” offspring of the same “type” (species, phenotypes, genotypes, traits etc.). The bounds of this process are in a sense limited, i.e. the number of individuals cannot be either infinite nor “too great”. That is why the “excessive” individuals die or are not even born. Each of the subpopulations of the same type of individuals may impact the particular surroundings or conditions for the remaining sub-populations.

For the described situation, we can apply a basic tenet of Darwinism: the subpopulations with greater fitness will survive and increase and the ones with smaller fitness will decline and die out. This statement suggest that the fitness of a sub-population is not a self-existent value, but is determined by fitnesses of the remaining sub-populations. A more precise formulation of the tenet is that surviving and increasing sub-populations are the ones with the fitness greater than a kind of “overall fitness”, e.g. the average fitness of the sub-populations.

The survival and increase of a subpopulation results in an increase of its magnitude or abundance. This does not mean that the prosperous sub-populations are the ones with increasing size. The size of a non-prosperous subpopulation can increase but increments of prosperous ones are greater. Thus the size of a subpopulation itself is not able to characterize the prosperity or fitness of a subpopulation. A more appropriate indicator is the relative abundance of subpopulation, the fraction of the subpopulation abundance in the whole population. Now, we can reformulate the considerations provided in the following way: *a change of the relative frequency of sub-population is proportional to difference of its fitness and an overall fitness.*

The current conclusion can be expressed in mathematical terms. Therefore, let us introduce the notation

$x_i$  – relative frequency of the  $i$ -th sub-population,

$f_i$  – fitness of the  $i$ -th sub-population;

having population of total size  $N$  split into  $n$  different types of subpopulations and size (abundance) of the  $i$ -th sub-population being  $N_i$ , we can write

$$x_i = \frac{N_i}{N}, \quad i = 1, 2, \dots, n, \quad \sum_{i=1}^n N_i = N, \quad \text{hence} \quad \sum_{i=1}^n x_i = 1.$$

The overall fitness can be expressed as the average of single fitnesses weighted by the relative frequencies, i.e.

$$\bar{f} = \sum_{j=1}^n x_j f_j.$$

We aim to describe a dynamics of the process under consideration. Therefore we consider the single relative frequencies to be functions of time,  $x_i = x_i(t)$ ,  $i = 1, 2, \dots, n$ . The fitness of one subpopulation depends on presence of subpopulations that stimulate or reduce its fitness. It may also be impacted by its size itself as the size of subpopulation may determine whether intraspecific competition or cooperation appears. The separate fitnesses are functions of presence constituent sub-populations,  $f_i = f_i(x_1, x_2, \dots, x_n)$ ,

consequently. Thus, we obtain the following “system of equations”

$$\text{time change } x_i \sim f_i(x_1, x_2, \dots, x_n) - \sum_{j=1}^n x_j f_j(x_1, x_2, \dots, x_n), \quad i = 1, 2, \dots, n.$$

Now, we must specify the proportionateness “ $\sim$ ” and “time change”. We choose the direct proportion with positive rate  $c$  and the relative change of relative frequency, i.e. time derivative over instant relative frequency. The previous “system of equations” acquires the form

$$\frac{x_i'}{x_i} = c \left( f_i(x_1, x_2, \dots, x_n) - \sum_{j=1}^n x_j f_j(x_1, x_2, \dots, x_n) \right), \quad i = 1, 2, \dots, n,$$

or the explicit and more concise one

$$x_i' = cx_i \left( f_i(x) - \sum_{j=1}^n x_j f_j(x) \right), \quad i = 1, 2, \dots, n.$$

The time unit can be chosen such that the rate of proportionality  $c$  equals one. Finally, we obtain *the general replicator equation*

$$x_i' = x_i \left( f_i(x) - \sum_{j=1}^n x_j f_j(x) \right), \quad i = 1, 2, \dots, n. \quad (1)$$

The equation (1) represents an autonomous system of  $n$  ordinary differential equations which can be rewritten in the form  $x_i' = x_i(e_i - x)^\top f(x)$ ,  $i = 1, 2, \dots, n$  and then in the form of one vector equation

$$x' = x \circ ((E - xI^\top)f(x)).$$

## 2.2 Basic properties of replicator equation solutions

From now on, we will assume that the equation (1) with the initial condition such that  $x_1(0) + x_2(0) + \dots + x_n(0) = 1$  possesses a unique solution. This property is guaranteed, e.g., if all of the functions  $f_i$ ,  $i = 1, 2, \dots, n$  are continuously differentiable. Let us show several simple properties of the equation (1).

**Lemma 1.** *Let the solution  $x$  of the equation (1) satisfy the initial condition*

$$x_1(0) + x_2(0) + \dots + x_n(0) = 1,$$

*i.e.  $I^\top x(0) = 1$ . Then*

$$x_1(t) + x_2(t) + \dots + x_n(t) = 1 \text{ for all } t \geq 0.$$

*Proof.* Let  $x$  be the solution of the equation (1). Denote  $S = x_1 + x_2 + \dots + x_n$ . Then

$$S' = \sum_{i=1}^n x_i \left( f_i(x) - \sum_{j=1}^n x_j f_j(x) \right) = \bar{f}(x) - S\bar{f}(x),$$

which is the linear equation for the unknown function  $S$ . Its unique solution is

$$S(t) = 1 + (S(0) - 1)e^{-\int_0^t \bar{f}(x(\tau)) d\tau}.$$

Hence,  $S(0) = 1$  implies  $S(t) = 1$  for all  $t \geq 0$ .  $\square$

**Lemma 2.** *If there exists a subscript  $i \in \{1, 2, \dots, n\}$  such that  $x_i(0) = 0$  then  $x_i(t) = 0$  for all  $t \geq 0$ .*

*Proof.* Let  $x$  be the solution of the equation (1). The function  $x_i(t) \equiv 0$  solves the scalar equation.

$$x_i' = x_i (f_i(x) - \bar{f}(x)).$$

Now, the statement follows from the assumed uniqueness of the system (1) solution.  $\square$

The lemmas 1 and 2 state that the  $n$ -dimensional simplex  $S_n$ , its boundary  $S_n^\partial$ , and, as a consequence of the assumed uniqueness of solution, its interior  $S_n^\circ$  are invariant sets of the system (1). Differently speaking, the replicator equation (1) models evolution which does not change the number of the subpopulation. That is, a subpopulation which is not present at the beginning cannot appear during evolution and a sub-population present at the beginning cannot disappear in a finite time. Of course, the lemmas do not imply non-existence of a component of solution  $x_i$  of the system (1) such that  $x_i(0) > 0$ ,  $\lim_{t \rightarrow \infty} x_i(t) = 0$ . A subpopulation can die out during “long time”.

From a biological perspective, the replicator equation describes the natural selection, i.e. the deterministic part of the biological evolution. Mutations and additional stochastic processes forming the evolution are not included into the model.

**Lemma 3.** *Let  $\Psi : S_n \rightarrow \mathbb{R}$  be a continuous function. Put  $g_i = f_i + \Psi \quad \forall i \in \{1, 2, \dots, n\}$ . Then  $x$  solves the equation (1) if and only if it solves the equation*

$$x_i' = x_i \left( g_i(x) - \sum_{j=1}^n x_j g_j(x) \right), \quad i = 1, 2, \dots, n$$

as well.

*Proof.*

$$\begin{aligned} x_i' &= x_i \left( f_i(x) - \sum_{j=1}^n x_j f_j(x) \right) = x_i \left( f_i(x) + \Psi(x) - \sum_{j=1}^n x_j f_j(x) - \Psi(x) \sum_{j=1}^n x_j \right) = \\ &= x_i \left( g_i(x) - \sum_{j=1}^n x_j (f_j(x) + \Psi(x)) \right) = x_i \left( g_i(x) - \sum_{j=1}^n x_j g_j(x) \right). \quad \square \end{aligned}$$

The equation appearing in Lemma 3 possesses the same form as the replicator equation (1). Consequently, the functions  $g_i$  represent fitnesses of subpopulations as well. Lemma 3 states that the addition of a constant to the fitnesses of sub-population does not influence the evolution of their relative frequencies. Hence, the fitnesses can be chosen in the way such that average fitness equals zero. That is, we need not think of fitnesses but of deviations from the overall fitness.

**Theorem 1 (Hofbauer *et al.* [7], Zeeman [17]).** *Let there exist a point  $\hat{x} \in S_n$  and its neighborhood  $U \subseteq \mathbb{R}^n$  such that*

$$\sum_{i=1}^n \hat{x}_i f_i(x) > \bar{f}(x) \quad \text{for all } x \in S_n \cap (U \setminus \{\hat{x}\}). \quad (2)$$

*Then  $\hat{x}$  is the asymptotically stable equilibrium of the system (1).*

*Proof.* The neighborhood  $U$  can be taken such that  $\text{supp } \hat{x} = \text{supp } x$  holds for each point  $x \in S_n \cap U$ . The Jensen inequality<sup>1</sup> implies that the following holds

$$\begin{aligned} \sum_{i \in \text{supp } \hat{x}} \hat{x}_i \ln \frac{\hat{x}_i}{x_i} &= \sum_{i \in \text{supp } \hat{x}} \hat{x}_i \left( -\ln \frac{x_i}{\hat{x}_i} \right) \geq -\ln \left( \sum_{i \in \text{supp } \hat{x}} \hat{x}_i \frac{x_i}{\hat{x}_i} \right) = \\ &= -\ln \sum_{i \in \text{supp } \hat{x}} x_i = -\ln 1 = 0, \end{aligned}$$

and the equality holds if and only if  $x = \alpha \hat{x}$  for some constant  $\alpha$ ; since  $x \in S_n$ ,  $\hat{x} \in S_n$ , the constant  $\alpha$  has to equal 1. Hence, the following holds

$$\sum_{i \in \text{supp } \hat{x}} \hat{x}_i \ln \hat{x}_i \geq \sum_{i \in \text{supp } \hat{x}} \hat{x}_i \ln x_i, \quad \text{or} \quad \prod_{i \in \text{supp } \hat{x}} \hat{x}_i^{\hat{x}_i} \geq \prod_{i \in \text{supp } \hat{x}} x_i^{\hat{x}_i},$$

for all  $x \in U \cap S_n$ . The equality holds for  $x = \hat{x}$ .

Denote

$$V(x) = \prod_{i \in \text{supp } \hat{x}} \hat{x}_i^{\hat{x}_i} - \prod_{i \in \text{supp } \hat{x}} x_i^{\hat{x}_i}, \quad P(x) = \prod_{i \in \text{supp } \hat{x}} x_i^{\hat{x}_i}.$$

Then

$$V(\hat{x}) = 0, \quad V(x) > 0 \text{ for } x \neq \hat{x}, \quad P(x) > 0 \text{ for } x \in U \cap S_n.$$

<sup>1</sup> Let  $\varphi$  be differentiable strictly convex function defined on the interval  $I$ . Then all of the numbers  $\xi_1, \xi_2, \dots, \xi_k \in I$  and all of the points  $p \in S_k^\circ$  satisfy

$$\varphi \left( \sum_{t=1}^k p_t \xi_t \right) \leq \sum_{t=1}^k p_t \varphi(\xi_t).$$

The equality holds if and only if  $\xi_1 = \xi_2 = \dots = \xi_k$ .

Further, the assumption yields

$$\begin{aligned} \frac{\frac{d}{dt}P(x)}{P(x)} &= \frac{d}{dt} \ln P(x) = \frac{d}{dt} \sum_{i \in \text{supp.} \hat{x}} \hat{x}_i \ln x_i = \sum_{i \in \text{supp.} \hat{x}} \hat{x}_i \frac{x'_i}{x_i} = \\ &= \sum_{i \in \text{supp.} \hat{x}} \hat{x}_i (f_i(x) - \bar{f}(x)) = \sum_{i \in \text{supp.} \hat{x}} \hat{x}_i f_i(x) - \bar{f}(x) \sum_{i \in \text{supp.} \hat{x}} \hat{x}_i = \\ &= \sum_{i \in \text{supp.} \hat{x}} \hat{x}_i f_i(x) - \bar{f}(x) > 0 \end{aligned}$$

and, consequently,

$$\frac{d}{dt}P(x) > 0 \quad \text{which implies} \quad \frac{d}{dt}V(x) = -\frac{d}{dt}P(x) < 0.$$

This means that the function  $V$  is the Lyapunov one of the equation (1) in the point  $\hat{x}$  and this point is uniformly asymptotically stable.  $\square$

Theorem 1 allows us to introduce the terminology: The point  $\hat{x} \in S_n$  satisfying the equality (2) is called *evolutionary stable state* (with respect to the fitnesses  $f_1, f_2, \dots, f_n$ ). If the relative frequencies of subpopulations reach this state they do not evolve further. If the structure of population (i.e. relative frequencies, not the number of subpopulation) “slightly deviates” from the evolutionary stable state it will return to the state  $\hat{x}$  again. In this way, the evolutionary stable state may be interpreted as a formal expression of the “frozen evolution” [4].

### 2.3 Equation with linear fitnesses

The replicator equation (1) with fitnesses  $f_i$  expressed by linear homogeneous functions

$$f_i(x_1, x_2, \dots, x_n) = \sum_{k=1}^n a_{ik}x_k, \quad i = 1, 2, \dots, n$$

is of particular interest. In this case, the replicator equation is of the form

$$x'_i = x_i \left( \sum_{k=1}^n a_{ik}x_k - \sum_{j=1}^n \sum_{k=1}^n x_j a_{jk}x_k \right), \quad i = 1, 2, \dots, n.$$

The coefficients  $a_{ij}$ ,  $i, j = 1, 2, \dots, n$  can be considered to be entries of a square  $n$ -order matrix  $A$ . In this way, the fitnesses are defined by expressions  $f_i(x) = (Ax)_i$  and the equation can be rewritten to the more concise form

$$x'_i = x_i((Ax)_i - x^T Ax), \quad i = 1, 2, \dots, n \quad (3)$$

or

$$x'_i = x_i(e_i - x)^T Ax, \quad i = 1, 2, \dots, n.$$

Again, this system can be written in the form of one vector equation

$$x' = x \circ ((E - xI^T)Ax).$$

**Lemma 4.** *The solution of the equation (3) does not change if a diagonal matrix is added to the matrix A, if a constant vector is added to a row of the matrix A or if a constant vector is added to a column of the matrix A.*

*Proof.* Let  $c$  be an arbitrary  $n$ -dimensional vector. The statements follow from the lemma 3; for the first part we put  $\Psi(x) = c \circ x$ , for the second one we put  $\Psi(x) = x_j c$  for some subscript  $j \in \{1, 2, \dots, n\}$ , and for the third one we put  $\Psi(x) = (0, 0, \dots, 0, c^T x, 0, \dots, 0)^T$ .  $\square$

Without loss of generality, we can assume that the diagonal of matrix A consists of zeroes only, or that one of the rows or columns of the matrix A (e.g. the last one) is the zero one.

In the case of fitnesses in the form of linear functions, the condition (2) can be reformulated: the point  $\hat{x} \in S_n$  represents an evolutionary stable state if there is a neighborhood  $U \subseteq \mathbb{R}^n$  of it such that

$$\hat{x}^T A x > x^T A x, \quad \text{for all } x \in S_n \cap (U \setminus \{\hat{x}\}).$$

In fact, the equation (3) represents a system of  $n$  nonlinear equations with cubic nonlinearities. The most important theorem of the present section states that it can be transformed into the system of  $n - 1$  equations with quadratic nonlinearities:

**Theorem 2 (Hofbauer [5]).** *Put  $b_{ij} = a_{nj} - a_{ij}$ ,  $r_i = a_{in} - a_{nn}$  for  $i, j = 1, 2, \dots, n - 1$ . The transformation of the independent variable (of the time) and the transformation of unknown functions defined by the equalities*

$$\tau = \int_0^t x_n(s) ds, \quad y_j = \frac{x_j}{x_n}, \quad j = 1, 2, \dots, n - 1$$

*map the orbits of the replicator equation (3) initializing in the interior of the simplex  $S_n^\circ$  onto the orbits of the Lotka-Volterra system*

$$\frac{dy_j}{d\tau} = y_j \left( r_j - \sum_{k=1}^{n-1} b_{jk} y_k \right), \quad j = 1, 2, \dots, n - 1 \quad (4)$$

*initializing in the interior of the positive orthant  $\mathbb{R}_+^{n-1}$ .*

*Proof.* The following holds  $\sum_{j=1}^{n-1} y_j = \frac{1}{x_n} \sum_{j=1}^{n-1} x_j = \frac{1}{x_n} (1 - x_n) = \frac{1}{x_n} - 1$ . Subsequently,

$$x_n = \frac{1}{1 + \sum_{j=1}^{n-1} y_j} \quad \text{and further} \quad x_i = \frac{y_i}{1 + \sum_{j=1}^{n-1} y_j}.$$

This means that the map  $y_j = \frac{x_j}{x_n}$ ,  $j = 1, 2, \dots, n - 1$  is a one-to-one map of the interior of the simplex  $S_n^\circ$  onto the interior of the  $n - 1$ -dimensional orthant.

By the lemmas 1 and 2, any solution  $x$  of the equation (3) satisfies

$$\frac{d\tau}{dt} = x_n(t) > 0;$$

the transformation of the independent variable is an injection. Now, we have

$$\begin{aligned} \frac{dy_j}{d\tau} &= \frac{d \frac{x_j}{x_n}}{\frac{d\tau}{dt}} \frac{dt}{d\tau} = \frac{x'_j x_n - x_j x'_n}{x_n^2} \frac{1}{x_n} = \frac{1}{x_n^2} \left( x'_j - x_j \frac{x'_n}{x_n} \right) = \\ &= \frac{1}{x_n^2} (x_j ((Ax)_j - x^T Ax) - x_j ((Ax)_n - x^T Ax)) = \\ &= \frac{x_j}{x_n^2} ((Ax)_j - (Ax)_n) = \frac{x_j}{x_n^2} \left( \sum_{k=1}^n a_{jk} x_k - \sum_{k=1}^n a_{nk} x_k \right) = \\ &= \frac{x_j}{x_n^2} \sum_{k=1}^n (a_{jk} - a_{nk}) x_k = \frac{x_j}{x_n^2} \left( \sum_{k=1}^{n-1} (a_{jk} - a_{nk}) x_k + (a_{jn} - a_{nn}) x_n \right) = \\ &= \frac{x_j}{x_n} \left( a_{jn} - a_{nn} - \sum_{k=1}^{n-1} (a_{nk} - a_{jk}) \frac{x_k}{x_n} \right) = y_j \left( r_j - \sum_{k=1}^{n-1} b_{jk} y_k \right). \quad \square \end{aligned}$$

Theorem 2 reveals a link between evolution (natural selection) and ecology. The validity of it justifies the choice of the relative change of relative frequencies of separate sub-populations during the derivation (or the construction) of the replicator equation on page 4.

**Example: evolution of two subpopulations.** Let  $n = 2$ ,  $A = \begin{pmatrix} a_{11} & a_{12} \\ a_{21} & a_{22} \end{pmatrix}$ . The equation

(4) is of the form  $\frac{dy}{d\tau} = y(a_{12} - a_{22} - (a_{21} - a_{11})y)$ . The solution of this equation with the initial condition  $y(0) = y_0 > 0$  is the function

$$y(\tau) = \frac{(a_{12} - a_{22})y_0}{(a_{21} - a_{11})y_0 + (a_{12} - a_{22} - (a_{21} - a_{11})y_0)e^{(a_{22} - a_{12})\tau}}.$$

Denote  $Q = \frac{a_{22} - a_{12}}{a_{11} - a_{21}}$ . The following holds

- if  $a_{12} - a_{22} > 0$ ,  $a_{21} - a_{11} > 0$ , then  $\lim_{\tau \rightarrow \infty} y(\tau) = Q$ ,  
i.e. the both subpopulations survive;
- if  $a_{12} - a_{22} > 0 > a_{21} - a_{11}$ , then  $\lim_{\tau \rightarrow \infty} y(\tau) = \infty$ ,  
i.e. the second subpopulation dies out;
- if  $a_{21} - a_{11} > 0 > a_{12} - a_{22}$ , then  $\lim_{\tau \rightarrow \infty} y(\tau) = 0$ ,  
i.e. the first subpopulation dies out;

– if  $a_{12} - a_{22} < 0$ ,  $a_{21} - a_{11} < 0$ , then

$$\lim_{\tau \rightarrow \infty} y(\tau) = \begin{cases} 0, & y_0 < Q, \\ Q, & y_0 = Q, \\ \infty, & y_0 > Q, \end{cases}$$

i.e. one of the subpopulations dies out; the initial conditions determine which one of the subpopulations survives.

**Example: Hawks and doves [8, p. 58].** John Maynard Smith has initiated a theory to explain the high frequency of conventional contests. It takes the form of a thought experiment: suppose there are only two possible behavioral types: one escalates the conflict until injury or the flight of the opponent settles the issue; the other sticks to displays and retreats if the opponent escalates. These two types of behavior are usually described as “hawks” and “doves”, although this is somewhat misleading. The conflicts, after all, are supposed to take place within one species and not between two; furthermore, real doves do escalate.

The contest may take place over a morsel of food, the boundary line between territories or a potential mate. The prize corresponds to a gain in fitness  $V$ , while an injury reduces fitness by  $-C$ . Fitness here means simply reproductive success.

If two doves meet, they posture, glare at each other, swell up, change color etc. but eventually, one of them retreats. The winner obtains  $V$ , the loser gets nothing, so that the average increase in fitness, for a dove meeting another dove, is  $\frac{1}{2}V$ . A dove meeting a hawk flees and its fitness remains unchanged, while that of the hawk increases by  $V$ . Finally, if a hawk meets a hawk, they escalate until one of the two gets knocked out. The fitness of the winner is increased by  $V$ , that of the loser reduced by  $C$ , so that the average increase in fitness is  $\frac{1}{2}(V - C)$ . This is encapsulated in the matrix

$$A = \begin{pmatrix} \frac{1}{2}(V - C) & V \\ 0 & \frac{1}{2}V \end{pmatrix}.$$

Now, adopting the notation from the previous example, we have

$$a_{12} - a_{22} = \frac{V}{2}, \quad a_{21} - a_{11} = \frac{C - V}{2}, \quad Q = \frac{V}{C - V}.$$

Subsequently, if  $V < C$ , then both behavioral types persist, if  $V > C$  the “hawk” tactic prevails and the “dove” tactic dies out. The hawk-dove conflict can be simulated by computer; the figures 1 and 2 introduce the Maple classic worksheets with solution of the corresponding equation.

### 3 (Bi)matrix games

The replicator equation (3) models the evolution of a population split into  $n$  subpopulations that mutually interact. The entries of matrix  $A$  characterize these interactions; we can say e.g. that if  $a_{ij} > 0$  then the  $i$ -th sub-population “wins a contribution to its

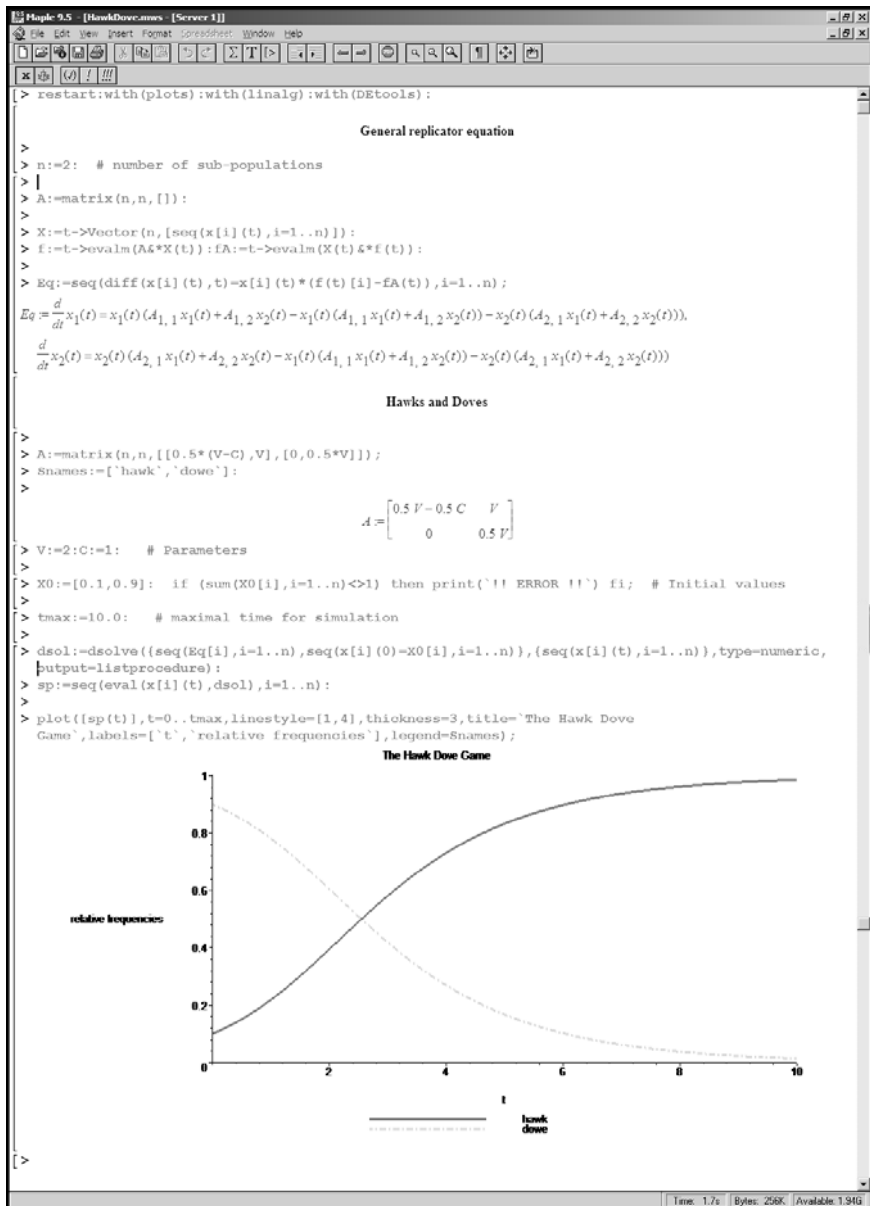


Fig. 1. Computer simulation of solution of replicator equation executed by Maple v. 9.5. The classic worksheet shows the hawk-dove conflict with diminishing of the dove tactic.

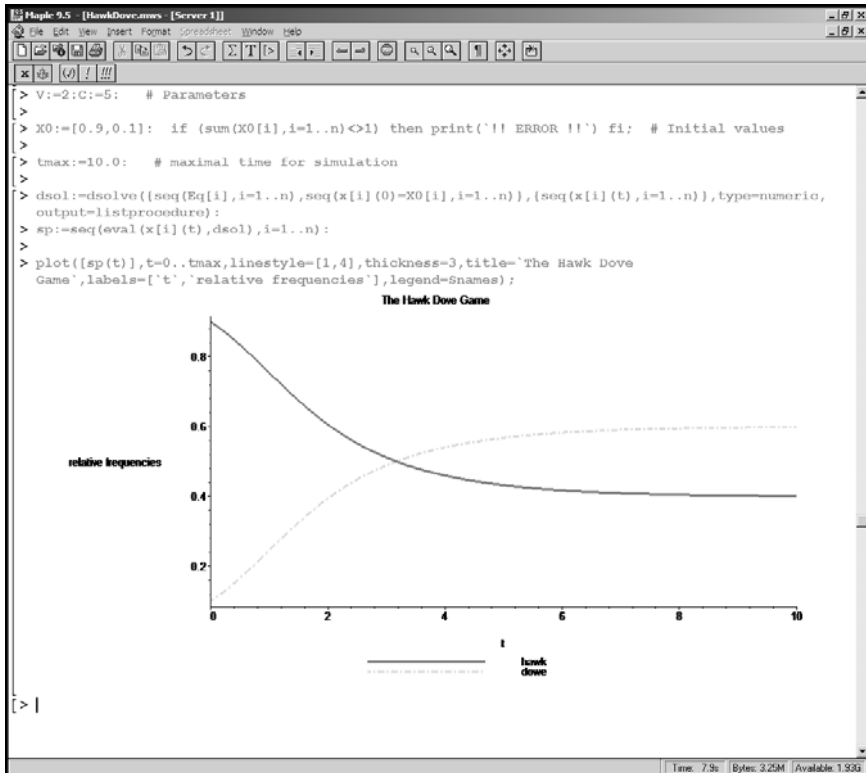


Fig. 2. Computer simulation of solution of replicator equation executed by Maple v. 9.5. The continuation of the classic worksheet from the figure 1 shows the hawk-dove conflict with persistence of the two tactics.

fitness” during a conflict with the  $j$ -th subpopulation. The similar situation — conflict between several participants — is usually studied by game theory. Therefore, this section deals briefly with concepts of game theory and shows their relations to replicator equations.

### 3.1 Basic notions

**Definition 1.** The finite normal form a two-player game (bimatrix game) is a 4-tuple  $\mathcal{G} = (X, Y, u, v)$ , where  $X, Y$  are finite sets and the functions  $u, v$  map the  $X \times Y$  into  $\mathbb{R}$ .

The sets  $X$  and  $Y$  are called sets of pure strategies of the first and of the second player, respectively. The functions  $u$  and  $v$  are called payoff functions of the first player and of the second one, respectively.

Since the sets  $X$  and  $Y$  are finite, we can put  $X = \{1, 2, \dots, n\}$  and  $Y = \{1, 2, \dots, m\}$ . Let us denote  $a_{ij} = u(i, j)$ ,  $b_{ji} = v(i, j)$ ,

$$A = \begin{pmatrix} a_{11} & a_{12} & \dots & a_{1m} \\ a_{21} & a_{22} & \dots & a_{2m} \\ \vdots & \vdots & \ddots & \vdots \\ a_{n1} & a_{n2} & \dots & a_{nm} \end{pmatrix}, \quad B = \begin{pmatrix} b_{11} & b_{12} & \dots & b_{1n} \\ b_{21} & b_{22} & \dots & b_{2n} \\ \vdots & \vdots & \ddots & \vdots \\ b_{m1} & b_{m2} & \dots & b_{mn} \end{pmatrix}.$$

Using this notation, we have

$$u(i, j) = a_{ij} = e_i^\top A e_j, \quad v(i, j) = b_{ji} = e_j^\top B e_i. \quad (5)$$

A bimatrix game is completely determined by the matrices  $A$  and  $B$  called *payoff matrices*. A game can be represented by the pair  $(A, B)$  and it can be described by the table

		player 2			
		1	2	...	$m$
player 1	1	$b_{11}$	$b_{21}$	...	$b_{m1}$
	$a_{11}$	$a_{12}$	...	$a_{1m}$	
	2	$b_{12}$	$b_{22}$	...	$b_{m2}$
	$a_{21}$	$a_{22}$	...	$a_{2m}$	
...	...	...	...	...	
$n$	$b_{1n}$	$b_{2n}$	...	$b_{mn}$	
$a_{n1}$	$a_{n2}$	...	$a_{nm}$		

**Definition 2.** Probability extension of a bimatrix game  $\mathcal{G} = (X, Y, u, v) = (A, B)$  is a 4-tuple  $\mathcal{G}^* = (X^*, Y^*, u^*, v^*)$ , where  $X^* = S_n$ ,  $Y^* = S_m$  and  $u^*, v^*$  are functions  $X^* \times Y^* \rightarrow \mathbb{R}$  defined by the following equalities

$$u^*(x, y) = x^\top A y, \quad v^*(x, y) = y^\top B x. \quad (6)$$

The maps  $\varphi : X \rightarrow X^*$  and  $\psi : Y \rightarrow Y^*$  defined by the equalities  $\varphi(i) = e_i$ ,  $\psi(j) = e_j$  are injective. That is why we can think of the sets  $X$  and  $Y$  as subsets of the sets  $X^*$  and  $Y^*$ , respectively. Comparing the formulas (5) and (6), we can see that the functions  $u$  and  $v$  are restrictions of the maps  $u^*$  and  $v^*$  to the sets  $X$  and  $Y$ . The elements of the sets  $X^*$  and  $Y^*$  are called *mixed strategies*.

**Definition 3.** The mixed strategy  $\bar{x} \in X^*$  is called the best reply to the strategy  $y \in Y^*$  if

$$u^*(\bar{x}, y) = \bar{x}^\top A y \geq x^\top A y = u^*(x, y)$$

for all strategies  $x \in X^*$ . In a similar way, the mixed strategy  $\bar{y} \in Y^*$  is called the best reply to the strategy  $x \in X^*$  if

$$v^*(x, \bar{y}) = \bar{y}^\top B x \geq y^\top B x = v^*(x, y)$$

for all strategies  $y \in Y^*$ . The pair of strategies  $(\bar{x}, \bar{y}) \in X^* \times Y^*$  is called the Nash equilibrium if  $\bar{x}$  is the best reply to  $\bar{y}$  and in the same time  $\bar{y}$  is the best reply to  $\bar{x}$ , i.e.

$$\bar{x}^T A \bar{y} \geq x^T A \bar{y}, \quad \bar{y}^T B \bar{x} \geq y^T B \bar{x} \quad \text{for all } x \in X^*, y \in Y^*.$$

A player adopting the equilibrium strategy is sure that his payoff cannot decrease in the case that his opponent adopts a strategy different from the equilibrium one. In this way, the equilibrium strategy is the most profitable for the both of the players.

**Definition 4.** The bimatrix game  $\mathcal{G} = (X, Y, u, v)$  is called symmetric if  $X = Y$  and  $u(i, j) = v(j, i)$  for all of the pure strategies  $i, j \in X$ . The symmetric game can be written down in a brief form  $\mathcal{G} = (X, u)$ .

The symmetric game satisfies the relation  $a_{ij} = u(i, j) = v(j, i) = b_{ij}$ , hence  $A = B$ . That is, a symmetric game is determined by the matrix  $A$  therefore it used to be called the *matrix game*.

The pair of strategies  $(\bar{x}, \bar{y}) \in X^{*2}$  of a matrix game is the Nash equilibrium if the following holds

$$\bar{x}^T A \bar{y} \geq x^T A \bar{y}, \quad \bar{y}^T A \bar{x} \geq y^T A \bar{x}, \quad \text{for all } x, y \in X^*.$$

The strategy  $\bar{x} \in X^*$  of a matrix game is called *symmetric Nash equilibrium* if the pair  $(\bar{x}, \bar{x})$  is equilibrium, i.e. if the following holds

$$\bar{x}^T A \bar{x} \geq x^T A \bar{x}, \quad \text{for all } x \in X^*.$$

### 3.2 Equilibria of symmetric matrix game and stationary points of replicator equation (3)

Conflict within a structured population can be modeled by games or by a replicator equation. The fundamental concept in the game theory is that of Nash equilibrium and the one in the qualitative theory is that of stationary point. This section shows that Nash equilibria of a matrix game corresponds to stationary solutions of the respective replicator equation.

**Theorem 3.** Let  $\mathcal{G}$  be symmetric finite game defined by the matrix  $A$ . The mixed strategy  $\bar{x}$  is symmetric Nash equilibrium if and only if

$$e_i^T A \bar{x} \leq \bar{x}^T A \bar{x} \quad \text{for all } i \notin \text{supp } \bar{x} \quad (7)$$

and

$$e_i^T A \bar{x} = \bar{x}^T A \bar{x} \quad \text{for all } i \in \text{supp } \bar{x}. \quad (8)$$

*Proof.* Let  $\bar{x}$  be an equilibrium strategy. Then

$$e_i^T A \bar{x} \leq \bar{x}^T A \bar{x} \quad \text{for all } i \in \{1, 2, \dots, n\}.$$

Let us suppose for contradiction that there exists  $k \in \text{supp } \bar{x}$  such that  $e_k^\top A \bar{x} < \bar{x}^\top A \bar{x}$ . Then

$$\begin{aligned} \bar{x}^\top A \bar{x} &= \sum_{i=1}^n \bar{x}_i e_i^\top A \bar{x} = \sum_{i \in \text{supp } \bar{x}} \bar{x}_i e_i^\top A \bar{x} = \bar{x}_k e_k^\top A \bar{x} + \sum_{i \in \text{supp } \bar{x} \setminus \{k\}} \bar{x}_i e_i^\top A \bar{x} < \\ &< \bar{x}_k \bar{x}^\top A \bar{x} + \sum_{i \in \text{supp } \bar{x} \setminus \{k\}} \bar{x}_i \bar{x}^\top A \bar{x} = \sum_{i=1}^n \bar{x}_i \bar{x}^\top A \bar{x} = \bar{x}^\top A \bar{x}. \end{aligned}$$

This contradiction proves the necessity of the conditions.

Let the conditions (7) and (8) hold. Then  $e_i^\top A \bar{x} \leq \bar{x}^\top A \bar{x}$  for all subscripts  $i \in \{1, 2, \dots, n\}$ . Now, if  $x \in X^*$  is an arbitrary mixed strategy, then

$$x^\top A \bar{x} = \sum_{i=1}^n x_i e_i^\top A \bar{x} \leq \sum_{i=1}^n x_i \bar{x}^\top A \bar{x} = \bar{x}^\top A \bar{x}.$$

Hence, the note above the theorem states that  $\bar{x}$  is a symmetric equilibrium strategy. The conditions are sufficient as well.  $\square$

**Theorem 4 (Nachbar [10]).**

- (i) If  $\bar{x}$  is a symmetric equilibrium strategy for a matrix game defined by the matrix  $A$  then  $\bar{x}$  is a stationary point of the autonomous differential equation system (3).
- (ii) If  $\hat{x} = (\hat{x}_1, \hat{x}_2, \dots, \hat{x}_n)^\top \in X^*$  is a stable stationary point of the system (3) then  $\hat{x}$  is a symmetric equilibrium strategy for the matrix game defined by the matrix  $A$ .

*Proof.* (i) The proposition follows directly Theorem 3 and the fact that the conditions (7) and (8) can be rewritten to the form

$$\begin{aligned} (e_i - \bar{x})^\top A \bar{x} &\leq 0 \quad \text{for all } i \notin \text{supp } \bar{x}, \\ (e_i - \bar{x})^\top A \bar{x} &= 0 \quad \text{for all } i \in \text{supp } \bar{x}. \end{aligned}$$

(ii) Denote

$$F_i(x) = x_i (e_i - x)^\top A x = x_i \left( \sum_{k=1}^n a_{ik} x_k - \sum_{l=1}^n \sum_{k=1}^n a_{lk} x_l x_k \right).$$

Then

$$\begin{aligned} \frac{\partial F_i}{\partial x_j}(x) &= \\ &= \delta_{ij} \left( \sum_{k=1}^n a_{ik} x_k - \sum_{l=1}^n \sum_{k=1}^n a_{lk} x_l x_k \right) + x_i \left( a_{ij} - \sum_{k=1}^n a_{jk} x_k - \sum_{l=1}^n a_{lj} x_l \right) = \\ &= \delta_{ij} (e_i^\top A x - x^\top A x) + x_i (a_{ij} - e_j^\top A x - x^\top A e_j). \end{aligned}$$

Hence, the entries of variational matrix of the system (3) at the stationary point  $\hat{x}$  are

$$\frac{\partial F_i}{\partial x_j}(\hat{x}) = \begin{cases} \hat{x}_i (a_{ij} - e_j^\top A \hat{x} - \hat{x}^\top A e_j), & \hat{x}_i \neq 0, \\ \delta_{ij} (e_i^\top A \hat{x} - \hat{x}^\top A \hat{x}), & \hat{x}_i = 0. \end{cases}$$

The eigenvalues of the variational matrix satisfy the equation

$$\det \left( \frac{\partial F_i}{\partial x_j}(\hat{x}) - \delta_{ij}\lambda \right) = 0.$$

Let  $i$  satisfying  $\hat{x}_i = 0$  be arbitrary. We expand the determinant by the  $i$ -th row:

$$(e_i^\top A\hat{x} - \hat{x}^\top A\hat{x} - \lambda) \cdot (\text{the respective algebraic complement}).$$

This calculation yields that the number  $e_i^\top A\hat{x} - \hat{x}^\top A\hat{x}$  is an eigenvalue of the variational matrix for all  $i$  such that  $\hat{x}_i = 0$ . The assumed stability of the stationary solution  $\hat{x}$  implies

$$e_i^\top A\hat{x} - \hat{x}^\top A\hat{x} \leq 0 \quad \text{for any } i \text{ such that } \hat{x}_i = 0.$$

Moreover, the following holds

$$e_i^\top A\hat{x} - \hat{x}^\top A\hat{x} = 0 \quad \text{for all } i \text{ such that } \hat{x}_i \neq 0,$$

because  $\hat{x}$  is the stationary solution of the system (3). Consequently,

$$e_i^\top A\hat{x} - \hat{x}^\top A\hat{x} \leq 0 \quad \text{for all } i \in \{1, 2, \dots, n\}.$$

Now, let  $x = \sum_{i=1}^n x_i e_i \in X^*$  be an arbitrary mixed strategy. Then

$$x^\top A\hat{x} = \sum_{i=1}^n x_i e_i^\top A\hat{x} \leq \sum_{i=1}^n x_i \hat{x}^\top A\hat{x} = \hat{x}^\top A\hat{x} \sum_{i=1}^n x_i = \hat{x}^\top A\hat{x},$$

hence,  $\hat{x}$  is a symmetric equilibrium strategy. □

Converse statements do not hold:

(i) Each pure strategy  $e_i$  is a stationary point of the system (3) but a pure strategy is not a equilibrium one, in general.

(ii) E.g., let us consider the symmetric matrix game defined by the matrix

$$A = \begin{pmatrix} 1 & 0 \\ 0 & 0 \end{pmatrix}.$$

Then the strategy  $\bar{x} = (0, 1)^\top$  is a symmetric equilibrium since

$$(x, 1-x) \begin{pmatrix} 1 & 0 \\ 0 & 0 \end{pmatrix} \begin{pmatrix} 0 \\ 1 \end{pmatrix} = 0 = (0, 1) \begin{pmatrix} 1 & 0 \\ 0 & 0 \end{pmatrix} \begin{pmatrix} 0 \\ 1 \end{pmatrix}$$

for any  $x \in [0, 1]$ . The corresponding ordinary differential system is the following

$$x' = x \left[ (1, 0) \begin{pmatrix} 1 & 0 \\ 0 & 0 \end{pmatrix} \begin{pmatrix} x \\ y \end{pmatrix} - (x, y) \begin{pmatrix} 1 & 0 \\ 0 & 0 \end{pmatrix} \begin{pmatrix} x \\ y \end{pmatrix} \right] = x(x - x^2) = x^2(1 - x),$$

$$y' = y \left[ (0, 1) \begin{pmatrix} 1 & 0 \\ 0 & 0 \end{pmatrix} \begin{pmatrix} x \\ y \end{pmatrix} - (x, y) \begin{pmatrix} 1 & 0 \\ 0 & 0 \end{pmatrix} \begin{pmatrix} x \\ y \end{pmatrix} \right] = y(-x^2) = -x^2 y.$$

The stationary points are  $(0, y)$ ,  $(1, 0)$  for any  $y \in [0, 1]$ . The variational matrix in a stationary point  $(x, y)$  takes the form

$$J(x, y) = \begin{pmatrix} 2x - 3x^2 & 0 \\ -2xy & -x^2 \end{pmatrix}.$$

In particular,

$$J(0, 1) = \begin{pmatrix} 0 & 0 \\ 0 & 0 \end{pmatrix}.$$

The characteristic polynomial of this matrix possesses the double root  $\lambda = 0$  which means that the stationary solution is not stable.

### 3.3 Replicator equation for a bimatrix game

As it was mentioned in the introduction to this section, the replicator equation (3) represents an alternative description of a matrix game. Sub-populations correspond to pure strategies and their fitnesses correspond to payoff functions. This observation suggests that bimatrix games could be represented by differential equations as well. A paradigmatic situation is Dawkins's battle of sexes game; this game has motivated a seminal paper [11]. This game models the interaction (either cooperation or contest) of males and females endeavoring to put their genes into effect. The females are considered to be the first player, their phenotypes (in a broad sense, e.g. behavior patterns) constitute strategies. In a similar way we can think of males. The payoff  $a_{ij}$  may be the number of offspring of the female with the  $i$ -th phenotype and of the male with the  $j$ -th phenotype.

Considerations similar to the ones provided in the section 2 lead to the equations

$$\begin{aligned} x'_i &= x_i((Ay)_i - x^T Ay), & i &= 1, 2, \dots, n, \\ y'_j &= y_j((Bx)_j - y^T Bx), & j &= 1, 2, \dots, m, \end{aligned} \quad (9)$$

or, in an equivalent form

$$\begin{aligned} x'_i &= x_i(e_i - x)^T Ay, & i &= 1, 2, \dots, n, \\ y'_j &= y_j(e_j - y)^T Bx, & j &= 1, 2, \dots, m. \end{aligned}$$

Also, this system can be rewritten to the form of one vector equation

$$\begin{pmatrix} x \\ y \end{pmatrix}' = \begin{pmatrix} x \\ y \end{pmatrix} \circ \begin{pmatrix} \mathbf{O} & (E - xI^T)A \\ (E - yI^T)B & \mathbf{O} \end{pmatrix} \begin{pmatrix} x \\ y \end{pmatrix}.$$

The system (9) possesses a unique solution, since the righthand sides are continuously differentiable by all of the variables  $x_i$  and  $y_j$ . In a similar way as in Section 2, lemmas 1 and 2 we can demonstrate that the sets  $S_n \times S_m$  and  $S_n^\circ \times S_m^\circ$  are invariants for the system (9). Moreover, we can show that the solution of the system (9) will not change after addition of a constant vector to the diagonal or to a some row or column of the matrices A and B; the proof repeats the arguments used in the proofs of the lemmas 3 and 4 in the section 2.

Theorem 2 in the section 2 states that the cubic nonlinearities appearing in the replicator equation (3) can be reduced to the quadratic ones. An analogy of this statement is not known for the system (9). But at least, we are able to reduce the dimension of the system (9).

Indeed, the invariantness of the set  $S_n \times S_m$  with respect to the system (9) implies

$$x_n = 1 - \sum_{i=1}^{n-1} x_i, \quad y_m = 1 - \sum_{j=1}^{m-1} y_j$$

which yields

$$\begin{aligned} \sum_{j=1}^m a_{ij}y_j - x^T A y &= \sum_{j=1}^m a_{ij}y_j - \sum_{l=1}^n \sum_{j=1}^n x_l a_{lj}y_j = \\ &= \sum_{j=1}^{m-1} a_{ij}y_j + a_{im} \left( 1 - \sum_{j=1}^{m-1} y_j \right) - \\ &\quad - \sum_{l=1}^n x_l \left[ \sum_{j=1}^{m-1} a_{lj}y_j + a_{lm} \left( 1 - \sum_{j=1}^{m-1} y_j \right) \right] = \\ &= \sum_{j=1}^{m-1} (a_{ij} - a_{im})y_j + a_{im} - \sum_{l=1}^n x_l \left[ \sum_{j=1}^{m-1} (a_{lj} - a_{lm})y_j + a_{lm} \right] = \\ &= \sum_{j=1}^{m-1} (a_{ij} - a_{im})y_j + a_{im} - \sum_{l=1}^{n-1} x_l \left[ \sum_{j=1}^{m-1} (a_{lj} - a_{lm})y_j + a_{lm} \right] - \\ &\quad - \left( 1 - \sum_{l=1}^{n-1} x_l \right) \left[ \sum_{j=1}^{m-1} (a_{nj} - a_{nm})y_j + a_{nm} \right] = \\ &= \sum_{j=1}^{m-1} (a_{ij} - a_{im})y_j + a_{im} - \sum_{j=1}^{m-1} (a_{nj} - a_{nm})y_j - a_{nm} - \\ &\quad - \sum_{l=1}^{n-1} x_l \left[ \sum_{j=1}^{m-1} (a_{lj} - a_{lm} - a_{nj} + a_{nm})y_j + a_{lm} - a_{nm} \right] = \\ &= \sum_{j=1}^{m-1} (a_{ij} - a_{im} - a_{nj} + a_{nm})y_j + a_{im} - a_{nm} - \\ &\quad - \sum_{l=1}^{n-1} x_l \left[ \sum_{j=1}^{m-1} (a_{lj} - a_{lm} - a_{nj} + a_{nm})y_j + a_{lm} - a_{nm} \right] = \end{aligned}$$

$$\begin{aligned}
&= \sum_{l=1}^{n-1} \sum_{j=1}^{m-1} \delta_{il} [(a_{lj} - a_{lm} - a_{nj} + a_{nm})y_j + a_{lm} - a_{nm}] - \\
&\quad - \sum_{l=1}^{n-1} \sum_{j=1}^{m-1} x_l [(a_{lj} - a_{lm} - a_{nj} + a_{nm})y_j + a_{lm} - a_{nm}] = \\
&= \sum_{l=1}^{n-1} \sum_{j=1}^{m-1} (\delta_{il} - x_l) [(a_{lj} - a_{lm} - a_{nj} + a_{nm})y_j + a_{lm} - a_{nm}].
\end{aligned}$$

Let us denote now

$$\tilde{a}_{ij} = a_{ij} - a_{im} - a_{nj} + a_{nm}, \quad \hat{a}_i = a_{nm} - a_{im}$$

for  $i = 1, 2, \dots, n-1, j = 1, 2, \dots, m-1$  and

$$\tilde{\mathbf{A}} = \begin{pmatrix} \tilde{a}_{11} & \tilde{a}_{12} & \cdots & \tilde{a}_{1(m-1)} \\ \tilde{a}_{21} & \tilde{a}_{22} & \cdots & \tilde{a}_{2(m-1)} \\ \vdots & \vdots & \ddots & \vdots \\ \tilde{a}_{(n-1)1} & \tilde{a}_{(n-1)2} & \cdots & \tilde{a}_{(n-1)(m-1)} \end{pmatrix}, \quad \hat{\mathbf{a}} = \begin{pmatrix} \hat{a}_1 \\ \hat{a}_2 \\ \vdots \\ \hat{a}_{n-1} \end{pmatrix}.$$

Analogous calculations imply

$$\sum_{i=1}^n b_{ji}x_i - y^T \mathbf{B}x = \sum_{j=1}^{m-1} \sum_{l=1}^{n-1} (\delta_{lj} - y_j) [(b_{lj} - b_{lm} - b_{mj} + b_{mn})x_l + b_{jn} - b_{mn}]$$

hence, the we can denote

$$\tilde{b}_{ij} = b_{ij} - b_{im} - b_{mj} + b_{mn}, \quad \hat{b}_j = b_{mn} - b_{jm}$$

for  $i = 1, 2, \dots, n-1, j = 1, 2, \dots, m-1$  and

$$\tilde{\mathbf{B}} = \begin{pmatrix} \tilde{b}_{11} & \tilde{b}_{12} & \cdots & \tilde{b}_{1(n-1)} \\ \tilde{b}_{21} & \tilde{b}_{22} & \cdots & \tilde{b}_{2(n-1)} \\ \vdots & \vdots & \ddots & \vdots \\ \tilde{b}_{(m-1)1} & \tilde{b}_{(m-1)2} & \cdots & \tilde{b}_{(m-1)(n-1)} \end{pmatrix}, \quad \hat{\mathbf{b}} = \begin{pmatrix} \hat{b}_1 \\ \hat{b}_2 \\ \vdots \\ \hat{b}_{m-1} \end{pmatrix}.$$

The consideration and calculations show that the  $(n+m)$ -dimensional system (9) can be reduced to the  $(n+m-2)$ -dimensional system

$$\begin{aligned}
x'_i &= x_i(e_i - x)^T (\tilde{\mathbf{A}}y - \hat{\mathbf{a}}), \quad i = 1, 2, \dots, n-1, \\
y'_j &= y_j(e_j - y)^T (\tilde{\mathbf{B}}x - \hat{\mathbf{b}}), \quad j = 1, 2, \dots, m-1.
\end{aligned} \tag{10}$$

Now, we adopt the notation  $x = (x_1, x_2, \dots, x_{n-1}), y = (y_1, y_2, \dots, y_{m-1})$ .

**Example: Conflict of two players with two strategies.** Let  $n = m = 2$ ,

$$A = \begin{pmatrix} a_{11} & a_{12} \\ a_{21} & a_{22} \end{pmatrix}, \quad B = \begin{pmatrix} b_{11} & b_{12} \\ b_{21} & b_{22} \end{pmatrix}.$$

Then the system of equations (10) takes the form

$$\begin{aligned} x' &= x(1-x)(\alpha_1 y - \alpha_2), \\ y' &= y(1-y)(\beta_1 x - \beta_2), \end{aligned}$$

where  $\alpha_1 = a_{11} - a_{12} - a_{21} + a_{22}$ ,  $\alpha_2 = a_{22} - a_{12}$ ,  $\beta_1 = b_{11} - b_{12} - b_{21} + b_{22}$ ,  $\beta_2 = b_{22} - b_{12}$ . The phase space for this system is the set  $[0, 1] \times [0, 1]$ . The system possesses the stationary points  $(0, 0)$ ,  $(0, 1)$ ,  $(1, 0)$ ,  $(1, 1)$  corresponding to the pure strategies. If further

$$\alpha_1 \neq 0, \quad 0 < \frac{\alpha_2}{\alpha_1} < 1, \quad \beta_1 \neq 0, \quad 0 < \frac{\beta_2}{\beta_1} < 1,$$

it possesses also the interior equilibrium

$$\left( \frac{\beta_2}{\beta_1}, \frac{\alpha_2}{\alpha_1} \right)$$

corresponding to the mixed strategies. The matrix

$$J(x, y) = \begin{pmatrix} (1-2x)(\alpha_1 y - \alpha_2) & \alpha_1 x(1-x) \\ \beta_1 y(1-y) & (1-2y)(\beta_1 x - \beta_2) \end{pmatrix}$$

is the variational matrix of the system, hence

$$\begin{aligned} J(0, 0) &= \begin{pmatrix} -\alpha_2 & 0 \\ 0 & -\beta_2 \end{pmatrix}, & J(0, 1) &= \begin{pmatrix} \alpha_1 - \alpha_2 & 0 \\ 0 & \beta_2 \end{pmatrix}, \\ J(1, 0) &= \begin{pmatrix} \alpha_2 & 0 \\ 0 & \beta_1 - \beta_2 \end{pmatrix}, & J(1, 1) &= \begin{pmatrix} \alpha_2 - \alpha_1 & 0 \\ 0 & \beta_2 - \beta_1 \end{pmatrix}, \\ J\left(\frac{\beta_2}{\beta_1}, \frac{\alpha_2}{\alpha_1}\right) &= \begin{pmatrix} 0 & \frac{\alpha_1 \beta_2 (\beta_1 - \beta_2)}{\beta_1^2} \\ \frac{\alpha_2 \beta_1 (\alpha_1 - \alpha_2)}{\alpha_1^2} & 0 \end{pmatrix}. \end{aligned}$$

Now we can see that the edge equilibria corresponding to the pure strategies are saddle points or nodes, while an interior equilibrium (provided it exists) corresponding to the mixed strategies is a saddle point or an unstable focus. Consequently, such a system evolves to pure strategies; just one of the extended phenotype of a particular player survives, and the other dies out.

**Example: The Battle of the Sexes [8, p. 114–115].** In many species, raising offspring requires a considerable amount of time and energy. Each parent might attempt to reduce its own share at the expense of the other. The outcome might depend on which sex is in a position to desert first. Whenever fertilization is internal, for example, females risk being deserted even before giving birth to the offspring. At an even more fundamental level, the game is rigged against the female by the fact that they produce relatively few, large gametes, whereas males produce many small gametes. Females are thereby much more committed and can less afford to lose a child. Thus, males are in many cases in a better position to desert. They can invest the corresponding gain in time and energy into increasing their offspring with the help of new mates.

The female counterstrategy is “coyness”, i.e. the insistence upon a long engagement period before copulation. Rather than undergoing a second costly engagement (for which it might be too late in the mating season), males would do better to stay faithfully at home and help raise their offspring. Roughly speaking, in a population of coy females, males would have to be faithful. Among faithful males, however, it would not pay a female to be coy: the long engagement period is an unnecessary cost. Thus, the proportion of “fast” females would grow. But then “philandering” males will have their chance and spread. Females, in that case, will do well to be coy. The argument thus runs full circle. In order to model this through game theory, let us assume that there are two types in the male population, namely “faithful” and “philandering” with frequencies  $x_1$  and  $x_2$ , respectively, and two types in the female population, namely “coy” and “fast” with frequencies  $y_1$  and  $y_2$ , respectively. Let us suppose that the successful raising of the offspring increases the fitness of both parents by  $V$ . The parental investment  $-2C$  will be entirely borne by the female if the male deserts. Otherwise, it is shared equally by both parents. A long engagement period represent a cost of  $-c$  to both parents.

Hence, the game can be represented by the following table:

		female	
		coy	fast
male	faithful	$V - C - c$	$V - C$
	philanderer	0	$V - 2C$

The analysis of stationary states of corresponding replicator equation provided in the previous example reveals that just one strategy (mating behavior pattern) of each sex can persist.

Figures 3 and 4 show a computer simulation provided by Maple v. 9.5. The example illustrates diminishing of the male “philanderer” and the female “fast” strategies.

### 3.4 Stationary points and invariant of replicator equation (9)

Section 3.2 shows that Nash equilibria of matrix game correspond to stationary solutions of replicator equation (3). The analogous statement is true also for bimatrix games and respective replicator equations. Moreover, replicator equation for a bimatrix game

```

Maple 9.5 - [BattleOfSexes.mws - (Server 1)]
> restart;with(plots):with(linalg):with(DRtools):

                                General replicator equation
>
> n:=2:m:=2: # numbers of strategies
>
> A:=matrix(n,m,[]):B:=matrix(m,n,[]):
>
> X:=t->Vector(n+m,[seq(x[i](t),i=1..n+m)]):
> Xp:=t->Vector(n,[seq(x[i](t),i=1..n)]):Yp:=t->Vector(m,[seq(x[j](t),j=n+1..n+m)]):
> M:=Vector(n+m,[]):
> f:=t->evalm(A&#x27;Yp(t)):fA:=t->evalm(Xp(t)&#x27;f(t)):
> g:=t->evalm(B&#x27;Xp(t)):gA:=t->evalm(Yp(t)&#x27;g(t)):
> for k from 1 to n do M[k]:=f(t)[k]-fA(t) end do:
> for l from 1 to m do M[l+n]:=g(t)[l]-gA(t) end do:
>
> Eq:=seq(diff(x[i](t),t)-x[i](t)*M[i],i=1..n+m):
Eq =
d
-- x1(t) = x1(t)(A1,1 x3(t) + A1,2 x4(t) - x1(t)(A1,1 x3(t) + A1,2 x4(t)) - x2(t)(A2,1 x3(t) + A2,2 x4(t)),
dt
d
-- x2(t) = x2(t)(A2,1 x3(t) + A2,2 x4(t) - x1(t)(A1,1 x3(t) + A1,2 x4(t)) - x2(t)(A2,1 x3(t) + A2,2 x4(t)),
dt
d
-- x3(t) = x3(t)(B1,1 x1(t) + B1,2 x2(t) - x3(t)(B1,1 x1(t) + B1,2 x2(t)) - x4(t)(B2,1 x1(t) + B2,2 x2(t)),
dt
d
-- x4(t) = x4(t)(B2,1 x1(t) + B2,2 x2(t) - x3(t)(B1,1 x1(t) + B1,2 x2(t)) - x4(t)(B2,1 x1(t) + B2,2 x2(t))

                                The Battle of the Sexes
>
> A:=matrix(n,m,[V-C-c,V-C],[0,V]):
> B:=matrix(m,n,[V-C-c,V-C],[0,V-2*C]):
> Snames:=['male - faithful`,`male - philanderer`,`female - coy`,`female - fast']:
>
                                A :=
                                [ V-C-c  V-C ]
                                [      0      V ]
                                B :=
                                [ V-C-c  V-C ]
                                [      0  V-2C ]

> V:=3.0:C:=2.0:c:=.5: # Parameters
>
> X0:=[0.6,0.4]: if (sum(X0[i],i=1..n)<>1) then print(`!! ERROR !! X0`) fi: # Initial values
> Y0:=[0.1,0.9]: if (sum(Y0[j],j=1..m)<>1) then print(`!! ERROR !! Y0`) fi:
>

```

Fig.3. Computer simulation of solution of replicator equation for bimatrix game provided by Maple v. 9.5. In particular, the battle of sexes game is modeled.

may have an invariant (constant of motion, Hamiltonian); that is, in the area of theoretical biology, replicator equations for bimatrix game may play a role similar to that of equations of analytical mechanics in physics.

**Theorem 5.** *The pair of mixed strategies  $(\bar{x}, \bar{y}) \in S_n \times S_m$  is the Nash equilibrium for the bimatrix game defined by matrices A, B if and only if*

$$\begin{aligned}
 (A\bar{y})_i &= e_i^T A\bar{y} = \bar{x}^T A\bar{y} \quad \text{for all } i \in \text{supp } \bar{x}, \\
 (A\bar{y})_i &= e_i^T A\bar{y} \leq \bar{x}^T A\bar{y} \quad \text{for all } i \notin \text{supp } \bar{x}, \\
 (B\bar{x})_j &= e_j^T B\bar{x} = \bar{y}^T B\bar{x} \quad \text{for all } j \in \text{supp } \bar{y}, \\
 (B\bar{x})_j &= e_j^T B\bar{x} \leq \bar{y}^T B\bar{x} \quad \text{for all } j \notin \text{supp } \bar{y}.
 \end{aligned}$$

*Proof.* We can repeat and slightly modify the arguments used in the proof of Theorem 3. □

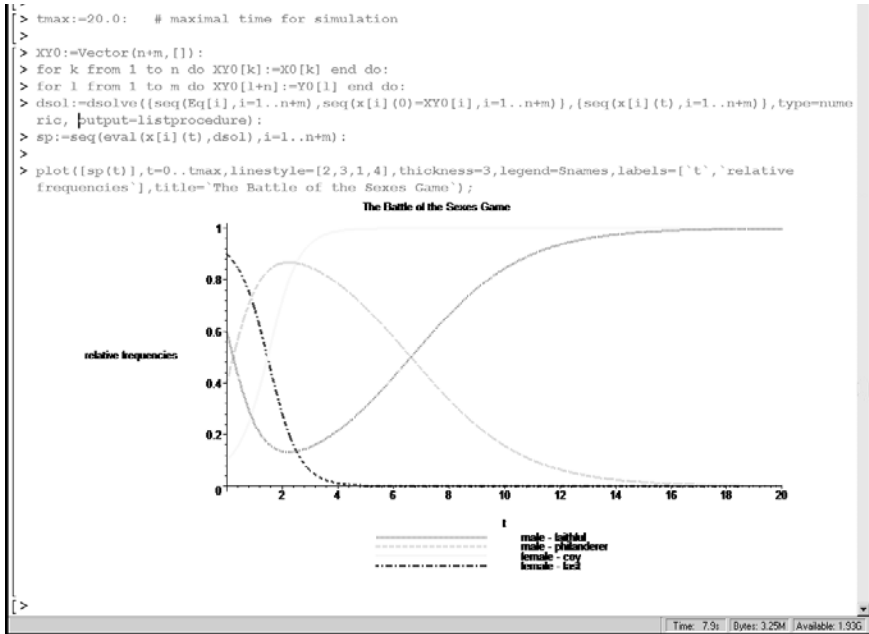


Fig. 4. Continuation of fig. 3

**Corollary 1.** If  $(\bar{x}, \bar{y}) \in S_n \times S_m$  is the Nash equilibrium for the bimatrix game  $(A, B)$  then  $(\bar{x}, \bar{y})$  is a stationary point of the system (9).

**Corollary 2.** Let  $(\bar{x}, \bar{y}) \in S_n^\circ \times S_m^\circ$ . Then the following statements are equivalent.

- (i)  $(\bar{x}, \bar{y})$  is Nash equilibrium of the game  $(A, B)$ .
- (ii)  $(\bar{x}, \bar{y})$  is a stationary point of the system (9).
- (iii)  $A\bar{y} = I\bar{x}^T A\bar{y}$ ,  $B\bar{x} = I\bar{y}^T B\bar{x}$ .
- (iv)  $x^T A\bar{y} = \bar{x}A\bar{y}$ ,  $y^T B\bar{x} = \bar{y}B\bar{x}$  for all  $x \in S_n$ ,  $y \in S_m$ .

*Proof.* The first implication is a particular case of Corollary 1.

(ii)  $\Rightarrow$  (iii): Let  $i$  be arbitrary. Then  $x_i > 0$ ,  $x_i ((A\bar{y})_i - x^T A\bar{y}) = 0$ , hence

$$(A\bar{y})_i = \bar{x}^T A\bar{y}.$$

In a similar way we can show that  $(B\bar{x})_j = \bar{y}^T B\bar{x}$ .

(iii)  $\Rightarrow$  (iv): Let  $y \in S_m$  be arbitrary. Then

$$\begin{aligned} B\bar{x} &= I\bar{y}^T B\bar{x} \\ y^T B\bar{x} &= y^T I\bar{y}^T B\bar{x} \\ y^T B\bar{x} &= \bar{y}^T B\bar{x}. \end{aligned}$$

In a similar way we can show that  $x^T A\bar{y} = \bar{x}A\bar{y}$ .

(iv) $\Rightarrow$ (i): This implication follows immediately the definition of Nash equilibrium.

□

**Definition 5.** Let  $(A, B)$  be a bimatrix game and assume that there exists matrices  $D$  and vectors  $p, q$  such that

$$A = D + Iq^T, \quad B = cD^T + Iq^T, \quad (11)$$

that is

$$a_{ij} = d_{ij} + q_j, \quad b_{ji} = cd_{ij} + p_i$$

for some  $c \neq 0$ . If  $c > 0$  then  $(A, B)$  is called  $c$ -partnership game, if  $c < 0$  then  $(A, B)$  is called  $c$ -zero-sum game.

**Theorem 6 (Hofbauer [6]).** Let  $(A, B)$  be a bimatrix game and  $c \neq 0$  such that the condition (11) holds. If  $(\bar{x}, \bar{y}) \in S_n^\circ \times S_m^\circ$  is Nash equilibrium then the function

$$H(x, y) = c \sum_{i=1}^n \bar{x}_i \ln x_i - \sum_{j=1}^m \bar{y}_j \ln y_j$$

is the invariant for the equation (9).

*Proof.* Taking into account Corollary 2, we can compute

$$\begin{aligned} \frac{d}{dt} H(x, y) &= c \sum_{i=1}^n \bar{x}_i \frac{x'_i}{x_i} - \sum_{j=1}^m \bar{y}_j \frac{y'_j}{y_j} = \\ &= c \sum_{i=1}^n \bar{x}_i ((Ay)_i - x^T Ay) - \sum_{j=1}^m \bar{y}_j ((Bx)_j - y^T Bx) = \\ &= c(\bar{x} - x)^T Ay - (\bar{y} - y)^T Bx = \\ &= c(\bar{x} - x)^T A(y - \bar{y}) - (\bar{y} - y)^T B(x - \bar{x}) + c(\bar{x} - x)^T A\bar{y} + (\bar{y} - y)^T B\bar{x} = \\ &= c(\bar{x} - x)^T (D + Iq^T)(y - \bar{y}) - (\bar{y} - y)^T (cD^T + Ip^T)(x - \bar{x}) = \\ &= c(\bar{x} - x)^T D(y - \bar{y}) - c(\bar{y} - y)^T D^T(x - \bar{x}) = 0. \end{aligned}$$

□

In particular, an interior stationary point  $(\bar{x}, \bar{y})$  for a  $c$ -zero-sum game is always stable but not asymptotically stable.

## 4 Alternative approaches

The replicator equations studied in sections 2 and 3 represent one possible model of selection. They possess “nice” properties — equation (3) admits transformation to the famous Lotka-Volterra equation, equation (9) may have the Hamiltonian. There exist people confident in the idea that a “mathematical beauty” is a necessary ingredient in any theory pretending to describe nature; on the other hand, there also exist people considering it suspicious as such abstract mathematical theory may express only a human way of thinking and not properties of nature itself (for discussion see e.g. [1], [9]). Hence, in this section we introduce two alternative models of selection that take into account additional phenomena.

#### 4.1 Discrete dynamics

Let us consider two populations with non-overlapping generations and assume that the lifespan of one generation is equal to  $h$ . That is, a change in relative frequencies of sub-populations may occur only in time instants  $t_0, t_0 + h, t_0 + 2h, \dots$ . The populations mutually interact and sub-populations of one population have no impact on each other. In another words, the interaction of populations can be expressed by a bimatrix game.

Let us suppose further that relative frequency of single sub-population in a subsequent generation is proportional to its frequency in a present generation and to its “payoff” in present interaction, i.e.

$$x_i(t+h) = c(t)x_i(t)(Ay(t))_i, \quad y_j(t+h) = d(t)y_j(t)(Bx(t))_j.$$

The coefficients of proportionality  $c$  and  $d$  may depend on time. The entries of time-dependent vectors  $x(t), y(t)$  express relative frequencies of constituent sub-populations over time, therefore a natural requirement is that the components of vectors  $x(t), y(t)$  are non-negative and  $I^T x(t) = 1 = I^T y(t)$  for all  $t \in \{t_0, t_0 + h, t_0 + 2h, \dots\}$ . The validity of the first condition is guaranteed by non-negativity of entries of the matrices  $A$  and  $B$ , the second condition requires that

$$1 = \sum_{i=1}^n x_i(t+1) = c(t) \sum_{i=1}^n x_i(t)(Ay(t))_i = c(t)x(t)^T Ay(t)$$

and, in a similar way,  $1 = d(t)y(t)^T Bx(t)$ . Subsequently

$$c(t) = \frac{1}{x(t)^T Ay(t)} \quad \text{and} \quad d(t) = \frac{1}{y(t)^T Bx(t)}.$$

Thus, the coefficients  $c$  and  $d$  do not depend on time directly and their time change is mediated by changing structure of populations. The provided considerations lead to discrete analog of replicator equations in the form

$$\begin{aligned} x_i(t+h) &= x_i(t) \frac{(Ay(t))_i}{x(t)^T Ay(t)}, & i &= 1, 2, \dots, n, \\ y_j(t+h) &= y_j(t) \frac{(Bx(t))_j}{y(t)^T Bx(t)}, & j &= 1, 2, \dots, m. \end{aligned} \tag{12}$$

A fundamental difference of this system and the continuous system (9) lies in the fact, that the matrices  $A$  and  $B$  appearing in (9) need not be non-negative. Hence, an interpretation of matrices  $A$  and  $B$  in systems (9) and (12) is different. The entry  $a_{ij}$  of matrix  $A$  in (12) expresses a multiplication rate from one generation to the next one of the  $i$ -th sub-population of the first population impacted by the  $j$ -th sub-population of the second population while in the replicator equation (9) it expresses a change in fitness of the  $i$ -th sub-population impacted by the  $j$ -th one.

The equations (12) can be rewritten to the form

$$\Delta x_i(t) = x_i(t+h) - x_i(t) = x_i(t) \frac{(Ay(t))_i - x(t)^T Ay(t)}{x(t)^T Ay(t)},$$

$$\Delta y_j(t) = y_j(t+h) - y_j(t) = y_j(t) \frac{(\mathbf{Bx}(t))_j - y(t)^\top \mathbf{Bx}(t)}{y(t)^\top \mathbf{Bx}(t)}.$$

This form shows that the systems (9) and (12) possess the same stationary states. In particular, stationary points of the system of difference equations (12) are Nash equilibria of the bimatrix game  $(\mathbf{A}, \mathbf{B})$ .

A continuous analogy of the difference equations (12) is the following system of differential equations

$$\begin{aligned} x'_i &= x_i \frac{(\mathbf{Ay})_i - x^\top \mathbf{Ay}}{x^\top \mathbf{Ay}}, & i = 1, 2, \dots, n, \\ y'_j &= y_j \frac{(\mathbf{Bx})_j - y^\top \mathbf{Bx}}{y^\top \mathbf{Bx}}, & j = 1, 2, \dots, m. \end{aligned}$$

The meaning of matrices  $\mathbf{A}$  and  $\mathbf{B}$  appearing in this system differs from that in the system (9).

## 4.2 Imitation dynamics

The replicator dynamics (3) mimics the effect of natural selection (although it blissfully disregards the complexities of sexual reproduction). In the context of “games” played in human societies, however, the spreading of successful strategies is more likely to occur through imitation than through inheritance. How should we model these imitation processes?

Let us suppose that a population consists of  $N$  individuals and these individuals are well mixed, i.e. each individual can meet another. It may occur that an individual adopting the  $j$ -th strategy meets an individual adopting the  $i$ -th strategy and after this encounter he adopts the  $i$ -th strategy, that is, he imitates his behavior. Let us assume further that a number of individuals that act in such a way during a time interval of the length (duration)  $\Delta t$  is proportional to  $\Delta T$  and to probability of encounter of individuals adopting the mentioned strategies. Let  $g_{ij}$  be the coefficient of proportionality. The probability that an individual adopting the  $i$ -th strategy meets an individual adopting the  $j$ -th strategy equals to the relative frequency of individuals with  $j$ -th strategy. Hence, the number of individuals adopting the  $i$ -th strategy after time interval  $\Delta t$  is

$$Nx_i(t + \Delta t) = Nx_i(t) + \sum_{j=1}^n Nx_i(t)x_j(t)g_{ij}\Delta t - \sum_{j=1}^n Nx_j(t)x_i(t)g_{ji}\Delta t.$$

Simple calculation and the limit transition  $\Delta t \rightarrow 0$  yields the differential equation

$$x'_i = x_i \sum_{j=1}^n (g_{ij} - g_{ji})x_j.$$

We need to specify the rates  $g_{ij}$  appearing in this equation. It is natural to assume that the rates depend on the current payoffs  $(\mathbf{Ax})_i$  and  $(\mathbf{Ax})_j$  earned by the two strategies in the population:

$$g_{ij} = \varphi((\mathbf{Ax})_i, (\mathbf{Ax})_j);$$

the function  $\varphi$  defines the *imitation rule*. The simplest rule would be “*imitate the better*”. i.e.

$$\varphi(u, v) = \begin{cases} 1, & u > v \\ 0, & u \leq v; \end{cases}$$

this has the disadvantage of being discontinuous. Hence, we will assume that the function  $\varphi$  is continuous and it depends on difference of its arguments, i.e.  $\varphi(u, v) = \psi(u - v)$  where  $\psi$  is continuous non-negative and increasing function such that  $\psi(w) = 0$  for  $w \leq 0$ . Now, we have

$$\begin{aligned} g_{ij} - g_{ji} &= \psi((Ax)_i - (Ax)_j) - \psi((Ax)_j - (Ax)_i) = \\ &= \operatorname{sgn}((Ax)_i - (Ax)_j) \psi(|(Ax)_i - (Ax)_j|). \end{aligned}$$

Denoting  $\Psi(w) = (\operatorname{sgn} w) \psi(|w|)$ , we obtain the equation

$$x'_i = x_i \sum_{j=1}^n x_j \Psi((Ax)_i - (Ax)_j), \quad i = 1, 2, \dots, n; \quad (13)$$

where  $\Psi$  is increasing odd continuous function. In particular, we can take  $\Psi(w) = |w|^\alpha \operatorname{sgn} w$  where  $\alpha$  is a positive number. For  $\alpha = 1$ , this yields  $\Psi(w) = w$ . Such an imitation rule effectively says “*imitate actions that perform better, with a probability proportional to the expected gain*”; it reduces the equation (13) to the usual replicator equation (3). In the limiting case  $\alpha \rightarrow 0$ , on the other hand, we are back to the rule “*imitate the better*”.

## References

1. Barrow, J. D.: Pi in the Sky: Counting, Thinking, and Being. Clarendon Press: New York, 1992 [Czech translation: Pí na nebesích. O počítání, myšlení a bytí. Mladá fronta: Praha, 2000]
2. Dawkins, R.: The Selfish Gene. Oxford Univ. Press: Oxford, 1989 [Czech translation: Sobecký gen. Mladá fronta: Praha, 1998]
3. Dercole, F., Rinaldi, S.: Analysis of Evolutionary Processes. The Adaptive Dynamic Approach and Its Applications. Princeton Univ. Press: Princeton and Oxford, 2008
4. Flegl, J.: Frozen Evolution: Or, that’s not the way it is, Mr. Darwin – Farewell to selfish gene. Charles University in Prague: Prague, 2008 [Czech original: Zamrzlá evoluce, aneb, Je to jinak, pane Darwin. Academia: Praha, 2006]
5. Hofbauer, J.: On the occurrence of limit cycles in the Volterra-Lotka equation. Nonlin. Analysis **5** (1981) 1003–1007
6. Hofbauer, J.: Evolutionary dynamics for bimatrix games: A Hamiltonian system? J. Math. Biol. **34** (1996) 675–688
7. Hofbauer, J., Schuster, P., Sigmund, K.: A note on evolutionarily stable strategies and game dynamics. J. Theor. Biol. **81** (1979) 609–612
8. Hofbauer, J., Sigmund, K.: Evolutionary Games and Population Dynamics. Cambridge Univ. Press: Cambridge, 2002
9. Livio, P.: Is God a Mathematician? Simon&Schuster: New York, 2009 [Czech translation: Je Bůh matematik? Argo/Dokořán: Praha, 2010]

10. Nachbar, J.: 'Evolutionary' selection dynamics in games: convergence and limit properties. *Intern. J. of Game Theory* **19** (1990) 59–89
11. Schuster, P., Sigmund, K.: Coyness, philandering and stable strategies. *Anim. Behavior* **29** (1981) 186–192
12. Maynard Smith, J.: *Evolution and the Theory of Games*. Cambridge Univ. Press: Cambridge, 1982
13. Maynard Smith, J., Price, G.: The logic of animal conflict. *Nature* **246** (1973) 15–18
14. Sigmund, K.: *The Calculus of Selfishness*. Princeton Univ. Press: Princeton and Oxford, 2010
15. Taylor, P. D., Jonker, L.: Evolutionary stable strategies and game dynamics. *Math. Biosci.* **44** (1978) 145–156
16. Vincent, T. L., Brown, J. S.: *Evolutionary Game Theory. Natural Selection and Darwinian Dynamics*. Cambridge Univ. Press: Cambridge, 2005
17. Zeeman, E. C.: *Population dynamics from game theory*. In: *Global Theory of Dynamical Systems*. Springer: New York, 1980



Deterministic and Stochastic  
Modelling in Biology and Medicine

**Computational Biology**  
**Students' Abstracts**





# Gene prediction from non-annotated sequences

Michaela Bayerlová, Supervisor: Mgr. Natália Martínková, Ph.D.

Institute of Biostatistics and Analyses, MU Brno, Department of Population Biology, IVB AS  
CR, v.v.i. Brno

## Introduction

Genomic databases contain large amount of unprocessed data. An example of such database is a whole-genome shotgun (WGS) database that collects non-annotated nucleotide sequences. I have compiled and applied a method to search the WGS database to predict a gene for a particular protein from non-annotated sequences. I have validated the method by putting predicted proteins into context with annotated sequences, i.e. I have verified the accuracy of prediction. Further, I was interested if the proposed design is more accurate than the automatic gene annotation in the Ensemble genome browser. This procedure was applied to the gene of ryanodine receptor (*ryr*). *Ryrs* are calcium release channel proteins of the sarcoplasmic reticulum and they are expressed in three distinct ways: *ryr1*, *ryr2* and *ryr3*.

## Methods

To search the WGS database, I used the tool BLAST that provides sequence similarity search. Regions of aligned annotated nucleotide sequences of gene for *ryr* proteins were used as input data; these sequences were conserved in the alignment. Different sequence lengths of randomly selected taxa were used subsequently. Retrieved sequences were then analyzed using GENSCAN. The program predicts genes, as well as their introns and exons. Predicted genes were then translated into individual proteins. Predicted proteins with length corresponding to *ryr* protein were selected and their identification was then checked using the BLAST search against a reference protein database. Verified sequences were collected into multiple sequence alignment for phylogenetic analysis. WGS sequence retrieval was reiterated until three consecutive BLAST searches (i.e., about 100 sequences) did not yield any other new sequence in which *ryr* protein could be predicted.

## Results

The analyses resulted into a phylogenetic tree for the gene of *ryr1*, *ryr2* and *ryr3* proteins composed of 35 annotated amino acid sequences, 35 sequences previously predicted by NCBI tool GNOMON and 23 sequences predicted with my design. Compared to the Ensemble gene tree, my tree contains fewer species, but is stable and devoid of any major errors in phylogenetic classification of taxa. Thus I am able to verify the accuracy of prediction from the evolutionary point of view, and to identify incorrectly annotated sequences present in the public databases. The prediction using this method is sensitive enough and provides evidence for the whole-genome duplication in fish evolution.

## **Conclusion**

In conclusion, I would like to summarize that the proposed method of gene prediction from non-annotated sequences works efficiently for small-scale projects and provides sufficiently accurate results.

# **Mathematical modelling of biodegradable processes**

Anna Gardavská

Faculty of Science, Masaryk University, Brno

## **Introduction**

The aim of my work is to map existing methods of mathematical modelling of biodegradable processes. This work presents an overview of the basic processes of degradation of biodegradable waste, describes the anaerobic and aerobic digestion, and gives more detail on the problems of biogas plants operating on the principle of anaerobic digestion. It also describes batch systems, single or multi-phase systems, and discusses problems of these reactors due to the inhibition by pH, bacteria or ammonia. The paper gives a brief overview of available mathematical models that describe the process of anaerobic digestion by the system of differential equations. The final section deals with the implementation of one model using the software Maple.

## **Methods and materials**

The first part of my paper presents processes of anaerobic digestion (or aerobic digestion) and describes stages of this process such as hydrolysis, acidogenesis, acetogenesis and methanogenesis. The next part describes problems of this process. The models presented in the work involve a model with phase separation (modified kinetic Monod model), a model from authors Hill and Bart (28 differential equations), a model BisWas (33 differential equations) and a model with distributed parameters (72 differential equations).

## **Results**

The final part of my work contains several graphs based on the simplified Hill and Bart model. Instead of 28 equations, the model was constructed from 10 equations. These graphs illustrate how the yield of the biogas (methan gas) changes with different concentration of ammonia or pH. This part also includes an analysis sensitivity test for all parameters of modified Bart and Hill models. This test clearly shows that pH and ammonia are the most sensitive parameters.

## **Conclusion**

The paper only describes some mathematical models, not all existing ones. That is due to a considerable number of those models, as well as the complexity of each of

them. The graphs based on models constructed in Maple show how the yield of biogas (methane or carbon dioxide) changes with the values of pH or ammonia concentration, which implies that it is advantageous to have such models and to have option to carry out studies based on mathematical models instead of conducting expensive real-time experiments.

## **Enabling pathway analysis - connecting genomic experiments and gene ontology databases**

Hana Imrichová

Faculty of Science, Masaryk University, Brno

### **Introduction**

DNA microarray technology has made it possible to monitor the changes in the expression of thousands of genes between different groups of interest. The usual output of the analysis is a list of differentially expressed genes. A mere glance at this list, however, is not enough to understand the complex mechanisms within the cell underlying the phenotype differences between the studied groups. Here comes the big challenge - a correct biological interpretation of these results, which can be achieved by mining online databases of gene sets and biological pathways. This leads to a better understanding of cellular processes as an intricate network of functionally related components. The goal of my work was to create a wide overview of recent methods for gene set and pathway analysis.

### **Methods and materials**

In my work, I have reviewed 25 methods of gene set analysis. These methods differ in several important aspects: the type of the tested null hypothesis; the type of the method searching for the enrichment of gene sets as well as the type of the statistical method to determine the significance of this enrichment; the number of samples in the dataset; whether the method considers both directions of expression and if unable to identify any enriched gene sets in individual samples. Furthermore, the methods differ in software implementations and the type of organism supported by the implementation.

Methods are divided into 3 main categories according to the null hypothesis:

- **Competitive methods**, testing whether the genes in the gene set are differentially expressed more than other genes. This group involves e.g.: Catmap (Breslin et al., 2004), GOAL (Volinia et al., 2004), PAGE (Kim and Volsky, 2005), GeneTrail (Backes et al., 2007).
- **Self-contained methods** that consider only genes within a gene set and test, if there is at least one differentially expressed gene. This group is represented by e.g.: Globaltest (Goeman et al., 2004), PLAGE (Tomfohr et al., 2005), SAM-GS (Dinu et al., 2007).

- **Mixed methods** that validate whole data set and test, if there is any gene set with differently expressed genes. This group involves a method called GSEA (Mootha et al., 2003) and its two extensions.

## Results

There are dozens of methods for gene set/pathway analysis. All of them have a common objective, which is to assign a value to a group of genes (P-value or a score) in order to determine which gene set (or pathway) is enriched in the list of differentially expressed genes from the microarray analysis. However, the user has to choose a method according to the type of the dataset and questions he would like to have answered. I have created two tables and a simple instruction scheme to simplify this choice. Three main aspects have to be taken into account when choosing an appropriate method:

1. The type of the data set that is analyzed (according to the number of samples and the type of organism).
2. The aim of the experiment (the type of the null hypothesis, gene sets with both directions of expression).
3. The programming capabilities of the user.

## Conclusion

In my work, I have created a wide review of methods for gene-set analysis together with the description of particular methods. Moreover, two tables and a decision scheme are given to choose the right method for a particular problem. Using the right method, the user can resolve his problem with the best results.

# Creation of a single initiation application with GUI generateb by MATLAB

Pavĺína Krečmerov

Faculty of Science, Masaryk University, Brno

## Introduction

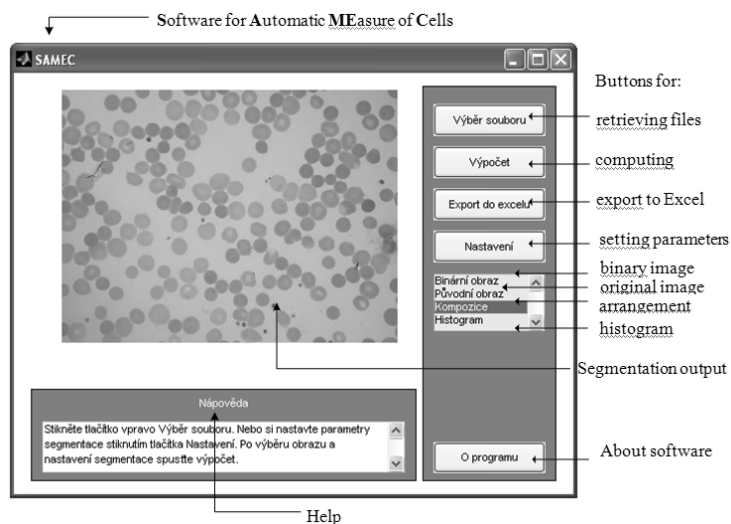
Aim of the study was creating GUI (Graphic user interface) as an extension of my bachelor thesis that dealt with extraction of cells' geometrical parameters in 2-D images from optical microscopy.

## Methods and materials

GUI is generated by MATLAB, it is a function that we call without parameters, so it creates interface with buttons. When we press the button, we call this function with parameter (in MATLAB it is called Callback). It uses global variables due to parameter passing in subfunction. Inputs are haematological images obtained by and optical microscope.

## Results

Outputs are labelled images, arrangement of images, histograms and outputs to Excel.



## Conclusion

The goal was achieved. My programme was devolved on the Department of Clinical Haematology, University Hospital Brno on 4 March.2010. It has been used for measurement of cells' parameters to date.

## Changes in long time monitoring of macrozoobenthos in the Czech Republic

Simona Littnerová

Faculty of Science, Masaryk University, Brno

## Introduction

The European Union Water Framework Directive (WFD) was created to assess and preserve water quality. Predictive models are used to assess the ecological status of streams. These models are based on the community-environment relationship modelling. Knowledge of variability of community and community-environment relationship is therefore essential. Predictive models are based on the assumption of assemblage stability. However, temporal changes in the structure of communities are one of the factors affecting water quality assessment systems. The aim of this work was to analyze the temporal variability of benthic macroinvertebrates and its consequences for the established typology. The analyzed data come from the biomonitoring of streams of the Czech Republic in 2002-2005. The changes were

observed in terms of both diversity indices and biotic indices describing the community, as well as in terms of actual changes in community composition. Subsequently, we tested whether the typology of sites had an impact beyond this change: typologies used in various types of assessment models of ecological status were adopted for this task.

## Methods and materials

RM ANOVA was applied to determine the indices changes over time and under the influence of typology of sites; overall changes in communities composition were analysed by means of Procrustean analysis, followed by a detailed analysis of changes of individual taxa occurrence in time. Consequently, the Spearman correlation coefficient was used to determine the correlation between change of chemical variables and change of structure of community.

## Results

<i>Environmental parameter</i>	<b>Saprobiotic index</b>				<b>Shannon index</b>				<b>Comm. struc. (Procrustes resid.)</b>		
	<i>Year</i>	<i>Seas.</i>	<i>Y. × S.</i>		<i>Year</i>	<i>Seas.</i>	<i>Y. × S.</i>		<i>2002</i>	<i>2002</i>	<i>2002</i>
									-	-	-
									<i>2003</i>	<i>2004</i>	<i>2005</i>
<b>Altitude</b>	✓	✓	×	✓	✓	×	×	×	×	×	×
<b>Stream order</b>	✓	×	×	×	✓	×	×	×	✓	×	×
<b>Hydroecoregion</b>	✓	×	×	×	✓	✓	✓	✓	×	×	×
<b>Land use: Fields</b>	✓	×	×	×	✓	×	×	×	×	×	×
<b>Land use: Forest</b>	✓	×	×	×	×	×	×	×	×	×	×
<b>Abiotic typology</b>	✓	✓	×	×	✓	×	×	×	×	×	✓
<b>Biotic typology</b>	✓	×	×	×	✓	×	×	×	×	×	✓
<i>Chem. parameter</i>											
<b>Biol. ox. demand</b>									✓	✓	✓
<b>Total phosphorus</b>									×	✓	×

× NON SIGNIFICANT; ✓ SIGNIFICANT

## Conclusion

The time-related shift in indices and the community composition was found; on the contrast, the influence of the localities typologies on this change was not found. The most significant change was recorded between 2002 and 2003. This change is a possible consequence of high precipitation amount and floods in 2002. The analysis of chemical measurements revealed the link of this change to the biological oxygen demand. We can conclude that the size of temporal changes of indices based on communities' structure allows us to adopt sites typologies based on one-year sampling for systems of ecological status assessments. On the other hand, detailed analyses of communities on the level of species have to take into account significant inter-annual changes in species composition.

# Population history of viruses causing rabies

Jiří Moravec

Faculty of Science, Masaryk University, Brno

## Introduction

Viruses causing rabies (genus *Lyssavirus*) are neurotrophic viruses that are potentially fatal to warm-blooded animals. *Lyssavirus* is commonly transmitted by a bite from an infected individual. Thanks to animal vaccination in developed countries, the pathogen was eliminated from most ground animal reservoirs of rabies. Several reservoirs of rabies still remain, such as bat or megabat populations.

My aim is to fully reconstruct phylogeny of all *Lyssaviruses* in order to better understand their evolution.

## Methods and materials

I have been working with complete sequences of *lyssavirus* CDS of N-gene, gene for nucleoprotein, which is a protein that binds to DNA. Its evolution is largely independent on the selective pressure caused by the co-evolution of the virus and the immune system of the host. The sequences were downloaded from the NCBI GenBank database using the Geneious programme. All complete CDS for nucleoprotein were aligned in BioEdit, and the RAXML programme was used to perform the final maximum likelihood analysis using polybenche Black Box online service.

## Results

All major bifurcations were supported by high bootstrap values (>75) and divided the phylogenetic tree into two major groups. The first group consisted of viruses potentially dangerous for humans. Viruses in the second group have not caused fatalities in humans, or are described from very few human infections.

Phylogroup 1		Phylogroup 2
European bat lyssavirus 1 (EBLV-1)	European Bat lyssavirus 2 (EBLV-2)	West Caucasian bat virus (WCBV)
Australian bat virus (ABLV)	Duvenhage virus (DUVV)	Shimoni bat virus (SHIBV)
Irkut virus (IRKV) and Ozernoe	Khujand virus (KHUV)	Mokola virus (MOKV)
Aravan virus (ARAV)	Rabies virus (RABV)	Lagos bat virus (LBV)

Rabies virus and Mokola virus are the most derived in phylogroups 1 and 2, respectively. European bat lyssavirus 1 and Aravan virus are the most similar to *Lyssavirus* common ancestor. Rabies virus, Australian bat lyssavirus, Lagos bat virus,

and possibly also Mokola virus have high intraspecific variability. Low genetic variability was found in European bat lyssavirus 1. Sample sizes from other viruses are too small to assess their genetic variability.

## **Conclusion**

I was able to fully reconstruct Lyssavirus phylogenetic tree with the basic sculpture of 7 original genotypes assembled into two phylogroups as it was previously classified, but with much larger sampling and including newly described viruses. The positions of new viruses correspond to other studies, but to date this is the first study analyzing all known genotypes.

# **Computational simulation of environmental pollution using Maple**

Markéta Novotná

Faculty of Science, Masaryk University, Brno

## **Introduction**

Maintenance of high water quality is a key problem for water management officials and for appropriate research centres nowadays. Computer simulation models play a crucial role in predictions and various analyses. There are numerous water quality and hydrodynamic models that have been used for surface water systems such as rivers, lakes, reservoirs and estuaries.

Aquatic ecosystems are very complex systems of physical, chemical and biological interactions. The occurrence of nutrients can bring about changes to the structure of ecosystem (the loss or overgrowth of fundamental organisms).

This work is focused on water pollution and models used in this area. Its aim is to predict the phosphorus concentration in selected water bodies.

## **Methods and materials**

The CE-QUAL-W2 is a two-dimensional (longitudinal-vertical) water quality and hydrodynamic computer simulation model that was developed at the Portland State University in the US and has been used in many river, reservoir, lake and estuary applications. In this work, the model has been applied to DeGray Lake in Arkansas, USA.

The main part deals with the classical modelling approach using the basic and modified ELS-model. The phosphorus concentration in a lake is described by the following differential equations:

$$\frac{dC}{dt} = \frac{Q \cdot (C_{in} - C) - KT \cdot V \cdot C}{V}$$

$$\frac{dC}{dt} = \frac{Q_1 \cdot C_{in} - Q_2 \cdot C - KT \cdot (a \cdot t + b) \cdot C}{(a \cdot t + b)}$$

$V = a \cdot t + b$  ... lake volume,  
 $dC/dt$  ... change of phosphorus concentration in the lake per unit of time,  
 $C$  ... phosphorus concentration in the lake,  
 $C_{in}$  ... phosphorus concentration in the tributary,  
 $Q$  ... tributary water discharge to the lake,  
 $Q_1$  ... averaged inflow,  $Q_2$  ... averaged outflow,  
 $KT$  ... turnover rate of phosphorus in the lake.

## Results

Capabilities of two basic models have been tested on measured data from the Brno Dam. Results for the first five months of 2008 are shown in Table 1.

TAB.1: COMPARISON OF BASIC AND MODIFIED ELS-MODEL TO MEASURED DATA, P [MG/L].

date	field data	basic model	modified model
09/01/08	0.050	0.050	0.050
04/02/08	0.048	0.067	0.075
05/03/08	0.077	0.057	0.054
31/03/08	0.027	0.121	0.175
06/05/08	0.031	0.068	0.085

We can see that the concentration predictions of the basic and the modified model are nearly the same. Detailed insight into studied area could support better agreement with field data.

## Conclusion

This work reviews several water quality models. The complex CE-QUAL-W2 model was used on a testing data set, while the classical and the modified version of ELS-model were applied on phosphorus concentration predictions in the Brno Dam. All the computations were performed in the Maple system.

# Bioclimatic modelling

Roman Richard Štěřba

Faculty of Science, Masaryk University, Brno

## Introduction

Kuneš (2008) tested a hypothesis that the glacial pollen spectrum of central Europe and recent pollen spectrum of southern Siberia are analogous and he proved the hypothesis to be true. Based on his work, I have focused to create a model of glacial vegetation of central Europe based not on pollen spectra but on the plant growing in southern Siberia.

## Methods and materials

The main part of my work was a review of presence-only based models used in bioclimatic modelling. Out of those, I eventually chose two: bioclimatic envelopes and ENFA (ecological niche factor analysis).

Bioclimatic envelope modelling is a simple model based on creating multidimensional convex envelope, each of its borders being based on minimum and maximum of particular ecological variable.

ENFA is a factor-based model. The first factor axis shows all the marginality – the difference between the optimum of species distribution and optimum of the whole tested area. Other axes, on the other hand, show the rest of variability.

In my work, I have used an available data set collected in southern Siberia. It contained data from 702 localities, each containing information about the environmental variables and the occurrence of species. Another data set which was used for modelling contained the whole tested area in the grid of 1 x 1 km.

## Results

The main benefit of my work is the proof that the distribution of vegetation is really based on bioclimatic variables, as bioclimatic envelopes which are generally supposed to give bad prediction actually gave good prediction. This means that the examination of other bioclimatic models is necessary in order to find those which give the best predictions possible.

As I mentioned before, bioclimatic envelopes are expected to give bad predictions as they do not concern any correlation among used variables. The best prediction proved to be 78 % well-predicted presences, though.

ENFA, due to its user unfriendly implementation and interface in Biomapper, gave only a raster output, so its prediction ability could not have been compared with bioclimatic envelopes.

# **Evaluation of Stress Test ECG Signal Parameters in Horses**

Jana Svačinová

Faculty of Science, Masaryk University, Brno

## **Introduction**

Examination and measuring of parameters of stress ECG is one method for the assessment of horses' health. The term "stress" here means exercise (such as walk, gallop, trot) on a conveyor-belt, while the ECG is being scanned. Basic processing of signal consists of QRS complexes detection and cardiac cycles length assessment. The detection is essential in order to establish other parameters, such as T-waves. QRS complexes detection in stress ECG is more complicated, because the horse's movements influence the measurement: consequently, significant unwanted effects appear in the signal. The goal of this work is to process and conveniently modify the horse's ECG to detect QRS complexes or eventually T- waves. This is performed using the computer programme Matlab.

## **Methods and materials**

The ECG report consists of three recordings which were scanned at a sampling frequency of 500 Hz. Initially, each recording is subject to filtration that points out QRS complexes in a signal. Consequently, each recording is smoothed by a rectangular window; and finally, individual recordings are amplified and summarized. In this way, we have successfully created a signal with distinctive peaks at QRS complexes. This signal is also suitable to detect T-waves, which are also clearly visible.

The principle of detection consists in the search of peak values of modified signal, that follow crossing of the detection threshold with QRS complex peak. The detection threshold is set to be one third of average of last three peak values. The detector also includes a zone that follows positive detection of a complex, in which next complex can't be detected. This tone is useful in case of high T-waves, or possibly extrasystols. Therefore, an important part of this work consisted in the search of best setting of a detector depending on the type of horse's exercise and, consequently, on the length of cardiac cycles, in order to perform the detection as accurately as possible.

## Results

CHART 1: RESULTS OF A QRS COMPLEXES DETECTION FOR TWO-MINUTE RECORDING

TYPE OF EXERC.	AMOUNT OF QRS COMPLEXES DETECTED	AMOUNT OF MISSED QRS COMPLEXES	AMOUNT OF FALSELY DETECTED QRS COMPLEXES	DETECTOR HIT RATE (%)	AVERAGE LENGTH OF CARDIAC CYCLE (S)	STAND. DEV.
WALK	177	0	0	100	0,68	0.06
CANTER	254	2	0	99,2	0,46	0,05
TROT	281	19	0	93	0,37	0,03

The hit rate of detection is best in case of a walk. With a higher speed of horse's movement, the ECG signal is being strongly disturbed and T-waves (which can be mistaken with QRS complex) start to appear. However, by a proper setting of detector parameters, it is possible to increase the hit rate of detection. Furthermore, we can see a considerable variability of cardiac cycle lengths.

## Conclusion

This detector is able to detect QRS complexes at walk and canter successfully. In case of trot, the detector does not work as efficiently as in the previous cases.

## The application of clustering methods on data of clinical registries

Bc. Hana Švihálková

Faculty of Science, Masaryk University, Brno

## Introduction

On many occasions, biologists collecting specific data ask whether their observations belong to any natural groups and if so, how many groups are there and which observations belong to each group.

The aim of this work is to try and detect these groups in clinical trials, and to classify patients into these groups.

## Methods and materials

The first part of this work is focused on the background research of methods of cluster analysis. In the next part, some of these methods are applied on selected clinical registries.

The software used in this work included Statistica for Windows, Matlab and Microsoft Office Excel.

Firstly, coefficients of association (Sokal-Michener, Rogers-Tanimoto, Hamann, Russel-Rao, Jaccard and Dice) were used to input data from the registry AHEAD (Acute HEArt failure Database, clinical registry for the monitoring and treatment of acute heart failure).

Secondly, the Principal Component Analysis (PCA) was used on these data in order to find whether they are correlated or not, and to select the most suitable parameters for further analyses.

And finally, hierarchic agglomerative clustering algorithms and partitional clustering methods were applied to both categorical and continuous data from the PCA.

## **Results**

The coefficients of association applied to the input data were helpful when a new patient appeared. The most similar patients were found, allowing us to assess how the condition of this patient might develop.

The clustering methods divided patients according to selected parameters and depicted their mutual distance in a multidimensional space. Moreover, these methods have discovered some duplicities, i.e. patients who were recorded twice in this registry.

## **Conclusion**

Using the available literature, various methods of dealing with clinical data were found, and cluster analysis divided them into natural groups.

At this time, an algorithm is being prepared to reveal duplicate or similar patients in a clinical registry. This algorithm should be implemented into the TRIALDB system.

# **Acquiring knowledge on anticancer chemotherapy from health insurance claims data**

Bc. Alena Zol'áková, Supervisor: RNDr. Daniel Klimeš

Faculty of Science, The Institute of Biostatistics and Analyses, Masaryk University, Brno

## **Introduction**

The chemotherapy is currently an important and much discussed way of treatment of malignant diseases. Specifically, it is a treatment with an anti-tumour effect using the so-called cytostatic agents, which affect the growth cycle of cancer cells and stop their division, or alleviate the symptoms of the disease. Those cytostatic agents usually given in various combinations, cycles, and setting of doses, i.e. in various regimens to enhance the therapeutic effect, to reduce the cumulation of adverse effects, and to prevent the resistance of the organism to the applied medicament.

Currently, the electronic library DIOS contains 214 pre-set regimens and it is still being updated according to the “Guidelines on cytostatic treatment of malignant tumours“ which are regularly released by the Czech Society for Oncology at the Czech Medical Association of J. E. Purkyne (CzMA JEP). Actually, there are much more applied regimens worldwide. This paper therefore aims to detect the applied regimens, to search for them in available resources, and to extend the digital library in this way.

## **Methods and materials**

This work involved the design and test of an algorithm, as well as the assessment of clinical relevance of differences among regimens. It was implemented on data of medical facilities in between 1 February 2007 and 11 September 2009. The data consisted of 1,870 patients’ records and 2,094 applied chemotherapies. After a subsequent correction and analysis, the data was compared to standard chemotherapy regimens, which originated in the electronic library of the DIOS project. After the comparison to scientific literature, the data of the years 2008, 2009, and 2010 were summarised, revised and analysed. The algorithm was designed in PL/SQL language (Procedural Language/Structured Query Language) and the obtained data was processed by the database software Oracle.

## **Results**

The suggested algorithm enables the diversification of practically applied regimens based on the type of administered cytostatic agents (step 1), on the length of the cycle of given substances (step 2), and on the range of given doses (step 3). The applied procedure distinguishes and entitles applied chemotherapy regimens and compares them to standard regimens from digital library (approximately 70% recognised applied regimens). Finally, the algorithm evaluates the compliance with the dose intensity in clinical practice (the most accurately dosed chemotherapy regimens in cases of breast cancer – C50). Another advantage of the suggested algorithm is the detection of potential mistakes and uncertainty in the application of chemotherapy regimens, which can be analysed and evaluated in cooperation with specialists. This brings about an improvement of the digital library, and increases clarity and accuracy of practical regimens’ applications in a certain medical facility.

## **Conclusion**

As a result, the algorithm proves a relatively high success rate in the recognition and evaluation of applied regimens. However, it is necessary to deal with certain issues, e.g. the recalculation of doses to the patient’s weight (not to a body surface), or an assessment of the cycle’s length when the cytostatic agent is given repeatedly within one cycle. Finally, due to applied methods and the implementation of various sets of chemotherapy data, the procedure becomes universal; therefore, it fulfils its long-term aim – to distinguish and to entitle applied chemotherapy regimens and to evaluate the adherence of dose intensity in clinical practice in various medical facilities on the whole territory of the Czech Republic. It can also enhance the quality of cancer patients treatment.